

The Charged Bowl in Toroidal Coordinates

Phil Lucht

Rimrock Digital Technology, Salt Lake City, Utah 84103

last update: January 5, 2016

rimrock@xmission.com

Maple code is available upon request. Comments and errata are welcome.

The material in this document is copyrighted by the author.

The graphics look ratty in Windows Adobe PDF viewers when not scaled up, but look just fine in this excellent freeware viewer: <http://www.tracker-software.com/pdf-xchange-products-comparison-chart>.

Overview and Summary.....	3
1. Bipolar and toroidal coordinates.....	7
1.1 Bipolar coordinates	7
1.2 Toroidal coordinates	9
2. The charged bowl potential in toroidal coordinates	16
2.1 Level curves, the charged ellipsoid problem and a dashed hope	16
2.2 Cartesian, spherical, toroidal and ellipsoidal atomic forms	17
2.3 Smythian forms and one for the bowl.....	18
2.4 Solution to the charged bowl potential problem: the Mehler-Fock Transform.....	19
2.5 Limiting cases of the potential	22
3. The charged double-bowl potential in toroidal coordinates.....	26
3.1 The general double bowl solution.....	26
3.2 Special case: a bowl with a flat lid.....	29
3.3 Special case: a sessile drop (lens-shaped double bowl)	29
4. The charged bowl surface charge densities and capacitance	31
4.1 Bowl surface charge densities.....	31
4.2 Comparison with known results, and the small-hole limit.....	35
4.3 The full-sphere and flat-disk limits of σ	39
4.4 Bowl capacitance	40
5. Plots of the toroidal coordinates $u(\rho,z)$ and $\xi(\rho,z)$.....	43
6. A selection of charged bowl potential plots.....	49
7. Mehler integrals	52
7.1 List of useful Mehler integrals	52
7.2 Evaluation of the integral X appearing in (4.1.10).....	53
7.3 Where to find Mehler integrals (some errata noted)	55
7.4 Mehler Functions: hypergeometric forms and plots	56
8. The bowl potential in elementary functions.....	61
9. Using Maple to plot the bowl potential	64
10. Potential and capacitance of a charged torus	67
10.1 The potential of a charged torus.....	67
10.2 How many terms should one keep in the potential series?	69

10.3 Using Maple to plot the torus potential.....	71
10.4 Capacitance of a torus	74
10.5 Surface charge density on a torus	77
10.6 Using Maple to plot the torus surface charge density	82
Appendix A. Maple code text for plotting the bowl and torus potentials	86
Appendix B : Converting expressions from toroidal to cylindrical coordinates	89
B.1 The conversions.....	89
B.2 Application: The Disk Potential	93
Appendix C: Kelvin's approach to the charged bowl problem.....	96
Appendix D: Smythe's approach to the charged bowl problem	100
Appendix E: Dual equations and their connection to the charged bowl problem	105
Appendix F: The Abel Transform in various forms	110
Appendix G: Solving the charged bowl problem using a double Abel transform	113
G.1 Find g_1	113
G.2 Run a check on g_1	117
G.3 Find a_n	117
G.4 Find Ψ and f_2	119
Appendix H: Support.....	121
H.1 Solving for $A(\tau)$ and $B(\tau)$ in (2.4.10) and double-bowl support	121
H.2 Computation of the integral in (2.4.7).....	127
H.3 Computation of the integral in (4.4.2).....	128
H.4 Computation of two integrals used in Appendix J and K	129
H.5 Limits of toroidal functions (and combinations) as $n \rightarrow \infty$	133
H.6 Limits of toroidal functions (and combinations) as $z \rightarrow \infty$	135
H.7 Limits of toroidal functions as $z \rightarrow 1$	137
H.8 Alternate series for $T(z)$ near $z = 1$	139
Appendix I. Capacitance in the thin-wire and horn torus limits	141
I.1 The torus thin wire limit $R \rightarrow 0$	141
I.2 Warm-up exercises to prepare for the degenerate torus limit.....	145
I.3 Capacitance of a degenerate torus (horn torus)	150
Appendix J. The Fourier Cosine Series Transform and the Mehler-Fock Transform.....	154
J.1 Regular boundary value problems and associated transforms.....	154
J.2 The Fourier Cosine Series Transform	156
J.3 Application to $f(\theta) = (a - b\cos\theta)^{1/2}$	159
J.4 The Q^2 and QQ' sums	162
J.5 The Generalized Mehler-Fock Transform	164
Appendix K: Integration of torus surface charge density	171
K.1 Warmup Exercises: Circumference and Area of a Torus.....	171
K.2 Integration of the toroidal surface charge density	173
Appendix L: Some Mehler Integrals	176
Appendix M: The behavior of $f(z) = (a + \cos z)^{1/2}$ as an analytic function.....	188
References	192

Overview and Summary

This document was motivated by a "stub" section appearing in an informal 2002 paper by Kirk McDonald (see References) which reviews various solutions of the charged bowl problem. Here is that section in its entirety:

2.5 Solution in Toroidal Coordinates

The problem of a charged, conducting spherical bowl can also be solved in toroidal coordinates [10].

where [10] is our Lebedev et al. reference. The present document is meant to fill in this stub section!

The phrase "charged bowl" refers to an isolated conducting spherical bowl, sometimes called a spherical cap, shell or segment. An arbitrary plane slicing through a full spherical shell divides that shell into two spherical bowls, each with the same circular lip. The "charged bowl problem" is this: put some charge Q on an isolated conducting bowl and determine the resulting electrostatic potential V everywhere as well as the charge densities σ on the inner and outer bowl surfaces. The reader versed in related problems (e.g., the charged disk) would not be surprised to find the charge densities to be divergent (but integrable) at the bowl edge and non-zero everywhere on the bowl. In practice, one normally assumes that the bowl is at some potential V_0 relative to infinity, and then the charge on the bowl is $Q = C_{\text{bowl}}V_0$. Of course finding capacitance C_{bowl} is part of the problem.

In 1869 Lord Kelvin used the method of inversion (last seen lurking in green Jackson) to solve the charged bowl problem for the inner and outer charge densities. Kelvin's "bowl paper" requires great patience to read, and is outlined in McDonald's paper. Modern readers might have forgotten things like "the chord theorem" and other geometric properties of circles. We comment more on Kelvin's bowl paper in Appendix C and discuss how Kelvin showed the now-well-known fact that the inner and outer bowl charge densities differ by the constant $V_0/(4\pi R)$ which is independent of the bowl's lip angle and of the location on the bowl. Certainly this result is valid for a fully closed bowl since $\sigma = 0$ inside and on the outside $\sigma = Q/A = C_{\text{sphere}}V_0/A = RV_0/(4\pi R^2) = V_0/(4\pi R)$.

In Appendix D we mention a fascinating variation of the Kelvin inversion approach indicated by Smythe in a set of problems.

Besides inversion, various other methods exist to obtain an exact solution of this problem. Perhaps the most well known is the use of "dual" Legendre series equations in friendly spherical coordinates as outlined by Sneddon and others. One series (Dirichlet) sets the potential to a constant on the bowl, while a radial derivative of that series (Neumann) sets the charge density to zero on the cap. The problem is then to find series coefficients which satisfy both equations, neither of which is invertible since it only covers a partial range of polar angle. In matrix language, these dual equations are $A\Psi = f$ and $B\Psi = g$ where Ψ is an infinite vector of unknown coefficients. Appendix E shows formally how such dual equations may be solved, and Appendix G solves the charged bowl problem using this method. A tool used in the dual equations approach is the Abel transform, a summary of which is given in Appendix F.

Our main concern, despite all these spherical coordinate appendices, is to obtain an exact solution of the charged bowl problem using the much less friendly toroidal coordinates. Surely this has been done many hundred times since 1869, but the author has not found much on the web -- certainly not much that is freely downloadable. But sources do exist and we quote some of them as needed for verification.

After doing the bowl, we turn our attention to the problem of the charged torus.

The general plan is shown in the Contents above. Appendix A provides simple Maple code to allow the reader to make plots of the bowl and torus potentials. Appendix I concerns a limit which seems to indicate that the capacitance of a degenerate (horn) torus of radius R is given by the strange value $C = 1.7413R$ which can be compared to the capacitance $C = 2.0000R$ of its embedding sphere.

In all that follows, we shall refer to the spherical conducting bowl as "the bowl", and shall refer to the unoccupied remainder of the bowl's sphere as "the cap".

The symbol ϵ_n stands for $2\delta_{n,0}$, sometimes called Neumann's factor or number.

We use cgs units as in (4.1.2). Multiply our charge and capacitance results by $4\pi\epsilon_0$ to convert them to SI units.

When an equation is repeated, its equation number is put in italics.

Section and Appendix summaries follow.

Legendre Functions

The Legendre functions we write as $P_v^\mu(z)$ and $Q_v^\mu(z)$ are the standard associated Legendre functions which are defined identically in our three main references Bateman (1953), NIST (2010), and GR7 (2007). These references all use a slightly italic font for these functions, but we use a non-italic font.

Morse and Feshbach's two-volume set came out around the same time as Bateman (1953) and their P and Q functions are unfortunately non-standard. For example, their toroidal $Q_{n-1/2}^\mu(z)$ function definition (p 1329) is different from their associated Legendre $Q_v^\mu(z)$ function definition (p 1327), when one sets $v = n-1/2$. We prefer to use the same standard analytically continued functions for all values of v (degree) and μ (order) and z (argument). There are phase issues which depend on how the cuts are taken away from the branch points at $z = -1$ and $z = 1$. We take them both to the left to clear the interval $(1, \infty)$ for z, and this is the way NIST thinks of their italic P and Q functions.

In addition to these standard italic P and Q functions, NIST has non-italic Ferrers functions which are slightly different. In addition, they use a bolded Q function and a bolded F function as follows:

$$Q_\nu^\mu(x) = e^{-\mu\pi i} \frac{Q_\nu^\mu(x)}{\Gamma(\nu + \mu + 1)}. \quad \mathbf{F}(a, b; c; x) = \frac{1}{\Gamma(c)} F(a, b; c; x)$$

where the unbolted Q and F are the standard Bateman functions

Generally all authors agree on the definitions of $P_v(z)$ and $Q_v(z)$.

The toroidal functions are $P_{n-1/2}^\mu(z)$ and $Q_{n-1/2}^\mu(z)$.

The Mehler and conical functions are $P_{i\tau-1/2}^\mu(z)$ and $Q_{i\tau-1/2}^\mu(z)$.

Section Summaries

Section 1 reviews bipolar (ξ, u) and toroidal (ξ, u, φ) coordinates.

Section 2 discusses the notion of atomic forms and Smythian forms. A Smythian form for the charged bowl is obtained and its coefficients computed, resulting in a solution for the **bowl potential** for which a preliminary Maple plot is displayed. The **Mehler-Fock Transform** is encountered. The potential is checked in various limiting cases such as the disk and large- r limit.

Section 3 addresses the problem of **two bowls** having a common but possibly insulated lip. Special cases of a bowl with a flat lid and a sessile droplet are considered.

Section 4 uses the bowl potential obtained in Section 2 to compute the **surface charge densities** on the two sides of the bowl. The results are compared with those of other workers including Kelvin. A quick look is taken at the case of a bowl with a very small opening. The limiting cases of a full sphere and flat disk are studied. The large- r limit is then examined to obtain the bowl **capacitance**.

Section 5 studies graphically the nature of the u and ξ toroidal coordinates.

Section 6 displays a selection of **bowl potential plots** for various bowl labels u_0 .

Section 7 discusses **Mehler integrals** and evaluates one as a detailed example. Some important integrals are stated but their derivations are relegated to Appendix L. The short list of available sources for Mehler integrals is reviewed and some errata in these sources are noted. The **Mehler functions** $P_{i\tau-1/2}(ch\xi)$ and $Q_{i\tau-1/2}(ch\xi)$ are then plotted in several ways to reveal their oscillatory nature. The notion of regional analytic continuation of functions is briefly addressed.

Section 8 evaluates the integral-form bowl potential into a relatively **simple expression** involving only elementary functions.

Section 9 describes the **Maple code** which plots the bowl potential.

Section 10 basically repeats all of the above for a **torus** instead of a bowl. Whereas the initial bowl potential is an integral over continuous variable τ , the **torus potential** is a sum of terms involving the discrete index n . The sums are generally reasonably convergent allowing for truncation. Maple code to plot the torus potential is presented and **plots** are shown. The torus **capacitance** is obtained, and the **surface charge density** is computed, checked in several limits, and plotted with more Maple code. Detailed discussion of the **thin-wire limit** and the **horn toroid limit** is presented in Appendix I.

Appendix Summaries

About half the content of this document is contained in the following set of appendices.

Appendix A contains copy-and-paste text **Maple code** for generating plots of the potential of a charged bowl and torus. The code is quite minimal.

Appendix B shows how to **convert** expressions from toroidal to cylindrical (and then Cartesian) coordinates, with application to the potential of a charged disk.

Appendix C reviews Lord **Kelvin's** approach to the charged bowl using the theory of inversion.

Appendix D summarizes a sequence of **Smythe** problems which use the theory of inversion to explore the properties of a charged bowl by first considering the Green's function of a conducting iris with a point charge located within the iris hole.

Appendix E presents a simple matrix theory for solving "**dual equations**". The theory is then applied to the charged disk in cylindrical coordinates and the charged bowl in spherical coordinates.

Appendix F states the generalized **Abel transforms** in several forms and comments on their connection to Legendre and Bessel functions.

Appendix G applies the dual equation matrix approach of Appendix E and the Abel transforms of Appendix F to find the bowl potential in spherical coordinates using a **double Abel transform**.

Appendix H contains **supporting** mathematical details that would further clutter the main text were they placed there. Equations are solved, integrals are evaluated, and limits are derived. Maple is often used to verify results.

Appendix I first examines the **thin-wire limit of a torus** and shows how capacitance lingers even as the wire is made extremely thin. In I.2 the theory of **series non-uniform convergence** is reviewed and applied to two simple series examples. Then in I.3 this theory is applied to determine the **capacitance of a horn torus** to 8 decimal places.

Appendix J reviews the general notion of a **transform**, and shows how the **Fourier Series Cosine Transform** fits into that framework. This last transform is then stated for the specific case that the transformed function is $f(x) = 1/\sqrt{a-b\cos x}$. This result is then used to state the free-space Green's function in cylindrical coordinates. Certain **sums of Q functions** that are needed in Appendix K are derived. The final section comments on the generalized **Mehler-Fock Transform**.

Appendix K does warmup integrations to compute the toroidal circumference and area using toroidal coordinates. The main act then is **integration of the toroidal charge density** σ to get the total torus charge Q and from that the capacitance C . This calculation is a check on result (10.5.10) for the torus surface charge density and makes use of the Q sums of Appendix J.

Appendix L derives a set of **six Mehler integrals**.

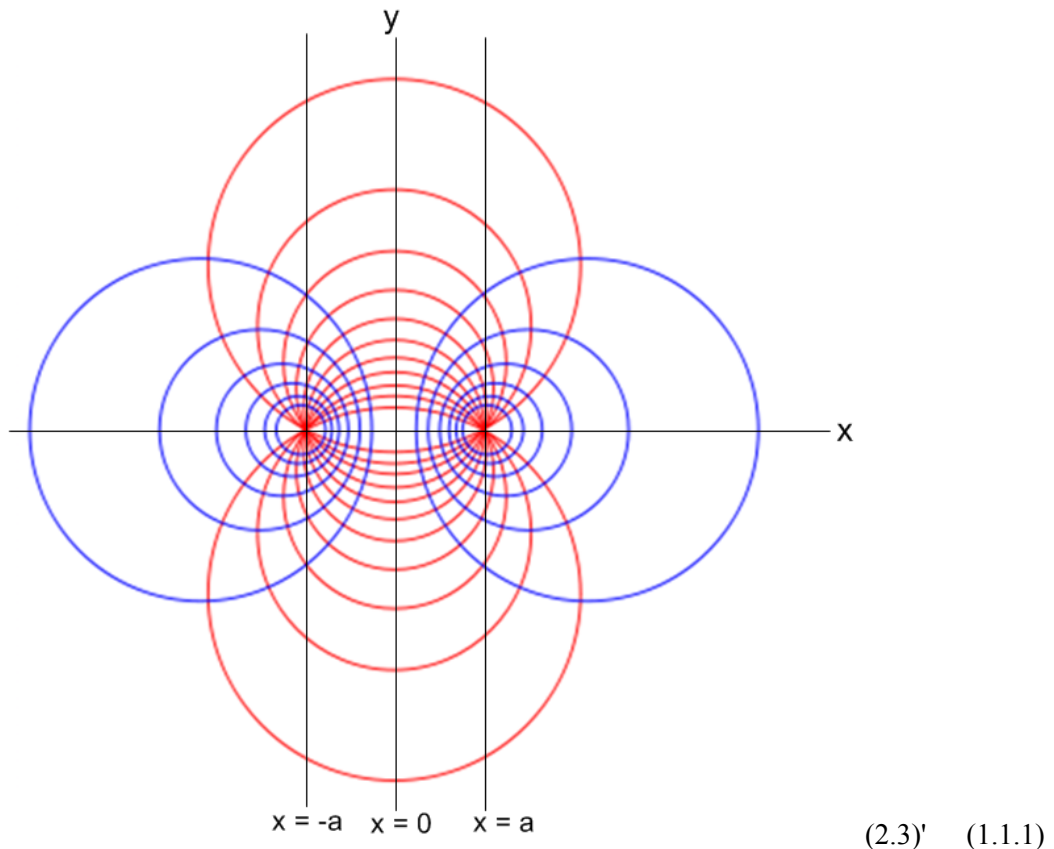
Appendix M examines the function $f(z) = \sqrt{a+\cos(z)}$ as an analytic mapping.

1. Bipolar and toroidal coordinates

1.1 Bipolar coordinates

To understand the toroidal coordinates ξ, u, φ , one must first understand bipolar coordinates ξ, u which form a 2D orthogonal coordinate system. These are described in detail in our monograph *Bipolar* (see Refs) from which we extract a brief summary. Equation numbers from *Bipolar* are shown with primes.

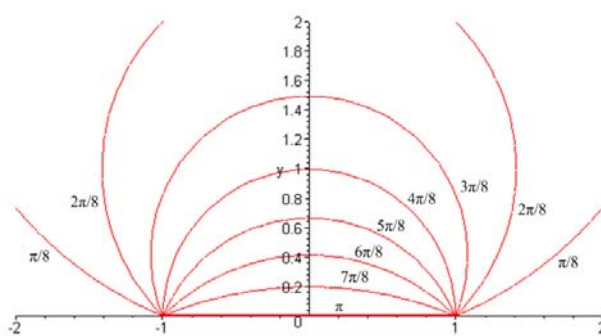
In the following drawing, the two "poles" of the bipolar system are located on the x-axis at points $x = \pm a$:



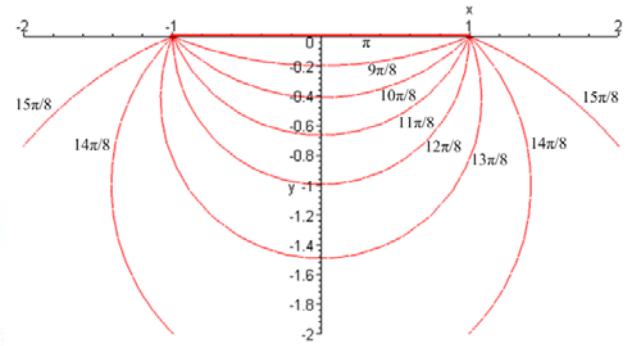
http://en.wikipedia.org/wiki/Toroidal_coordinates

The blue circles are loci of constant ξ while the *truncated* red circles are loci of constant u . The red circles are truncated at the x-axis.

The u parameter ranges from $u = 0$ to $u = 2\pi$ as indicated in these drawings



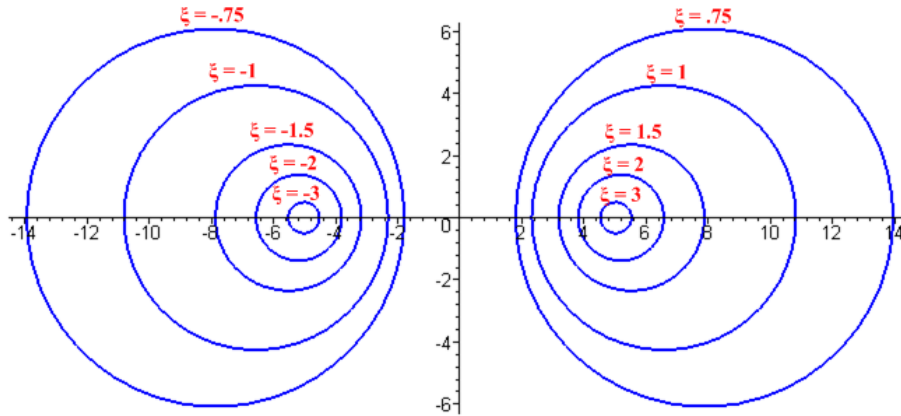
(2.8)' (a)



(2.9)' (b) (1.1.2)

As $u \rightarrow \pi$, the truncated circles approach a line segment between the two focal points. As $u \rightarrow 0$, the upper truncated circles get very large and approach the union of the half lines $(-\infty, -a)$ and (a, ∞) . As $u \rightarrow 2\pi$, the lower truncated circles approach this same union locus, but from below.

Meanwhile, here are some of the blue circles of constant ξ with labels,



(2.5)' (1.1.3)

As $\xi \rightarrow +\infty$, the blue circles contract around the right focal point. As $\xi \rightarrow -\infty$, they contract around the left focal point. As $\xi \rightarrow 0$, the circles become very large and approach the vertical axis.

There are many equations related to bipolar coordinates which are derived in *Bipolar* and which we just quote here:

$$-\infty \leq \xi \leq \infty \quad 0 \leq u \leq 2\pi \quad // \text{both } \xi \text{ and } u \text{ are dimensionless} \quad (2.1)' \quad (1.1.4)$$

$$\begin{aligned} x &= a \operatorname{sh}\xi / (\operatorname{ch}\xi - \cos u) && // \text{defining equations (forward transformation)} \\ y &= a \sin u / (\operatorname{ch}\xi - \cos u) && y/x = \sin u / \operatorname{sh}\xi \end{aligned} \quad (2.2)' \quad (1.1.5)$$

$$\begin{aligned} \xi &= \tanh^{-1} [2ax/(x^2 + y^2 + a^2)] && // \text{inverse transformation} \\ u &= \tan^{-1} [2ay/(x^2 + y^2 - a^2)] . \end{aligned} \quad (4.1)' \quad (1.1.6)$$

$$h_\xi = h_u = a / (\operatorname{ch}\xi - \cos u) \quad // \text{scale factors} \quad (3.3)' \quad (1.1.7)$$

$$x^2 + (y - y_c)^2 = R^2 \quad y_c = a / \tan u \quad R = a / |\sin u| \quad // \text{ red circles} \quad (2.6)' \quad (1.1.8)$$

$$(x - x_c)^2 + y^2 = R^2 \quad x_c = a / \operatorname{th} \xi \quad R = a / |\operatorname{sh} \xi| \quad // \text{ blue circles} \quad (2.4)' \quad (1.1.9)$$

The same symbol R is used above to indicate two unrelated radii.

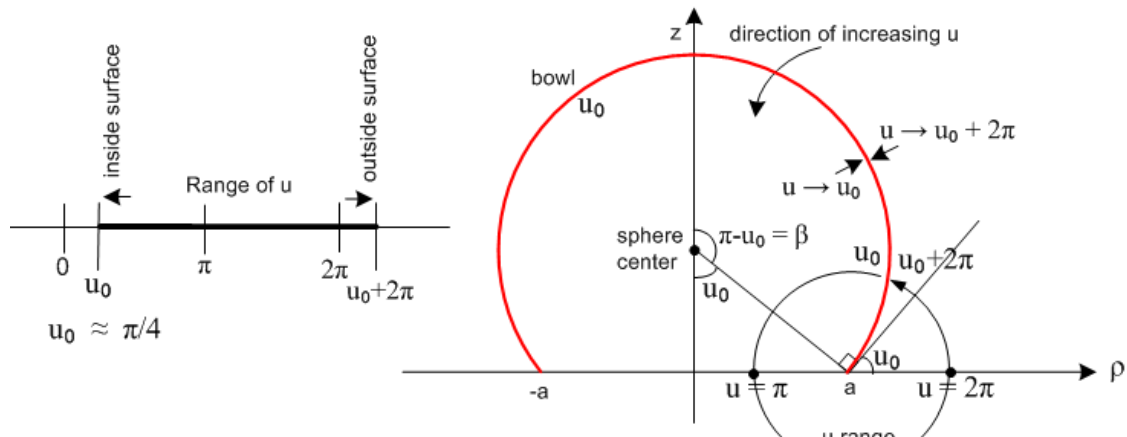
1.2 Toroidal coordinates

To form toroidal coordinates, we take just the right side of Fig (1.1.1) (which has $0 \leq \xi \leq \infty$) and we rotate it about the vertical axis. The red truncated circles become bowls, while the blue circles become tori. In making this change, we rename the vertical axis of Fig (1.1.1) to be z instead of y, and we rename the x axis to be $\rho = \sqrt{x^2 + y^2}$. Thus the symmetry axis is z. The new coordinate ϕ of (ξ, u, ϕ) is the azimuthal angle measured away from the positive x axis toward the positive y axis. The level surfaces in toroidal coordinates are thus tori, bowls and vertical half planes -- surfaces of constant ξ , u and ϕ .

With these 3D coordinates, the bowl limiting case $u = \pi$ is a flat disk of radius a in the $z=0$ plane. The case $u = 0$ and 2π is the entire $z=0$ plane with a hole of radius a in the center -- an iris. For the tori, as $\xi \rightarrow \infty$, a torus becomes an infinitely thin wire of radius $R = a / \operatorname{sh} \xi$ which forms a circle of radius a. As $\xi \rightarrow 0$, we get an extremely fat torus with no hole which fills all space. However, if we take $\xi \rightarrow 0$ and $a \rightarrow 0$ at the same time such that $a/\xi = R$, this fat torus becomes a degenerate or "horn" torus which is a torus of tube radius R whose hole has just vanished, as shown in Fig (I.3.4). We do not consider the self-intersecting "spindle torus" in this document.

Comment: A toroid with a circular cross section is a torus, so a torus is a toroid and tori are toroids.

When dealing with a bowl labeled by u_0 , it will be convenient to shift the range of u from $(0, 2\pi)$ to $(u_0, u_0 + 2\pi)$, as indicated in this drawing,



(1.2.1)

The drawing requires some explanation:

First of all, the red bowl is a surface of constant u , that is to say, $u = u_0$ on the entire red surface. So u_0 is the "label" for this particular (upside-down) bowl.

The drawing shows two geometric interpretations of the angle u_0 . First, u_0 is the polar angle of a point on the lip of the bowl, measured from the $-\hat{z}$ axis. Second, u_0 is the tangent angle which the bowl makes where it contacts the $z = 0$ plane.

The black circle schematically shows the range of u . It starts from u_0 on the inner surface and ends up at $u_0 + 2\pi$ on the outer surface.

With the u range convention adopted on the left of Fig (1.2.1), when studying the bowl with label u_0 the discontinuity in the u coordinate is placed right at the bowl surface and so u has "free range" out in the open, both inside and outside the bowl.

The two small facing arrows top right show how one approaches the surface of the bowl from the inside and from the outside, while the curved arrow nearby shows the direction in which u increases, consistent with the left side of Fig (1.1.2). Approaching a point on the bowl from the inside means we are doing $\varepsilon \rightarrow 0$ with $u = u_0 + \varepsilon$, as indicated by the left-pointing arrow in the range picture on the left. On the other hand, approaching a point on the bowl from the outside means we are doing $\varepsilon \rightarrow 0$ with $u = u_0 + 2\pi - \varepsilon$, and this is suggested by the other small arrow. We will use these two limits later to specify boundary conditions for the electrostatic potential on the two sides of the bowl surface.

The defining equations for toroidal coordinates are these :

$$\begin{aligned} x &= a \cos\phi \operatorname{sh}\xi / (\operatorname{ch}\xi - \cos u) & \rho &= a \operatorname{sh}\xi / (\operatorname{ch}\xi - \cos u) = \sqrt{x^2 + y^2} \\ y &= a \sin\phi \operatorname{sh}\xi / (\operatorname{ch}\xi - \cos u) & z/\rho &= \sin u / \operatorname{sh}\xi \quad 0 \leq \phi \leq 2\pi \\ z &= a \sin u / (\operatorname{ch}\xi - \cos u) & 0 \leq \xi \leq \infty, 0 \leq u \leq 2\pi \text{ (or } u_0 \leq u \leq u_0 + 2\pi\text{)} . \end{aligned} \quad (1.2.2)$$

From the relation $z/\rho = \sin u / \operatorname{sh}\xi$ we see that $\xi = 0$ corresponds to points on the z axis where $\rho = 0$.

Metric Tensor

From equations (1.2.2), one may construct the metric tensor for toroidal coordinates using the method outlined in *Bipolar* Section 12. Here is Maple code which does the task. We start by entering the coordinate names and the above equations,

```

xp[1] := xi;
xp1 :=  $\xi$ 
xp[2] := u;
xp2 :=  $u$ 
xp[3] := phi;
xp3 :=  $\phi$ 
x[1] := a * cos(xp[3]) * sinh(xp[1]) / (cosh(xp[1]) - cos(xp[2]));
x1 :=  $\frac{a \cos(\phi) \sinh(\xi)}{\cosh(\xi) - \cos(u)}$ 
x[2] := a * sin(xp[3]) * sinh(xp[1]) / (cosh(xp[1]) - cos(xp[2]));
x2 :=  $\frac{a \sin(\phi) \sinh(\xi)}{\cosh(\xi) - \cos(u)}$ 
x[3] := a * sin(xp[2]) / (cosh(xp[1]) - cos(xp[2]));
x3 :=  $\frac{a \sin(u)}{\cosh(\xi) - \cos(u)}$ 

```

The notation x_p means x' , with the idea that $(\xi, u, \phi) = (x'_1, x'_2, x'_3) = x'$. Writing $\mathbf{x} = (x, y, z)$, the toroidal defining equations may be interpreted as $\mathbf{x} = \mathbf{F}^{-1}(x')$ where $\mathbf{x}' = \mathbf{F}(\mathbf{x})$ is a non-linear but invertible transformation from Cartesian x -space to curvilinear x' -space. The transformation has a differential matrix S where $S_{ij}(x') \equiv (\partial x_i / \partial x'_j)$, which we now compute,

```
s_ := (i,j) -> diff(x[i],xp[j]);
```

$$S_{ij} := (i,j) \rightarrow \frac{\partial}{\partial x' j} x_i$$

```
S := matrix(3,3,s_); simplify(%);
```

$$\begin{bmatrix} -\frac{a \cos(\phi) (\cosh(\xi) \cos(u) - 1)}{\cosh(\xi)^2 - 2 \cosh(\xi) \cos(u) + \cos(u)^2} & -\frac{a \cos(\phi) \sinh(\xi) \sin(u)}{\cosh(\xi)^2 - 2 \cosh(\xi) \cos(u) + \cos(u)^2} & \frac{a \sin(\phi) \sinh(\xi)}{\cosh(\xi) - \cos(u)} \\ -\frac{a \sin(\phi) (\cosh(\xi) \cos(u) - 1)}{\cosh(\xi)^2 - 2 \cosh(\xi) \cos(u) + \cos(u)^2} & -\frac{a \sin(\phi) \sinh(\xi) \sin(u)}{\cosh(\xi)^2 - 2 \cosh(\xi) \cos(u) + \cos(u)^2} & \frac{a \cos(\phi) \sinh(\xi)}{\cosh(\xi) - \cos(u)} \\ -\frac{a \sin(u) \sinh(\xi)}{\cosh(\xi)^2 - 2 \cosh(\xi) \cos(u) + \cos(u)^2} & \frac{a (\cosh(\xi) \cos(u) - 1)}{\cosh(\xi)^2 - 2 \cosh(\xi) \cos(u) + \cos(u)^2} & 0 \end{bmatrix}$$

The metric tensor in x' -space (the space of the toroidal coordinates) is $\bar{g}' = S^T S$ which we compute next,

```
gp := evalm(transpose(S) &* S); simplify(%);
```

$$\begin{bmatrix} \frac{a^2}{\cosh(\xi)^2 - 2 \cosh(\xi) \cos(u) + \cos(u)^2} & 0 & 0 \\ 0 & \frac{a^2}{\cosh(\xi)^2 - 2 \cosh(\xi) \cos(u) + \cos(u)^2} & 0 \\ 0 & 0 & \frac{a^2 (\cosh(\xi)^2 - 1)}{\cosh(\xi)^2 - 2 \cosh(\xi) \cos(u) + \cos(u)^2} \end{bmatrix}$$

The metric tensor is diagonal, indicating that toroidal coordinates form an orthogonal coordinate system. The diagonal elements are the squares of the scale factors h_ξ , h_u and h_ϕ . We then read off from the above,

$$h_\xi = h_u = a / (\cosh \xi - \cos u) \quad h_\phi = a \operatorname{sh} \xi / (\cosh \xi - \cos u) \quad . \quad (1.2.3)$$

For more details on this subject, see the author's *Tensor Analysis* document where $\bar{g}' = S^T S$ appears as (5.7.9). The overbar on \bar{g}' indicates that \bar{g}' is the covariant metric tensor, whereas g' is the contravariant one (in all-indices-down notation).

Inverse equations

To find the inverse of the toroidal defining equations (1.2.2) we start with two of those equations,

$$\begin{aligned} \rho &= a \operatorname{sh} \xi / (\cosh \xi - \cos u) \\ z &= a \sin u / (\cosh \xi - \cos u) \end{aligned} \quad . \quad (1.2.2)$$

Since this is just (1.1.5) with $x \rightarrow \rho$ and $y \rightarrow z$, we read off from (1.1.6) that

$$\begin{aligned}\xi &= \tanh^{-1}[2a\rho/(\rho^2 + z^2 + a^2)] \\ u &= \tan^{-1}[2az/(\rho^2 + z^2 - a^2)] .\end{aligned}\quad (1.2.4)$$

From the definition of φ we know that $x = \rho \cos \varphi$ and $y = \rho \sin \varphi$, so $\varphi = \tan^{-1}(y/x)$. Therefore, the inverse transformation of the toroidal defining equations is as follows

$$\begin{aligned}\xi &= \tanh^{-1}[2a\rho/(\rho^2 + z^2 + a^2)] & \rho &= \sqrt{x^2 + y^2} \\ u &= \tan^{-1}[2az/(\rho^2 + z^2 - a^2)] \\ \varphi &= \tan^{-1}(y/x)\end{aligned}\quad (1.2.5)$$

and this is the transformation $\mathbf{x}' = \mathbf{F}(\mathbf{x})$ alluded to above where $\mathbf{x}' = (\xi, u, \varphi)$ and $\mathbf{x} = (x, y, z)$. Here \tan^{-1} returns a value in the range $0, 2\pi$ and will be called arctan2Pi later in this document.

Equations of bowls and tori

The bowls are formed as surfaces of revolution of the red truncated circles in Fig (1.1.2).

The equation describing the sphere on which the bowl of label u_0 in Fig (1.2.1) lies is, from (1.1.8),

$$\text{sphere: } \rho^2 + (z - z_c)^2 = R^2 \quad z_c = a / \tan u_0 \quad R = a / |\sin u_0| \quad \rho = \sqrt{x^2 + y^2} . \quad (1.2.6)$$

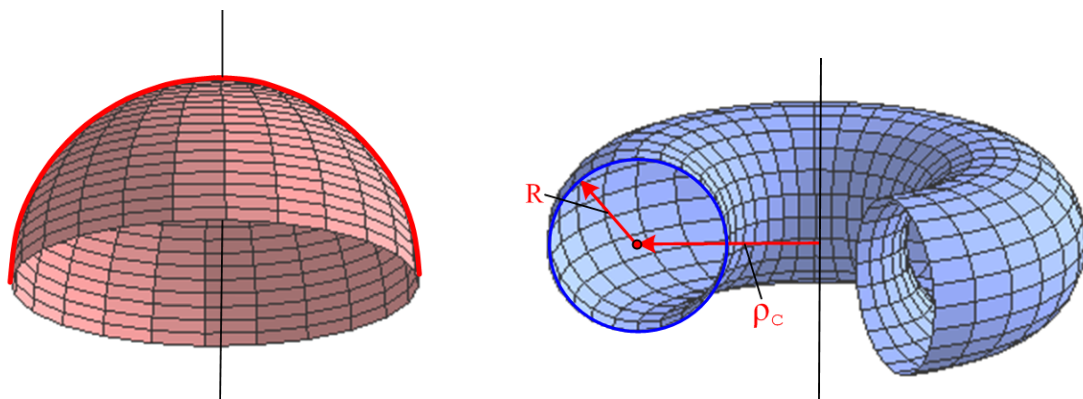
The tori are formed as surfaces of revolution of the blue circles on the right side of Fig (1.1.3).

The equation describing the toroidal surface of label ξ_0 is, from (1.1.9),

$$\text{torus: } (\rho - \rho_c)^2 + z^2 = R_t^2 \quad \rho_c = a / \operatorname{th} \xi_0 \quad R = a / \operatorname{sh} \xi_0 \quad \rho = \sqrt{x^2 + y^2} . \quad (1.2.7)$$

The tube center is located distance ρ_c from the z symmetry axis, and the tube radius is R .

Below are Maple plots of a bowl with $u_0 = \pi/2$ and a partial torus with $\rho_c = 2$ and $R = 1$. For this plot we see from (1.2.7) that $\operatorname{ch} \xi_0 = \rho_c/R$ so $\xi_0 = \operatorname{ch}^{-1}(\rho_c/R) = \operatorname{ch}^{-1}(2/1) \approx 1.3$.



The r coordinate and the large-r region

Finally, from (1.2.2) one can develop an expression for the spherical coordinate r as follows:

$$\begin{aligned} r^2 &= \rho^2 + z^2 = a^2 \operatorname{sh}^2 \xi / (\operatorname{ch} \xi - \cos u)^2 + a^2 \sin^2 u / (\operatorname{ch} \xi - \cos u)^2 \\ &= a^2 (\operatorname{sh}^2 \xi + \sin^2 u) / (\operatorname{ch} \xi - \cos u)^2 \end{aligned}$$

so

$$r = a \sqrt{\operatorname{sh}^2 \xi + \sin^2 u} / (\operatorname{ch} \xi - \cos u) . \quad (1.2.8)$$

From this equation, one can see that the limit $r \rightarrow \infty$ is reached when $\xi \rightarrow 0$ and $u \rightarrow 2\pi^*$ integer, because the denominator then goes to 0. Since for the bowl we require $u_0 < u < u_0 + 2\pi$, we must select u near 2π as the region of interest for large r .

Fact: The region of (ξ, u) space that corresponds to large r (in spherical coordinates) is that region where ξ is small, and where u is near 2π . (1.2.9)

To be more precise, define small ϵ by

$$u = 2\pi + \epsilon . \quad // \epsilon \text{ could have either sign} \quad (1.2.10)$$

Then in the region of large r we have u close to 2π and ξ small, so

$$\begin{aligned} \cos u &= \cos \epsilon \approx 1 - \epsilon^2/2 & \sin u &= \sin(2\pi + \epsilon) = \sin \epsilon \approx \epsilon \\ \sqrt{\operatorname{sh}^2 \xi + \sin^2 u} &\approx \sqrt{\xi^2 + \epsilon^2} \\ \operatorname{ch} \xi - \cos u &\approx (1 + \xi^2/2) - (1 - \epsilon^2/2) = (\xi^2 + \epsilon^2)/2 . \end{aligned} \quad (1.2.11)$$

Then from (1.2.8),

$$r = a \sqrt{\operatorname{sh}^2 \xi + \sin^2 u} / (\operatorname{ch} \xi - \cos u) \approx a \sqrt{\xi^2 + \epsilon^2} / [(\xi^2 + \epsilon^2)/2] = 2a/\sqrt{\xi^2 + \epsilon^2} . \quad (1.2.12)$$

From (1.2.2) one can relate small ξ to small ϵ in this way,

$$\rho/z = \operatorname{sh} \xi / \sin u \approx \xi / \epsilon \Rightarrow \xi = (\rho/z)\epsilon \quad (1.2.13)$$

so one can write things in terms of a single smallness parameter ϵ ,

$$\xi^2 + \epsilon^2 = [1 + (\rho/z)^2]\epsilon^2 \Rightarrow \sqrt{\xi^2 + \epsilon^2} = \sqrt{1 + \rho^2/z^2} \epsilon . \quad (1.2.14)$$

Therefore,

$$r \approx 2a/\sqrt{\xi^2 + \varepsilon^2} = [2a/\sqrt{1+\rho^2/z^2}] (1/\varepsilon)$$

$$(1/r) \approx \sqrt{\xi^2 + \varepsilon^2}/2a = [\sqrt{1+\rho^2/z^2}/2a] \varepsilon \quad \varepsilon = (u-2\pi) \quad (1.2.15)$$

Finally, from (1.2.11) and (1.2.12),

$$\sqrt{ch\xi - cosu} \approx \sqrt{(\xi^2 + \varepsilon^2)/2} = (1/\sqrt{2}) \sqrt{\xi^2 + \varepsilon^2} = (1/\sqrt{2})(2a/r) = \sqrt{2} a/r. \quad (1.2.16)$$

We now collect the above results in one place:

Toroidal Coordinates (1.2.17)

$x = a \cos\phi \operatorname{sh}\xi / (\operatorname{ch}\xi - \cos u)$	$\rho = a \operatorname{sh}\xi / (\operatorname{ch}\xi - \cos u) = \sqrt{x^2 + y^2}$
$y = a \sin\phi \operatorname{sh}\xi / (\operatorname{ch}\xi - \cos u)$	$z/\rho = \sin u / \operatorname{sh}\xi$
$z = a \sin u / (\operatorname{ch}\xi - \cos u)$	$0 \leq \xi \leq \infty, 0 \leq u \leq 4\pi, 0 \leq \phi \leq 2\pi$

(1.2.2)

$$h_\xi = h_u = a / (\operatorname{ch}\xi - \cos u) \quad h_\phi = a \operatorname{sh}\xi / (\operatorname{ch}\xi - \cos u) \quad (1.2.3)$$

$\xi = \tanh^{-1}[2ap/(\rho^2 + z^2 + a^2)]$	$\rho = \sqrt{x^2 + y^2}$
$u = \tan^{-1}[2az/(\rho^2 + z^2 - a^2)]$	
$\phi = \tan^{-1}(y/x)$	$\xi = 0 \leftrightarrow \rho = 0$ (the z axis)

(1.2.5)

$$\text{sphere: } \rho^2 + (z - z_c)^2 = R^2 \quad z_c = a / \tan u_0 \quad R = a / |\sin u_0| \quad \rho = \sqrt{x^2 + y^2}. \quad (1.2.6)$$

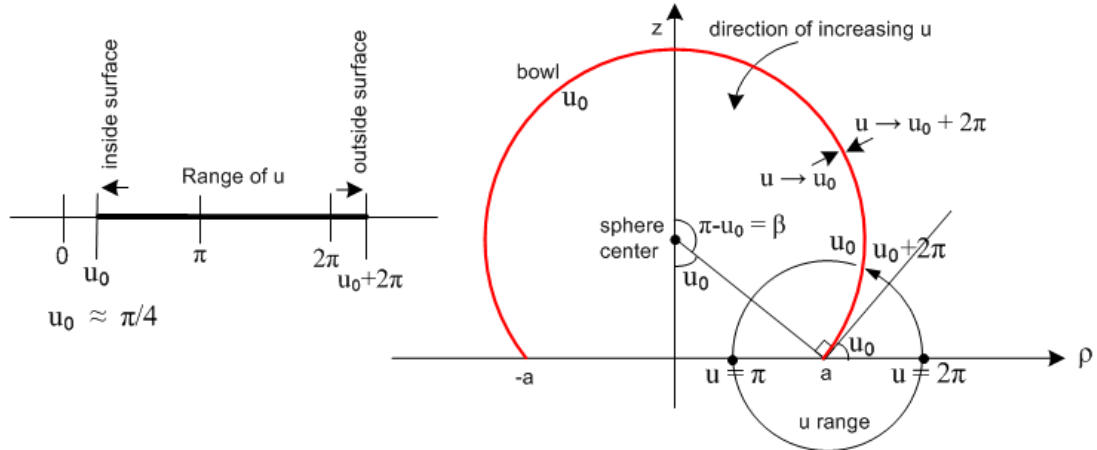
$$\text{torus: } (\rho - \rho_c)^2 + z^2 = R^2 \quad \rho_c = a / \operatorname{th}\xi \quad R = a / \operatorname{sh}\xi \quad \rho = \sqrt{x^2 + y^2}. \quad (1.2.7)$$

$$r = a \sqrt{\operatorname{sh}^2 \xi + \sin^2 u} / (\operatorname{ch}\xi - \cos u). \quad // \text{spherical coordinate } r \quad (1.2.8)$$

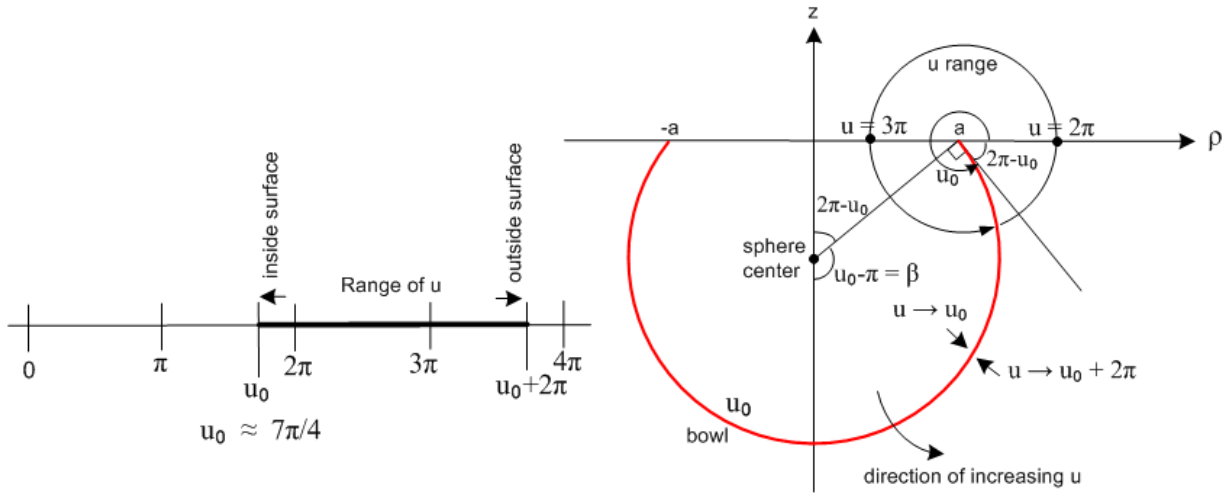
$$(1/r) \approx [\sqrt{1+\rho^2/z^2}/2a] \varepsilon \quad \text{with } \varepsilon = u-2\pi \quad // \text{large } r \quad (1.2.15)$$

$$\sqrt{ch\xi - cosu} \approx \sqrt{2} a/r \quad // \text{large } r \quad (1.2.16)$$

The first drawing below is a repeat of (1.2.1) showing a bowl for $u_0 < \pi$. The second drawing shows a corresponding bowl which has $u_0 > \pi$. In both cases the u range is $u_0 \leq u \leq u_0 + 2\pi$. In both cases we denote by β the polar angle from the bowl base to the bowl lip.



(1.2.18a)



(1.2.18b)

2. The charged bowl potential in toroidal coordinates

2.1 Level curves, the charged ellipsoid problem and a dashed hope

As one sees scanning through the beautiful pictures in Moon & Spencer's strangely but correctly named *Field Theory Handbook*, each orthogonal coordinate system has its characteristic level surfaces. In spherical coordinates these are spheres, polar cones and azimuthal half-planes, whereas in toroidal coordinates they are bowls and tori and azimuthal half-planes as seen above. In spherical coordinates a bowl has a hole in it since the polar angle runs only part of its range, but in toroidal coordinates there is no such "hole". That is to say, a bowl has a label u_0 (a value of one of the toroidal coordinates u) and as the other two coordinates sweep their *full ranges*, a bowl is swept out. The fact that the bowl is a level surface in toroidal coordinates makes one interested in solving the charged bowl problem in this system.

In ellipsoidal coordinates the level surfaces are ellipsoids and asymmetric hyperboloids of one and two sheets, which certainly sounds foreboding. One can solve the "charged ellipsoid problem" and the result is shockingly simple (as Kelvin also showed) and σ on the ellipsoid is simple even in Cartesian coordinates (more magic geometry). A family of confocal ellipsoids can be described by the equation $x^2/(\xi_1^2 - a^2) + y^2/(\xi_1^2 - b^2) + z^2/(\xi_1^2) = 1$ where ξ_1 in $(0, \infty)$ is the "label" of an ellipsoid. It happens then that the label ξ_1 is also the largest semi-major axis of the ellipsoid, while $a > b$ are focal distances associated with the other two axes. Ellipsoidal coordinates are fully separable, and a Laplace-satisfying potential function which is constant on each of these ellipsoids and which vanishes at infinity is given by

$$\begin{aligned} V(\xi_1)/\text{const} &= F_0^0(\xi_1) E_0^0(\xi_2) E_0^0(\xi_3) = [(1/a) \operatorname{sn}^{-1}(a/\xi_1, b/a)] * 1 * 1 = (1/a) \operatorname{sn}^{-1}(a/\xi_1, b/a) \\ &= (1/a) F(\sin^{-1}(a/\xi_1), b/a) . \end{aligned} \quad (2.1.1)$$

Here (ξ_1, ξ_2, ξ_3) are the three ellipsoidal coordinates in Morse & Feshbach notation, E and F are first and second kind Lamé functions, and a different F is the first kind elliptic integral. By setting $V = V_0$ on a *particular* ellipsoid $\xi_1 = c$, one then obtains the potential anywhere outside this charged ellipsoid,

$$V(\xi_1) = V_0 F(\sin^{-1}(a/\xi_1), k=b/a) / F(\sin^{-1}(a/c), k=b/a) . \quad (2.1.2)$$

Although not immediately obvious, this expression is exactly the same if one swaps $a \leftrightarrow b$ and such a swap is necessary to show that the above form agrees with that of Kelvin. [There is some confusion in elliptic F notation to beware: $F(\phi, k) = F(\phi | k^2) = F(\phi \setminus \sin^{-1}k)$, the first notation being that of GR7 8.111.2.]

One might *hope* that the bowl potential in toroidal coordinates could be as simply stated as the ellipsoid potential in ellipsoidal coordinates, but alas it is not so, but only in the following sense. In toroidal coordinates a certain weight factor cross-links the bowl and torus coordinates (labels), which makes the Laplace equation separable only in the form of three separated functions times the weight factor $\sqrt{\operatorname{ch}\xi \cdot \cos u}$, where ξ is a torus label and u a bowl label. This weaker kind of separability is called R-separability by Moon and Spencer. A solution $\sqrt{\operatorname{ch}\xi \cdot \cos u} [A(\xi)=1]B(u)[C(\phi)=1]$ evaluated on the surface of bowl u_0 gives $V = \sqrt{\operatorname{ch}\xi \cdot \cos u_0} B(u_0)$ which varies with ξ , not allowing $V = V_0$ on the bowl. *Nevertheless*, it will turn out that the charged bowl potential can be expressed in simple inverse trig functions, and is in that sense even simpler than the charged ellipsoid potential.

2.2 Cartesian, spherical, toroidal and ellipsoidal atomic forms

"Atomic forms" or just "atoms" are the author's private phrases for "harmonics", which word means simple solutions of the Laplace equation which can be superposed to construct non-simple solutions. The Cartesian atoms illustrate the idea that if you curve toward axis in 2 dimensions, you must curve away from axis in the 3rd:

$$(1) \begin{array}{ccc} \text{osc} & \text{osc} & \text{expo} \\ [\sin(k_x x), \cos(k_x x)], [\sin(k_y y), \cos(k_y y)], [\exp(k_z z), \exp(-k_z z)] \\ \text{toward} & \text{toward} & \text{away} \end{array} \quad k_z = \text{imaginary} = ik_z \quad k_z = \sqrt{k_x^2 + k_y^2} \quad (2.2.1)$$

For solving practical 3D problems, two of the three coordinates have to be oscillatory to allow for functional completeness (above on a surface of x and y) so that expansions can be inverted and problems solved. For spherical atoms, two interesting atomic forms can be written in which azimuthal ϕ is oscillatory:

$$\begin{aligned} & r \text{ in } (0, \infty) \quad z \text{ in } (-1, 1) \quad \phi \text{ in } (0, 2\pi) \\ (1) \quad & \begin{array}{ccc} \text{expo} & \text{osc} & \text{osc} \\ [r^n, r^{-n-1}] [P_n^m(z), Q_n^m(z)] [\sin(m\phi), \cos(m\phi)] \end{array} \quad z = \cos\theta \\ (2) \quad & \begin{array}{ccc} \text{osc} & \text{expo} & \text{osc} \\ (1/\sqrt{r}) [r^{i\tau}, r^{-i\tau}] [P_{i\tau-1/2}^m(z), Q_{i\tau-1/2}^m(z)] [\sin(m\phi), \cos(m\phi)] \end{array} \quad n = i\tau - 1/2 \\ & \sim (1/\sqrt{r}) [\sin(\tau \ln r), \cos(\tau \ln r)] [P_{i\tau-1/2}^m(z), Q_{i\tau-1/2}^m(z)] [\sin(m\phi), \cos(m\phi)] . \end{aligned} \quad (2.2.2)$$

The first is doubtless more familiar to the reader, but the second is appropriate for, say, a Dirichlet problem involving a cone, since the atomic form is oscillatory both ways across the surface of a cone, allowing a prescribed potential there to be inverted. The underlying fact is that each oscillatory coordinate becomes a 1D Sturm-Liouville problem with a complete set of eigenfunctions (see Appendix J.1), and then these two sets provide a complete set of eigenfunctions for a 2D surface spanned by those coordinates. In passing, we note that the Legendre functions in form (2) above are called **conical functions** and have $|z|<1$.

Without further ado, we can write two similar atomic forms for toroidal coordinates,

$$\begin{aligned} & \xi \text{ in } (0, \infty) \quad u \text{ in } (0, 2\pi) \quad \phi \text{ in } (0, 2\pi) \\ (1) \quad & \begin{array}{ccc} \text{expo} & \text{osc} & \text{osc} \\ \sqrt{\text{ch}\xi - \cos u} [P_{n-1/2}^m(\text{ch}\xi), Q_{n-1/2}^m(\text{ch}\xi)] [\sin(nu), \cos(nu)] [\sin(m\phi), \cos(m\phi)] \end{array} \\ (2) \quad & \begin{array}{ccc} \text{osc} & \text{expo} & \text{osc} \\ \sqrt{\text{ch}\xi - \cos u} [P_{i\tau-1/2}^m(\text{ch}\xi), Q_{i\tau-1/2}^m(\text{ch}\xi)] [\exp(tu), \exp(-tu)] [\sin(m\phi), \cos(m\phi)] \end{array} . \end{aligned} \quad (2.2.3)$$

To solve bowl problems, we need the two coordinates other than the bowl label u to be oscillatory, and that means we must use form (2). To solve torus problems, we need the two coordinates other than the torus label ξ to be oscillatory, and that means we must use form (1).

In form (1), if a problem has a full azimuth, the parameter m gets quantized to integers, and this indirectly causes parameter n on $P_{n-1/2}^m(ch\xi)$ to be quantized to integers, so the spectra of both Sturm-Liouville problems are discrete. In form (2) even if m is quantized, parameter τ remains unquantized and, since $P_v = P_{-v-1}$, the τ spectrum can be restricted to the positive real axis (see Appendix J.5).

The Legendre functions in system (1) are called **toroidal functions or ring functions**, argument $z = ch\xi > 1$, whereas those appearing in (2) are called **Mehler functions** with argument $z = ch\xi > 1$.

In reference to our earlier charged ellipsoid comments, we just mention the atomic form for ellipsoidal coordinates,

$$[E_m^P(\xi_1), F_m^P(\xi_1)] [E_m^P(\xi_2), F_m^P(\xi_2)] [E_m^P(\xi_3), F_m^P(\xi_3)] \quad (2.2.4)$$

where $0 < \xi_3 < b < \xi_2 < a < \xi_1$ with $a > b$ the confocal ellipsoid focal distances. As noted earlier, E and F are the first and second kind Lamé functions. The ξ_i are the three roots of the cubic equation which is the equation of the ellipsoid given above. In this system there is no azimuthal coordinate, and the separated solutions are triply cross-linked in that all three functions bear the same quantum numbers m and p (separation constants arising when the Laplace equation is separated). This system, though quite complicated, is well explained in full detail in the last chapter of Hobson's classic 1931 book.

2.3 Smythian forms and one for the bowl

Please forgive the author's predilection for strange phrases. A Smythian form refers to a linear combination (sum and/or integral) of atomic forms, having some to-be-determined "coefficients", which provides a candidate solution to some problem. Such a form usually "builds in" certain boundary conditions, such as continuity between two regions of space on whose boundary a Green's point charge lies in a Green's Function problem. Smythe's book makes excellent use of such forms, and one might even refer to "the method of Smythian forms" in a list of effective methods of solving boundary value problems.

So based on (2.2.3) we propose the following Smythian form for the potential of a charged bowl (since things are azimuthally symmetric, we have only $m = 0$ atoms),

$$V(\xi, u) = \sqrt{ch\xi - cosu} \int_0^\infty dt P_{i\tau-1/2}(ch\xi) [A(\tau)ch(u\tau) + B(\tau)sh(u\tau)], \quad (2.3.1)$$

where A and B are to-be-determined coefficient functions.

Why do we reject the $Q_{i\tau-1/2}(ch\xi)$ atom? From box (1.2.17) we note that $\xi = 0$ corresponds to the z axis, where we expect the potential to be finite and smooth. But $Q_v(x) \sim \ln(x-1)$ as $x \rightarrow 1$, so the function $Q_v(ch\xi) \sim \ln(ch\xi-1) \approx \ln(\xi^2/2)$ for small ξ is singular at $\xi = 0$. The leading factor provides no rescue since $\sqrt{ch\xi - cosu} \rightarrow \sqrt{1 - cosu_0}$ which is just some finite number.

Since the Mehler P functions form a complete orthogonal set for ξ in $(0, \infty)$, it is possible to set in some prescribed potential $V = f(\xi, u_0)$ on the surface of a bowl, and invert to find the coefficient functions. At first it seems odd that there are two functions A and B to be found, and only one boundary condition, but the dilemma is quickly resolved by realizing that we apply the boundary condition separately on each surface of the bowl, so really there are two boundary conditions and two unknown coefficient functions. For our charged bowl problem, the prescribed Dirichlet potential is $f(\xi, u_0) = V_0 = \text{a constant}$.

2.4 Solution to the charged bowl potential problem: the Mehler-Fock Transform

The generalized Mehler-Fock (Mehler-Fok) transform (Oberhettinger and Higgins page 2 or NIST 14.20.11,12 p 373) is this,

$$\begin{aligned} g(y) &= \int_0^\infty d\tau P_{i\tau-1/2}^{\mu}(y) f(\tau) && // \text{expansion} \\ f(\tau) &= (\tau/\pi) \operatorname{sh}(\pi\tau) \Gamma(1/2-\mu+i\tau) \Gamma(1/2-\mu-i\tau) \int_1^\infty dy P_{i\tau-1/2}^{\mu}(y) g(y) && // \text{projection} \end{aligned} \quad (2.4.1)$$

and for $\mu = 0$, using $\Gamma(1/2+i\tau)\Gamma(1/2-i\tau) = \pi/\cosh(\pi\tau)$, one obtains the regular Mehler-Fock transform,

$$\begin{aligned} g(y) &= \int_0^\infty d\tau P_{i\tau-1/2}(y) f(\tau) && // \text{expansion} \\ f(\tau) &= \tau \operatorname{th}(\pi\tau) \int_1^\infty dy P_{i\tau-1/2}(y) g(y) && // \text{projection} \end{aligned} \quad (2.4.2)$$

(Oberhettinger and Higgins page 1) which can also be written

$$\begin{aligned} G(\xi) &= \int_0^\infty d\tau P_{i\tau-1/2}(\operatorname{ch}\xi) f(\tau) && // \text{expansion} \\ f(\tau) &= \tau \operatorname{th}(\pi\tau) \int_0^\infty d\xi \operatorname{sh}\xi P_{i\tau-1/2}(\operatorname{ch}\xi) G(\xi) . && // \text{projection} \end{aligned} \quad (2.4.3)$$

For azimuthally symmetric bowl problems, this transform is the one associated with the Sturm Liouville problem in the ξ coordinate. Every reasonable Sturm-Liouville problem defines a complete set of functions and therefore defines a transform (there are thousands of them), and this happens to be the transform for our oscillatory ξ coordinate. Admittedly, this transform is more sparsely found in the literature than, say, the Fourier Integral Cosine Transform. See Appendix J.1 for a general review of transforms and J.5 for comments on the Mehler-Fock transform.

It is convenient to define $u_0' \equiv u_0 + 2\pi$ and to note then that $\cos(u_0') = \cos(u_0)$. Here then are the two boundary conditions on the Smythian form (2.3.1) evaluated at the inner and outer surface of the bowl, as was discussed below Fig (1.2.1),

$$\begin{aligned} V_0 &= \sqrt{\operatorname{ch}\xi - \cos u_0} \int_0^\infty d\tau P_{i\tau-1/2}(\operatorname{ch}\xi) [A(\tau)\operatorname{ch}(u_0\tau) + B(\tau)\operatorname{sh}(u_0\tau)] \quad u'_0 \equiv u_0 + 2\pi \\ V_0 &= \sqrt{\operatorname{ch}\xi - \cos u_0} \int_0^\infty d\tau P_{i\tau-1/2}(\operatorname{ch}\xi) [A(\tau)\operatorname{ch}(u'_0\tau) + B(\tau)\operatorname{sh}(u'_0\tau)] \end{aligned} \quad (2.4.4)$$

where $\cos u'_0 = \cos u_0$ in the leading factor. We now apply the Mehler-Fock transform (2.4.3) with

$$\begin{aligned} G(\xi) &= V_0 / \sqrt{\operatorname{ch}\xi - \cos u_0} \quad \text{and} \quad f(\tau) = [A(\tau)\operatorname{ch}(u_0\tau) + B(\tau)\operatorname{sh}(u_0\tau)] \\ G(\xi) &= V_0 / \sqrt{\operatorname{ch}\xi - \cos u_0} \quad \text{and} \quad f(\tau) = [A(\tau)\operatorname{ch}(u'_0\tau) + B(\tau)\operatorname{sh}(u'_0\tau)] \end{aligned} \quad (2.4.5)$$

which allows us to invert (2.4.4) for the coefficient functions,

$$\begin{aligned} [A(\tau)\operatorname{ch}(u_0\tau) + B(\tau)\operatorname{sh}(u_0\tau)] &= V_0 \tau \operatorname{th}(\pi\tau) \int_0^\infty d\xi \operatorname{sh}(\xi) P_{i\tau-1/2}(\operatorname{ch}\xi) / \sqrt{\operatorname{ch}\xi - \cos u_0} \\ [A(\tau)\operatorname{ch}(u'_0\tau) + B(\tau)\operatorname{sh}(u'_0\tau)] &= V_0 \tau \operatorname{th}(\pi\tau) \int_0^\infty d\xi \operatorname{sh}(\xi) P_{i\tau-1/2}(\operatorname{ch}\xi) / \sqrt{\operatorname{ch}\xi - \cos u_0} . \end{aligned} \quad (2.4.6)$$

Notice that these two equations have identical right hand sides. In (H.2.1) we derive the following integral,

$$\int_1^\infty dx P_{i\tau-1/2}(x) / \sqrt{x - \cos u_0} = \sqrt{2} \operatorname{ch}[\tau(u_0 - \pi)] / (\tau \operatorname{sh}(\pi\tau)) \quad 0 \leq u_0 \leq 2\pi . \quad (2.4.7)$$

Setting $x = \operatorname{ch}\xi$ ($dx = \operatorname{sh}\xi d\xi$) this may be restated as,

$$\int_0^\infty d\xi \operatorname{sh}(\xi) P_{i\tau-1/2}(\operatorname{ch}\xi) / \sqrt{\operatorname{ch}\xi - \cos u_0} = \sqrt{2} \operatorname{ch}[\tau(u_0 - \pi)] / (\tau \operatorname{sh}(\pi\tau)) . \quad (2.4.8)$$

The right side expression in (2.4.6) then becomes

$$V_0 \tau \operatorname{th}(\pi\tau) * \sqrt{2} \operatorname{ch}[\tau(u_0 - \pi)] / (\tau \operatorname{sh}(\pi\tau)) = V_0 \sqrt{2} \operatorname{ch}[\tau(u_0 - \pi)] / \operatorname{ch}(\pi\tau) . \quad (2.4.9)$$

Thus, equations (2.4.6) become

$$\begin{aligned} [A(\tau)\operatorname{ch}(u_0\tau) + B(\tau)\operatorname{sh}(u_0\tau)] &= V_0 \sqrt{2} \operatorname{ch}[\tau(u_0 - \pi)] / \operatorname{ch}(\pi\tau) \\ [A(\tau)\operatorname{ch}(u'_0\tau) + B(\tau)\operatorname{sh}(u'_0\tau)] &= V_0 \sqrt{2} \operatorname{ch}[\tau(u_0 - \pi)] / \operatorname{ch}(\pi\tau) . \end{aligned} \quad (2.4.10)$$

This is a standard 2x2 Cramer's Rule problem, but in order to get the solution into the form shown below, a certain amount of work is required, which we relegate to Appendix H.1. The result from (H.1.12) is then,

$$\begin{aligned} A(\tau) &= V_0 \sqrt{2} \operatorname{ch}[(\pi - u_0)\tau] \operatorname{ch}[(\pi + u_0)\tau] / \operatorname{ch}^2(\pi\tau) \\ B(\tau) &= -V_0 \sqrt{2} \operatorname{ch}[(\pi - u_0)\tau] \operatorname{sh}[(\pi + u_0)\tau] / \operatorname{ch}^2(\pi\tau) . \end{aligned} \quad (2.4.11)$$

Inserting these coefficients into the square bracket of (2.3.1) gives

$$\begin{aligned}
[A(\tau) \operatorname{ch}(u\tau) + B(\tau) \operatorname{sh}(u\tau)] &= V_0 \sqrt{2} \operatorname{ch}[(\pi-u_0)\tau] / \operatorname{ch}^2(\pi\tau) * \{ \operatorname{ch}[(\pi+u_0)\tau] \operatorname{ch}(u\tau) - \operatorname{sh}[(\pi+u_0)\tau] \operatorname{sh}(u\tau) \} \\
&= V_0 \sqrt{2} \operatorname{ch}[(\pi-u_0)\tau] / \operatorname{ch}^2(\pi\tau) * \{ \operatorname{ch}[(\pi+u_0-u)\tau] \} \\
&= V_0 \sqrt{2} \operatorname{ch}[(\pi-u_0)\tau] \operatorname{ch}[(\pi+u_0-u)\tau] / \operatorname{ch}^2(\pi\tau)
\end{aligned} \tag{2.4.12}$$

and then the Smythian form (2.3.1) for the bowl potential becomes

$$V(\xi, u) = V_0 \sqrt{2} \sqrt{\operatorname{ch}\xi - \cos u} \int_0^\infty d\tau P_{1\tau-1/2}(\operatorname{ch}\xi) \frac{\operatorname{ch}[(\pi-u_0)\tau] \operatorname{ch}[(\pi+u_0-u)\tau]}{\operatorname{ch}^2(\pi\tau)}. \tag{2.4.13}$$

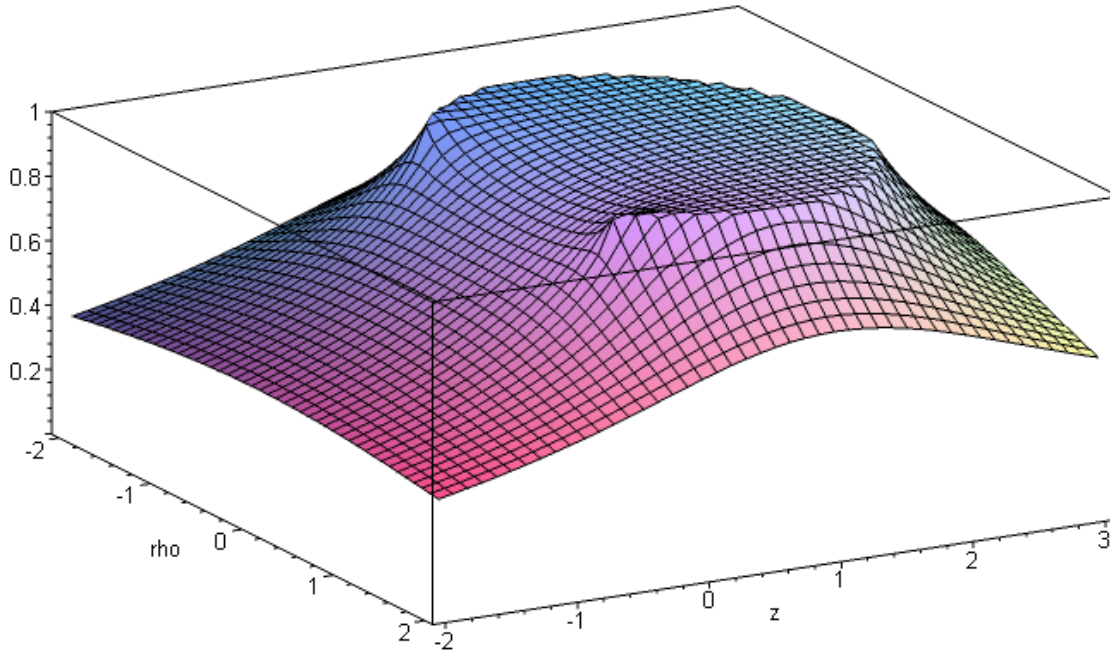
It is shown below in (8.8) that this integral can be evaluated into the following set of elementary functions,

$$V(\xi, u) = (V_0/\pi) \left\{ \cot^{-1} \left[-\frac{\sqrt{2} \cos(u/2)}{\sqrt{\operatorname{ch}\xi - \cos u}} \right] + \frac{\sqrt{\operatorname{ch}\xi - \cos u}}{\sqrt{\operatorname{ch}\xi - \cos(2u_0 - u)}} \cot^{-1} \left[\frac{\sqrt{2} \cos(u_0 - u/2)}{\sqrt{\operatorname{ch}\xi - \cos(2u_0 - u)}} \right] \right\} \tag{2.4.14}$$

$$= (V_0/\pi) \left\{ \pi - \cot^{-1} \left[\frac{\sqrt{2} \cos(u/2)}{\sqrt{\operatorname{ch}\xi - \cos u}} \right] + \frac{\sqrt{\operatorname{ch}\xi - \cos u}}{\sqrt{\operatorname{ch}\xi - \cos(2u_0 - u)}} \cot^{-1} \left[\frac{\sqrt{2} \cos(u_0 - u/2)}{\sqrt{\operatorname{ch}\xi - \cos(2u_0 - u)}} \right] \right\} \tag{b}$$

where we show two equivalent forms. There are many other ways to express this same potential using \tan^{-1} (flip the ratios) or \sin^{-1} or \cos^{-1} (draw right triangles to get new ratios).

We can throw this equation into Maple (Section 9) and obtain very nice plots of the charged bowl potential across a symmetric slice of the bowl. Here is the plot for a bowl with $u_0 = \pi/4$. Along the bowl edge the potential is constant at the value $V_0 = 1$, and outside the region shown it drops off to 0 at infinity. Kelvin would have liked Maple.



(2.4.15)

This picture shows the potential $V(\xi, u, \varphi)$ in any plane $\varphi = \text{constant}$, so this is a slice through the center of the bowl which includes the z axis. One can interpret $V(\xi, u)$ as a 2D potential in bipolar coordinates, where then (ρ, z) are the Cartesian coordinates normally called (x, y) . As in all 2D problems, the potential surface has the look of a stretched rubber membrane where at each point the curvature in one direction is the negative of that in the other direction, as required by Laplace $\nabla^2 V = \partial_x^2 V + \partial_y^2 V = 0$.

We are unaware of any external references that can verify the results (2.4.13) and (2.4.14). However, below we shall use the bowl potential to find the surface charge densities on the bowl surfaces, and these densities do agree with external sources.

2.5 Limiting cases of the potential

Since we have not found our result (2.4.14) in a quick web and book search, we shall check the result as much as possible by looking at four limits.

1. Check the potential approaching the bowl surfaces.

Start with (2.4.14b),

$$V(\xi, u) = (V_0/\pi) \left\{ \pi - \cot^{-1} \left[\frac{\sqrt{2} \cos(u/2)}{\sqrt{\text{ch}\xi - \cos u}} \right] + \frac{\sqrt{\text{ch}\xi - \cos u}}{\sqrt{\text{ch}\xi - \cos(2u_0 - u)}} \cot^{-1} \left[\frac{\sqrt{2} \cos(u_0 - u/2)}{\sqrt{\text{ch}\xi - \cos(2u_0 - u)}} \right] \right\} .$$

Then if $u \rightarrow u_0$ and $u \rightarrow u_0 + 2\pi$ we first evaluate,

$$\begin{array}{ll} \underline{u_0} & \underline{u_0 + 2\pi} \\ \cos(u_0 - u/2) = \cos(u_0/2) & \cos([u_0 + 2\pi]/2) = \cos(u_0/2 + \pi) = -\cos(u_0/2) \\ \cos(2u_0 - u) = \cos u_0 & \cos(2u_0 - u) = \cos u_0 \\ \text{ch}\xi - \cos(2u_0 - u) = \text{ch}\xi - \cos u_0 & \text{ch}\xi - \cos(2u_0 - u) = \text{ch}\xi - \cos u_0 \\ \cos(u/2) = \cos(u_0/2) & \cos(u/2) = \cos([u_0 + 2\pi]/2) = -\cos(u_0/2) . \end{array} \quad (2.5.1)$$

Inserting these into the above gives the following for $u \rightarrow u_0$ (+) and for $u \rightarrow u_0 + 2\pi$ (-),

$$\begin{aligned} V(\xi, u) &= (V_0/\pi) \left\{ \pi - \cot^{-1} \left[\frac{\pm\sqrt{2} \cos(u_0/2)}{\sqrt{\text{ch}\xi - \cos u_0}} \right] + \frac{\sqrt{\text{ch}\xi - \cos u}}{\sqrt{\text{ch}\xi - \cos u_0}} \cot^{-1} \left[\frac{\pm\sqrt{2} \cos(u_0/2)}{\sqrt{\text{ch}\xi - \cos u_0}} \right] \right\} \\ &= (V_0/\pi) \left\{ \pi - \cot^{-1}[x] + \cot^{-1}[x] \right\} = (V_0/\pi) \left\{ \pi \right\} = V_0 . \end{aligned} \quad (2.5.2)$$

Thus the potential (2.4.14) equals V_0 on both sides of the bowl surface, as required.

2. Check The Disk Limit

Start with (2.4.14a),

$$V(\xi, u) = (V_0/\pi) \left\{ \cot^{-1} \left[\frac{\sqrt{2} \cos(u/2)}{\sqrt{\text{ch}\xi - \cos u}} \right] + \frac{\sqrt{\text{ch}\xi - \cos u}}{\sqrt{\text{ch}\xi - \cos(2u_0 - u)}} \cot^{-1} \left[\frac{\sqrt{2} \cos(u_0 - u/2)}{\sqrt{\text{ch}\xi - \cos(2u_0 - u)}} \right] \right\}.$$

Then if $u_0 \rightarrow \pi$ we find

$$\begin{aligned} \cos(u_0 - u/2) &= \cos(\pi - u/2) = -\cos(u/2) \\ \cos(2u_0 - u) &= \cos(2\pi - u) = \cos u \\ \text{ch}\xi - \cos(2u_0 - u) &= \text{ch}\xi - \cos u \end{aligned} \quad (2.5.3)$$

so

$$\begin{aligned} V(\xi, u) &= (V_0/\pi) \left\{ \cot^{-1} \left[\frac{-\sqrt{2} \cos(u/2)}{\sqrt{\text{ch}\xi - \cos u}} \right] + \frac{\sqrt{\text{ch}\xi - \cos u}}{\sqrt{\text{ch}\xi - \cos u}} \cot^{-1} \left[\frac{-\sqrt{2} \cos(u/2)}{\sqrt{\text{ch}\xi - \cos u}} \right] \right\} \\ &= (2V_0/\pi) \cot^{-1} \left[\frac{-\sqrt{2} \cos(u/2)}{\sqrt{\text{ch}\xi - \cos u}} \right]. \end{aligned} \quad (2.5.4)$$

It is shown in Appendix B that, when the above is converted to cylindrical coordinates, the result is

$$V_{\text{disk}}(\xi, u) = (2V_0/\pi) \sin^{-1} \left[\frac{2a}{\sqrt{(\rho-a)^2+z^2} + \sqrt{(\rho+a)^2+z^2}} \right] \quad (2.5.5)$$

which agrees with green Jackson p 92 (3.178).

3. Check The Large r Limit

Start with (2.4.14a),

$$V(\xi, u) = (V_0/\pi) \left\{ \cot^{-1} \left[\frac{\sqrt{2} \cos(u/2)}{\sqrt{\text{ch}\xi - \cos u}} \right] + \frac{\sqrt{\text{ch}\xi - \cos u}}{\sqrt{\text{ch}\xi - \cos(2u_0 - u)}} \cot^{-1} \left[\frac{\sqrt{2} \cos(u_0 - u/2)}{\sqrt{\text{ch}\xi - \cos(2u_0 - u)}} \right] \right\}.$$

In the large r region we know from (1.2.16) that

$$\sqrt{\text{ch}\xi - \cos u} \approx \sqrt{2} a/r$$

$$\xi \ll 1$$

$$u = 2\pi + \epsilon \quad \text{with } |\epsilon| \ll 1. \quad (2.5.6)$$

One can then approximate various expressions in the above potential

$$\cos(u/2) \approx \cos(2\pi/2) = \cos(\pi) = -1$$

$$\cos(2u_0 - u) \approx \cos(2u_0 - 2\pi) = \cos(2u_0)$$

$$\text{ch}\xi - \cos(2u_0 - u) \approx 1 - \cos(2u_0) = 2\sin^2 u_0$$

$$\sqrt{\text{ch}\xi - \cos(2u_0 - u)} = \sqrt{2} |\sin u_0|$$

$$\cos(u_0 - u/2) \approx \cos(u_0 - \pi) = -\cos u_0 . \quad (2.5.7)$$

Then the ratios appearing in (2.4.14a) may be approximated as

$$\begin{aligned} -\frac{\sqrt{2} \cos(u/2)}{\sqrt{\text{ch}\xi - \cos u}} &\approx -\frac{-\sqrt{2}}{\sqrt{2} a/r} = r/a \\ \frac{\sqrt{\text{ch}\xi - \cos u}}{\sqrt{\text{ch}\xi - \cos(2u_0 - u)}} &\approx \frac{\sqrt{2} a/r}{\sqrt{2} |\sin u_0|} = R/r \quad R = a |\sin u_0| \\ \frac{\sqrt{2} \cos(u_0 - u/2)}{\sqrt{\text{ch}\xi - \cos(2u_0 - u)}} &\approx \frac{-\sqrt{2} \cos u_0}{\sqrt{2} |\sin u_0|} = \frac{-\cos u_0}{|\sin u_0|} . \end{aligned} \quad (2.5.8)$$

The potential shown above is then, for large r ,

$$V(\xi, u) = (V_0/\pi) \left\{ \cot^{-1}[r/a] + (R/r) \cot^{-1}\left[\frac{-\cos u_0}{|\sin u_0|}\right] \right\} . \quad (2.5.9)$$

The first term may be written

$$\cot^{-1}[r/a] = \tan(a/r) \approx a/r \text{ (large } r\text{)} = (R/r) |\sin u_0| \quad // (1.2.6) \quad (2.5.10)$$

The second term may be written

$$(R/r) \cot^{-1}\left[\frac{-\cos u_0}{|\sin u_0|}\right] = (R/r) \tan^{-1}\left[\frac{|\sin u_0|}{-\cos u_0}\right] = (R/r) \arctan 2\pi(-\cos u_0, |\sin u_0|) \quad (2.5.11)$$

where $\theta = \arctan 2\pi(x, y)$ returns θ in the range $(0, 2\pi)$ as in (9.2). This is the intended meaning of the ambiguous function \tan^{-1} . We can consider u_0 in each of the four quadrants of $(0, 2\pi)$ as follows:

$$\begin{array}{lllll} u_0 \text{ in Q1} & -\cos u_0 < 0 & \theta \text{ in Q2} & \Rightarrow & \theta = \pi - u_0 \\ u_0 \text{ in Q2} & -\cos u_0 > 0 & \theta \text{ in Q1} & \Rightarrow & \theta = \pi - u_0 \\ u_0 \text{ in Q3} & -\cos u_0 > 0 & \theta \text{ in Q1} & \Rightarrow & \theta = u_0 - \pi \\ u_0 \text{ in Q4} & -\cos u_0 < 0 & \theta \text{ in Q2} & \Rightarrow & \theta = u_0 - \pi . \end{array} \quad (2.5.12)$$

If this seems unclear, draw a picture of the four cases. The conclusion is that

$$\arctan 2\pi(-\cos u_0, |\sin u_0|) = |\pi - u_0| \quad \text{for } u_0 \text{ in any quadrant Q1, Q2, Q3, Q4} \quad (2.5.13)$$

and therefore,

$$V(\xi, u) = (V_0/\pi) (R/r) (|\sin u_0| + |\pi - u_0|) . \quad 0 \leq u_0 \leq 2\pi . \quad (2.5.14)$$

Look first at Fig (1.2.18a) where $0 < u_0 < \pi$ and where $\beta = \pi - u_0 > 0$. Then

$$|\sin u_0| = \sin \beta \quad |\pi - u_0| = \beta \quad V(\xi, u) = (V_0/\pi) (R/r) (\sin \beta + \beta) . \quad (2.5.15)$$

Look next at Fig (1.2.18b) where $\pi < u_0 < 2\pi$ and where $\beta = u_0 - \pi > 0$. Then

$$|\sin u_0| = \sin \beta \quad |\pi - u_0| = \beta \quad V(\xi, u) = (V_0/\pi) (R/r) (\sin \beta + \beta) . \quad (2.5.16)$$

The potential is the same in either case when expressed in terms of angle β . Far away the bowl looks like a point charge $Q = CV_0$ with potential $V = Q/r$. Thus the capacitance must be

$$C = Q/V_0 = (Vr/V_0) = (R/\pi) (\beta + \sin \beta) . \quad (2.5.17)$$

Since this is the known correct result and also the result we get later in (4.4.10), we regard our potential (2.4.14) as passing the large- r limit check.

4. Check The Full Sphere Limit

Start with (2.4.14b),

$$V(\xi, u) = (V_0/\pi) \left\{ \pi - \cot^{-1} \left[\frac{\sqrt{2} \cos(u/2)}{\sqrt{\text{ch} \xi - \cos u}} \right] + \frac{\sqrt{\text{ch} \xi - \cos u}}{\sqrt{\text{ch} \xi - \cos(2u_0 - u)}} \cot^{-1} \left[\frac{\sqrt{2} \cos(u_0 - u/2)}{\sqrt{\text{ch} \xi - \cos(2u_0 - u)}} \right] \right\} .$$

Then if $u_0 \rightarrow 0$ we find

$$\begin{aligned} \cos(2u_0 - u) &= \cos(-u) = \cos u \\ \cos(u_0 - u/2) &= \cos(-u/2) = \cos(u/2) \\ \text{ch} \xi - \cos(2u_0 - u) &= \text{ch} \xi - \cos u \end{aligned} \quad (2.5.18)$$

so

$$\begin{aligned} V(\xi, u) &= (V_0/\pi) \left\{ \pi - \cot^{-1} \left[\frac{\sqrt{2} \cos(u/2)}{\sqrt{\text{ch} \xi - \cos u}} \right] + \frac{\sqrt{\text{ch} \xi - \cos u}}{\sqrt{\text{ch} \xi - \cos u}} \cot^{-1} \left[\frac{\sqrt{2} \cos(u/2)}{\sqrt{\text{ch} \xi - \cos u}} \right] \right\} \\ &= (V_0/\pi) \left\{ \pi - \cot^{-1}[x] + \cot^{-1}[x] \right\} = (V_0/\pi) \{\pi\} = V_0 . \end{aligned} \quad (2.5.19)$$

This result is at first a little surprising, since one might be expecting $V = Q/r$, especially when looking at a plot like the first one in Section 6 (notice the axis scale compared to the other plots). Looking at Fig (1.1.2a) one sees that the $u_0 = 0$ sphere slice is so large that it fills the entire upper half plane so naturally the potential in that half plane is the constant value V_0 . In the lower half plane, although one can move a finite distance away from the sphere, the sphere is overwhelmingly large so V does not taper off and we then have $V = V_0$ as well in the lower half plane. So the limit computed above is correct.

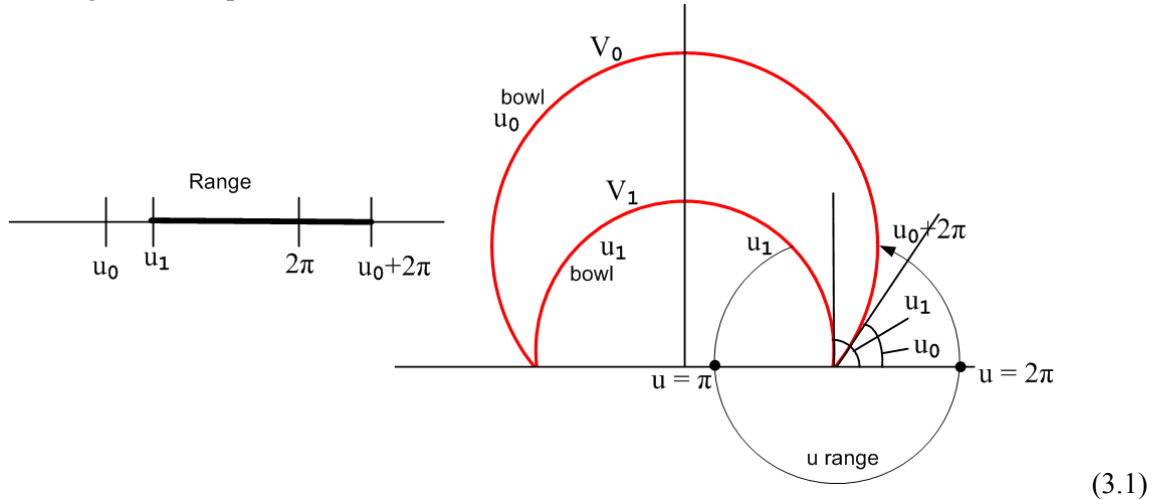
3. The charged double-bowl potential in toroidal coordinates

3.1 The general double bowl solution

This seems a good place to address this related problem. Sneddon (Sec 7.7) deals with the problem of two separated bowls having a common symmetry axis. *That* problem seems to have no closed form solution and Sneddon reduces its solution to solving one or more second-kind Fredholm integral equations. *Our* double-bowl problem is much simpler in that both bowls have a common lip. First we imagine that the bowls are somehow insulated from each other at the lip and so can have constant potentials V_0 and V_1 resulting in a strange two-bowl capacitor. Then we remove the insulation and set $V_1 = V_0$.

The 3D shapes formed in this way from two bowls can vary from a sort of 3D lune, to a bowl with a flat lid on it, to a "lens" composed of two spherical surfaces (two facing attached bowls). If the two bowls of the lens have the same size, the solution to this problem describes the evaporation from the surface of a liquid drop sitting on a flat surface, which drop then is half the lens shape. See Hu and Larson regarding such "sessile droplets". It is nice to see that solutions to 19th century electrostatic and heat flow potential theory problems have 21st century application to DNA sequencing.

The solution to the double bowl problem follows exactly that of the single-bowl problem. Here is the picture showing a lune-shaped cross section,



If the potential on both lune surfaces is V_0 , we know (from Laplace) that the entire interior region is at V_0 . For the exterior region, we show how coordinate u ranges from u_1 on the inner surface of the smaller lune surface to $u_0+2\pi$ on the outer surface of the larger lune.

We use the exact same Smythian form (2.3.1) as for the single bowl,

$$V(\xi, u) = \sqrt{\operatorname{ch}\xi - \cos u} \int_0^\infty dt P_{i\tau-1/2}(\operatorname{ch}\xi) [A(\tau)\operatorname{ch}(u\tau) + B(\tau)\operatorname{sh}(u\tau)] . \quad (2.3.1) \quad (3.2)$$

As before we define $u'_0 \equiv u_0 + 2\pi$ and note that $\cos(u'_0) = \cos(u_0)$. Here then are the boundary conditions for the exterior double-bowl problem, where for the moment we assume $V_0 \neq V_1$,

$$\begin{aligned} V_1 &= \sqrt{\text{ch}\xi - \cos u_1} \int_0^\infty d\tau P_{i\tau-1/2}(\text{ch}\xi) [A(\tau)\text{ch}(u_1\tau) + B(\tau)\text{sh}(u_1\tau)] \\ V_0 &= \sqrt{\text{ch}\xi - \cos u_0} \int_0^\infty d\tau P_{i\tau-1/2}(\text{ch}\xi) [A(\tau)\text{ch}(u_0'\tau) + B(\tau)\text{sh}(u_0'\tau)] . \quad u_0' \equiv u_0 + 2\pi \end{aligned} \quad (3.3)$$

As in going from (2.4.4) to (2.4.6), we use the Mehler transform to extract the square brackets,

$$\begin{aligned} [A(\tau)\text{ch}(u_1\tau) + B(\tau)\text{sh}(u_1\tau)] &= V_1 \tau \text{th}(\pi\tau) \int_0^\infty d\xi \text{sh}(\xi) P_{i\tau-1/2}(\text{ch}\xi) / \sqrt{\text{ch}\xi - \cos u_1} \\ [A(\tau)\text{ch}(u_0'\tau) + B(\tau)\text{sh}(u_0'\tau)] &= V_0 \tau \text{th}(\pi\tau) \int_0^\infty d\xi \text{sh}(\xi) P_{i\tau-1/2}(\text{ch}\xi) / \sqrt{\text{ch}\xi - \cos u_0} . \end{aligned} \quad (3.4)$$

Using integral (2.4.8) we then get, in analogy with (2.4.10),

$$\begin{aligned} [A(\tau)\text{ch}(u_1\tau) + B(\tau)\text{sh}(u_1\tau)] &= V_1 \sqrt{2} \text{ch}[\tau(u_1-\pi)] / \text{ch}(\pi\tau) \\ [A(\tau)\text{ch}(u_0'\tau) + B(\tau)\text{sh}(u_0'\tau)] &= V_0 \sqrt{2} \text{ch}[\tau(u_0-\pi)] / \text{ch}(\pi\tau) . \end{aligned} \quad (3.5)$$

Comparison with (2.4.10) shows that we have set $u_0 \rightarrow u_1$ in the first condition and the second condition is the same. The coefficients this time are a little more complicated, and are computed in (H.1.20),

$$\begin{aligned} A(\tau) &= V_0 \sqrt{2} Q \frac{\text{ch}[\tau(\pi-u_0)]}{[Q \text{ch}(u_0'\tau) + P \text{sh}(u_0'\tau)] \text{ch}(\pi\tau)} \\ B(\tau) &= V_0 \sqrt{2} P \frac{\text{ch}[\tau(\pi-u_0)]}{[Q \text{ch}(u_0'\tau) + P \text{sh}(u_0'\tau)] \text{ch}(\pi\tau)} \end{aligned}$$

where

$$\begin{aligned} P &= \{ V_1 \text{ch}(u_0'\tau) \text{ch}[\tau(\pi-u_1)] - V_0 \text{ch}(u_1\tau) \text{ch}[\tau(\pi-u_0)] \} \\ Q &= \{ V_0 \text{sh}(u_1\tau) \text{ch}[\tau(\pi-u_0)] - V_1 \text{sh}(u_0'\tau) \text{ch}[\tau(\pi-u_1)] \} . \end{aligned} \quad (3.6)$$

Inserting $A(\tau)$ and $B(\tau)$ into the Smythian form (3.2) gives this result for the potential outside the insulated-lip double bowl combination with bowl u_0 at V_0 and bowl u_1 at V_1 ,

$$V(\xi, u) = V_0 \sqrt{2} \sqrt{\text{ch}\xi - \cos u} \int_0^\infty d\tau P_{i\tau-1/2}(\text{ch}\xi) \frac{\text{ch}[\tau(\pi-u_0)]}{\text{ch}(\pi\tau)} \frac{P \text{ch}(u\tau) + Q \text{sh}(u\tau)}{Q \text{ch}(u_0'\tau) + P \text{sh}(u_0'\tau)} . \quad (3.7)$$

Setting $u_0' \equiv u_0 + 2\pi$ and $V_1 = V_0$ one finds, after much algebra verified below (H.1.22), the following potential (3.2) outside the common-lip bowls at the same potential V_0 (the potential inside is V_0),

$$V(\xi, u) = V_0 \sqrt{2} \sqrt{\text{ch}\xi - \cos u} \int_0^\infty d\tau P_{i\tau-1/2}(\text{ch}\xi) \frac{\text{ch}[(\pi-u_0)\tau] \text{sh}[(u-u_1)\tau] + \text{ch}[(\pi-u_1)\tau] \text{sh}[(2\pi+u_0-u)\tau]}{\text{ch}(\pi\tau) \text{sh}[(2\pi+u_0-u_1)\tau]} . \quad (3.8)$$

If one takes the limit $u_1 \rightarrow u_0$, the solution (2.4.13) to the single-bowl problem is recovered, as shown below (H.1.27). We have not made any attempt to evaluate (3.8) but it may yield an expression involving elementary functions as is the case for the single-bowl potential.

For comparison purposes, we replace $u, u_0, u_1, \xi \rightarrow \beta, \beta_1, \beta_2, \alpha$ to get

$$V(\alpha, \beta) = V_0 \sqrt{2} \sqrt{\cosh \alpha - \cos \beta} \int_0^\infty d\tau P_{i\tau-1/2}(\cosh \alpha) * \frac{\cosh[(\pi-\beta_1)\tau] \sinh[(\beta-\beta_2)\tau] + \cosh[(\pi-\beta_2)\tau] \sinh[(2\pi+\beta_1-\beta)\tau]}{\cosh(\pi\tau) \sinh[(2\pi+\beta_1-\beta_2)\tau]} \quad (3.9)$$

This matching result appears in the Hu and Larson paper mentioned above,

$$u = V \sqrt{2 \cosh \alpha - 2 \cos \beta} \int_0^\infty \frac{\cosh[(\pi - \beta_1)\tau] \sinh[(\beta - \beta_2)\tau] + \cosh[(\pi - \beta_2)\tau] \sinh[(2\pi + \beta_1 - \beta)\tau]}{\cosh(\pi\tau) \sinh[(2\pi + \beta_1 - \beta_2)\tau]} P_{-(1/2)+i\tau}(\cosh \alpha) d\tau \quad (22) \quad (3.10)$$

Comment: The exterior double-bowl solution above is based on the boundary conditions (3.3). When V_1 and V_0 are different, there is also an interior double-bowl problem of interest. For this problem the range of u is (see Fig 3.1) $u_0 \leq u \leq u_1$. The boundary conditions are then (3.3) with $u'_0 \rightarrow u_0$. The coefficients A and B are then given by (3.6) with $u'_0 \rightarrow u_0$, and the interior solution is then (3.7) with $u'_0 \rightarrow u_0$.

Reader exercise: With the double-bowl exterior and interior potentials described above, use the methods of Section 4 below to compute the surface charge densities on all four bowl surfaces. Integrate the charge densities to find the total charges Q_0 and Q_1 on the bowls. Find V_0 and V_1 such that $Q_1 = -Q_0 = Q$. Then use $Q = C(V_1 - V_0)$ to determine the capacitance of such a common-lip double-bowl capacitor. Is there some simpler way to find this capacitance, perhaps using (D.6) ?

3.2 Special case: a bowl with a flat lid

Taking $u_1 = \pi$ in Fig (3.1) to get the flat lid, the solution (3.8) reduces to,

$$V(\xi, u) = V_0 \sqrt{2} \sqrt{\cosh \xi - \cos u} \int_0^\infty d\tau P_{i\tau-1/2}(\cosh \xi) \frac{\cosh[(\pi-u_0)\tau] \sinh[(u-\pi)\tau] + \sinh[(2\pi+u_0-u)\tau]}{\cosh(\pi\tau) \sinh[(\pi+u_0)\tau]}. \quad (3.11)$$

Again for comparison, we take $u, u_0 \rightarrow \beta, \beta_0$ and $\xi \rightarrow \alpha$ to get

$$V(\alpha, \beta) = V_0 \sqrt{2} \sqrt{\cosh \alpha - \cos \beta} \int_0^\infty d\tau P_{i\tau-1/2}(\cosh \alpha) \frac{\cosh[(\pi-\beta_0)\tau] \sinh[(\beta-\pi)\tau] + \sinh[(2\pi+\beta_0-\beta)\tau]}{\cosh(\pi\tau) \sinh[(\pi+\beta_0)\tau]}. \quad (3.12)$$

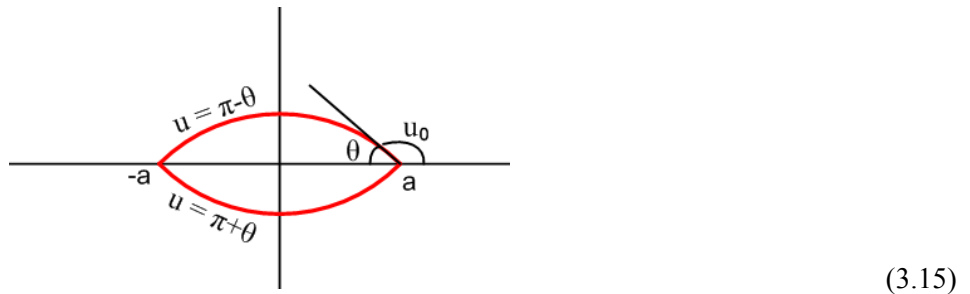
This agrees with the result quoted in Lebedev et al. Problem 503 (page 241),

$$\begin{aligned} u(\alpha, \beta) &= V \sqrt{2 \cosh \alpha - 2 \cos \beta} \\ &\times \int_0^\infty [\sinh(2\pi + \beta_0 - \beta)\tau - \cosh(\pi - \beta_0)\tau \\ &\times \sinh(\pi - \beta)\tau] \frac{P_{-1/2+i\tau}(\cosh \alpha)}{\sinh(\pi + \beta_0)\tau \cosh \pi\tau} d\tau, \end{aligned} \quad (3.13)$$

3.3 Special case: a sessile drop (lens-shaped double bowl)

Here we select in Fig (3.1), with θ being a relatively small angle,

$$\begin{aligned} u_0 &= [\pi-\theta] && // \text{a shallow upper bowl} && \pi-u_0 = \theta && u_1-u_0 = 2\theta \\ u_1 &= [\pi+\theta] && // \text{a shallow lower bowl} && \pi-u_1 = -\theta && \end{aligned} \quad (3.14)$$



The upper part of this figure (rotated about the vertical axis) represents a liquid droplet on a flat surface. Angle θ is called the "contact angle" of the droplet. Potential (3.8) then becomes

$$V(\xi, u) = V_0 \sqrt{2} \sqrt{\cosh \xi - \cos u} \int_0^\infty d\tau P_{i\tau-1/2}(\cosh \xi) \frac{\cosh[\theta\tau] \sinh[(u-\pi-\theta)\tau] + \cosh[\theta\tau] \sinh[(3\pi-\theta-u)\tau]}{\cosh(\pi\tau) \sinh[(2\pi-2\theta)\tau]}. \quad (3.16)$$

We show in (H.1.30) that (3.16) can be written in this simpler form,

$$V(\xi, u) = V_0 \sqrt{2} \sqrt{\cosh \xi - \cos u} \int_0^\infty d\tau P_{i\tau-1/2}(\cosh \xi) \frac{\cosh(\theta\tau) \cosh[(2\pi-u)\tau]}{\cosh(\pi\tau) \cosh[(\pi-\theta)\tau]}. \quad (3.17)$$

Again setting $\xi \rightarrow \alpha$ and $u \rightarrow \beta$ one gets

$$V(\alpha, \beta) = V_0 \sqrt{2} \sqrt{\cosh \alpha - \cos \beta} \int_0^\infty d\tau P_{i\tau-1/2}(\cosh \alpha) \frac{\cosh(\theta\tau) \cosh[(2\pi-\beta)\tau]}{\cosh(\pi\tau) \cosh[(\pi-\theta)\tau]} \quad (3.18)$$

which appears in the Hu and Larson paper as

$$\begin{aligned} \frac{c - c_\infty}{c_v - c_\infty} &= \sqrt{2 \cosh \alpha - 2 \cos \beta} \int_0^\infty \\ \frac{\cosh(\theta\tau)}{\cosh(\pi\tau)} \frac{\cosh[(2\pi-\beta)\tau]}{\cosh[(\pi-\theta)\tau]} P_{-(1/2)+i\tau}(\cosh \alpha) d\tau \quad (26) \end{aligned} \quad (3.19)$$

The connection to electrostatics is that the vapor concentration just above the droplet solves the Laplace equation and then plays the role of the electrostatic potential, and the electric field becomes the diffusive evaporation flux of liquid off the droplet surface. Hu and Larson quote applications to DNA sequencing.

4. The charged bowl surface charge densities and capacitance

4.1 Bowl surface charge densities

We restrict our interest to "upper bowls" of Fig (1.2.18a) which have $0 \leq u_0 \leq \pi$ so $\sin(u_0) > 0$. Such bowls always have their opening on the bottom in our drawings. Since this calculation is one of the main results of this document, we show every detail of the calculation. The methods can be used for other curvilinear coordinate systems.

We start with the bowl potential (2.4.13) and set up to compute the surface charge densities,

$$V(\xi, u) = V_0 \sqrt{2} \sqrt{\cosh\xi - \cos u} \int_0^\infty d\tau P_{1/2}(\cosh\xi) \frac{\cosh[(\pi-u_0)\tau] \cosh[(\pi+u_0-u)\tau]}{\cosh^2(\pi\tau)} . \quad (4.1.1)$$

$$\begin{aligned} \sigma_+ &= -(1/4\pi) (1/h_u) \partial_u V(\xi, u)|^{u=u_0} = \sigma_{in} & 1/h_u &= (\cosh\xi - \cos u)/a \\ \sigma_- &= +(1/4\pi) (1/h_u) \partial_u V(\xi, u)|^{u=u_0+2\pi} = \sigma_{out} & // \text{ cgs units selected here} \end{aligned} \quad (4.1.2)$$

Explanation: Recall that the above σ equations arise from positioning a tiny Gaussian pillbox with one end inside a "metal" conductor with the result that $\sigma = (1/4\pi)E_s$ (cgs) if \hat{s} is a local Cartesian-coordinate out-facing normal at the surface. Then $\sigma = -(1/4\pi)\partial_s V$. For a curvilinear coordinate u one has $ds = h_u du$ (for example, $ds = r d\theta$ in polar coordinates) so $\partial_s = (1/h_u)\partial_u$. Quantity $h_u = a/(\cosh\xi - \cos u)$ is the curvilinear scale factor $\sqrt{g_{uu}}$ in the u direction, and a is the radius of the circular lip of the bowl. For an upper bowl having $0 \leq u \leq \pi$, coordinate u increases away from inner surface, which explains the - sign in the σ_+ equation. But the reverse is true for the outer surface, so the σ_- equation has a + sign.

Now, define the integral part of (4.1.1) to be $f(u, \xi)$,

$$f(u, \xi) \equiv \int_0^\infty d\tau P_{1/2}(\cosh\xi) \cosh[(\pi-u_0)\tau] \cosh[(\pi+u_0-u)\tau]/\cosh^2(\pi\tau) \quad (4.1.3)$$

so that then

$$V(\xi, u) = V_0 \sqrt{2} \sqrt{\cosh\xi - \cos u} f(u, \xi) . \quad (4.1.4)$$

The boundary conditions at the inside and outside bowl surfaces require that,

$$\begin{aligned} V(\xi, u_0) &= V_0 \sqrt{2} \sqrt{\cosh\xi - \cos u_0} f(u_0, \xi) = V_0 & \Rightarrow \sqrt{2} \sqrt{\cosh\xi - \cos u_0} f(u_0, \xi) &= 1 \\ V(\xi, u_0+2\pi) &= V_0 \sqrt{2} \sqrt{\cosh\xi - \cos u_0} f(u_0+2\pi, \xi) = V_0 \Rightarrow \sqrt{2} \sqrt{\cosh\xi - \cos u_0} f(u_0+2\pi, \xi) &= 1 . \end{aligned} \quad (4.1.5)$$

Now define

$$\begin{aligned} f^+ &\equiv f(u_0, \xi) \\ f^- &\equiv f(u_0 + 2\pi, \xi) . \end{aligned} \quad (4.1.6)$$

Then we have just shown in (4.1.5) that

$$f^\pm = 1/\sqrt{2 \sqrt{\text{ch}\xi - \cos u}} . \quad (4.1.7)$$

Next, compute $\partial_u f$,

$$\begin{aligned} \partial_u f &= \int_0^\infty d\tau P_{i\tau-1/2}(\text{ch}\xi) \text{ch}[(\pi-u_0)\tau] \partial_u \{\text{ch}[(\pi+u_0-u)\tau]\} / \text{ch}^2(\pi\tau) \\ &= \int_0^\infty d\tau P_{i\tau-1/2}(\text{ch}\xi) \text{ch}[(\pi-u_0)\tau] \text{sh}[(\pi+u_0-u)\tau] (-\tau) / \text{ch}^2(\pi\tau) , \end{aligned} \quad (4.1.8)$$

so that

$$\begin{aligned} (\partial_u f)^+ &\equiv \partial_u f^{u=u_0} = - \int_0^\infty d\tau P_{i\tau-1/2}(\text{ch}\xi) \text{ch}[(\pi-u_0)\tau] \tau \text{sh}[\pi\tau] / \text{ch}^2(\pi\tau) \\ (\partial_u f)^- &\equiv \partial_u f^{u=u_0+2\pi} = \int_0^\infty d\tau P_{i\tau-1/2}(\text{ch}\xi) \text{ch}[(\pi-u_0)\tau] \text{sh}[(-\pi)\tau] (-\tau) / \text{ch}^2(\pi\tau) \\ &= + \int_0^\infty d\tau P_{i\tau-1/2}(\text{ch}\xi) \text{ch}[(\pi-u_0)\tau] \tau \text{sh}[\pi\tau] / \text{ch}^2(\pi\tau) . \end{aligned} \quad (4.1.9)$$

Then defining this last integral to be X,

$$X \equiv \int_0^\infty d\tau P_{i\tau-1/2}(\text{ch}\xi) \text{ch}[(\pi-u_0)\tau] \tau \text{sh}(\pi\tau) / \text{ch}^2(\pi\tau) , \quad (4.1.10)$$

the results (4.1.9) are

$$(\partial_u f)^\pm = \mp X . \quad (4.1.11)$$

Going back to the full potential V in (4.1.4), we compute next $\partial_u V$:

$$\begin{aligned} V(\xi, u) &= V_0 \sqrt{2} \sqrt{\text{ch}\xi - \cos u} f(u) \\ \partial_u V &= V_0 \sqrt{2} [\partial_u (\sqrt{\text{ch}\xi - \cos u}) f(u, \xi) + \sqrt{\text{ch}\xi - \cos u} \partial_u f(u, \xi)] \\ &= V_0 \sqrt{2} [(1/2)(1/\sqrt{\text{ch}\xi - \cos u}) \sin(u) f(u, \xi) + \sqrt{\text{ch}\xi - \cos u} \partial_u f(u, \xi)] . \end{aligned} \quad (4.1.12)$$

Then,

$$\begin{aligned}
(\partial_u V)^\pm &= V_0 \sqrt{2} \left\{ (1/2)(1/\sqrt{\text{ch}\xi - \cos u_0}) \sin(u_0) f^\pm + \sqrt{\text{ch}\xi - \cos u_0} (\partial_u f)^\pm \right\} \\
&= V_0 \sqrt{2} \left\{ (1/2)(1/\sqrt{\text{ch}\xi - \cos u_0}) \sin(u_0) 1/[\sqrt{2} \sqrt{\text{ch}\xi - \cos u_0}] \mp \sqrt{\text{ch}\xi - \cos u_0} X \right\} \\
&\quad (4.1.7) \qquad \qquad \qquad (4.1.11) \\
&= V_0 \sqrt{2} \left\{ 1/(2\sqrt{2})^* \sin(u_0) * (\text{ch}\xi - \cos u_0)^{-1} \mp \sqrt{\text{ch}\xi - \cos u_0} X \right\} \\
&= V_0 \sqrt{2} \left\{ 1/(2\sqrt{2})^* \sin(u_0) * B^{-2} \mp B X \right\} \quad \text{where } B \equiv \sqrt{\text{ch}\xi - \cos u_0} \\
&= V_0 \sin(u_0)/(2B^2) \mp V_0 \sqrt{2} B X . \qquad \qquad \qquad (4.1.13)
\end{aligned}$$

The charge densities from (4.1.2) are then

$$\sigma_\pm = \mp (1/4\pi) (1/h_u) (\partial_u V)^\pm \qquad \qquad 1/h_u = (\text{ch}\xi - \cos u)/a = B^2/a \qquad \qquad (4.1.2)$$

$$\begin{aligned}
&= \mp (1/4\pi) * B^2/a * V_0 * [\sin(u_0)/(2B^2) \mp \sqrt{2} B X] \qquad \qquad (4.1.13) \\
&= \mp (V_0/4\pi a) [\sin(u_0)/(2) \mp \sqrt{2} B^3 X] \\
&= \mp (V_0/4\pi) (\sin(u_0)/a) [1/2 \mp \sqrt{2} B^3 X / \sin(u_0)] \\
&= \mp (V_0/4\pi R) [1/2 \mp \sqrt{2} B^3 X / \sin(u_0)] \quad // (1.2.6) \quad R = a/\sin(u_0) \\
&= (V_0/4\pi R) [\sqrt{2} B^3 X / \sin(u_0) \mp 1/2] . \qquad \qquad \qquad (4.1.14)
\end{aligned}$$

Even without knowing the integral X , we discover at once the famous fact,

$$\sigma_{\text{out}} - \sigma_{\text{in}} = \sigma_- - \sigma_+ = (V_0/4\pi R) \qquad \qquad (4.1.15)$$

which Kelvin obtained by doing inversion and superposition, see Appendix C. This does seem a remarkable result, considering that σ_{in} varies violently over the bowl's surface.

The integral X of (4.1.10) is evaluated in (7.2.8) below to be

$$X = \frac{1}{\pi} \frac{\sin(u_0/2)}{\text{ch}\xi - \cos u_0} \left[1 + \frac{A}{B} \tan^{-1}\left(\frac{A}{B}\right) \right] \qquad \qquad (7.2.8) \qquad \qquad (4.1.16)$$

$$\text{where } A = \sqrt{2} \cos(u_0/2) \text{ and } B = \sqrt{\text{ch}\xi - \cos u_0} .$$

Looking at (4.1.14) we evaluate,

$$\begin{aligned}
& \sqrt{2} B^3 X / \sin(u_0) = \sqrt{2} B^3 X / [2 \sin(u_0/2) \cos(u_0/2)] \\
&= \sqrt{2} B^3 (1/\pi) [\sin(u_0/2)/B^2] [1 + (A/B) \tan^{-1}(A/B)] / [2 \sin(u_0/2) \cos(u_0/2)] \\
&= (B/\pi) [1 + (A/B) \tan^{-1}(A/B)] / [\sqrt{2} \cos(u_0/2)] \\
&= (B/\pi A) [1 + (A/B) \tan^{-1}(A/B)] \\
&= (1/\pi) [(B/A) + \tan^{-1}(A/B)]. \tag{4.1.17}
\end{aligned}$$

The charge densities on the bowl are now,

$$\begin{aligned}
\sigma_{\pm} &= (V_0/4\pi R) \{ \sqrt{2} B^3 [X] / \sin(u_0) \mp 1/2 \} \\
&= (V_0/4\pi R) \{ (1/\pi) [(B/A) + \tan^{-1}(A/B)] \mp 1/2 \} \\
&= (V_0/4\pi^2 R) \{ (B/A) + \tan^{-1}(A/B) \mp \pi/2 \}. \tag{4.1.18}
\end{aligned}$$

Now use the following fact which one can easily verify by drawing a right triangle,

$$\pi/2 - \tan^{-1}(x/y) = \tan^{-1}(y/x). \tag{4.1.19}$$

Then

$$\tan^{-1}(A/B) - \pi/2 = -\tan^{-1}(B/A) \tag{4.1.20}$$

so that

$$\begin{aligned}
\sigma_{in} &= \sigma_+ = (V_0/4\pi^2 R) \{ (B/A) - \tan^{-1}(B/A) \} & A &= \sqrt{2} \cos(u_0/2) \\
&& B &= \sqrt{\text{ch}\xi - \cos u_0} \\
\sigma_{out} &= \sigma_{in} + (V_0/4\pi R). \tag{4.1.21}
\end{aligned}$$

Installing A and B gives our final result for the bowl inner and outer charge densities:

$$\sigma_{in} = \frac{V_0}{4\pi^2 R} \left\{ \frac{\sqrt{\text{ch}\xi - \cos u_0}}{\sqrt{2} \cos(u_0/2)} - \tan^{-1} \left[\frac{\sqrt{\text{ch}\xi - \cos u_0}}{\sqrt{2} \cos(u_0/2)} \right] \right\}, \quad \sigma_{out} = \sigma_{in} + \frac{V_0}{4\pi R} \tag{4.1.22}$$

The bowl has label u_0 and (ξ, ϕ) vary on the bowl, but of course there is no azimuthal dependence. The bowl has radius R and is at potential V_0 relative to the Great Sphere at infinity where $V = 0$. We shall check this result by taking two important limits below, but first we verify (4.1.22) against some external sources.

4.2 Comparison with known results, and the small-hole limit

- Lebedev et al. (Problem Number 501 p 239) obtain the following result for σ_{in} ,

Ans. The charged density is

$$\sigma_i = \frac{V}{4\pi^2 a} \left[\frac{\sqrt{2 \cosh \alpha - 2 \cos \beta_0}}{2 \cos \frac{1}{2}\beta_0} - \arctan \frac{\sqrt{2 \cosh \alpha - 2 \cos \beta_0}}{2 \cos \frac{1}{2}\beta_0} \right]$$

on the inner surface of the bowl, and

$$\sigma_o = \sigma_i + \frac{V}{4\pi a}$$

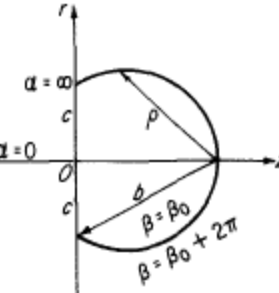


FIGURE 139

$$\sin \beta_0 = \frac{c}{a} \quad (4.2.1)$$

With the translations $a \rightarrow R$, $c \rightarrow a$, $\alpha \rightarrow \xi$ and $\beta_0 \rightarrow u_0$, this result is in agreement with (4.1.22) above.

- Kelvin (page 185) obtained the following result,

$$\rho = \frac{V}{2\pi^2 f} \left\{ \sqrt{\frac{\cos \alpha + 1}{\cos \eta - \cos \alpha}} - \tan^{-1} \sqrt{\frac{\cos \alpha + 1}{\cos \eta - \cos \alpha}} \right\} \dots (18), \quad (4.2.2)$$

To translate this to our notation, we take $\rho \rightarrow \sigma_{in}$ (surface charge), $f \rightarrow 2R$ (diameter), $\eta \rightarrow \pi - \theta$ (η and θ are shown in Figure (4.2.6) below), $\alpha \rightarrow \pi - u_0$, and $V \rightarrow V_0$. Then $\cos(\alpha) \rightarrow -\cos(u_0)$ and $\cos(\eta) \rightarrow -\cos(\theta)$ and Kelvin's result becomes,

$$\sigma_{in}^{(K)} = \frac{V_0}{4\pi^2 R} \left\{ \frac{\sqrt{1-\cos u_0}}{\sqrt{\cos u_0 - \cos \theta}} - \tan^{-1} \left[\frac{\sqrt{1-\cos u_0}}{\sqrt{\cos u_0 - \cos \theta}} \right] \right\}. \quad (4.2.3)$$

Replacing $\sqrt{1-\cos u_0} = \sqrt{2} \sin(u_0/2)$ this becomes the first line below, while our result is the second line,

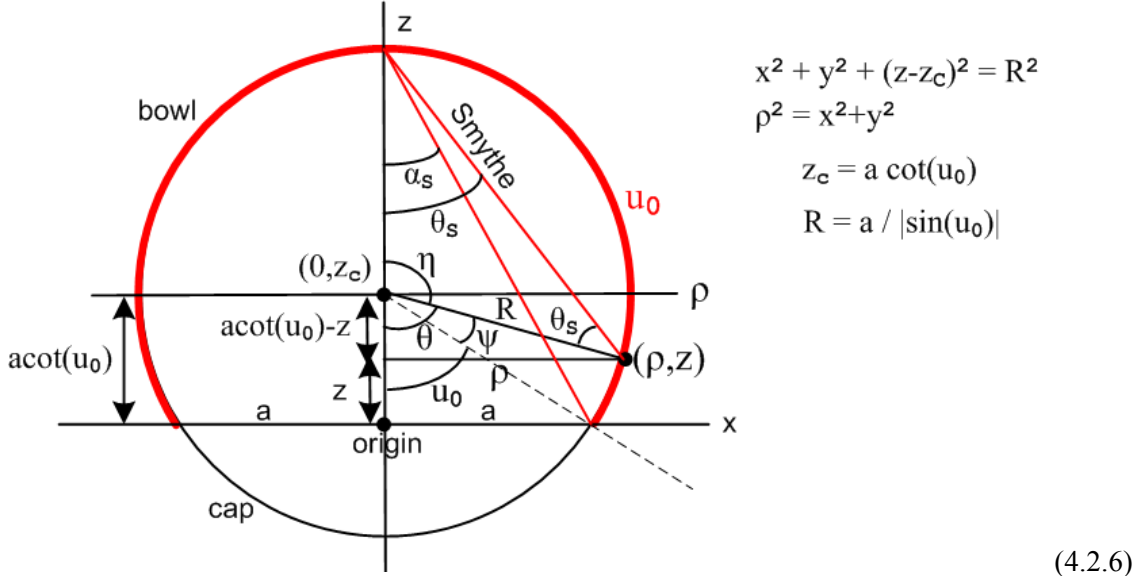
$$\sigma_{in}^{(K)} = \frac{V_0}{4\pi^2 R} \left\{ \frac{\sqrt{2} \sin(u_0/2)}{\sqrt{\cos u_0 - \cos \theta}} - \tan^{-1} \left[\frac{\sqrt{2} \sin(u_0/2)}{\sqrt{\cos u_0 - \cos \theta}} \right] \right\} \quad (4.2.4)$$

$$\sigma_{in} = \frac{V_0}{4\pi^2 R} \left\{ \frac{\sqrt{\cosh \xi - \cos u_0}}{\sqrt{2} \cos(u_0/2)} - \tan^{-1} \left[\frac{\sqrt{\cosh \xi - \cos u_0}}{\sqrt{2} \cos(u_0/2)} \right] \right\}. \quad (4.1.22)$$

We will show below that the following relation is true,

$$\frac{\sqrt{\cosh \xi - \cos u_0}}{\sqrt{2} \cos(u_0/2)} = \frac{\sqrt{2} \sin(u_0/2)}{\sqrt{\cos u_0 - \cos \theta}} \quad (4.2.5)$$

and therefore the above equations are the same. Consider the following drawing, where θ and η are complementary polar angles of a point of interest on the bowl,



This "bowl figure" is a bit complicated because it is trying to show many things at once. The small black right triangle shows that

$$\cos\theta = (\cot(u_0) - z) / R . \quad (4.2.7)$$

From box (1.2.17) we know that $z = a \sin u_0 / (\cosh \xi - \cos u_0)$ and $R = a / \sin u_0$. Inserting these into (4.2.7) and doing some brute-force algebra (this is typical of what one constantly does reading Kelvin's bowl paper), one finds that,

$$\cos\theta = [a \cot u_0 - a \sin u_0 / (\cosh \xi - \cos u_0)] / [a / \sin u_0]$$

$$\cos\theta = \sin u_0 [\cot(u_0) - \sin u_0 / (\cosh \xi - \cos u_0)] = \cos u_0 - \sin^2 u_0 / (\cosh \xi - \cos u_0)$$

$$\cos u_0 - \cos\theta = \sin^2 u_0 / (\cosh \xi - \cos u_0)$$

$$\sqrt{\cos u_0 - \cos\theta} = \sin(u_0) / \sqrt{\cosh \xi - \cos u_0} = 2 \sin(u_0/2) \cos(u_0/2) / \sqrt{\cosh \xi - \cos u_0}$$

$$\sqrt{\cos u_0 - \cos\theta} / [\sqrt{2} \sin(u_0/2)] = [\sqrt{2} \cos(u_0/2)] / \sqrt{\cosh \xi - \cos u_0} , \quad (4.2.8)$$

and inverting both sides gives (4.2.5).

- Smythe provides the following result (page 204 Problem 42, in SI units)

$$\sigma_i = \frac{\epsilon V_0}{\pi a} \left[\frac{\sin \alpha}{(\sin^2 \theta - \sin^2 \alpha)^{1/2}} - \sin^{-1} \frac{\sin \alpha}{\sin \theta} \right], \quad \sigma_o = \frac{\epsilon V_0}{a} + \sigma_i \quad (4.2.9)$$

Smythe's angles θ and α (we shall call them θ_s and α_s) are shown in Fig (4.2.6) above. Basic geometry of a chord tells us that $\theta_s = \theta/2$ and $\alpha_s = u_0/2$. Then,

$$\sin^2 \theta_s - \sin^2 \alpha_s = \sin^2(\theta/2) - \sin^2(u_0/2) = (1/2) [(1-\cos\theta) - (1 - \cos u_0)] = (\cos u_0 - \cos \theta)/2 \quad (4.2.10)$$

so Smythe's first term inside [...] is $\frac{\sqrt{2} \sin(u_0/2)}{\sqrt{\cos u_0 - \cos \theta}}$. Drawing a triangle, one easily shows that Smythe's \sin^{-1} expression can be written as \tan^{-1} of this first term. Dividing by $4\pi\epsilon$ to go to cgs units and taking $a \rightarrow R$ one then gets,

$$\sigma_{in}^{(s)} = \frac{V_0}{4\pi^2 R} \left[\frac{\sqrt{2} \sin(u_0/2)}{\sqrt{\cos u_0 - \cos \theta}} - \tan^{-1} \left(\frac{\sqrt{2} \sin(u_0/2)}{\sqrt{\cos u_0 - \cos \theta}} \right) \right] \quad (4.2.11)$$

which is the same as Kelvin's result (4.2.4).

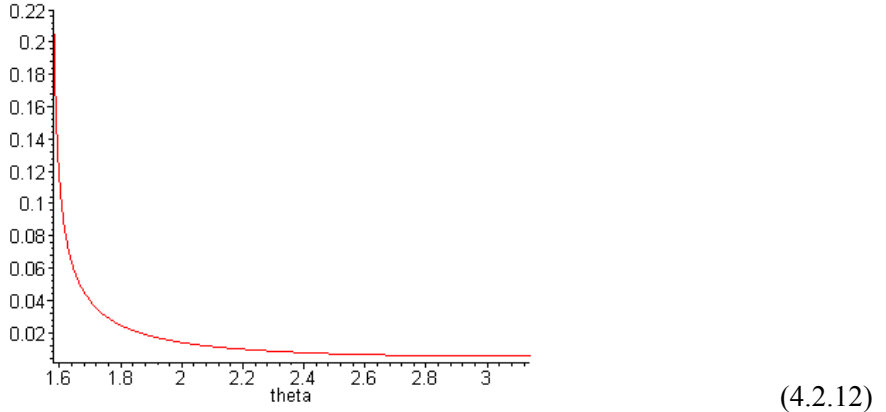
Plots of charge density: general case and small hole case

In Fig (4.2.6) the angle θ runs along the bowl surface from u_0 to π . Using (4.2.11) one can plot σ_{in} from the bowl edge to the bowl base center. The plots have a similar shape for any selection of u_0 , so here is the case of a hemispherical bowl with $u_0 = \pi/2$:

```

ratio := sqrt(2)*sin(u0/2)/sqrt(cos(u0)-cos(theta));
sigma := V/(4*Pi^2*R)*(ratio - arctan(ratio));
sigma := 1/4 * V * ( sqrt(2) * sin(pi/4) / sqrt(cos(pi/2) - cos(theta)) - arctan( sqrt(2) * sin(pi/4) / sqrt(cos(pi/2) - cos(theta)) ) )
pi^2 R
V := 1; R := 1;
u0 := Pi/2;
plot(sigma, theta = u0+.01..Pi);

```

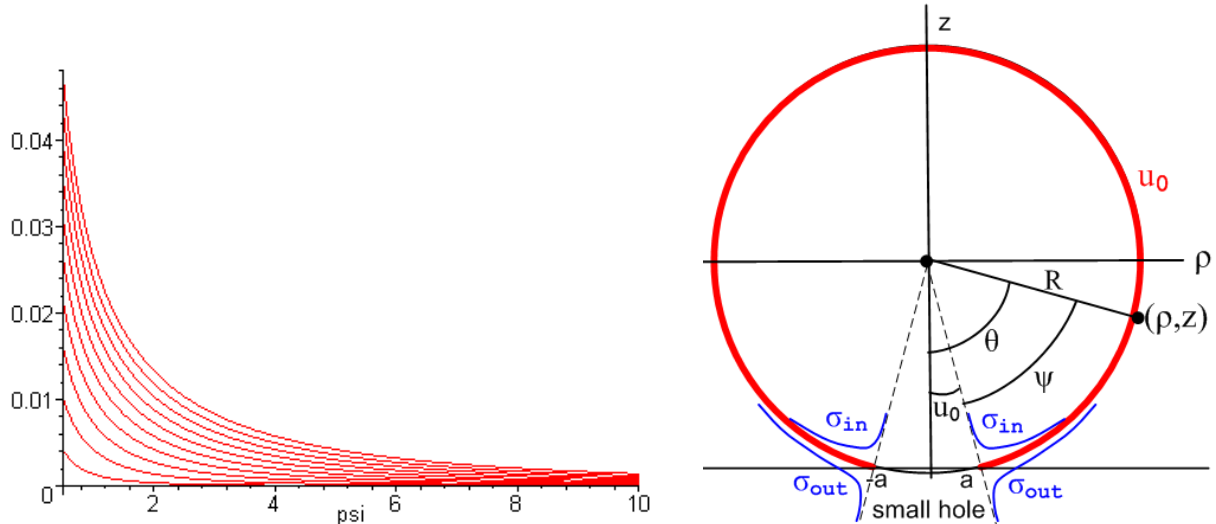


The charge density σ_{in} is infinite at the bowl edge $\theta = u_0$ and tapers off to a finite value at the bowl base center. Despite the edge singularity, the integrated charge density is finite. Notice that the graph starts off at $\theta = u_0 + .01$ to avoid the singularity.

What happens to the charge density σ_{in} on the inside of a bowl as the opening (hole) gets very small?

No matter how small u_0 (and the hole) gets, σ_{in} still blows up at the hole edge, according to (4.2.11), since $\theta = u_0$ at the hole edge. It is helpful to define $\psi = \theta - u_0$ so $\psi = 0$ at the bowl edge. Using (4.2.11), we plot $\sigma_{in}(\psi)$ (in degrees) for holes which subtend 1 to 10 degrees polar angle u_0 : (plots start at $\psi = 0.5^\circ$)

```
u0 := (n/180)*Pi;
theta := u0+psi*(Pi/180);
plot([seq(sigma, n=1..10)], psi = .5..10, color=red);
```



The lowest curve is for a tiny 1 degree hole and one sees that most of σ_{in} is piled up within 2 degrees of angle going into the bowl from the hole edge. It is this distance that gets smaller as the hole closes up, and the integrated charge on the bowl interior decreases toward 0. According to (4.1.15) $\sigma_{out} = \sigma_{in} + \text{constant}$, so the outer charge density has a similar shape but with a constant tail.

4.3 The full-sphere and flat-disk limits of σ

The Full Sphere Limit

The limit of interest here is $u_0 \rightarrow 0$. Rather than let the bowl become large, we force R to maintain its value by taking $a \rightarrow 0$ as well in such a way that $R = a/\sin u_0$ stays constant. In terms of the drawing (4.2.6), the red bowl rises up vertically until it just touches the x -axis. Since focal points $x = \pm a$ have moved way in to the origin, when one draws the constant ξ circles, only those large ones with $\xi \approx 0$ intersect the red bowl at finite points away from the origin. So the point is that $\xi \rightarrow 0$ as well in this limit so $\operatorname{ch} \xi \rightarrow 1$. Formally, from box (1.2.17) one has $\xi = \tanh^{-1}[2ap/(\rho^2+z^2+a^2)]$ and $R = a/|\sin u_0|$ so,

$$\begin{aligned}\xi &= \tanh^{-1}[2ap/(\rho^2+z^2+a^2)] = \tanh^{-1}[2 R |\sin u_0| \rho / (\rho^2 + z^2 + R^2 \sin^2 u_0)] \\ &\approx 2 R |\sin u_0| * \rho / (\rho^2 + z^2) \rightarrow 0 \text{ as } u_0 \rightarrow 0 .\end{aligned}\quad (4.3.1)$$

But of course $\cos u_0 \rightarrow 1$ as well, so that $\sqrt{\operatorname{ch} \xi - \cos u_0} \rightarrow 0$. Looking then at (4.1.22),

$$\sigma_{in} = \frac{V_0}{4\pi^2 R} \left\{ \frac{\sqrt{\operatorname{ch} \xi - \cos u_0}}{\sqrt{2} \cos(u_0/2)} - \tan^{-1} \left[\frac{\sqrt{\operatorname{ch} \xi - \cos u_0}}{\sqrt{2} \cos(u_0/2)} \right] \right\}, \quad (4.1.22)$$

since $\sqrt{\operatorname{ch} \xi - \cos u_0} / (\sqrt{2} \cos(u_0/2)) \approx \sqrt{\operatorname{ch} \xi - \cos u_0} / (\sqrt{2}) \rightarrow 0$, and since $\tan^{-1} x \approx x$ for small argument, the two terms cancel near the limit, in addition to each going to 0 at the limit, so without question one has $\sigma_{in} \rightarrow 0$, as appropriate for a full sphere held at a constant potential.

Meanwhile, from (4.1.21) we have $\sigma_{out} = \sigma_{in} + (V_0/4\pi R) = (V_0/4\pi R)$ uniformly on the outer surface of the sphere. The total charge Q on the sphere is then $Q = 4\pi R^2 (V_0/4\pi R) = V_0 R$, as appropriate for a sphere which has the known capacitance $C = R$.

The Flat Disk Limit

Working backwards, we start with the known charge density on a charged disk of radius a ,

$$\sigma(\rho) = (V/\pi^2) / \sqrt{a^2 - \rho^2} . \quad // \text{sum of charge density on both sides, cgs units} \quad (4.3.2)$$

This result may be found on page 64 (3.1.7) of Sneddon, and on page p 93 of green Jackson (3.179) with $V = q\pi/2a$ on page 92. Below we shall be taking the limit $u_0 \rightarrow \pi$ which causes $\cos u_0 \rightarrow -1$. Going ahead with this limit, and using (1.2.2) that $\rho = a \operatorname{sh} \xi / (\operatorname{ch} \xi - \cos u_0) = a \operatorname{sh} \xi / (\operatorname{ch} \xi + 1)$ one finds,

$$a^2 - \rho^2 = a^2 [1 - \operatorname{sh}^2 \xi / (\operatorname{ch} \xi + 1)^2] = a^2 [(\operatorname{ch} \xi + 1)^2 - \operatorname{sh}^2 \xi] / (\operatorname{ch} \xi + 1)^2 = 2a^2 / (\operatorname{ch} \xi + 1) . \quad (4.3.3)$$

Then the hoped-for disk limit is the following,

$$\sigma(\xi) = (V/a\pi^2) (1/\sqrt{2}) \sqrt{\operatorname{ch} \xi + 1} . \quad // \text{sum of both sides} \quad (4.3.4)$$

Visually, the red bowl in Fig (4.2.6) deflates like a soap bubble until it becomes a red disk between the two focal points $\pm a$, see Fig (1.1.2a).

As is clear from (4.3.2), the disk charge density blows up at the disk edge as $\rho \rightarrow a$, and takes the finite value ($V/\pi^2 a$) at disk center. The same behavior is seen in (4.3.4): At the disk edge, very tiny ξ circles intersect the region of the disk edge, and tiny means $\xi \rightarrow \infty$ so (4.3.4) blows up as well. At disk center only ξ circles with $\xi \approx 0$ intersect the central disk region so we find $\sigma(\xi) = (V/a\pi^2) (1/\sqrt{2}) \sqrt{1+1} = (V/a\pi^2)$, the same constant value.

Now that we have established (4.3.4) as our *desired* result, we take the $u_0 \rightarrow \pi$ limit of (4.1.22) to see if we obtain that result. To have a visible limit, we set $u_0 = \pi - \varepsilon$ and then we later take $\varepsilon \rightarrow 0$. In this limit,

$$\begin{aligned} \cos(u_0) &\rightarrow -1 & u_0 &= \pi - \varepsilon \\ \cos(u_0/2) &= \cos(\pi/2 - \varepsilon/2) = \sin(\varepsilon/2) \approx \varepsilon/2 \\ \sin(u_0) &= \sin(\pi - \varepsilon) = +\sin(\varepsilon) \approx \varepsilon . \end{aligned} \quad (4.3.5)$$

We must replace $1/R = \sin u_0/a \approx \varepsilon/a$ since R is going to infinity. Then starting with (4.1.22),

$$\begin{aligned} \sigma_{\text{in}} &= \frac{V_0}{4\pi^2 R} \left\{ \frac{\sqrt{\text{ch}\xi - \cos u_0}}{\sqrt{2} \cos(u_0/2)} - \tan^{-1} \left[\frac{\sqrt{\text{ch}\xi - \cos u_0}}{\sqrt{2} \cos(u_0/2)} \right] \right\} \\ &\approx \frac{V_0 \varepsilon}{4\pi^2 a} \left\{ \frac{\sqrt{\text{ch}\xi + 1}}{\varepsilon/\sqrt{2}} - \tan^{-1} \left[\frac{\sqrt{\text{ch}\xi + 1}}{\varepsilon/\sqrt{2}} \right] \right\} \approx \frac{V_0 \varepsilon}{4\pi^2 a} \left\{ \frac{\sqrt{\text{ch}\xi + 1}}{\varepsilon/\sqrt{2}} - \pi/2 \right\} \\ &= \frac{V_0}{4\pi^2 a} \left\{ \sqrt{2} \sqrt{\text{ch}\xi + 1} - \varepsilon\pi/2 \right\} \approx \frac{V_0}{4\pi^2 a} (\sqrt{2} \sqrt{\text{ch}\xi + 1}) \\ &= \frac{V_0}{2\sqrt{2} \pi^2 a} \sqrt{\text{ch}\xi + 1} . \end{aligned} \quad (4.3.6)$$

Notice that σ_{in} is the surface charge on the lower side of the disk. On the upper side (4.1.15) says $\sigma_{\text{out}} = \sigma_{\text{in}} + (V_0/4\pi R)$, but since $R \rightarrow \infty$ we get $\sigma_{\text{out}} = \sigma_{\text{in}}$, as symmetry requires. Then,

$$\sigma = 2\sigma_{\text{in}} = \frac{V_0}{\sqrt{2} \pi^2 a} \sqrt{\text{ch}\xi + 1} \quad // \text{ both sides} \quad (4.3.7)$$

and this agrees with our expectation (4.3.4).

4.4 Bowl capacitance

The bowl capacitance was inadvertently obtained in (2.5.17) in taking the large- r limit of the bowl potential (2.4.14) expressed in elementary functions. Here we repeat this calculation working directly with the Mehler integral form of the potential (2.4.13),

$$V(\xi, u) = V_0 \sqrt{2} \sqrt{\text{ch}\xi - \cos u} \int_0^\infty d\tau P_{i\tau-1/2}(\text{ch}\xi) \text{ch}[(\pi - u_0)\tau] \text{ch}[(\pi + u_0 - u)\tau] / \text{ch}^2(\pi\tau) . \quad (4.4.1)$$

To find the capacitance of the bowl, we study the potential "far away". From (1.2.9) we know that the large-r region corresponds to $\xi \ll 1$ and $u = 2\pi + \varepsilon$ with $|\varepsilon| \ll 1$. In this region, since $P_{i\tau-1/2}(1) = 1$ from (H.7.2), the above integral becomes,

$$\begin{aligned} & \int_0^\infty d\tau P_{i\tau-1/2}(\text{ch}\xi) \text{ch}[(\pi-u_0)\tau] \text{ch}[(\pi+u_0-u)\tau] / \text{ch}^2(\pi\tau) \\ & \approx \int_0^\infty d\tau \text{ch}[(\pi-u_0)\tau] \text{ch}[(\pi+u_0-2\pi)\tau] / \text{ch}^2(\pi\tau) = \int_0^\infty d\tau \text{ch}^2[(\pi-u_0)\tau] / \text{ch}^2(\pi\tau) \\ & = (1/2\pi) 2 \int_0^\infty dx \text{ch}^2[(1-u_0/\pi)x] / \text{ch}^2(x) . \quad // x = \pi\tau, dx = \pi d\tau \end{aligned} \quad (4.4.2)$$

The following integral is evaluated in Appendix H.3,

$$2 \int_0^\infty dx \text{ch}^2(bx) / \text{ch}^2(x) = [\pi b / \sin(\pi b) + 1] . \quad 0 < |b| < 1 \quad (H.3.1)$$

Apply this with $b = (1-u_0/\pi)$ to find,

$$\begin{aligned} 2 \int_0^\infty dx \text{ch}^2[(1-u_0/\pi)x] / \text{ch}^2(x) &= \pi(1-u_0/\pi) / \sin(\pi(1-u_0/\pi)) + 1 = (\pi-u_0) / \sin(\pi-u_0) + 1 \\ &= (\pi-u_0) / \sin u_0 + 1 . \end{aligned} \quad (4.4.3)$$

Therefore the integral in (4.4.1) has the following very simple evaluation,

$$\begin{aligned} \int_0^\infty d\tau P_{i\tau-1/2}(\text{ch}\xi) \text{ch}[(\pi-u_0)\tau] \text{ch}[(\pi+u_0-u)\tau] / \text{ch}^2(\pi\tau) &\approx (1/2\pi) [(\pi-u_0) / \sin u_0 + 1] \\ &= (1/2\pi) [(\pi-u_0) + \sin u_0] / \sin u_0 . \end{aligned} \quad (4.4.4)$$

Meanwhile, from (1.2.11), (1.2.14) and (1.2.15) we know that in the large r region,

$$\sqrt{2} \sqrt{\text{ch}\xi - \cos u} \approx \sqrt{2} \sqrt{(\xi^2 + \varepsilon^2)/2} = \sqrt{\xi^2 + \varepsilon^2} = \sqrt{1 + \rho^2/z^2} \varepsilon \approx 2a/r . \quad (4.4.5)$$

Therefore (4.4.1) with (4.4.4) may be written,

$$\begin{aligned} V(\xi, u) &= V_0 \sqrt{2} \sqrt{\text{ch}\xi - \cos u} \int_0^\infty d\tau P_{i\tau-1/2}(\text{ch}\xi) \text{ch}[(\pi-u_0)\tau] \text{ch}[(\pi+u_0-u)\tau] / \text{ch}^2(\pi\tau) \\ &\approx V_0 (2a/r) (1/2\pi) [(\pi-u_0) + \sin u_0] / \sin u_0 \\ &= V_0 (a/r \sin u_0) (1/\pi) [(\pi-u_0) + \sin u_0] . \end{aligned} \quad (4.4.6)$$

But from (1.2.6) one has $R = a/|\sin u_0|$ so then, assuming $0 \leq u_0 \leq \pi$,

$$\begin{aligned} V(\xi, u) &= V_0 (R/r) (1/\pi) [(\pi - u_0) + \sin u_0] \\ &= (V_0/r) (R/\pi) [(\pi - u_0) + \sin u_0]. \end{aligned} \quad (4.4.7)$$

Far away the bowl looks like a point charge $Q = CV_0$ with potential $V = Q/r$. Thus

$$V = Q/r = (CV_0)/r = (V_0/r) C. \quad (4.4.8)$$

Comparing the last two equations one reads off that

$$C = (R/\pi) [(\pi - u_0) + \sin u_0]. \quad // \text{capacitance of bowl } u_0 \quad (4.4.9)$$

Defining $\beta = \pi - u_0$ as the "bowl angle" from base to lip as in Fig (1.2.1), one has $\sin \beta = \sin u_0$ so

$$C = (R/\pi) (\beta + \sin \beta) \quad // \text{SI units: } C = 4\epsilon_0 R(\beta + \sin \beta) \quad (4.4.10)$$

This result agrees with (2.5.17) and the SI unit version agrees with Smythe p 204 Prob. 41.

Disk limit: Replace $R = a/\sin u_0$ in (4.4.9) to get

$$\begin{aligned} C &= (a/\pi) [(\pi - u_0) + \sin u_0] / \sin u_0 \\ &= (a/\pi) [(\pi - u_0)/\sin(\pi - u_0) + 1]. \end{aligned} \quad (4.4.11)$$

The disk is the limit of the bowl as $u_0 \rightarrow \pi$ as is clear from the left side of Fig (1.1.2). As $u_0 \rightarrow \pi$ the bowl deflates and ends up being a disk in the mouth of the former bowl. In this limit the first term in (4.4.11) is $\sin x/x \rightarrow 1$ and the result is

$$C_{\text{disk}} = (2a/\pi). \quad (4.4.12)$$

This agrees with green Jackson page 92.

Full sphere limit: Again as shown in Fig (1.1.2), the full bowl is a "big bowl" as $u_0 \rightarrow 0$ and one finds from (4.4.9) that

$$C_{\text{sphere}} = (R/\pi) [(\pi - u_0) + \sin u_0] = (R/\pi) [(\pi - 0) + 0] = R \quad (4.4.13)$$

which is the correct result for the capacitance of a sphere of radius R in cgs units.

5. Plots of the toroidal coordinates $u(\rho,z)$ and $\xi(\rho,z)$

The u coordinate

Recall from box (1.2.17) the equation

$$u = \tan^{-1} [2az / (\rho^2 + z^2 - a^2)] . \quad (5.1)$$

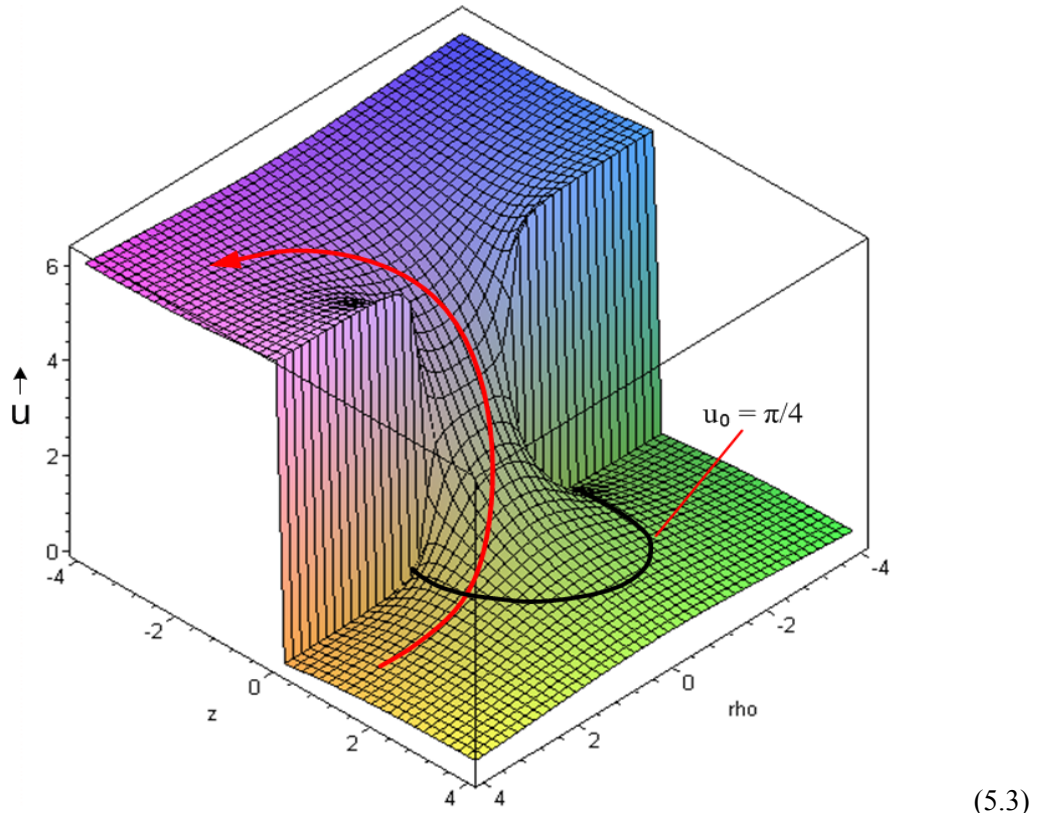
This is a misleading equation because it implies that u lies on the principle branch of the function \tan^{-1} which then gives $-\pi/2 < u < \pi/2$. One should in fact interpret the above equation in this operational sense, using other equations in box (1.2.17):

1. Compute $\xi = \tanh^{-1} [2ap / (\rho^2 + z^2 + a^2)]$
 2. Compute $\cos u = \operatorname{ch} \xi - (a/\rho) \operatorname{sh} \xi \quad // \text{from } \rho = a \operatorname{sh} \xi / (\operatorname{ch} \xi - \cos u)$
 3. Compute $\sin u = (z/\rho) \operatorname{sh} \xi$
 4. Compute $u = \operatorname{arctan2Pi}(\cos u, \sin u) \quad // \operatorname{arctan2Pi}(x,y) \sim \tan^{-1}(y/x)$
- (5.2)

where $\operatorname{arctan2Pi}(x,y)$ is a function of two arguments which returns an angle in the range $(0, 2\pi)$. The Maple code for this function is shown in (9.2) below.

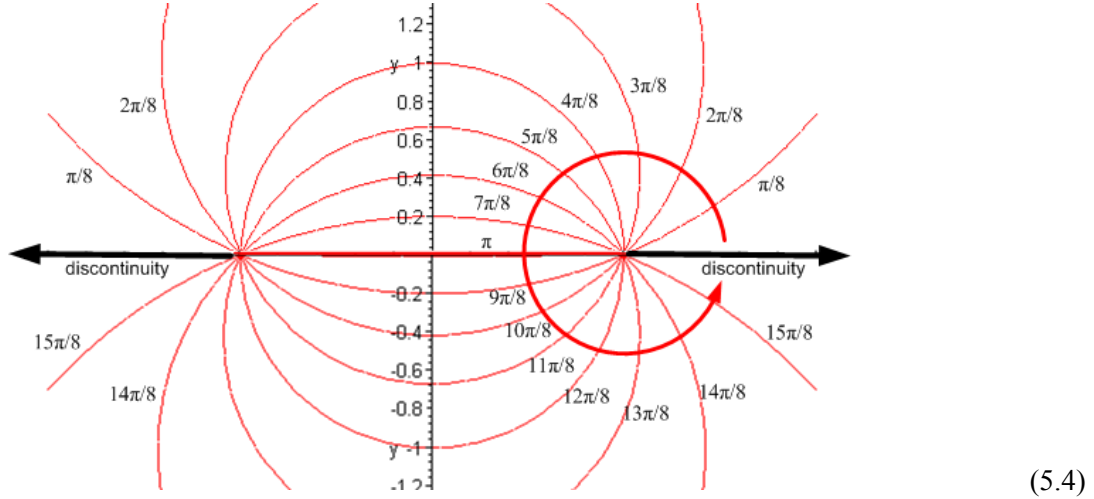
Here then is a plot of the function $u(\rho,z)$ for u in the standard range $0 \leq u \leq 2\pi$:

```
u := arctan2Pi(rho^2+z^2-a^2, 2*a*z);
a := 1;
plot3d(u, rho = -4..4, z = -4..4, axes=BOXED, grid=[50,50], scaling = constrained);
```



The black curve shows the locus in the (ρ, z) plane of a particular value $u = u_0 = \pi/4$. Near this black locus the plotted surface is very smooth. On the other hand, there are vertical cliffs on the $z = 0$ axis for $\rho > 1$ and $\rho < -1$.

The red arrow shows a hiking path from the lower level $u = 0$ to the upper level $u = 2\pi$. This path corresponds to the red path in the ρ - z plane below, where we have now combined the two parts of Fig (1.1.2),



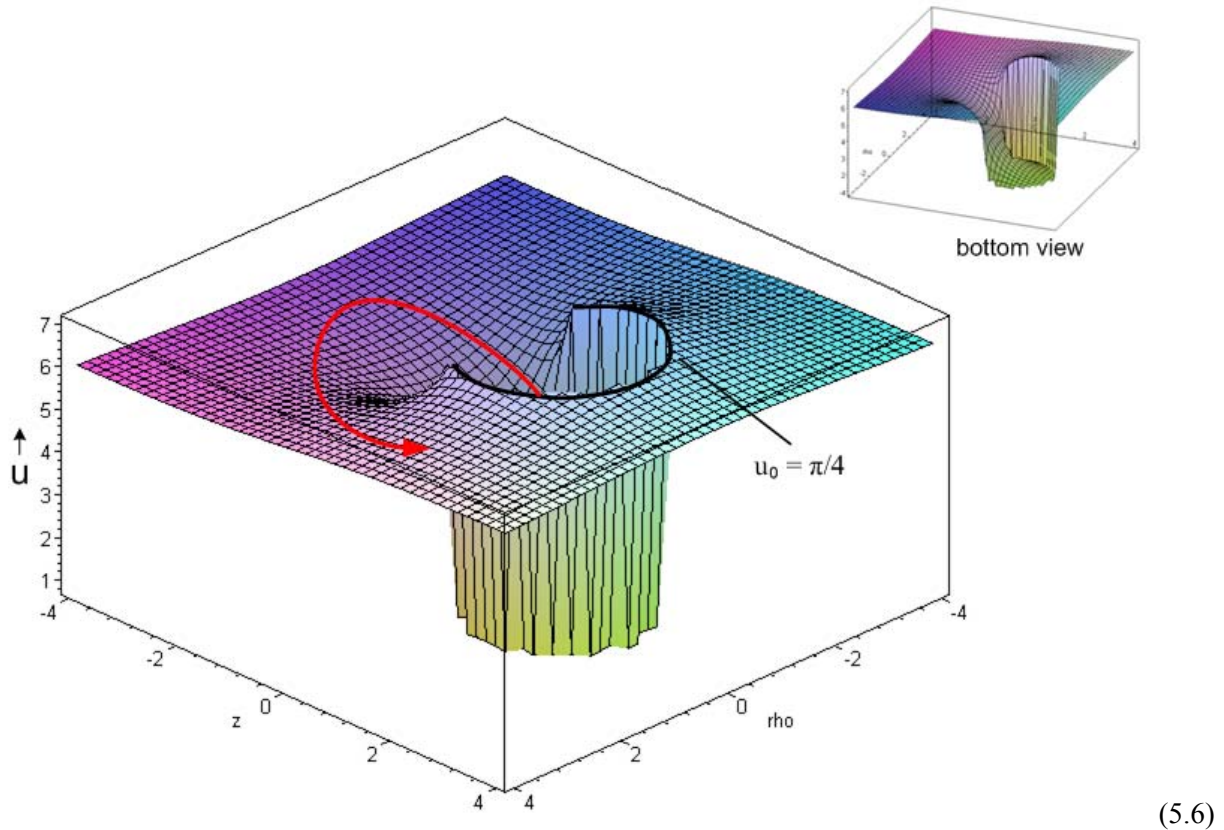
The vertical cliffs in (5.3) correspond to the discontinuities in (5.4).

In the treatment of a bowl of label u_0 , we use the range $u_0 \leq u \leq u_0 + 2\pi$, and compute this as follows in the get(u) function of (9.4),

```
u = arctan2Pi(cosu,sinu);           // the old u(rho,z)
if u < u0 then u := u+2pi;          // the new u(rho,z)      (5.5)
```

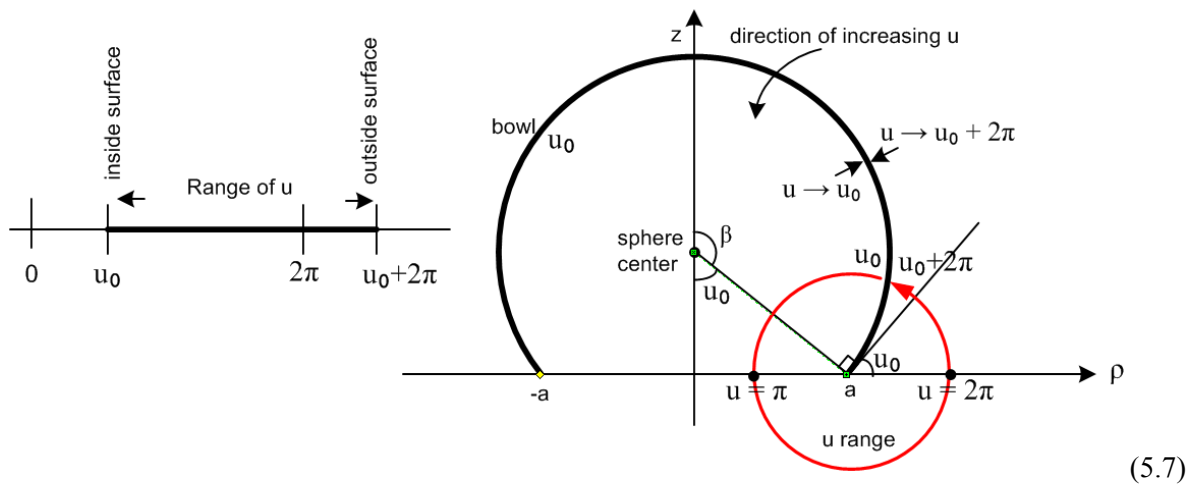
Here then is a plot of this new $u(\rho, z)$ where we select $u_0 = \pi/4$:

```
u := getu(rho,z);
plot3d(u, rho = -4..4, z = -4..4, axes=BOXED, grid = [50,50]);
```



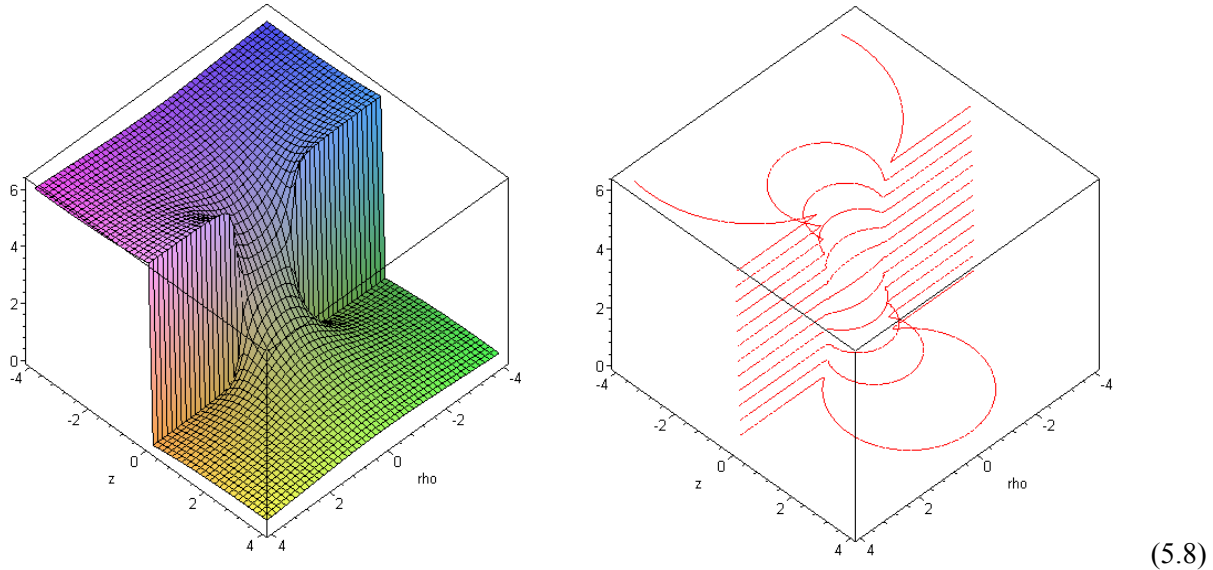
The same black $u_0 = \pi/4$ locus is shown, but now it represents the circular edge of Niagara Falls. The new function $u(\rho, z)$ has a discontinuity: it has value $u = \pi/4$ at the foot of the falls and a value $u = \pi/4 + 2\pi$ at the top of the falls. In terms of the bowl, u has a value of $\pi/4$ on its inner surface and $\pi/4 + 2\pi$ on its outer surface. The red arrow in Fig (5.6) shows a new hiking path from the lower level $u = \pi/4$ to the upper level $u = \pi/4 + 2\pi$.

As a reminder, here is Fig (1.2.1) showing the range $(u_0, u_0 + 2\pi)$ in the (ρ, z) plane:



The red hiking path in (5.6) corresponds roughly to the red path in (5.7).

To make the connection between Fig (5.3) and Fig (1.1.2) showing curves of constant u , we recall Fig (5.3) on the left below, then display that in "contour style" on the right.



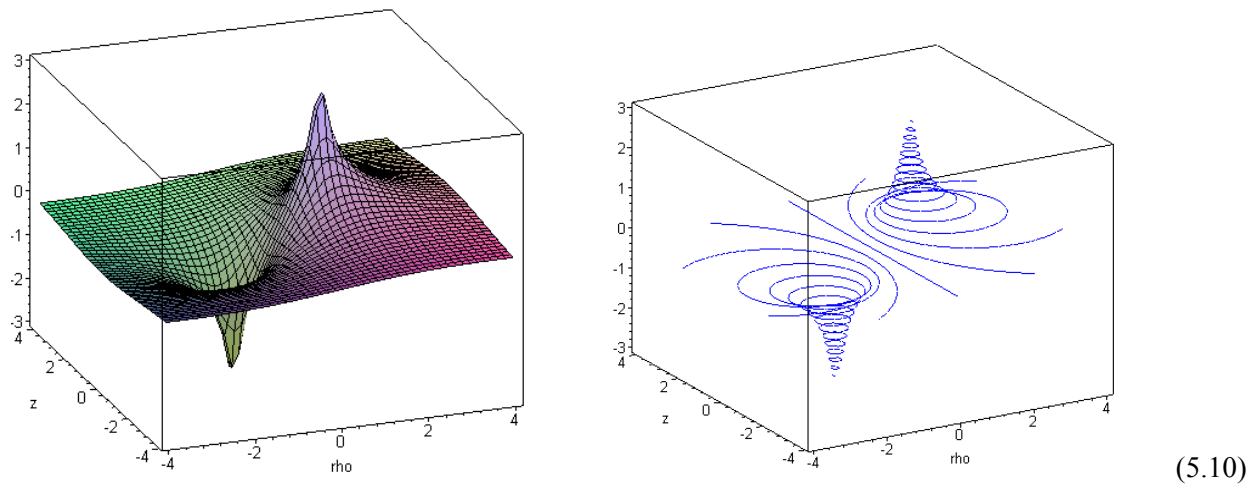
The ξ coordinate

Recall from box (1.2.17) the equation

$$\xi = \tanh^{-1} \left[\frac{2ap}{\rho^2 + z^2 + a^2} \right]. \quad (5.9)$$

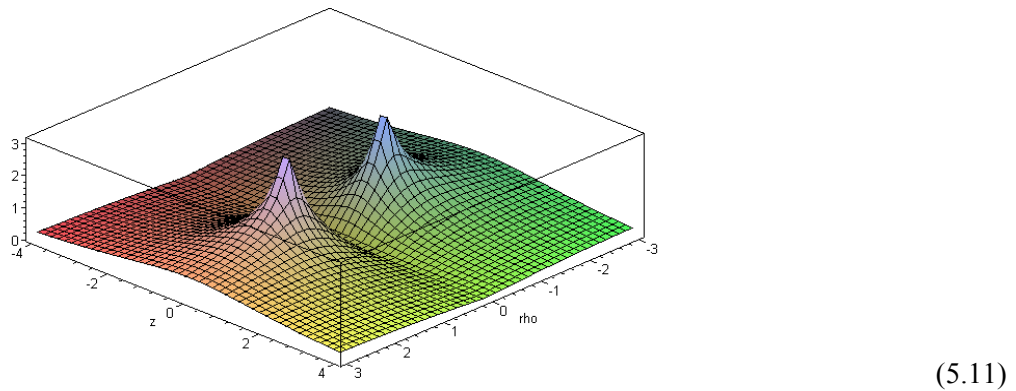
Here is a plot of $\xi(\rho, z)$ for the same argument ranges used above,

```
xi := arctanh(2*a*rho/(a^2+rho^2+z^2));
plot3d(xi, rho = -4..4, z = -4..4, axes=BOXED, grid =[50,50],
style = patch, contours = 20, scaling = constrained);
```



The peaks at the two focal points are infinite, though this plot cannot display that fact. The contour plot on the right appears as Fig (1.1.3) when viewed from the top.

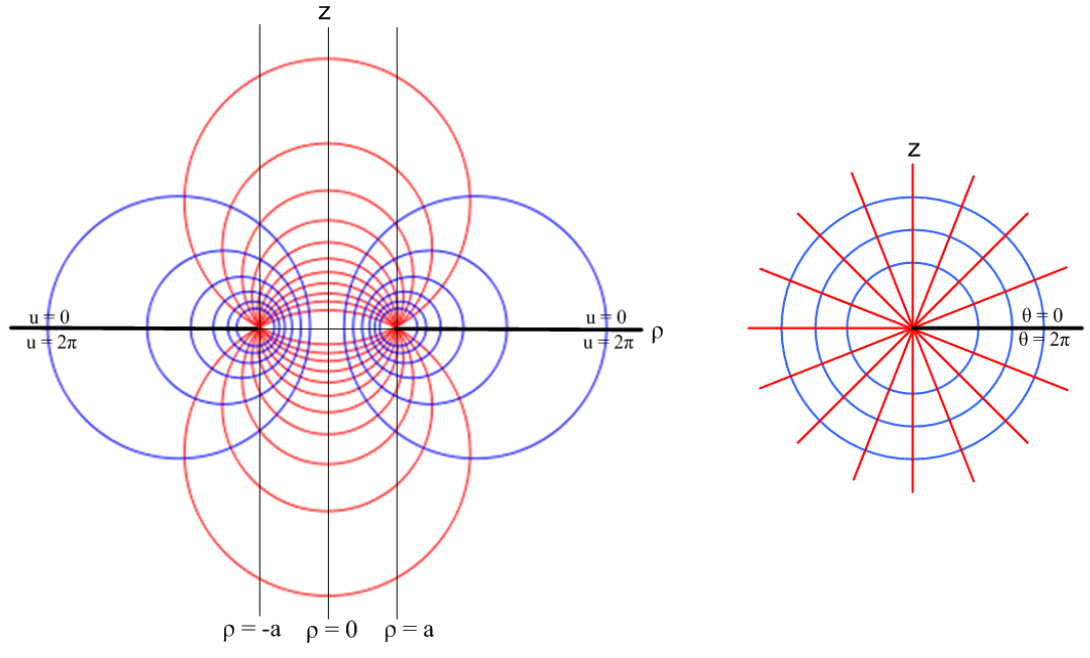
A plot of $|\xi|$ better reveals that fact that $\xi = 0$ along the line $\rho = 0$:



Spherical Coordinates r and θ

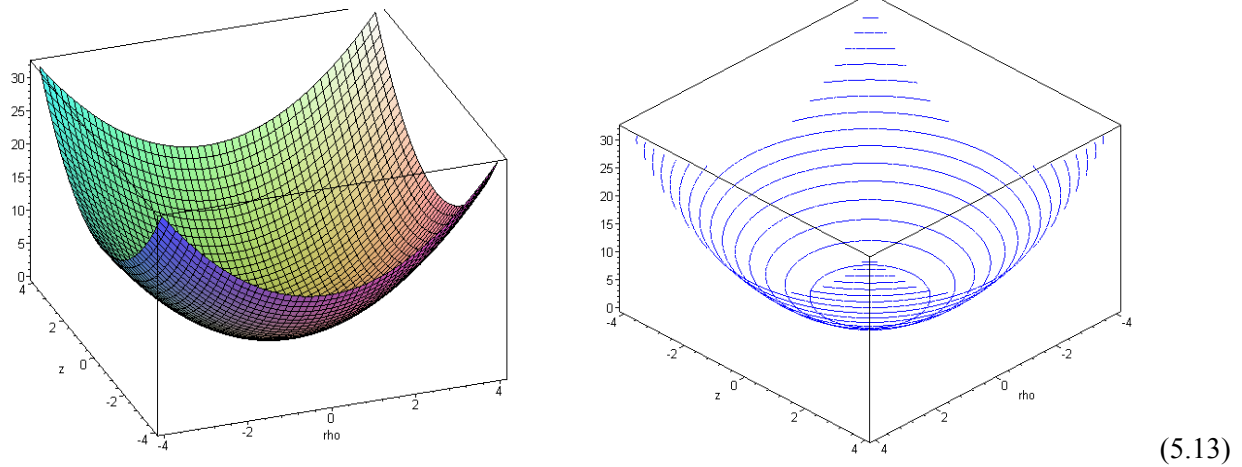
The plots (5.8) for $u(\rho, z)$ and (5.10) for $\xi(\rho, z)$ seem a bit strange. These plots show surfaces constructed by stacking the level curves of the 2D bipolar coordinate system. In each "stack", the height of the level curve is the label attached to that level curve. In the case of u , the vertical headwall of (5.8) or the waterfall of (5.6) show areas of discontinuity of u .

A more familiar situation arises with spherical coordinates (r, θ, ϕ) generated by rotating 2D polar coordinates (r, θ) . Here we show the bipolar level curves on the left, and the polar ones on the right. In each case, any locus of discontinuity in a coordinate is shown in black.

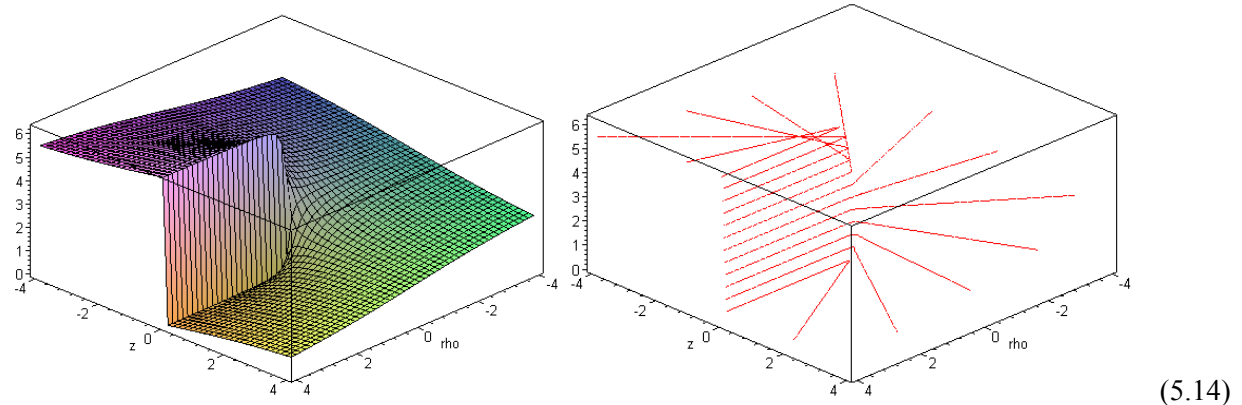


In each case, rotation about the vertical z axis generates a 3D coordinate system, toroidal on the left and spherical on the right. The level surfaces on the left are bowls and tori, while on the right they are spheres and cones. For spherical coordinates we can plot $r(\rho, z)$ and $\theta(\rho, z)$ as follows:

```
r := rho^2+z^2;
plot3d(r, rho = -4..4, z = -4..4, axes=BOXED,grid=[50,50],scaling = unconstrained);
```



```
theta := arctan2Pi(rho,z);
plot3d(theta, rho = -4..4, z = -4..4, axes=BOXED,grid=[50,50],scaling = unconstrained);
```



Again, in each case the surface on the left is formed by stacking the level curves on the right, where the height of each level curve equals the label of that curve. The headwall (cliff) in (5.14) results from the black discontinuity in (5.12).

6. A selection of charged bowl potential plots

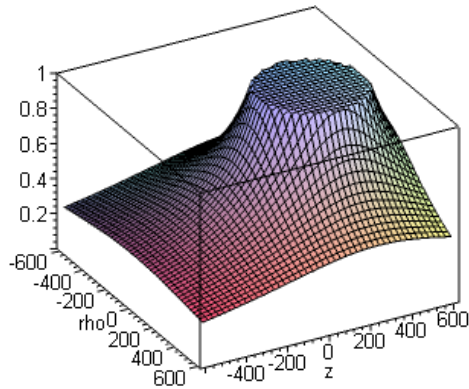
For a graph of the surface $z = f(x,y)$ the gradient $\nabla_{2D}f = (\partial_x f, \partial_y f)$ points in a 2D direction in the (x,y) plane which directs one locally uphill on the surface. This is so because $df = \nabla_{2D}f \bullet d\mathbf{r}_{2D}$ is a maximum when one's displacement $d\mathbf{r}_{2D}$ is aligned with $\nabla_{2D}f$.

Applying this to the potential function surface $V = V(\rho,z)$, one concludes that the electric field $\mathbf{E} = -\nabla_{2D}V$ is a 2D vector in the (ρ,z) plane which directs one downhill on the surface. The steeper the downhill slope at any point, the larger the 2D electric field : $\mathbf{E} = (E_\rho, E_z) = (-\partial_\rho V, -\partial_z V)$. Since the bowl is azimuthally symmetric, there is no \mathbf{E} field in the $\hat{\phi}$ direction.

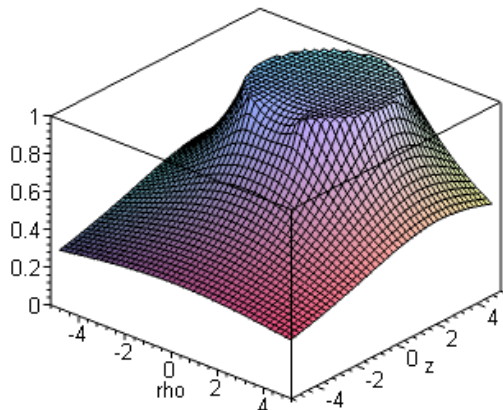
Thus, in the following graphs, one can regard the electric field as pointing in the 2D direction which is the projection of the 3D downhill surface vector onto the ρ,z plane. So generally the \mathbf{E} field points away from the bowl, as one would expect for a positively charged bowl with $V_0 > 0$. The field is strongest where the surface slope is largest. Not surprisingly, the slope is steepest right at the bowl surface.

Here then are plots of $V(\rho,z)$ for several values of the bowl parameter u_0 . Recall the rubber sheet comment below (2.4.15). The second plot ($u_0 = \pi/8$) shows the nature of the potential for a sphere with a relatively small hole.

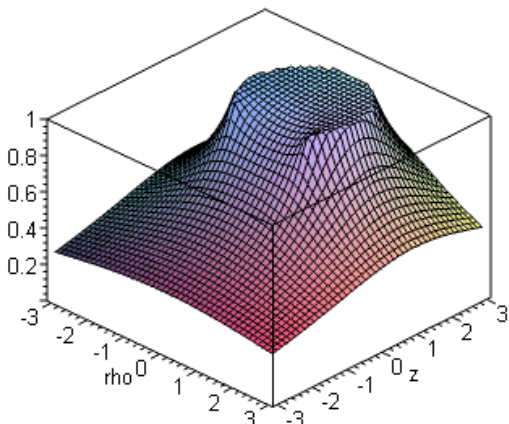
$u_0 = .01\pi/8$: (basically, $u_0 = 0$)



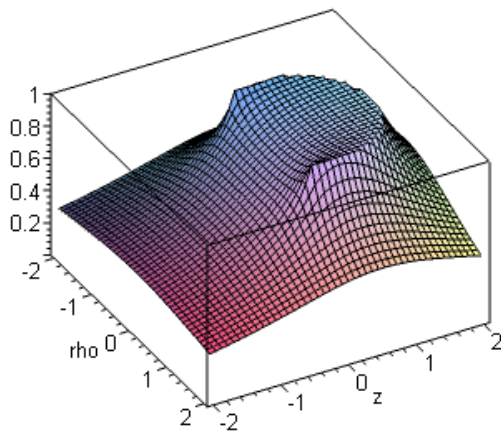
$u_0 = \pi/8$: a bowl that is almost a complete sphere



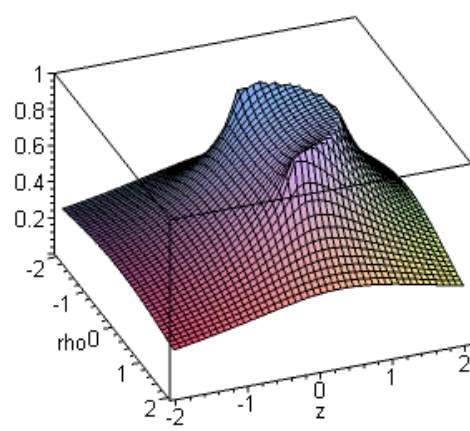
$u_0 = 2\pi/8$:



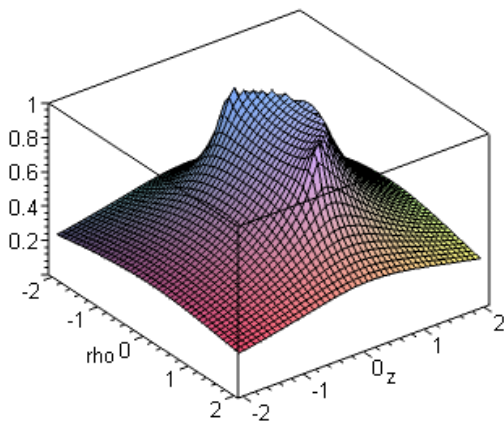
$u_0 = 3\pi/8$:



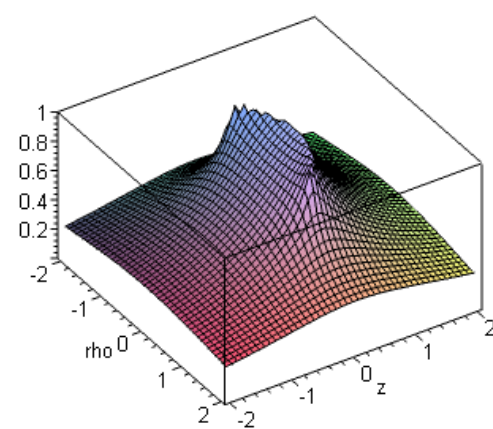
$u_0 = 4\pi/8$, the hemispherical bowl



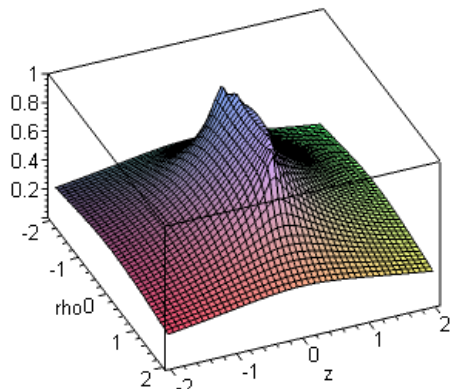
$u_0 = 5\pi/8$



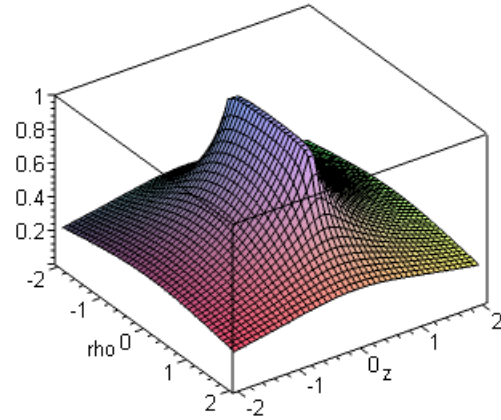
$u_0 = 6\pi/8$



$u_0 = 7\pi/8$, a very shallow bowl



$u_0 = \pi$, potential of a disk



When $u_0 = \pi$, the bowl slice becomes the line between the two foci, and the bowl becomes a perfect disk of radius a . So built into this problem solution is an exact plot of the disk potential.

7. Mehler integrals

7.1 List of useful Mehler integrals

Mehler integration is the seamy underside of using toroidal coordinates in the Mehler function atomic forms (2.2.3) (2), and is worth some comment. The general form of a "Mehler integral" is this,

$$g(y) = \int_0^\infty d\tau P_{i\tau-1/2}(y) f(\tau) . \quad y \geq 1 \quad (2.4.1)$$

About the best we can do for $P_{i\tau-1/2}$ is a form like

$$P_v(ch\xi) = e^{\xi v} F(v, 1/2; 1; 1 - e^{-2\xi}) \quad // Bateman (28) [EH I p 128]$$

so

$$P_{i\tau-1/2}(ch\xi) = e^{-(1/2)\xi} e^{i\xi\tau} F(1/2-i\tau, 1/2; 1; 1 - e^{-2\xi})$$

which at least isolates the variable τ into just one of the hypergeometric function's parameter arguments. But even so, there is very little literature available on such integrals, so changing from P to F really buys little. There are some integrals of $P_{i\tau-1/2}(y) f(\tau)$ appearing in the literature (see below), but one often has to do one's own integrals.

The starting point for doing a Mehler integral is to elevate P into some integral representation, such as

$$P_{i\tau-1/2}(cha) = (\sqrt{2}/\pi) \int_0^\alpha dx \cos(\tau x) / \sqrt{cha - chx} \quad (L.I.2)$$

$$P_{i\tau-1/2}(y) = (\sqrt{2}/\pi) ch(\pi\tau) \int_0^\infty dx \cos(\tau x) / \sqrt{y + chx} \quad (L.3.5)$$

which exposes a simple τ dependence. The τ integration can then usually be done, and one is faced with the final x integration which can hopefully be looked up somewhere. The following Mehler integrals are derived in Appendix L :

$$\int_0^\infty d\tau P_{i\tau-1/2}(y) = \frac{1}{\sqrt{2}} \frac{1}{\sqrt{y-1}} \quad (7.1.1)$$

$$\int_0^\infty d\tau P_{i\tau-1/2}(y) \cos(a\tau) = \frac{1}{\sqrt{2}} \frac{1}{\sqrt{y-cha}} \text{Heaviside}(y-cha) \quad (7.1.2)$$

$$\int_0^\infty d\tau P_{i\tau-1/2}(y) \cos(a\tau) / ch(\pi\tau) = \frac{1}{\sqrt{2}} \frac{1}{\sqrt{y+cha}} \quad (7.1.3)$$

$$\int_0^\infty d\tau P_{i\tau-1/2}(y) \cos(a\tau) / ch^2(\pi\tau) = \frac{\sqrt{2}}{\pi} \frac{1}{\sqrt{y-cha}} \tan^{-1}\left[\frac{\sqrt{y-cha}}{\sqrt{1+cha}}\right] \quad (7.1.4)$$

$$\int_0^\infty d\tau P_{i\tau-1/2}(y) \operatorname{ch}(b\tau) / \operatorname{ch}^2(\pi\tau) = \frac{\sqrt{2}}{\pi} \frac{1}{\sqrt{y-\cos b}} \cot^{-1}\left[\frac{\sqrt{1+\cos b}}{\sqrt{y-\cos b}}\right] \quad (7.1.5)$$

$$\int_0^\infty d\tau P_{i\tau-1/2}(y) \operatorname{sh}(b\tau) \operatorname{sh}(\pi\tau) / \operatorname{ch}^2(\pi\tau) = \frac{\sqrt{2}}{\pi} \frac{1}{\sqrt{y+\cos b}} \tan^{-1}\left(\frac{\sqrt{1-\cos b}}{\sqrt{y+\cos b}}\right). \quad (7.1.6)$$

This set of integrals includes all those needed to obtain results given earlier in this monograph.

One can replace $\cot^{-1}(x/y) = \tan^{-1}(y/x)$ in (7.1.5) to make it look more like (7.1.4) but we have chosen \cot^{-1} since it puts $\sqrt{1 \pm \cos b}$ in the numerator and since $\sqrt{1 \pm \cos b} = 0$ for certain values of b .

In the last two integrals one sees the expressions $\sqrt{1+\cos b}$ and $\sqrt{1-\cos b}$. If these are properly treated as analytic functions of b , then as b sweeps along the real axis, these functions change sign at odd multiples of π . This fact is more obvious when one writes these functions as $\sqrt{2} \cos(b/2)$ and $\sqrt{2} \sin(b/2)$. See Appendix M.

7.2 Evaluation of the integral X appearing in (4.1.10)

As a Mehler integral example, the integral (4.1.10) above has this form

$$X = \int_0^\infty d\tau P_{i\tau-1/2}(y) \operatorname{ch}(b\tau) \tau \operatorname{sh}(\pi\tau) / \operatorname{ch}^2(\pi\tau) \quad // y = \operatorname{ch}\xi \text{ and } b = \pi-u_0 \quad (7.2.1)$$

which has an unpleasant τ factor in the integrand. This integral can be done as $X = \partial_b Y$ where

$$Y = \int_0^\infty d\tau P_{i\tau-1/2}(y) \operatorname{sh}(b\tau) \operatorname{sh}(\pi\tau) / \operatorname{ch}^2(\pi\tau). \quad (7.2.2)$$

We know how to evaluate Y from (7.1.6),

$$\int_0^\infty d\tau P_{i\tau-1/2}(y) \operatorname{sh}(b\tau) \operatorname{sh}(\pi\tau) / \operatorname{ch}^2(\pi\tau) = (\sqrt{2}/\pi) \frac{1}{\sqrt{y+\cos b}} \tan^{-1}\left(\frac{\sqrt{1-\cos b}}{\sqrt{y+\cos b}}\right) \quad (7.1.6)$$

so we compute X as,

$$X = \partial_b Y = \partial_b \left\{ (\sqrt{2}/\pi) \frac{1}{\sqrt{y+\cos b}} \tan^{-1}\left(\frac{\sqrt{1-\cos b}}{\sqrt{y+\cos b}}\right) \right\}. \quad (7.2.3)$$

Maple computes ∂_b with this result,

```

Y := (sqrt(2)/Pi)*(1/sqrt(y+cos(b)))*arctan(sqrt(1-cos(b))/sqrt(y+cos(b))) ;
Y:= 
$$\frac{\sqrt{2} \arctan\left(\frac{\sqrt{1-\cos(b)}}{\sqrt{y+\cos(b)}}\right)}{\pi \sqrt{y+\cos(b)}}$$

X := diff(Y,b):simplify(%);

$$\frac{1}{2} \frac{\left(y + \arctan\left(\frac{\sqrt{1-\cos(b)}}{\sqrt{y+\cos(b)}}\right) \sqrt{y+\cos(b)} \sqrt{1-\cos(b)} + \cos(b)\right) \sqrt{2} \sin(b)}{\sqrt{1-\cos(b)} \pi (y^2 + 2y \cos(b) + \cos(b)^2)}$$


```

We manually rewrite this last result as

$$\begin{aligned}
X &= \frac{1}{\pi\sqrt{2}} \frac{1}{y+\cos b} \frac{\sin b}{\sqrt{1-\cos b}} \left\{ 1 + \frac{\sqrt{1-\cos b}}{\sqrt{y+\cos b}} \tan^{-1}\left(\frac{\sqrt{1-\cos b}}{\sqrt{y+\cos b}}\right) \right\} \\
&= \frac{1}{\pi\sqrt{2}} \frac{1}{y+\cos b} \frac{\sin b}{\sqrt{2} \sin(b/2)} \left\{ 1 + \frac{\sqrt{2} \sin(b/2)}{\sqrt{y+\cos b}} \tan^{-1}\left(\frac{\sqrt{2} \sin(b/2)}{\sqrt{y+\cos b}}\right) \right\} . \\
&= \frac{1}{\pi\sqrt{2}} \frac{1}{y+\cos b} \frac{2\sin(b/2)\cos(b/2)}{\sqrt{2} \sin(b/2)} \left\{ 1 + \frac{\sqrt{2} \sin(b/2)}{\sqrt{y+\cos b}} \tan^{-1}\left(\frac{\sqrt{2} \sin(b/2)}{\sqrt{y+\cos b}}\right) \right\} . \\
&= \frac{1}{\pi} \frac{\cos(b/2)}{y+\cos b} \left\{ 1 + \frac{\sqrt{2} \sin(b/2)}{\sqrt{y+\cos b}} \tan^{-1}\left(\frac{\sqrt{2} \sin(b/2)}{\sqrt{y+\cos b}}\right) \right\} .
\end{aligned} \tag{7.2.4}$$

Setting $y = \operatorname{ch}\xi$ and $b = \pi - u_0$ one finds

$$\begin{aligned}
\sin(b/2) &= \sin(\pi/2 - u_0/2) = \cos(u_0/2) \\
\cos(b/2) &= \cos(\pi/2 - u_0/2) = \sin(u_0/2) \\
\cos(b) &= -\cos(u_0) \\
\sin(b) &= \sin(\pi - u_0) = \sin(u_0)
\end{aligned} \tag{7.2.5}$$

so then

$$X = \frac{1}{\pi} \frac{\sin(u_0/2)}{\operatorname{ch}\xi - \cos u_0} \left\{ 1 + \frac{\sqrt{2} \cos(u_0/2)}{\sqrt{\operatorname{ch}\xi - \cos u_0}} \tan^{-1}\left(\frac{\sqrt{2} \cos(u_0/2)}{\sqrt{\operatorname{ch}\xi - \cos u_0}}\right) \right\} \tag{7.2.6}$$

and therefore we have shown that our X integral (4.1.10) has this evaluation:

$$\begin{aligned}
X &= \int_0^\infty d\tau P_{i\tau-1/2}(\operatorname{ch}\xi) \operatorname{ch}[(\pi - u_0)\tau] \tau \operatorname{sh}(\pi\tau) / \operatorname{ch}^2(\pi\tau) \\
&= \frac{1}{\pi} \frac{\sin(u_0/2)}{\operatorname{ch}\xi - \cos u_0} \left[1 + \frac{\sqrt{2} \cos(u_0/2)}{\sqrt{\operatorname{ch}\xi - \cos u_0}} \tan^{-1}\left(\frac{\sqrt{2} \cos(u_0/2)}{\sqrt{\operatorname{ch}\xi - \cos u_0}}\right) \right]
\end{aligned} \tag{7.2.7}$$

$$= \frac{1}{\pi} \frac{\sin(u_0/2)}{\operatorname{ch}\xi - \cos u_0} \left[1 + \frac{A}{B} \tan^{-1}\left(\frac{A}{B}\right) \right]. \quad A = \sqrt{2} \cos(u_0/2), \quad B = \sqrt{\operatorname{ch}\xi - \cos u_0} \quad (7.2.8)$$

With $u_0 \rightarrow \beta_0$ and $\xi \rightarrow \alpha$, this result agrees with Lebedev et al. Problem 501 p 239,

Hint. To calculate the density, use the integral

$$\int_0^\infty \frac{\tau \sinh \pi\tau \cosh(\pi - \beta_0)\tau}{\cosh^2 \pi\tau} P_{-\frac{1}{2}+\imath\tau}(cosh \alpha) d\tau = \frac{2}{\pi} \frac{\sin \frac{1}{2}\beta_0}{2 \cosh \alpha - 2 \cos \beta_0} \\ \times \left[1 + \frac{2 \cos \frac{1}{2}\beta_0}{\sqrt{2 \cosh \alpha - 2 \cos \beta_0}} \operatorname{arc tan} \frac{2 \cos \frac{1}{2}\beta_0}{\sqrt{2 \cosh \alpha - 2 \cos \beta_0}} \right]. \quad (7.2.9)$$

7.3 Where to find Mehler integrals (some errata noted)

The **largest source** of such integrals known to the author is an extremely obscure 1961 Boeing Report #246 written by no less than Professor Fritz Oberhettinger and coworker Theodore Higgins. It contains over 100 Mehler integrals involving $P_{i\tau-1/2}(y)$ and $P_{i\tau-1/2}^m(y)$ ("generalized" Mehler integrals), along with integrals against $K_{ix}(y)$ known as Lebedev transforms.

Integral (7.1.6) appears for example as page 20 #3.

Integral (7.1.4) above appears as page 20 #5 for $y > \operatorname{cha}$, but the corresponding log form for $y < \operatorname{cha}$ has a typo in that the leading factor should be $1/2$ instead of $1/\sqrt{2}$.

Integral (7.1.5) appears as page 20 #6 expressed as \tan^{-1} but the upper right exponent should be $-1/2$ instead of $+1/2$. That same erroneous exponent also appears in PBM mentioned next (this is from PBM volume 3 on Special Functions (2003), Russian page 181, integral 2.17.24.6),

$$6. \int_0^\infty \frac{\operatorname{ch} bx}{\operatorname{ch}^2 \pi x} P_{ix-1/2}(c) dx = \frac{1}{\sqrt{2(c - \cos b)}} - \frac{\sqrt{2(c - \cos b)}}{\pi} \operatorname{arctg} \sqrt{\frac{1 + \cos b}{c - \cos b}} \quad [c > 1].$$

// wrong

Using $\cot^{-1} = \pi/2 - \tan^{-1}$ for the principle branch of the arc trig functions, our (7.1.5) above becomes

$$\int_0^\infty dt P_{i\tau-1/2}(y) \operatorname{ch}(b\tau) \operatorname{sech}^2(\pi\tau) \\ = \frac{1}{\sqrt{2}} \frac{1}{\sqrt{y - \cos b}} - \frac{\sqrt{2}}{\pi} \frac{1}{\sqrt{y - \cos b}} \tan^{-1} \left[\frac{\sqrt{1 + \cos b}}{\sqrt{y - \cos b}} \right] \quad (7.1.5a)$$

which shows the correct placement of the radicals.

The **second largest source** is the just-mentioned volume 3 of the special functions series of PBM which has about 20 integrals of $P_{i\tau-1/2}(y)$ against elementary functions and many more against special functions.

Bateman ET II has a handful of Mehler integrals (p 329-30), and **GR7** has somewhat more (Section 7.21, all taken from ET II). Perhaps there is some recent collection of Mehler integrals unknown to the author.

7.4 Mehler Functions: hypergeometric forms and plots

As noted in (2.2.3), the Mehler functions $P_{i\tau-1/2}^m(\text{ch}\xi)$ and $Q_{i\tau-1/2}^m(\text{ch}\xi)$ are oscillatory for ξ in $(0, \infty)$. Here we shall demonstrate this fact with a few plots for the $m=0$ functions.

Maple V has built-in LegendreP and LegendreQ functions with an ability to adjust the cut locations. However, these provided functions don't always evaluate where we need them. For example ($I = i$),

```
LegendreP(-1/2+I, 1.2);
.8844005605
LegendreQ(-1/2+I, 1.2);
LegendreQ(-1/2+I, 1.2) // meaning: does not compute
```

Since we don't own Maple 2015, we cannot check whether this problem has been remedied. We therefore roll our own Legendre functions, using specific hypergeometric representations that are geared toward evaluation in the range $z = \text{ch}\xi > 1$:

$$P_v(z) = z^v F(-v/2, 1/2-v/2; 1; 1-1/z^2) \quad // \text{Bateman (24)}$$

$$P(v, \xi) \equiv P_v(\text{ch}\xi) = (\text{ch}\xi)^v F(-v/2, 1/2-v/2; 1; \text{th}^2\xi) \quad (7.4.1)$$

$$Q_v(z) = \sqrt{\pi} \Gamma(1+v) (z + \sqrt{z^2 - 1})^{-1-v} (\Gamma(v+3/2))^{-1} F(1/2, 1+v; 3/2+v; \frac{z - \sqrt{z^2 - 1}}{z + \sqrt{z^2 - 1}}) \quad // \text{Bateman (45)}$$

$$Q_v(\text{ch}\xi) = \sqrt{\pi} \Gamma(1+v) (e^\xi)^{-1-v} (\Gamma(v+3/2))^{-1} F(1/2, 1+v; 3/2+v; e^{-2\xi}). \quad (7.4.2)$$

These are from a Bateman EH I table, pages 129 and 136. Our application will then use $v = i\tau-1/2$,

$$\begin{aligned} P_{i\tau-1/2}(\text{ch}\xi) &= P(i\tau-1/2, \xi) \\ Q_{i\tau-1/2}(\text{ch}\xi) &= Q(i\tau-1/2, \xi). \end{aligned} \quad (7.4.3)$$

We have found that Bateman (45) works better than Bateman (36) for the Q function over all our computations in this document. (45) seems more convergent and faster than (36). See Comment below.

We first enter and test these new P and Q functions:

$$P := (\nu, \xi) \rightarrow \text{evalf}(\cosh(\xi)^{\nu} \text{hypergeom}([-nu/2, 1/2-nu/2], [1], \tanh(\xi)^2));$$

$$P := (\nu, \xi) \rightarrow \text{evalf}\left(\cosh(\xi)^{\nu} \text{hypergeom}\left(\left[-\frac{1}{2}\nu, \frac{1}{2}-\frac{1}{2}\nu\right], [1], \tanh(\xi)^2\right)\right)$$

Now show that these two functions agree at least somewhere!

$$\text{evalf}(P(3, 0.5));$$

$$1.893115746$$

$$\text{evalf}(\text{LegendreP}(3, \cosh(0.5)));$$

$$1.893115745$$

$$Q := (\nu, \xi) \rightarrow$$

$$\text{evalf}(\sqrt{\pi} \Gamma(1+\nu) e^{-(1+\nu)\xi} \text{hypergeom}\left(\left[\frac{1}{2}, 1+\nu\right], \left[\frac{3}{2}+\nu\right], e^{(-2)\xi}\right))$$

$$Q := (\nu, \xi) \rightarrow \text{evalf}\left(\frac{\sqrt{\pi} \Gamma(1+\nu) e^{-(1+\nu)\xi} \text{hypergeom}\left(\left[\frac{1}{2}, 1+\nu\right], \left[\frac{3}{2}+\nu\right], e^{(-2)\xi}\right)}{\Gamma\left(\frac{3}{2}+\nu\right)}\right)$$

Now show that these two functions agree at least somewhere!

$$\text{evalf}(Q(1, 1));$$

$$.1911607780$$

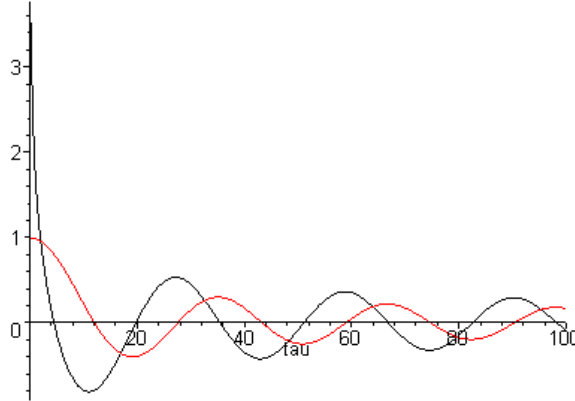
$$\text{evalf}(\text{LegendreQ}(1, \cosh(1)));$$

$$.191160779$$

(7.4.4)

Here we plot $P_{i\tau-1/2}(\text{ch}\xi)$ [red] and $Q_{i\tau-1/2}(\text{ch}\xi)$ [black] for $\xi = 0.2$ and for τ in range (0,100):

$$\text{plot}([\text{Re}(P(I*\tau-1/2, 0.2)), \text{Re}(Q(I*\tau-1/2, 0.2))], \tau = 0..100, \text{color} = [\text{red}, \text{black}]);$$



(7.4.5)

The evaluation produces spurious tiny imaginary parts which we filter out using the Maple `Re()` operator. At $\tau = 0$ the Mehler functions have these forms,

$$\begin{aligned} P_{-1/2}(\text{ch}\xi) &= (2/\pi) K(\text{th}[\xi/2])/\text{ch}(\xi/2) & K(0) &= \pi/2 && // \text{NIST } (14.5.25) \text{ and } (19.6.1) \\ Q_{-1/2}(\text{ch}\xi) &= (2/\sqrt{\pi}) e^{-\xi/2} K(e^{-\xi}) & K(1) &= \infty && // \text{NIST } (14.5.27) \text{ and } (19.6.1) \end{aligned}$$

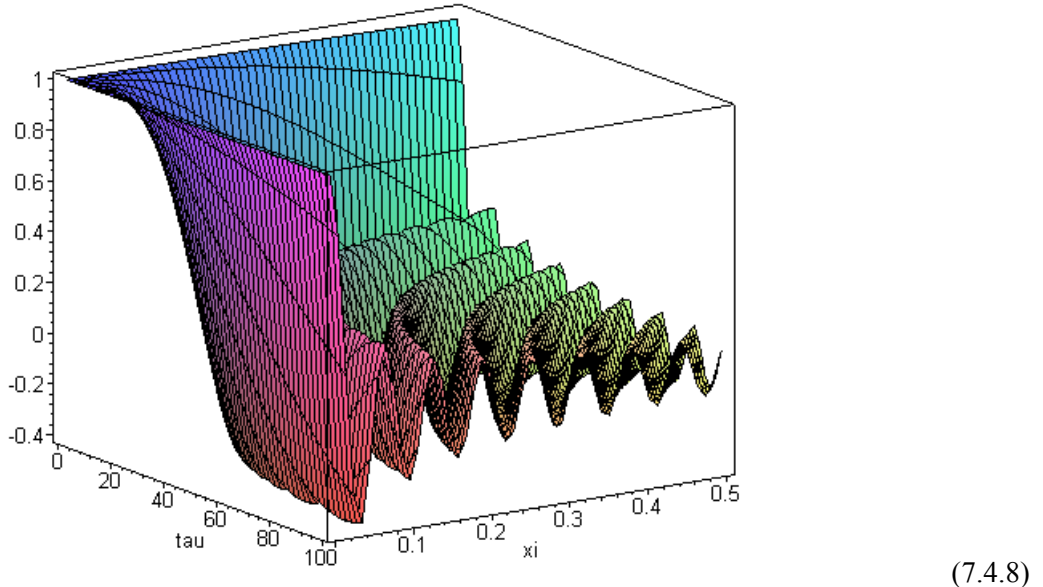
(7.4.6)

where K is the first-kind complete elliptic integral. Evaluating at $\xi = 0$ one then finds

$$\begin{aligned} P_{-1/2}(1) &= (2/\pi)(\pi/2)/1 = 1 && // \text{as expected} \\ Q_{-1/2}(1) &= (2/\sqrt{\pi}) 1 K(1) = \infty && // \text{blows up at } \tau = 0 \text{ and } \xi = 0 \end{aligned} \quad (7.4.7)$$

Here then is a 3D plot showing $P_{i\tau-1/2}(\operatorname{ch}\xi)$ for τ in $(0,100)$ and ξ in $(0.0,0.5)$,

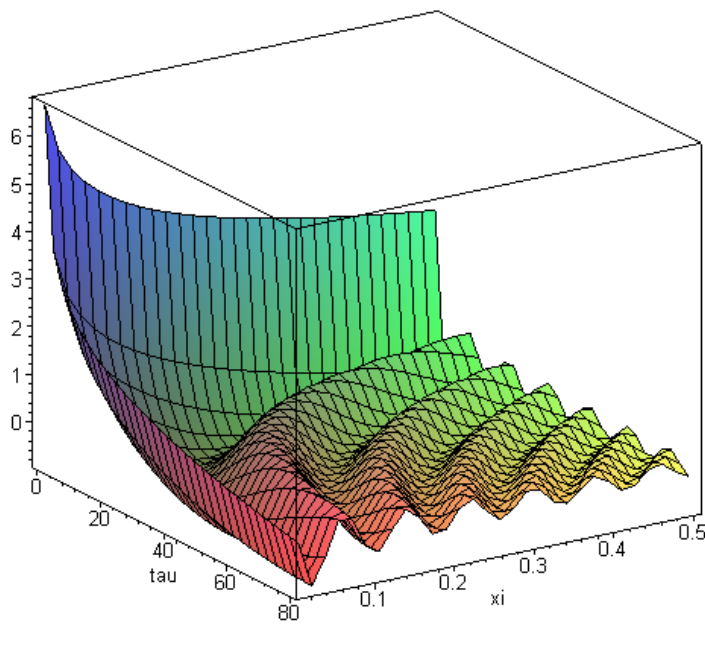
```
plot3d(Re(P(I*tau-1/2, xi)), tau=0..100, xi = 0..0.5, axes = boxed,
grid = [50,50]);
```



Slices at $\xi = \xi = \text{constant}$ produce curves like the red one above in (7.4.5) for $\xi = 0.2$. As noted in (7.4.7), the function takes the value 1 when $\tau = 0$ and $\xi = 0$.

Here is a similar plot showing $Q_{i\tau-1/2}(\operatorname{ch}\xi)$ for τ in $(0.01,80)$ and ξ in $(0.0,0.5)$,

```
plot3d(Re(Q(I*tau-1/2, xi)), tau=0..80, xi = 0.01..0.5, axes =
boxed, grid = [30,30]);
```



(7.4.9)

Slices at $\xi = \text{constant}$ produce curves like the black one above in (7.4.5) for $\xi = 0.2$. As noted in (7.4.7), the function is infinite when $\tau = 0$ and $\xi = 0$ (our plot starts at $\xi = .01$).

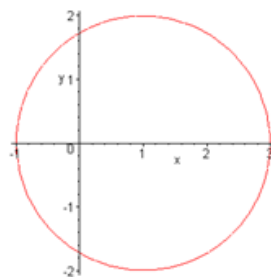
Comment on the hypergeometric function. We use the Bateman forms (7.4.1) and (7.4.2) for P and Q. The basic hypergeometric function (series) $F(a,b;c;z)$ is analytic for $|z| < 1$ and has a branch point at $z = 1$ which limits that circle of convergence. There are many other hypergeometric forms for $P_v(z)$ and $Q_v(z)$ listed in Bateman EH I pp 124-139 (Kummer's solutions p 105), and each has its own region of analyticity in the z-plane. Wherever two forms have overlapping analytic regions, they agree. One can think of moving from form to form as if one were navigating the Northwest Passage (sailing = doing analytic continuation),



(7.4.10)

There are always at least two "forms" that are analytic (blue water) in a region of interest. In a given region, the series of one form might converge more rapidly than that of another form.

The convergence regions are not always disks. Here are two examples showing the Bateman table form numbers for P and Q. On the top regions are disk and iris, but on the bottom we have a bowtie boundary separating two regions of convergence. The bowtie and disk have some overlap.



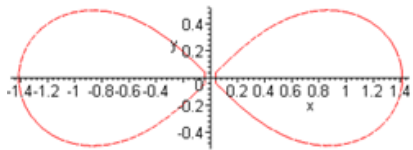
$$(1-z)/2$$

$$2/(1-z)$$

$$(14) (32)$$

$$(19) (37)$$

inside
outside



$$1-z^2$$

$$1/(1-z^2)$$

$$(20) (38)$$

$$(21) (39)$$

inside

outside

(7.4.11)

8. The bowl potential in elementary functions

Start with the bowl potential derived above in (2.4.13),

$$V(\xi, u) = V_0 \sqrt{2} \sqrt{\cosh \xi - \cos u} \int_0^\infty d\tau P_{i\tau-1/2}(\cosh \xi) \frac{\cosh[(\pi-u_0)\tau] \cosh[(\pi+u_0-u)\tau]}{\cosh^2(\pi\tau)} . \quad (2.4.13) \quad (8.1)$$

Recall the identity,

$$2\cosh[(x+y)/2]\cosh[(x-y)/2] = \cosh(x) + \cosh(y) . \quad (8.2)$$

$$\begin{aligned} \text{Set } x = (2\pi-u)\tau \text{ and } y = (2u_0-u)\tau &\Rightarrow (x+y)/2 = (2\pi-u+2u_0-u)\tau/2 = (\pi+u_0-u)\tau \\ &\Rightarrow (x-y)/2 = (2\pi-u-2u_0+u)\tau/2 = (\pi-u_0)\tau . \end{aligned} \quad (8.3)$$

Therefore (8.2) reads,

$$2 \cosh[(\pi+u_0-u)\tau] \cosh[(\pi-u_0)\tau] = \cosh[(2\pi-u)\tau] + \cosh[(2u_0-u)\tau] . \quad (8.4)$$

Use this to break (8.1) into two terms,

$$\begin{aligned} V(\xi, u) &= V_0 \sqrt{2} \sqrt{\cosh \xi - \cos u} \int_0^\infty d\tau P_{i\tau-1/2}(\cosh \xi) \frac{\cosh[(2\pi-u)\tau] + \cosh[(2u_0-u)\tau]}{2\cosh^2(\pi\tau)} \\ &= (V_0 / \sqrt{2}) \sqrt{\cosh \xi - \cos u} \left\{ \int_0^\infty d\tau P_{i\tau-1/2}(\cosh \xi) \frac{\cosh[(2\pi-u)\tau]}{\cosh^2(\pi\tau)} + \int_0^\infty d\tau P_{i\tau-1/2}(\cosh \xi) \frac{\cosh[(2u_0-u)\tau]}{\cosh^2(\pi\tau)} \right\} . \end{aligned} \quad (8.5)$$

Recall integral (7.1.5) with $y = \cosh \xi$ and $\sqrt{1+\cos b} = \sqrt{2} \cos(b/2)$,

$$\int_0^\infty d\tau P_{i\tau-1/2}(\cosh \xi) \frac{\cosh(b\tau)}{\cosh^2(\pi\tau)} = (\sqrt{2}/\pi) \frac{1}{\sqrt{\cosh \xi - \cos b}} \cot^{-1}\left[\frac{\sqrt{2} \cos(b/2)}{\sqrt{\cosh \xi - \cos b}}\right] . \quad (8.6)$$

Use this integral twice in (8.5): the first term has $b_1 = (2\pi-u)$ and the second has $b_2 = (2u_0-u)$,

$$\begin{aligned} V(\xi, u) &= (V_0 / \sqrt{2}) \sqrt{\cosh \xi - \cos u} * (\sqrt{2}/\pi) \\ &\quad \left\{ \frac{1}{\sqrt{\cosh \xi - \cos(2\pi-u)}} \cot^{-1}\left[\frac{\sqrt{2} \cos(\pi-u/2)}{\sqrt{\cosh \xi - \cos(2\pi-u)}}\right] + \frac{1}{\sqrt{\cosh \xi - \cos(2u_0-u)}} \cot^{-1}\left[\frac{\sqrt{2} \cos(u_0-u/2)}{\sqrt{\cosh \xi - \cos(2u_0-u)}}\right] \right\} . \end{aligned}$$

Making the obvious simplifications,

$$V(\xi, u) = (V_0/\pi) \left\{ \cot^{-1}\left[\frac{\sqrt{2} \cos(\pi-u/2)}{\sqrt{\cosh \xi - \cos u}}\right] + \frac{\sqrt{\cosh \xi - \cos u}}{\sqrt{\cosh \xi - \cos(2u_0-u)}} \cot^{-1}\left[\frac{\sqrt{2} \cos(u_0-u/2)}{\sqrt{\cosh \xi - \cos(2u_0-u)}}\right] \right\} . \quad (8.7)$$

Finally, replace $\cos(\pi-u/2) = -\cos(u/2)$ and then use $\cot^{-1}(-x) = \pi - \cot(x)$ to get these final forms

$$V(\xi, u) = (V_0/\pi) \left\{ \cot^{-1} \left[\frac{-\sqrt{2} \cos(u/2)}{\sqrt{\text{ch}\xi - \cos u}} \right] + \frac{\sqrt{\text{ch}\xi - \cos u}}{\sqrt{\text{ch}\xi - \cos(2u_0 - u)}} \cot^{-1} \left[\frac{\sqrt{2} \cos(u_0 - u/2)}{\sqrt{\text{ch}\xi - \cos(2u_0 - u)}} \right] \right\} \quad (8.8)$$

$$V(\xi, u) = (V_0/\pi) \left\{ \pi - \cot^{-1} \left[\frac{\sqrt{2} \cos(u/2)}{\sqrt{\text{ch}\xi - \cos u}} \right] + \frac{\sqrt{\text{ch}\xi - \cos u}}{\sqrt{\text{ch}\xi - \cos(2u_0 - u)}} \cot^{-1} \left[\frac{\sqrt{2} \cos(u_0 - u/2)}{\sqrt{\text{ch}\xi - \cos(2u_0 - u)}} \right] \right\} \quad (b)$$

u_0 in $(0, 2\pi)$
 u in $(u_0, 2\pi + u_0)$ $\text{ch}\xi$ in $(1, \infty)$. // potential of bowl u_0

Convergence of (8.6)

Does the integral (8.6) converge for our two values of parameter b ?

$$\int_0^\infty d\tau P_{i\tau-1/2}(\text{ch}\xi) \frac{\text{ch}(b\tau)}{\text{ch}^2(\pi\tau)} = (\sqrt{2}/\pi) \frac{1}{\sqrt{\text{ch}\xi - \cos b}} \cot^{-1} \left[\frac{\sqrt{2} \cos(b/2)}{\sqrt{\text{ch}\xi - \cos b}} \right]. \quad (8.6)$$

For large τ one finds that $|P_{i\tau-1/2}(y)| \sim \tau^{-1/2}$ (see (H.5.7) with $n = i\tau-1/2$). On the other hand,

$$\frac{\text{ch}(b\tau)}{\text{ch}^2(\pi\tau)} \rightarrow \frac{e^{|b|\tau/2}}{(e^{\pi\tau}/2)^2} = 2 e^{(|b| - 2\pi)\tau} \quad \text{as } \tau \rightarrow \infty. \quad (8.9)$$

Therefore the integral converges for sure if $|b| < 2\pi$. At $|b| = 2\pi$ it also converges as shown in (7.1.1). Are we respecting this requirement that $|b| \leq 2\pi$?

Above we use,

$$\begin{aligned} b_1 &= (2\pi - u) \\ b_2 &= (2u_0 - u) \end{aligned}$$

$$u_0 \leq u \leq u_0 + 2\pi \quad \text{where } 0 \leq u_0 \leq 2\pi. \quad (8.10)$$

Therefore, for fixed u_0 we find

$$\begin{aligned} b_{1\min} &= \min(2\pi - u) = 2\pi - \max(u) = 2\pi - (u_0 + 2\pi) = -u_0 \\ b_{1\max} &= \max(2\pi - u) = 2\pi - \min(u) = 2\pi - u_0 \\ b_{2\min} &= \min(2u_0 - u) = 2u_0 - \max(u) = 2u_0 - (u_0 + 2\pi) = u_0 - 2\pi \\ b_{2\max} &= \max(2u_0 - u) = 2u_0 - \min(u) = 2u_0 - u_0 = u_0 \end{aligned} \quad (8.11)$$

If we now consider all possible values of u_0 , our ranges increase:

$$\begin{aligned}
b_{1\min} &= \min(-u_0) = -\max(u_0) = -2\pi \\
b_{1\max} &= \max(2\pi - u_0) = 2\pi - \min(u_0) = 2\pi \\
b_{2\min} &= \min(u_0 - 2\pi) = \min(u_0) - 2\pi = -2\pi \\
b_{2\max} &= \max(u_0) = 2\pi
\end{aligned} \tag{8.12}$$

In all cases we have $|b| \leq 2\pi$ so the integral (8.6) is convergent for our application.

9. Using Maple to plot the bowl potential

We use old Maple V because we have it; any computer algebra system will do, though the syntax changes slightly. The code text is given in Appendix A, here we use screen clips. The first order of business is to enter the bowl potential from (8.8b) and set a few parameter values: $V_0 = 1$, $a = 1$, $u_0 = \pi/4$.

Construct the charged bowl potential in toroidal coordinates using (2.4.14b)

```

A := sqrt(cosh(xi)-cos(u));
B := sqrt(2)*cos(u/2);
C := sqrt(cosh(xi)-cos(2*u0-u));
E := sqrt(2)*cos(u0-u/2);
V := (V0/Pi)*(Pi-arccot(B/A)+(A/C)*arccot(E/C));
V:=  


$$\frac{V_0 \left( \pi - \operatorname{arccot} \left( \frac{\sqrt{2} \cos \left( \frac{1}{2} u \right)}{\sqrt{\cosh(\xi) - \cos(u)}} \right) + \frac{\sqrt{\cosh(\xi) - \cos(u)}}{\sqrt{\cosh(\xi) - \cos(-2u_0 + u)}} \operatorname{arccot} \left( \frac{\sqrt{2} \cos \left( -u_0 + \frac{1}{2} u \right)}{\sqrt{\cosh(\xi) - \cos(-2u_0 + u)}} \right) \right)}{\pi}$$

V0 := 1;
a := 1;
u0 := evalf(Pi/4);
u0 = .3926990818
(9.1)

```

Next, we need a special routine which takes a point (x,y) on a circle and returns a \tan^{-1} angle which lies in the range $(0,2\pi)$, where the angle is measured CCW away from the x axis. Maple has an internal function that does something like this, but we want to see what is happening. The basic Maple arctan function used below returns values in $(-\pi/2,\pi/2)$ which is the principle branch.

Routine arctan2Pi

Given (x,y) somewhere on a circle, return the angle in $(0,2\pi)$ measured CCW from the x axis.

Warning: returned result may include unevaluated multiples of π

```

:> arctan2Pi := proc(x,y)
    local q;
    if type(x,numeric) and type(y,numeric) then
        if x = 0 and y = 0 then print("arctan2Pi(0,0) error."); RETURN(0) fi;
        if x = 0 and y > 0 then RETURN(Pi/2) fi;
        if x = 0 and y < 0 then RETURN(3*Pi/2) fi;
        if x > 0 and y = 0 then RETURN(0) fi;
        if x < 0 and y = 0 then RETURN(Pi) fi;
        if x > 0 and y > 0 then q := 0 fi;
        if x < 0 and y > 0 then q := Pi fi;
        if x < 0 and y < 0 then q := Pi fi;
        if x > 0 and y < 0 then q := 2*Pi fi;
        RETURN(arctan(y/x)+q);
    else
        'arctan2Pi(x,y)';
    fi;
end:
(9.2)

```

The type functions relate to an obscure evaluation quirk of Maple and should be ignored.

The following routine uses the box (1.2.17) inverse equation for u ,

$$u = \tan^{-1} \left[\frac{2az}{\rho^2 + z^2 - a^2} \right] = \tan^{-1}(y/x) = \arctan 2\pi(x, y) = \arctan 2\pi(\rho^2 + z^2 - a^2, 2az) \quad (9.3)$$

then adjusts the result to be in the proper range $(u_0, u_0 + 2\pi)$:

Routine `getu`

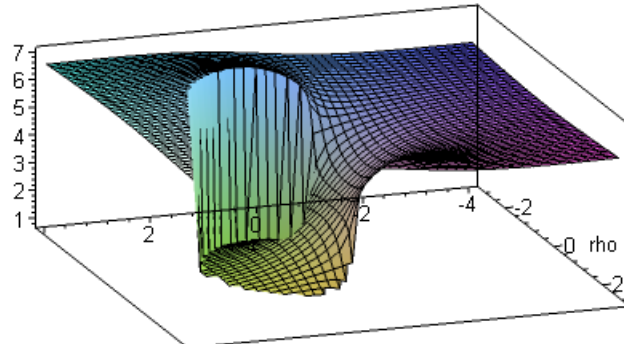
Given a, u_0, ρ, z , compute toroidal bowl-label parameter u in range $(u_0, u_0 + 2\pi)$

```
> getu := proc(rho, z)
    global a, u0; local u;
    if type(rho, numeric) and type(z, numeric) then
        u := arctan2Pi(rho^2 + z^2 - a^2, 2*a*z);
        if u < u0 then u := u + evalf(2*Pi) fi; # get in range
        RETURN(u);
    else
        'getu(rho, z)';
    fi;
end:
```

(9.4)

We used this `getu` function to plot the surfaces of u shown in Fig (5.6) (you may have to stare at this picture for awhile, it is a camera shot from below the plane)

```
u := getu(rho, z);
plot3d(u, rho = -3..3, z = -4..4, axes=BOXED, numpoints=2000);
```

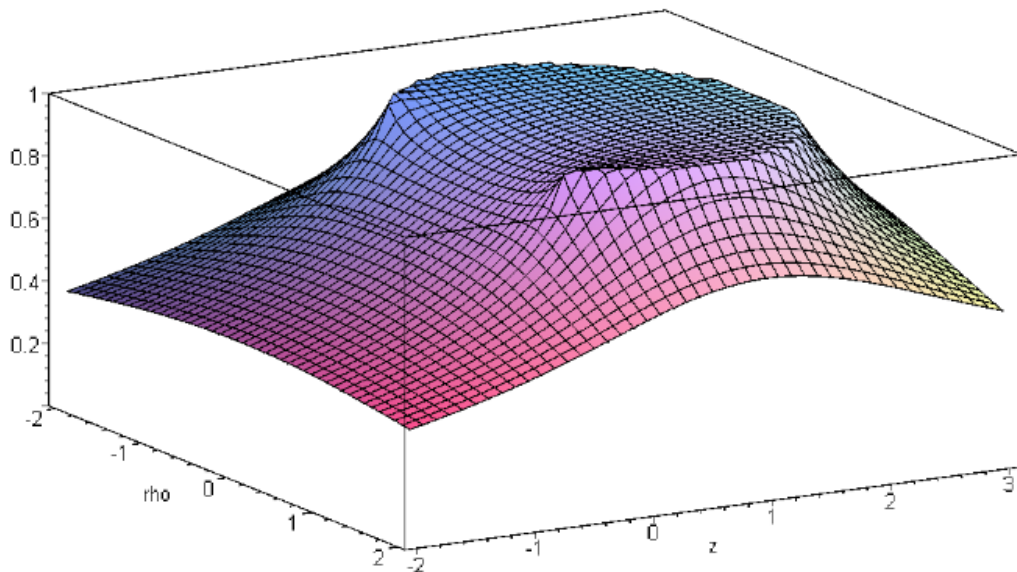


(9.5)

Finally, here is the code to plot the potential surface:

Plot the potential of the charged bowl (an azimuthal slice)

```
> xi := arctanh(2*a*abs(rho)/(a^2+rho^2+z^2));
> u := getu(rho,z);
> plot3d(V, rho = -2..2, z = -2..3, numpoints=2000, axes=BOXED, view=0..1);
```



(9.6)

10. Potential and capacitance of a charged torus

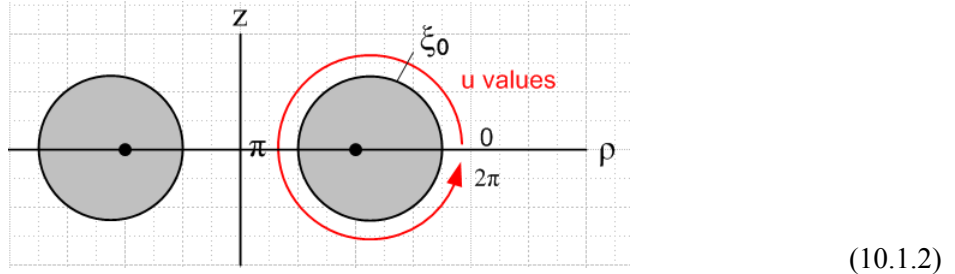
The charged torus problem provides an interesting contrast to the bowl problem. In particular, the spectrum of the eigenvalues appearing in the atomic forms is discrete instead of continuous, so solutions are sums instead of integrals.

10.1 The potential of a charged torus

Looking back at the two toroidal atomic forms in (2.2.3), one can see that for problems involving a torus as boundary ($\xi = \xi_0$) one must be oscillatory in the other two coordinates u and φ . Thus we select

$$(1) \quad \begin{array}{cccc} \text{expo} & \text{osc} & \text{osc} \\ \sqrt{\text{ch}\xi - \cos u} [P_{n-1/2}(m(\text{ch}\xi)), Q_{n-1/2}(m(\text{ch}\xi))] & [\sin(nu), \cos(nu)] & [\sin(m\varphi), \cos(m\varphi)] \end{array} \quad (10.1.1)$$

We take the range for u to be the normal unadjusted $(0, 2\pi)$,



Unlike the situation with the bowl problem, the red path of u values around the grey torus tube is unobstructed so the potential must be periodic in u with period 2π , and this fact causes quantization to integers of the parameter n appearing in the atomic form. Furthermore, $V(\xi, u) = V(\xi, 2\pi - u)$ by symmetry in the $z=0$ plane. Since $\cos(n(2\pi - u)) = \cos(nu)$ whereas $\sin(n(2\pi - u)) = -\sin(nu)$, only the $\cos(nu)$ atoms can contribute. Thus we quickly arrive at the following Smythian form for the potential of a charged torus,

$$V(\xi, u) = \sqrt{\text{ch}\xi - \cos u} \sum_{n=0}^{\infty} P_{n-1/2}(\text{ch}\xi) A_n \cos(nu) \quad (10.1.3)$$

where A_n are coefficients to be determined. A possible $Q_{n-1/2}(\text{ch}\xi)$ term is rejected for the exact same reason described below (2.3.1): the potential must be smooth on the z axis (which is $\xi = 0$), but $Q_n(\text{ch}\xi)$ is log singular at $\xi = 0$, as shown in (H.7.5).

From (10.1.3) the boundary condition of constant potential V_0 on the torus of label ξ_0 is this

$$V_0 / \sqrt{\text{ch}\xi_0 - \cos u} = \sum_{n=0}^{\infty} P_{n-1/2}(\text{ch}\xi_0) A_n \cos(nu) . \quad (10.1.4)$$

Unlike the bowl situation, here we have a single boundary condition because the torus has only a single surface "exposed to the outside world". The inside of the torus is completely separated from the outside, and the Smythian form (10.1.4) only applies to the outside region. Inside the torus the potential is $V = V_0$, since this is the constant potential of the closed bounding toroidal surface.

To solve (10.1.4) for the coefficients A_n , apply $\int_0^\pi du \cos(mu)$ to both sides to get

$$V_0 \int_0^\pi du \cos(mu) (1/\sqrt{\cosh\xi_0 - \cos u}) = \sum_{n=0}^{\infty} P_{n-1/2}(\cosh\xi_0) A_n \int_0^\pi du \cos(mu) \cos(nu). \quad (10.1.5)$$

On the right side, make use of this well-known orthogonality relation (see (J.2.8) line 3),

$$\int_0^\pi du \cos(nu) \cos(mu) = (\pi/\varepsilon_n) \delta_{n,m}, \quad \varepsilon_n = 2 - \delta_{n,0} = \text{"Neumann's Factor"} \quad (10.1.6)$$

to get

$$V_0 \int_0^\pi du \cos(mu) (1/\sqrt{\cosh\xi_0 - \cos u}) = (\pi/\varepsilon_m) P_{m-1/2}(\cosh\xi_0) A_m. \quad (10.1.7)$$

Next, make use of the second equation of the following nameless transform, derived in (J.3.8),

$$1/\sqrt{a - b \cos(x)} = (1/\pi) \sqrt{2/b} \sum_{n=0}^{\infty} \varepsilon_n Q_{n-1/2}(a/b) \cos(nx) \quad // \text{expansion} \quad (10.1.8a)$$

$$\int_0^\pi dx \cos(nx)/\sqrt{a - b \cos(x)} = \sqrt{2/b} Q_{m-1/2}(a/b) \quad // \text{projection} \quad (10.1.8b)$$

with $a = \cosh\xi_0$ and $b = 1$ to write (10.1.7) as,

$$V_0 \sqrt{2} Q_{m-1/2}(\cosh\xi_0) = (\pi/\varepsilon_m) P_{m-1/2}(\cosh\xi_0) A_m. \quad (10.1.9)$$

The coefficients are therefore

$$A_n = V_0 (\sqrt{2} \varepsilon_n / \pi) [Q_{n-1/2}(\cosh\xi_0) / P_{n-1/2}(\cosh\xi_0)]. \quad (10.1.10)$$

Inserting this A_n into our Smythian form (10.1.3) gives the following potential for a torus of label ξ_0 ,

$$V(\xi, u) = V_0 \frac{\sqrt{2}}{\pi} \sqrt{\cosh\xi - \cos u} \sum_{n=0}^{\infty} \varepsilon_n P_{n-1/2}(\cosh\xi) \frac{Q_{n-1/2}(\cosh\xi_0)}{P_{n-1/2}(\cosh\xi_0)} \cos(nu). \quad (10.1.11)$$

This can be compared with Morse and Feshbach p 1304 ($\xi = \mu$ and $u = \eta$)

$$\psi = \frac{V_0}{\pi} \sqrt{2(\cosh \mu - \cos \eta)} \sum_{n=0}^{\infty} \left[\frac{Q_{n-1/2}(\cosh \mu_0)}{P_{n-1/2}(\cosh \mu_0)} \right] P_{n-1/2}(\cosh \mu) \cos(n\eta) \quad (10.3.80)$$

// wrong

where the ε_n factor has been erroneously omitted. In May 2010 I asked Mark Feshbach if he knew of an errata collection for the massive 2000 page masterwork coauthored by his father, but he did not. The source of the missing ε_n factor is tracked down a bit in (J.3.9). The correct result (10.1.11) appears as (8.11.7) in Lebedev's *Special Functions*, where $\xi = \alpha$, $\xi_0 = \alpha_0$ and $u = \beta$,

$$\begin{aligned} \psi = & \frac{V}{\pi} \sqrt{2 \cosh \alpha - 2 \cos \beta} \left[\frac{P_{-1/2}(\cosh \alpha)}{P_{-1/2}(\cosh \alpha_0)} Q_{-1/2}(\cosh \alpha_0) \right. \\ & \left. + 2 \sum_{n=1}^{\infty} \frac{P_{n-1/2}(\cosh \alpha)}{P_{n-1/2}(\cosh \alpha_0)} Q_{n-1/2}(\cosh \alpha_0) \cos n\beta \right]. \end{aligned} \quad (8.11.7)$$

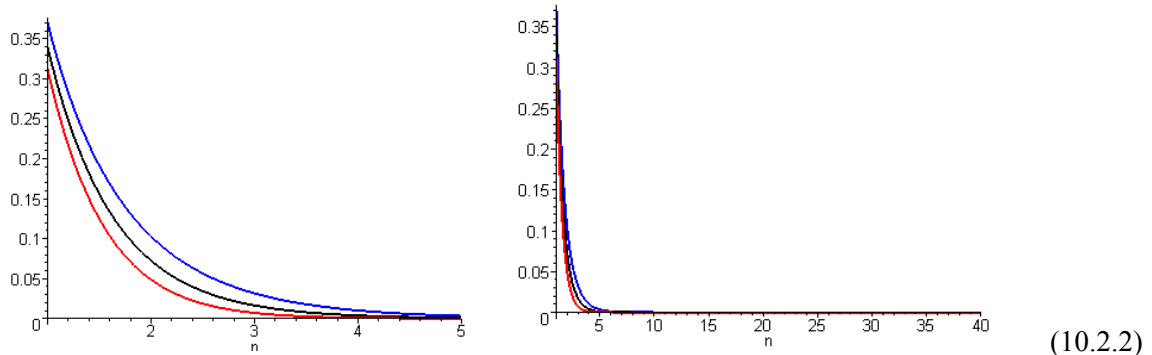
10.2 How many terms should one keep in the potential series?

To study the series (10.1.11) we write it in terms of coefficients A_n (new A_n) as follows,

$$\begin{aligned} V(\xi, u) = & V_0 \frac{\sqrt{2}}{\pi} \sqrt{\cosh \xi - \cos u} \sum_{n=0}^{\infty} \varepsilon_n A_n \cos(nu) \\ A_n \equiv & P_{n-1/2}(\cosh \xi) \frac{Q_{n-1/2}(\cosh \xi_0)}{P_{n-1/2}(\cosh \xi_0)}. \end{aligned} \quad (10.2.1)$$

For this discussion, we consider only the range $0 \leq \xi \leq \xi_0$ which corresponds to the region outside the torus of Fig (10.1.2). For any pair of values (ξ_0, ξ) that meet this condition, the A_n are positive and exponentially decreasing with n . Here is an illustration for $\xi_0 = 1$ and $\xi = 0.1$ (red), 0.7 and 1.0 (blue) :

```
A := (n) -> P(n-1/2, xi)* Q(n-1/2, xi0)/ P(n-1/2, xi0):
xi0 := 1:
plot([seq(A(n), xi = [0.1, 0.7, 1.0])], n=1..5, color = [red, black, blue], thickness=2);
```



The upper blue curve with $\xi = \xi_0$ shows the worst convergence with n . Maple of course interpolates smoothly between our integer n values.

In (H.5.10) we show that the asymptotic limit of A_n for large n is,

$$A_n \equiv P_{n-1/2}(\text{ch}\xi) \frac{Q_{n-1/2}(\text{ch}\xi_0)}{P_{n-1/2}(\text{ch}\xi_0)} \rightarrow \sqrt{\frac{\pi}{2n\text{sh}\xi}} e^{-n(2\xi_0 - \xi)} . \quad \text{as } n \rightarrow \infty \quad (10.2.3)$$

Here A_n decreases exponentially for very large n , and the least convergence occurs when $\xi = \xi_0$. We just showed that both these claims are valid (approximately) for small n as well.

Therefore, in trying to determine the number of terms needed in the series (10.2.1) to get a given amount of accuracy, we shall make the worst-case assumption that $\xi = \xi_0$. But in this situation the two P functions in A_n cancel leaving just

$$A_n = Q_{n-1/2}(\text{ch}\xi_0) , \quad \xi = \xi_0 \quad (10.2.4)$$

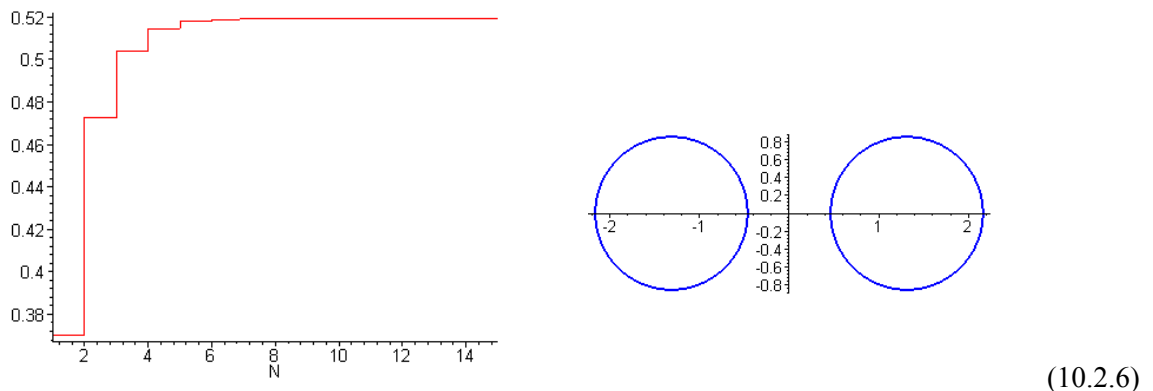
and then the potential series becomes (now evaluated at the toroidal surface),

$$V(\xi_0, u) = V_0 \frac{\sqrt{2}}{\pi} \sqrt{\text{ch}\xi_0 - \cos u} \sum_{n=0}^{\infty} \varepsilon_n Q_{n-1/2}(\text{ch}\xi_0) \cos(nu) . \quad (10.2.5)$$

Although this equation is an identity according to (10.1.8a), we still use it to evaluate sum convergence. We ignore $\varepsilon_n = 1 - \delta_{n,0}$ in the following convergence discussion. We also assume the worst case situation $u = 0$ or 2π so that $\cos(nu) = 1$ so there is no convergence assistance from $\cos(nu)$.

To see how many terms in (10.2.5) give a reasonable result, a brute force method is to add up the series with a variable number of terms and see at what n the sum stabilizes. For example, for $\xi_0 = 1$,

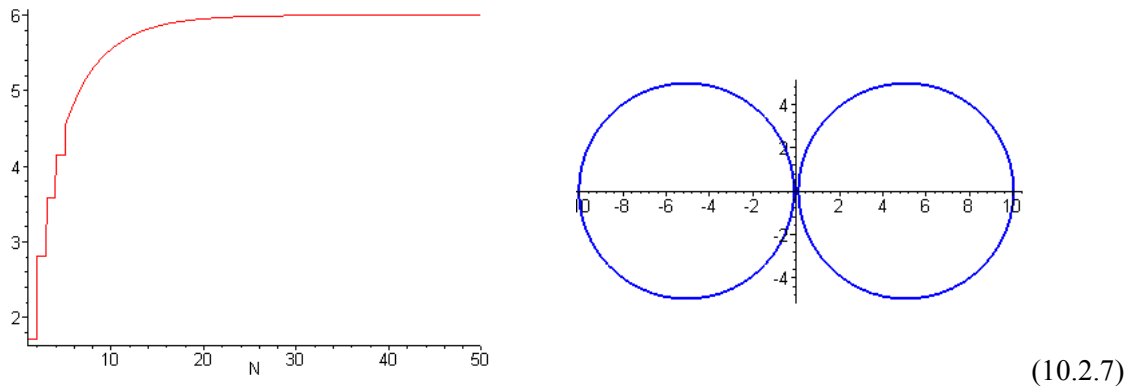
```
S := (N) -> sum(Q(n-1/2, xi0), n=1..N);
S := N -> sum(Q(n-1/2, xi0), n=1..N)
xi0 := 1;
plot(S(N), N=1..15);
```



In this case about 10 terms gives a stable result. On the right we show a torus cross section for $\xi_0 = 1$.

It turns out that as ξ_0 is decreased, the number of terms required increases. We repeat the above plot now for the case $\xi_0 = 0.2$ which makes the hole in the torus very small (close to a degenerate torus),

```
xi0 := 0.2;
plot(s(N), N = 1..50);
```



In this case one might regard 40 terms as a reasonable number of terms to keep in the series (10.2.5) and therefore in (10.2.1).

10.3 Using Maple to plot the torus potential

The method is similar to that used to plot the bowl potential in Section 9. The Legendre functions are those of (7.4.1) and (7.4.2) while the arctanh2Pi function is shown in (9.2). The u coordinate is unaltered so there is no getu routine, but there is now a getxi routine which pins the potential at V_0 whenever a location inside the torus is detected ($\xi = \tanh^{-1}[2ap/(\rho^2 + z^2 + a^2)]$ from (1.2.5)),

```
getxi := proc(rho,z)
  global a,xi0; local xi;
  if type(rho,numeric) and type(z,numeric) then
    xi := arctanh(2*a*abs(rho)/(a^2+rho^2+z^2));
    if xi > xi0 then xi := xi0 fi; # pin at torus
    RETURN(xi);
  else
    'getxi(rho,z)';
  fi;
end:
```

(10.3.1)

```
eps := proc(n) if type(n,numeric) then
  if n=0 then RETURN(1) else RETURN(2) fi;
else 'eps(n)'; fi end: // to generate  $\varepsilon_n$ 
```

(10.3.2)

Here then is the plotting code using (10.1.11) for $V(\xi, u)$.

$$V(\xi, u) = V_0 \frac{\sqrt{2}}{\pi} \sqrt{\text{ch}\xi - \cos u} \sum_{n=0}^{\infty} \varepsilon_n P_{n-1/2}(\text{ch}\xi) \frac{Q_{n-1/2}(\text{ch}\xi_0)}{P_{n-1/2}(\text{ch}\xi_0)} \cos(nu). \quad (10.1.11)$$

$V_0 = 10$ to allow for a "constrained" plot where all axes have the same scale (otherwise the torus cross section is not round), and $\xi_0 = 1$:

```

V := (v0*sqrt(2)/Pi)*sqrt(cosh(xi)-cos(u))*sum(term(n),n=0..N);

$$V = \frac{V_0 \sqrt{2} \sqrt{\cosh(\xi) - \cos(u)} \left( \sum_{n=0}^N \text{term}(n) \right)}{\pi}$$

term := (n) -> eps(n)*(Q(n-1/2, xi0)/P(n-1/2, xi0))*P(n-1/2, xi)*cos(n*u);

$$\text{term} := n \rightarrow \frac{\text{eps}(n) Q\left(n - \frac{1}{2}, \xi_0\right) P\left(n - \frac{1}{2}, \xi\right) \cos(n u)}{P\left(n - \frac{1}{2}, \xi_0\right)}$$

v0 := 10; a := 1; xi0 := 1.0; N := 10;
u := arctan2Pi(rho^2+z^2-a^2, 2*a*z);

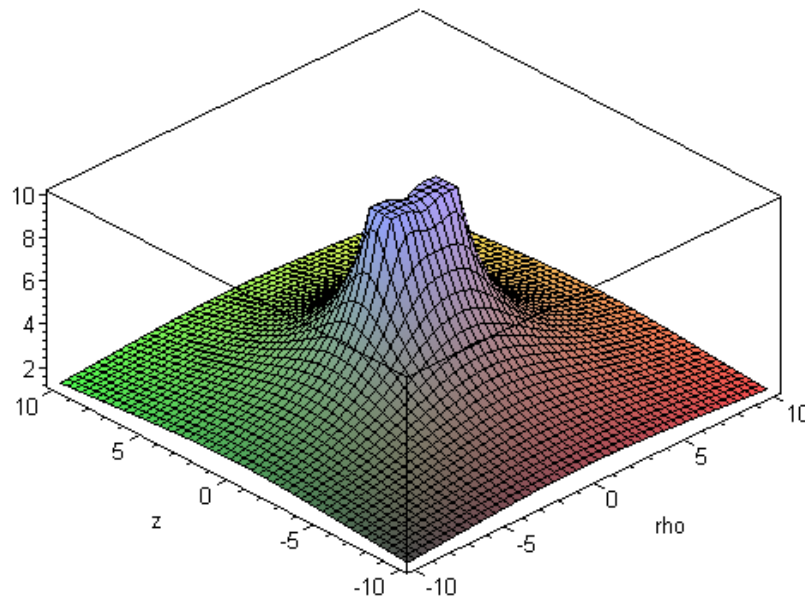
$$u = \arctan2\text{Pi}(\rho^2 + z^2 - a^2, 2az)$$

xi := getxi(rho, z);

$$\xi = \text{get}\xi(\rho, z)$$

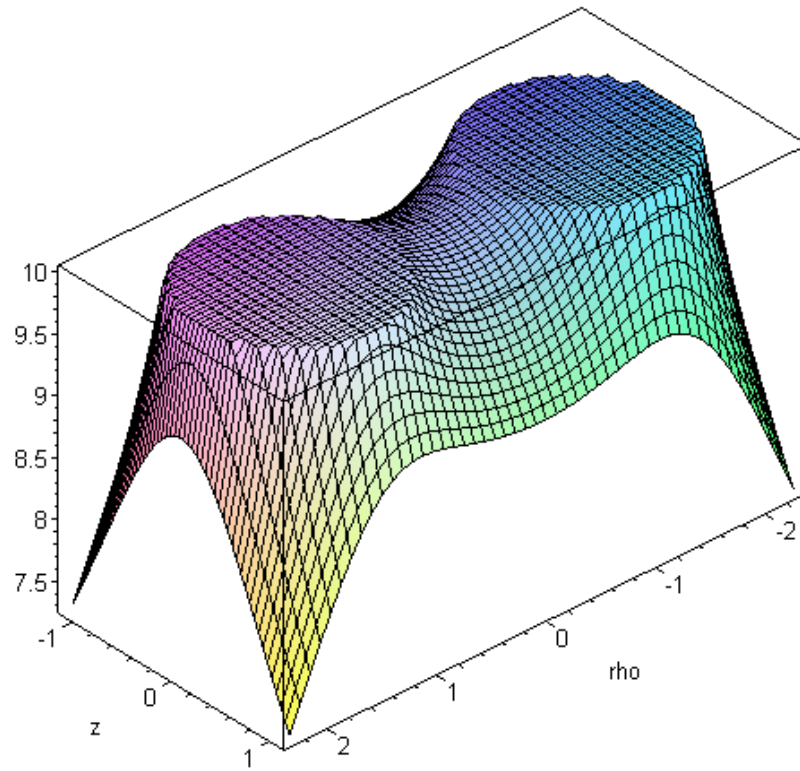
plot3d(Re(V), rho = -3..3, z = -2..2, grid = [50,50], axes = boxed, scaling = constrained);

```

(10.3.3)


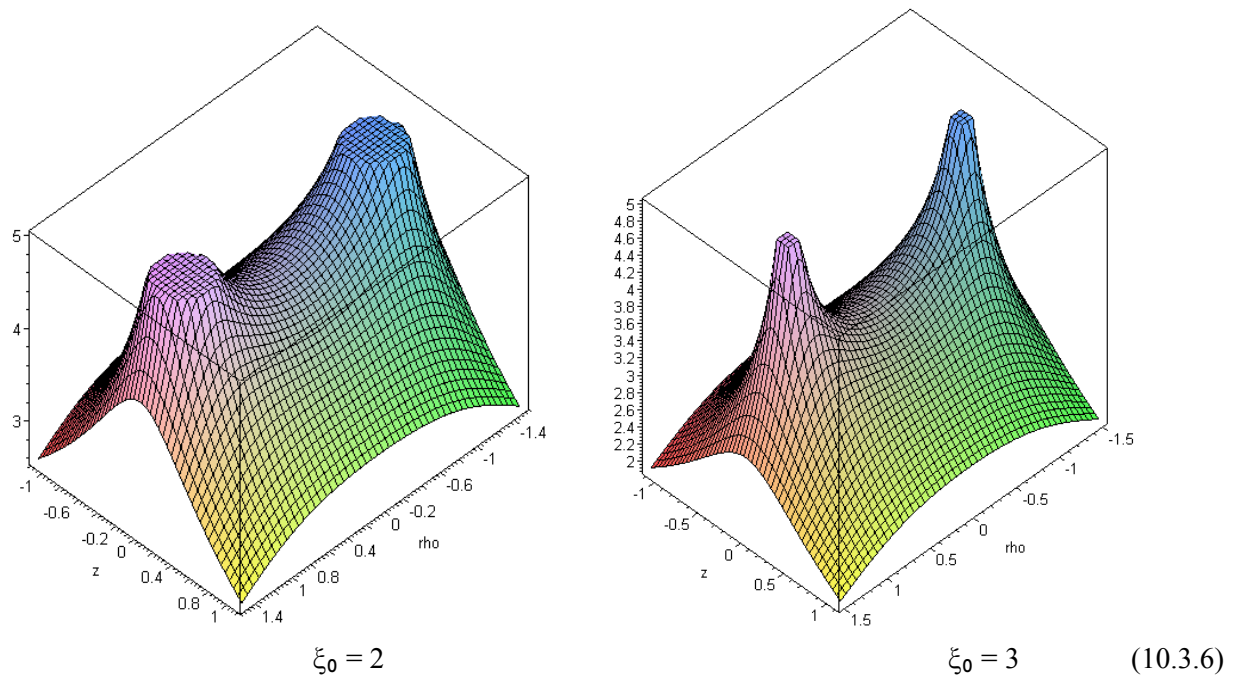
A close-in shot is more interesting, showing how the potential drops a bit in the center of the $\xi_0 = 1$ torus,

```
plot3d(Re(V), rho = -2.3..2.3, z = -1.1..1.1, grid = [50,50], axes = boxed, scaling = constrained);
```



(10.3.5)

For a thinner torus (larger ξ_0) the potential drops more in the toroid center. Here $V_0 = 5$:



These are plots of the potential of a charged conducting torus taken on any 2D azimuthal slice.

10.4 Capacitance of a torus

Recall from the text below (1.2.8) that large r means $\xi \rightarrow 0$ and $u \rightarrow 0$ in toroidal coordinates. We can therefore set $P_{n-1/2}(\text{ch}\xi) = 1$ [see (H.7.2)] and $\cos(nu) = 1$ in (10.1.11) to get

$$V(\xi, u) \approx V_0 \frac{\sqrt{2}}{\pi} \sqrt{\text{ch}\xi - \cos u} \sum_{n=0}^{\infty} \varepsilon_n \frac{Q_{n-1/2}(\text{ch}\xi_0)}{P_{n-1/2}(\text{ch}\xi_0)} . \quad // \text{large } r \quad (10.4.1)$$

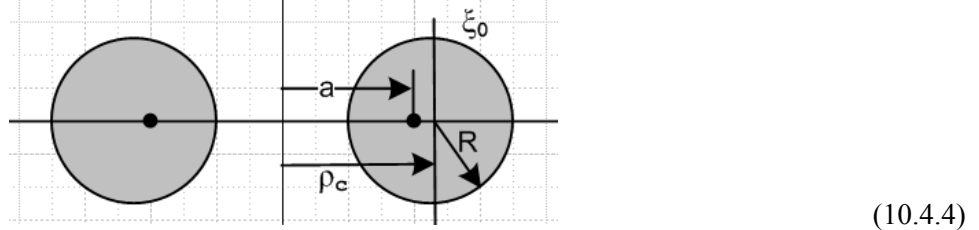
As in the bowl problem, we know from (1.2.16) that $\sqrt{\text{ch}\xi - \cos u} \approx \sqrt{2} a/r$ for large r , so

$$V(\xi, u) \approx V_0 \frac{\sqrt{2}}{\pi} (\sqrt{2} a / r) \sum_{n=0}^{\infty} \varepsilon_n \frac{Q_{n-1/2}(\text{ch}\xi_0)}{P_{n-1/2}(\text{ch}\xi_0)} . \quad (10.4.2)$$

Thinking of this as $V = Q/r$ and using $Q = CV_0$ so that $V(\xi, u) = V_0 C / r$ we find that the capacitance of a torus of label ξ_0 is given by

$$C = \frac{2a}{\pi} \sum_{n=0}^{\infty} \varepsilon_n \frac{Q_{n-1/2}(\text{ch}\xi_0)}{P_{n-1/2}(\text{ch}\xi_0)} \quad \varepsilon_n = 2 - \delta_{n,0} . \quad (10.4.3)$$

Sometimes this result is expressed in terms of R and ρ_c shown below (R is the tube radius, ρ_c is the torus radius to the center line of the tube),



From box (1.2.17) or (1.2.7) we know that

$$\rho_c = a \coth \xi_0 \quad R = a / \sinh \xi_0 \quad \Rightarrow \quad \sqrt{\rho_c^2 - R^2} = a , \quad \rho_c/R = \text{ch} \xi_0 \quad (10.4.5)$$

so that the C formula can be written (reminder: this is cgs units, multiply by $4\pi\varepsilon_0$ to get SI units),

$$C = (2/\pi) \sqrt{\rho_c^2 - R^2} \sum_{n=0}^{\infty} \varepsilon_n \frac{Q_{n-1/2}(\rho_c/R)}{P_{n-1/2}(\rho_c/R)} \quad \varepsilon_n = 2 - \delta_{n,0} . \quad (10.4.6)$$

Were we to define $\varepsilon'_n \equiv \varepsilon_n/2$ we could write,

$$C = (4/\pi) \sqrt{\rho_c^2 - R^2} \sum_{n=0}^{\infty} \epsilon'_n \frac{Q_{n-1/2}(\rho_c/R)}{P_{n-1/2}(\rho_c/R)} , \quad \epsilon'_n = 1/2 \text{ if } n=0, \text{ else } \epsilon'_n = 1 . \quad (10.4.7)$$

This is in agreement with the 1954 result of Snow, for whom our ρ_c and R are his A and a :

$$C = \frac{4\sqrt{A^2 - a^2}}{\pi} \sum_{n=0}^{\infty} \epsilon'_n \frac{Q_{n-1/2}(\cosh \beta_1)}{P_{n-1/2}(\cosh \beta_1)} (\epsilon'_0 = 1/2, \epsilon'_n = 1 \text{ if } n \neq 0), \quad \cosh \beta_1 = \frac{2}{k^2} - 1 = \frac{A}{a} \quad (10.4.8)$$

This Chester Snow result appears on page 9 of a fascinating 1954 "Circular 544" he wrote for the National Bureau of Standards which contains many unusual capacitance and inductance calculations.

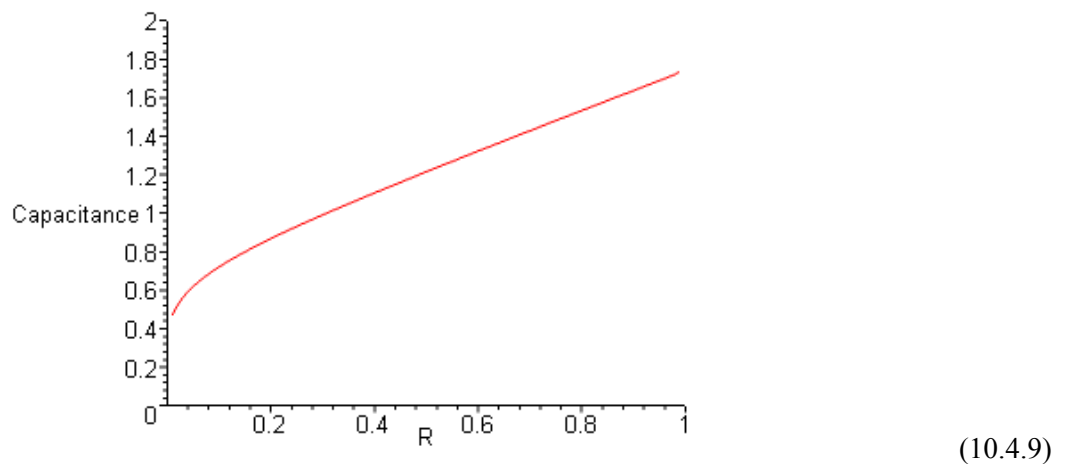
The series (10.4.6) is exponentially convergent, and (H.5.9) shows that,

$$B_n \equiv \frac{Q_{n-1/2}(\operatorname{ch} \xi_0)}{P_{n-1/2}(\operatorname{ch} \xi_0)} \rightarrow \pi e^{-2n\xi_0} \quad \text{as } n \rightarrow \infty . \quad (H.5.9)$$

Using the Legendre functions $P(v, \xi) = P_v(\operatorname{ch} \xi)$ and $Q(v, \xi) = Q_v(\operatorname{ch} \xi)$ described in (7.4.1) and (7.4.2), Maple plots the torus capacitance C in (10.4.6) as a function of R/ρ_c where we set $\rho_c = 1$. The first 20 terms give a stable plot -- adding more terms does not visibly change the curve.

```
eps := proc(n) if type(n, numeric) then
    if n=0 then RETURN(1) else RETURN(2) fi
else 'eps(n)' ; fi end:

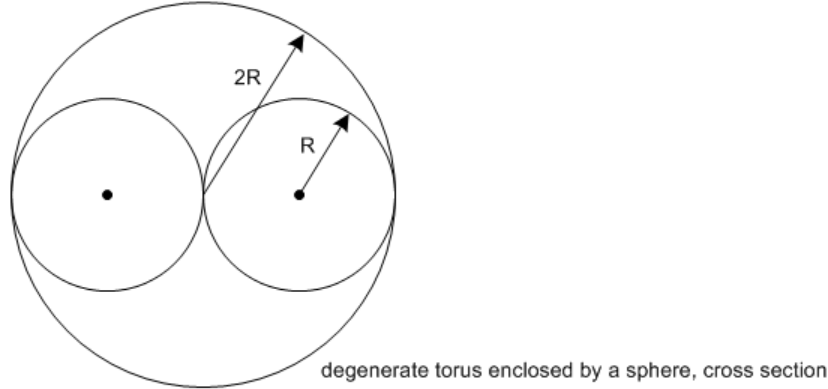
term := (n) -> eps(n)*Q(n-1/2, arccosh(1/R))/P(n-1/2, arccosh(1/R)):
sumterms := sum(term(n), n=0..20):
plot((2/Pi)*sqrt(1-R^2)*sumterms, R =
0..1, y=0..2, numpoints=100, labels=["R", "Capacitance"]);
```



$R/\rho_c = 1$ describes a degenerate torus where the hole just disappears (upper right of plot), and $R \rightarrow 0$ gives a limiting thin wire ring (lower left of plot). Both these limits are quite fascinating and are discussed in some detail in Appendix I.

The degenerate torus limit $R=1$ gives the mysterious value $C \approx 1.7414$. The author would love to know if this number is a simple function of π , small integers and simple roots (see Appendix I.3).

A comparison of this degenerate torus to a sphere which just encloses it ($r=2R$),



(10.4.10)

reveals these facts :

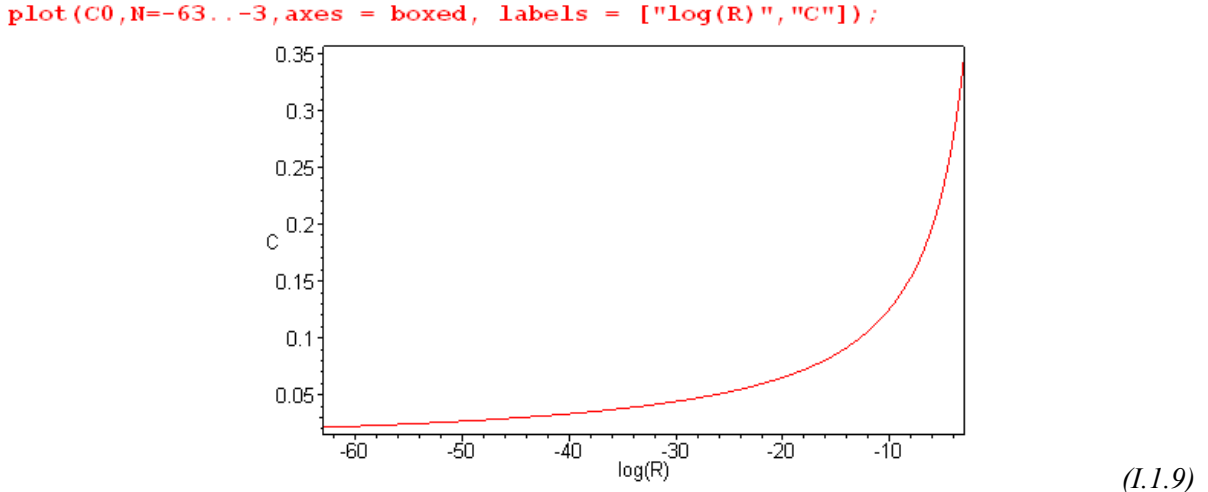
$$\begin{aligned}
 C_{\text{toroid}} &= 1.7414 R && // \text{mystery number} \\
 C_{\text{sphere}} &= 2.0000 R && \text{ratio sphere/torus} = 2.0000/1.741 = 1.149 \\
 \text{AREA}_{\text{toroid}} &= 4\pi^2 R^2 && // \text{area} = 4\pi^2 R \rho_c \\
 \text{AREA}_{\text{sphere}} &= 16\pi R^2 && \text{ratio sphere/torus} = 4/\pi = 1.273 \quad // \text{area} = 4\pi(2R)^2 .
 \end{aligned} \tag{10.4.11}$$

So the sphere has 27% more area and 15% more capacitance than the enclosed degenerate torus. We expect the sphere to have more capacitance since it is the optimal shape for keeping the charges apart. That is to say, the energy stored in the electric field, $(1/2)CV_0^2 = (1/2)Q^2/C$, is the work needed to assemble the charge Q from $r = \infty$. Since this work is less for a sphere than for the enclosed toroid, the sphere has a larger C than the enclosed toroid.

In (I.1.7) it is shown that for $R < 10^{-3}$ (the thin-wire limit), the torus capacitance is given by

$$C(R) \approx \pi / \ln(8/R) \equiv C_0(R) . \quad // \rho_c = 1 \tag{I.1.7} \tag{10.4.12}$$

Here is a plot of $C_0(R)$ versus $\log R$,



If we go from $R/\rho_c = 10^{-3}$ to $R/\rho_c = 10^{-63}$, capacitance drops only by a factor of 10, so one might say that a wire ring "holds its capacitance quite well" as the wire gets thinner and thinner. Ultimately the capacitance goes to 0 as the wire vanishes out of existence. This can be compared to the capacitance of a metal sphere which is shrunk to a point, in which case $C = R \rightarrow 0$ in a more reasonable fashion.

If a metal sphere carrying fixed charge Q is gradually shrunk to a point, work must be done to get the charges closer together which raises the sphere's potential V relative to infinity ($E = CV^2/2 = QV/2$). The charges are all piled on top of each other in the limit, so $C = Q/V$ goes to 0 quickly. In the torus case, the charges can stay away from each other to some extent by being spread out around the wire ring, so V rises more slowly as the ring is made thinner.

10.5 Surface charge density on a torus

The torus surface charge density may be obtained from the potential in this manner,

$$\sigma = + (1/4\pi) (1/h_{\xi_0}) [\partial_\xi V(\xi, u)]^{\xi=\xi_0} \quad 1/h_{\xi_0} = (\operatorname{ch}\xi_0 - \cos u)/a . \quad (10.5.1)$$

An explanation is given below (4.1.2), and the sign here is + because ξ decreases moving outward from the torus surface. The torus potential was found in (10.1.11) to be

$$V(\xi, u) = V_0 \frac{\sqrt{2}}{\pi} \sqrt{\operatorname{ch}\xi - \cos u} \sum_{n=0}^{\infty} \varepsilon_n P_{n-1/2}(\operatorname{ch}\xi) \frac{Q_{n-1/2}(\operatorname{ch}\xi_0)}{P_{n-1/2}(\operatorname{ch}\xi_0)} \cos(nu) \quad (10.1.11) \quad (10.5.2)$$

$$= V_0 \frac{\sqrt{2}}{\pi} \sum_{n=0}^{\infty} \varepsilon_n \frac{Q_{n-1/2}(\operatorname{ch}\xi_0)}{P_{n-1/2}(\operatorname{ch}\xi_0)} \cos(nu) [\sqrt{\operatorname{ch}\xi - \cos u} P_{n-1/2}(\operatorname{ch}\xi)] .$$

Therefore (10.5.1) reads,

$$\sigma = + \frac{1}{4\pi} V_0 \frac{\sqrt{2}}{\pi} \sum_{n=0}^{\infty} \varepsilon_n \frac{Q_{n-1/2}(\operatorname{ch}\xi_0)}{P_{n-1/2}(\operatorname{ch}\xi_0)} \cos(nu) * \frac{1}{h_{\xi_0}} \partial_\xi [\sqrt{\operatorname{ch}\xi - \cos u} P_{n-1/2}(\operatorname{ch}\xi)] |^{\xi=\xi_0} . \quad (10.5.3)$$

We need then to compute,

$$\begin{aligned}
& \partial_\xi [\sqrt{\text{ch}\xi - \cos u} P_{n-1/2}(\text{ch}\xi)] \\
&= \sqrt{\text{ch}\xi - \cos u} [P'_{n-1/2}(\text{ch}\xi) \text{sh}\xi] + [(1/2)(1/\sqrt{\text{ch}\xi - \cos u}) * \text{sh}\xi] P_{n-1/2}(\text{ch}\xi) \\
&= \text{sh}\xi [\sqrt{\text{ch}\xi - \cos u} P'_{n-1/2}(\text{ch}\xi) + (1/2)(1/\sqrt{\text{ch}\xi - \cos u}) P_{n-1/2}(\text{ch}\xi)] |^{\xi=\xi_0} \\
&= \text{sh}\xi_0 [\sqrt{\text{ch}\xi_0 - \cos u} P'_{n-1/2}(\text{ch}\xi_0) + (1/2)(1/\sqrt{\text{ch}\xi_0 - \cos u}) P_{n-1/2}(\text{ch}\xi_0)] , \tag{10.5.4}
\end{aligned}$$

where $P'_v(z)$ means $\partial_z P_v(z)$. Then using $1/h_{\xi_0} = (\text{ch}\xi_0 - \cos u)/a$,

$$\begin{aligned}
& (1/h_{\xi_0}) \partial_\xi [\sqrt{\text{ch}\xi - \cos u} P_{n-1/2}(\text{ch}\xi)] |^{\xi=\xi_0} \\
&= (\text{sh}\xi_0/a) (\text{ch}\xi_0 - \cos u) [\sqrt{\text{ch}\xi_0 - \cos u} P'_{n-1/2}(\text{ch}\xi_0) + (1/2)(1/\sqrt{\text{ch}\xi_0 - \cos u}) P_{n-1/2}(\text{ch}\xi_0)] . \\
&= (\text{sh}\xi_0/a) [(\text{ch}\xi_0 - \cos u)^{3/2} P'_{n-1/2}(\text{ch}\xi_0) + (1/2)\sqrt{\text{ch}\xi_0 - \cos u} P_{n-1/2}(\text{ch}\xi_0)] . \tag{10.5.5}
\end{aligned}$$

Inserting this into (10.5.3) gives, using $\text{sh}\xi_0/a = 1/R$ from (1.2.7), this preliminary result,

$$\begin{aligned}
\sigma &= +\frac{1}{4\pi R} V_0 \frac{\sqrt{2}}{\pi} \sum_{n=0}^{\infty} \varepsilon_n \frac{Q_{n-1/2}(\text{ch}\xi_0)}{P_{n-1/2}(\text{ch}\xi_0)} \cos(nu) \\
&\quad [(\text{ch}\xi_0 - \cos u)^{3/2} P'_{n-1/2}(\text{ch}\xi_0) + (1/2)\sqrt{\text{ch}\xi_0 - \cos u} P_{n-1/2}(\text{ch}\xi_0)] . \tag{10.5.6}
\end{aligned}$$

We now write this as the sum of the two terms $\sigma = \sigma_1 + \sigma_2$ where

$$\begin{aligned}
\sigma_1 &= +\frac{1}{4\pi R} V_0 \frac{\sqrt{2}}{\pi} \sum_{n=0}^{\infty} \varepsilon_n \frac{Q_{n-1/2}(\text{ch}\xi_0)}{P_{n-1/2}(\text{ch}\xi_0)} \cos(nu) * (\text{ch}\xi_0 - \cos u)^{3/2} P'_{n-1/2}(\text{ch}\xi_0) \\
\sigma_2 &= \frac{1}{4\pi R} V_0 \frac{\sqrt{2}}{\pi} \sum_{n=0}^{\infty} \varepsilon_n \frac{Q_{n-1/2}(\text{ch}\xi_0)}{P_{n-1/2}(\text{ch}\xi_0)} \cos(nu) * \sqrt{\text{ch}\xi_0 - \cos u} * \frac{1}{2} P_{n-1/2}(\text{ch}\xi_0)
\end{aligned}$$

which we then reorganize to get

$$\begin{aligned}
\sigma_1 &= \frac{1}{4\pi R} V_0 \frac{\sqrt{2}}{\pi} (\text{ch}\xi_0 - \cos u)^{3/2} \sum_{n=0}^{\infty} \varepsilon_n P'_{n-1/2}(\text{ch}\xi_0) \frac{Q_{n-1/2}(\text{ch}\xi_0)}{P_{n-1/2}(\text{ch}\xi_0)} \cos(nu) \\
\sigma_2 &= \frac{1}{4\pi R} V_0 \frac{\sqrt{2}}{\pi} \sqrt{\text{ch}\xi_0 - \cos u} \frac{1}{2} \sum_{n=0}^{\infty} \varepsilon_n Q_{n-1/2}(\text{ch}\xi_0) \cos(nu) . \tag{10.5.7}
\end{aligned}$$

Recall (10.1.8a) with $a = \text{ch}\xi_0$ and $b = 1$ and $x = u$,

$$1 = \sqrt{\text{ch}\xi_0 - \cos u} \frac{\sqrt{2}}{\pi} \sum_{n=0}^{\infty} \varepsilon_n Q_{n-1/2}(\text{ch}\xi_0) \cos(nu). \quad (10.5.8)$$

This "sum rule" greatly simplifies σ_2 so that now,

$$\sigma_2 = \frac{1}{4\pi R} V_0 \frac{1}{2} = \frac{1}{4\pi R} V_0 \frac{\sqrt{2}}{\pi} \left\{ \frac{\pi}{2\sqrt{2}} \right\}. \quad (10.5.9)$$

Reconstruct the sum $\sigma = \sigma_2 + \sigma_1$ to get

$$\begin{aligned} \sigma(u; \xi_0) &= \frac{1}{4\pi R} V_0 \frac{\sqrt{2}}{\pi} \\ &\left\{ \frac{\pi}{2\sqrt{2}} + (\text{ch}\xi_0 - \cos u)^{3/2} \sum_{n=0}^{\infty} \varepsilon_n P'_{n-1/2}(\text{ch}\xi_0) \frac{Q_{n-1/2}(\text{ch}\xi_0)}{P_{n-1/2}(\text{ch}\xi_0)} \cos(nu) \right\}. \end{aligned}$$

Next, extract a factor $\pi/\sqrt{2}$ from $\{ \dots \}$ and replace $(\text{sh}\xi_0/a) = 1/R$ from (1.2.7) to get,

$$\sigma(u; \xi_0) = \frac{V_0}{4\pi R} \left[\frac{1}{2} + \frac{\sqrt{2}}{\pi} (\text{ch}\xi_0 - \cos u)^{3/2} \sum_{n=0}^{\infty} \varepsilon_n P'_{n-1/2}(\text{ch}\xi_0) \frac{Q_{n-1/2}(\text{ch}\xi_0)}{P_{n-1/2}(\text{ch}\xi_0)} \cos(nu) \right]. \quad (10.5.10)$$

This is our final result for the surface charge density on a torus having label ξ_0 and tube radius R held at potential V_0 . We have scanned all our known sources, but cannot find verification of this result, so we shall be extra attentive in doing "checks".

First Check: The thin-wire torus limit

In the thin wire limit the parameter ξ_0 gets large as shown in Fig (1.1.3). The distance ρ_σ to the tube center line approaches a , and the tube radius R approaches 0. Since $\text{ch}\xi_0$ gets large, we invoke the large-x limits of the P and Q functions from Appendix H.

Consider first the terms in the sum in (10.5.10) which have $n > 0$. With $x = \text{ch}\xi_0$, one finds

$$P'_{n-1/2}(x) \rightarrow x^{n-3/2} \quad x \rightarrow \infty \quad (H.6.3)$$

$$\frac{Q_{n-1/2}(x)}{P_{n-1/2}(x)} \rightarrow x^{-2n} \quad (H.6.7)$$

$$(\text{ch}\xi_0 - \cos u)^{3/2} \rightarrow x^{3/2}.$$

Therefore, the n^{th} sum term goes as

$$x^{3/2} x^{n-3/2} x^{-2n} = x^{-n}. \quad (10.5.11)$$

For large x , these terms all decay away, relative to the constant term $1/2$ appearing in (10.5.10).

The $n = 0$ term has different behavior. Again from Appendix H,

$$P'_{-1/2}(x) \rightarrow \frac{\sqrt{2}}{\pi} x^{-3/2} [1 - (1/2)\ln(8x)] \quad x \rightarrow \infty \quad (H.6.16)$$

$$\frac{Q_{-1/2}(x)}{P_{-1/2}(x)} \rightarrow = (\pi^2/2) 1/\ln(8x) \quad (H.6.15)$$

$$(\operatorname{ch}\xi_0 - \cos u)^{3/2} \rightarrow x^{3/2}.$$

For large $x = \operatorname{ch}\xi_0$ the $n = 0$ term in (10.5.1) is then

$$\begin{aligned} & \frac{\sqrt{2}}{\pi} * x^{3/2} * 1 * \frac{\sqrt{2}}{\pi} x^{-3/2} [1 - (1/2)\ln(8x)] * (\pi^2/2) 1/\ln(8x) \\ &= [1 - (1/2)\ln(8x)] (1/\ln(8x)) = 1/\ln(8x) - 1/2 \end{aligned} \quad (10.5.12)$$

This $-1/2$ cancels the $+1/2$ appearing in (10.5.10) and we end up with

$$\sigma(u; \xi_0) \approx \frac{V_0}{4\pi R} \frac{1}{\ln(8x)}. \quad (10.5.13)$$

We keep in mind that $R \rightarrow 0$ in our limit, but we maintain R for a while longer. Meanwhile,

$$x = \operatorname{ch}\xi_0 \approx \operatorname{sh}\xi_0 = a/R \quad // (1.2.7)$$

so

$$\ln(8x) = \ln(8a/R) = \ln(a) + \ln(8/R) \approx \ln(8/R) \quad \text{as } R \rightarrow 0$$

Then we find

$$\sigma(u; \xi_0) \approx \frac{V_0}{4\pi R} \frac{1}{\ln(8/R)}. \quad (10.5.14)$$

This charge density is uniform in u , as one would expect since a piece of the thin ring thinks it is a piece of straight wire with uniform σ . The curvature radius $\rho_c = a$ is huge compared to the wire radius R . Thus, to find the total charge on the torus, we multiply σ by the area of a torus,

$$A = 4\pi^2 R \rho_c \quad // \text{torus area}$$

to get

$$Q = \sigma A = \frac{V_0}{4\pi R} \frac{1}{\ln(8/R)} \cdot 4\pi^2 R \rho_c = V_0 \pi \rho_c \frac{1}{\ln(8/R)} = CV_0$$

Setting $\rho_c = 1$ as in Section 10.4 below, one gets

$$C = \frac{\pi}{\ln(8/R)} \quad (10.5.15)$$

which agrees with (10.4.12) as the capacitance of the torus in the thin-wire limit. We therefore regard our σ result (10.5.10) as being correct in the thin-wire limit.

Second Check: Integrating the surface charge

This task is anything but simple and is carried out in Appendix K with support from other Appendices. The integration of course is performed directly in toroidal coordinates. We outline the main steps here.

1. Start with the charge density (10.5.10),

$$\sigma(u; \xi_0) = \frac{V_0}{4\pi R} \left[\frac{1}{2} + \frac{\sqrt{2}}{\pi} (\text{ch}\xi_0 - \cos u)^{3/2} \sum_{n=0}^{\infty} \varepsilon_n P'_{n-1/2}(\text{ch}\xi_0) \frac{Q_{n-1/2}(\text{ch}\xi_0)}{P_{n-1/2}(\text{ch}\xi_0)} \cos(nu) \right]. \quad (K.2.1)$$

2. Integrate over the toroidal surface to get the total charge Q ,

$$Q = \frac{V_0}{2R} a^2 \text{sh}\xi_0 \left\{ \pi (\text{ch}\xi_0)(1/\text{sh}^3\xi_0) + \frac{4}{\pi} \sum_{n=0}^{\infty} \varepsilon_n P'_{n-1/2}(\text{ch}\xi_0) \frac{[Q_{n-1/2}(\text{ch}\xi_0)]^2}{P_{n-1/2}(\text{ch}\xi_0)} \right\}. \quad (K.2.6)$$

3. Use the Wronskian (H.8.2), $1/(1-z^2) = P_v(z) Q'_v(z) - P'_v(z) Q_v(z)$, to rewrite the above sum as

$$\sum_{n=0}^{\infty} \varepsilon_n P'_{n-1/2}(\text{ch}\xi_0) \frac{[Q_{n-1/2}(\text{ch}\xi_0)]^2}{P_{n-1/2}(\text{ch}\xi_0)} = (1/\text{sh}\xi_0)^2 \sum_{n=0}^{\infty} \varepsilon_n \frac{Q_{n-1/2}(\text{ch}\xi_0)}{P_{n-1/2}(\text{ch}\xi_0)} \quad (K.2.9)$$

$$+ \sum_{n=0}^{\infty} \varepsilon_n Q_{n-1/2}(\text{ch}\xi_0) Q'_{n-1/2}(\text{ch}\xi_0). \quad (K.2.10)$$

4. Evaluate the second sum using these two facts, where the second is the derivative of the first,

$$\sum_{n=0}^{\infty} \varepsilon_n [Q_{n-1/2}(z)]^2 = (\pi^2/2) \frac{1}{\sqrt{z^2-1}} \quad (J.4.1)$$

$$\sum_{n=0}^{\infty} \varepsilon_n Q_{n-1/2}(z) Q'_{n-1/2}(z) = -(\pi^2/4) z (z^2-1)^{-3/2}. \quad (J.4.2)$$

The QQ' sum term in item 3 exactly cancels the first term in item 2 above, giving this result

$$Q = V_0 \frac{2a}{\pi} \sum_{n=0}^{\infty} \varepsilon_n \frac{Q_{n-1/2}(\text{ch}\xi_0)}{P_{n-1/2}(\text{ch}\xi_0)} \quad (10.5.16)$$

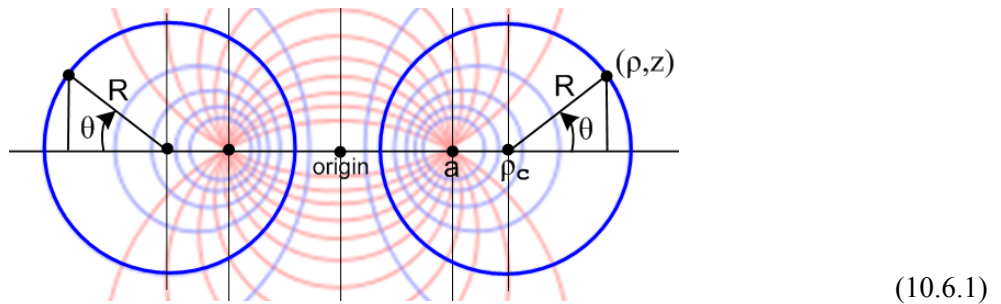
which implies that the torus has capacitance

$$C = \frac{2a}{\pi} \sum_{n=0}^{\infty} \epsilon_n \frac{Q_{n-1/2}(\text{ch}\xi_0)}{P_{n-1/2}(\text{ch}\xi_0)} . \quad (10.5.17)$$

This agrees with the result (10.4.3) which was found completely independently by taking the far-away limit of the potential (10.1.11).

10.6 Using Maple to plot the torus surface charge density

We wish to plot the surface charge not against toroidal coordinate u , but against the "circle angle" θ illustrated in this drawing of a torus cross section,



To do this, we write an expression for the total charge dQ in a patch of area dA on the torus,

$$dQ = \sigma dA = \sigma (h_u du)(h_\phi d\phi) = \sigma h_u h_\phi du d\phi = \sigma h_u h_\phi \frac{du}{d\theta} d\theta d\phi . \quad (10.6.2)$$

In *Bipolar* we derive a set of relations between θ and (ξ, u) which we quote here,

Relations between θ and (ξ, u)	$\frac{du}{d\theta} = \frac{\text{sh}\xi}{\text{ch}\xi + \cos\theta}$	$(7.10)'$
$\sin\theta = \frac{ \text{sh}\xi \sin u}{\text{ch}\xi - \cos u}$	$\sin u = \frac{ \text{sh}\xi \sin\theta}{\text{ch}\xi + \cos\theta}$	$\text{ch}\xi - \cos u = \frac{\text{sh}^2\xi}{\text{ch}\xi + \cos\theta}$
$\cos\theta = \frac{\text{ch}\xi \cos u - 1}{\text{ch}\xi - \cos u}$	$\cos u = \frac{\text{ch}\xi \cos\theta + 1}{\text{ch}\xi + \cos\theta}$	$\frac{1}{\text{ch}\xi - \cos u} = \frac{\text{ch}\xi + \cos\theta}{\text{sh}^2\xi}$
$\tan\theta = \frac{ \text{sh}\xi \sin u}{\text{ch}\xi \cos u - 1}$	$\tan u = \frac{ \text{sh}\xi \sin\theta}{\text{ch}\xi \cos\theta + 1}$	$h = \frac{a}{\text{ch}\xi - \cos u} = a \frac{\text{ch}\xi + \cos\theta}{\text{sh}^2\xi}$
		$(10.6.3)$

Then, from (1.2.17) and the bottom right equation in the above box,

$$h_u h_\phi = \operatorname{sh} \xi h_u^2 = \operatorname{sh} \xi h^2 = \operatorname{sh} \xi a^2 (\operatorname{ch} \xi + \cos \theta)^2 / \operatorname{sh}^4 \xi = a^2 (\operatorname{ch} \xi + \cos \theta)^2 / \operatorname{sh}^3 \xi . \quad (10.6.4)$$

Using $\frac{du}{d\theta} = \frac{\operatorname{sh} \xi}{\operatorname{ch} \xi + \cos \theta}$ also from the above box we get, now setting $\xi = \xi_0$ (torus label),

$$\begin{aligned} dQ_\theta &= \sigma h_u h_\phi \frac{du}{d\theta} d\theta d\varphi = \sigma a^2 (\operatorname{ch} \xi_0 + \cos \theta)^2 / \operatorname{sh}^3 \xi_0 * \operatorname{sh} \xi_0 / (\operatorname{ch} \xi_0 + \cos \theta) * d\theta d\varphi \\ &= \sigma a^2 (\operatorname{ch} \xi_0 + \cos \theta) / \operatorname{sh}^2 \xi_0 * d\theta d\varphi \\ &= \sigma R^2 (\operatorname{ch} \xi_0 + \cos \theta) d\theta d\varphi . \quad // \text{using } R = a / \operatorname{sh} \xi_0 \text{ from box (1.2.17)} \end{aligned} \quad (10.6.5)$$

The quantity we want to plot is then

$$"dQ_\theta" \equiv dQ_\theta / (d\theta d\varphi) = \sigma(u(\theta); \xi_0) R^2 (\operatorname{ch} \xi_0 + \cos \theta) . \quad (10.6.6)$$

Letting N being the number of terms to sum, the charge density σ from (10.5.10) is

$$\begin{aligned} \sigma(N) &= \frac{V_0}{4\pi R} \left[\frac{1}{2} + \frac{\sqrt{2}}{\pi} (\operatorname{ch} \xi_0 - \cos u)^{3/2} \sum_{n=0}^N \varepsilon_n P'_{n-1/2}(\operatorname{ch} \xi_0) \frac{Q_{n-1/2}(\operatorname{ch} \xi_0)}{P_{n-1/2}(\operatorname{ch} \xi_0)} \cos(nu) \right] . \\ &= \frac{V_0}{4\pi R} \left[\frac{1}{2} + \frac{\sqrt{2}}{\pi} (\operatorname{ch} \xi_0 - \cos u)^{3/2} * \text{sum1}(N) \right] \end{aligned}$$

where

$$\text{sum1}(N) = \sum_{n=0}^N \varepsilon_n P'_{n-1/2}(\operatorname{ch} \xi_0) \frac{Q_{n-1/2}(\operatorname{ch} \xi_0)}{P_{n-1/2}(\operatorname{ch} \xi_0)} \cos(nu) . \quad (10.6.7)$$

Expressions for dQ_θ , $\sigma = \text{sigma}$ and sum1 are duly entered,

$$\begin{aligned} dQ &:= (N) \rightarrow \text{sigma}(N) * R^2 * (\cosh(xi0) + \cos(theta)) ; \\ dQ &:= N \rightarrow \sigma(N) R^2 (\cosh(\xi_0) + \cos(\theta)) \\ \text{sigma} &:= (N) \rightarrow (V_0 / (4 * \pi * R)) * (1/2 + (\sqrt{2} / \pi) * (\cosh(xi0) - \cos(u))^{3/2} * \text{sum1}(N)) ; \\ \sigma &:= N \rightarrow \frac{1}{4} \frac{V_0 \left(\frac{1}{2} + \frac{\sqrt{2} (\cosh(\xi_0) - \cos(u))^{3/2}}{\pi} \text{sum1}(N) \right)}{\pi R} \\ \text{sum1} &:= (N) \rightarrow \sum(\text{eps}(n) * dP(n-1/2, xi0) * (Q(n-1/2, xi0) / P(n-1/2, xi0)) * \cos(n * u), n=0 .. N) ; \\ \text{sum1} &:= N \rightarrow \sum_{n=0}^N \frac{\text{eps}(n) dP\left(n - \frac{1}{2}, \xi_0\right) Q\left(n - \frac{1}{2}, \xi_0\right) \cos(n u)}{P\left(n - \frac{1}{2}, \xi_0\right)} \end{aligned} \quad (10.6.8)$$

It is easy to replace the $(ch\xi_0 - cosu)^{3/2}$ factor in σ by a function of u and θ using the box (10.6.3), but it is not easy to write $cos(nu)$ as a simple function of θ . We shall avoid this issue by having Maple compute u from θ as needed, again using expressions in the above box,

$$\begin{aligned}
 \sinu &:= \text{abs}(\sinh(xi0)) * \sin(theta) / (\cosh(xi0) + \cos(theta)); \\
 sinu &:= \frac{|\sinh(\xi_0)| \sin(\theta)}{\cosh(\xi_0) + \cos(\theta)} \\
 \cosu &:= (\cosh(xi0) * \cos(theta) + 1) / (\cosh(xi0) + \cos(theta)); \\
 cosu &:= \frac{\cosh(\xi_0) \cos(\theta) + 1}{\cosh(\xi_0) + \cos(\theta)} \\
 u &:= \text{arctan2Pi}(cosu, sinu); \\
 u &:= \text{arctan2Pi}\left(\frac{\cosh(\xi_0) \cos(\theta) + 1}{\cosh(\xi_0) + \cos(\theta)}, \frac{|\sinh(\xi_0)| \sin(\theta)}{\cosh(\xi_0) + \cos(\theta)}\right)
 \end{aligned} \tag{10.6.9}$$

Much of the other Maple code has been displayed earlier: the P and Q functions in (7.4.4), arctan2Pi in (9.2) and eps in (10.3.2). The P' function is computed as follows,

$$P'_v(ch\xi) = \frac{dP_v(ch\xi)}{d(ch\xi)} = \frac{dP_v(ch\xi)}{(sh\xi)d\xi} = (1/sh\xi) \partial_\xi P_v(ch\xi) = (1/sh\xi) \partial_\xi P(v,\xi) \equiv dP(v,\xi)$$

$$P(v,\xi) \equiv P_v(ch\xi) = (ch\xi)^v F(-v/2, 1/2-v/2; 1; th^2\xi) \tag{7.4.1}$$

$$\partial_z F(a,b;c;z) = (ab/c)F(a+1,b+1;c+1;z) \tag{10.6.10}$$

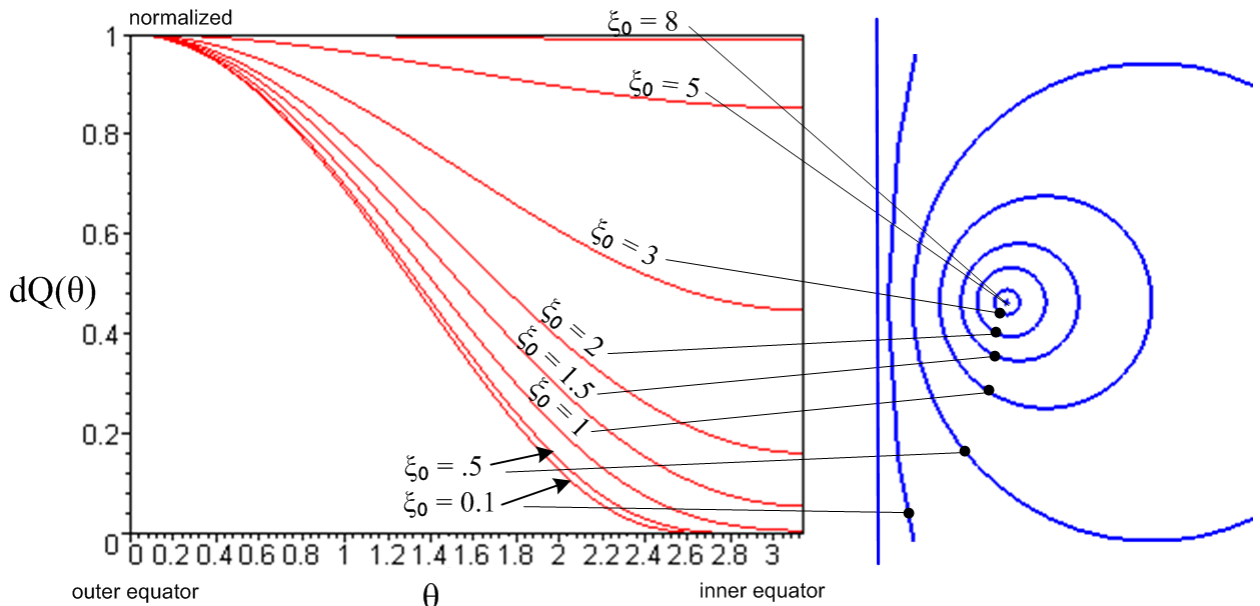
Maple is happy to compute $dP(v,\xi) = P'_v(ch\xi)$ with a little prodding,

$$\begin{aligned}
 > P &:= (nu, xi) \rightarrow \text{evalf}(\cosh(xi)^nu * \text{hypergeom}([-nu/2, 1/2-nu/2], [1], \tanh(xi)^2)); \\
 P &:= (v, \xi) \rightarrow \text{evalf}\left(\cosh(\xi)^v \text{hypergeom}\left(\left[-\frac{1}{2}v, \frac{1}{2}-\frac{1}{2}v\right], [1], \tanh(\xi)^2\right)\right) \\
 > \text{temp1} &:= (1/sinh(xi)) * \text{diff}(P(nu, xi), xi); \\
 \text{temp1} &:= \left(\frac{\cosh(\xi)^v v \sinh(\xi) \text{hypergeom}([.50 - .50 v, -.50 v], [1], \tanh(\xi)^2)}{\cosh(\xi)} \right. \\
 &\quad \left. - 1.0 \cosh(\xi)^v (.50 - .50 v) v \text{hypergeom}([1.5 - .50 v, -.50 v + 1], [2], \tanh(\xi)^2) \tanh(\xi) (1 - \tanh(\xi)^2) \right) / \sinh(\xi) \\
 > \text{dP} &:= \text{unapply}(\text{temp1}, nu, xi); \\
 dP &:= (v, \xi) \rightarrow \left(\frac{\cosh(\xi)^v v \sinh(\xi) \text{hypergeom}([.50 - .50 v, -.50 v], [1], \tanh(\xi)^2)}{\cosh(\xi)} \right. \\
 &\quad \left. - 1.0 \cosh(\xi)^v (.50 - .50 v) v \text{hypergeom}([1.5 - .50 v, -.50 v + 1], [2], \tanh(\xi)^2) \tanh(\xi) (1 - \tanh(\xi)^2) \right) / \sinh(\xi)
 \end{aligned} \tag{10.6.11}$$

Here the "unapply" command causes the temp1 expression to be a function $dP(v,\xi)$ of v and ξ .

Finally, we make plots of "dQ_θ" versus θ for a selection of ξ_0 values. These plots are normalized so dQ_θ(0) = 1, which is a location on the outer equator of the torus.

```
R := 1:v0 := 1:
M := 50:
k := 1:
for xi0 in [5,3,2,1.5,1.0,.75,.50,.25] do
  theta := 0: dQmax := dQ(M): unassign('theta'):
  p[k] := plot(dQ(M)/dQmax,theta = 0..pi,y=0..1):
  k := k+1:
od:
with(plots): display(seq(p[k],k=1..8));
```



(10.6.12)

The main idea in the dQ(θ) sum is that near θ = 0 (u=0) the terms are additive since cos(nu) ~ 1, whereas in the "backward direction" especially near θ = π (u = π) there is term interference from cos(nu) ~ (-1)ⁿ, causing the charge to concentrate on the outer toroidal surface just as one would expect. This situation is akin to the forward peak in a scattering amplitude in partial wave analysis.

For $\xi_0 = 8$ the torus is close to the thin-wire limit, so dQ is practically uniform in θ as indicated by the top red curve above. Once again, the thin wire thinks it is an isolated infinite straight wire which naturally has uniform σ. As the tori get fatter, the dQ distribution becomes more peaked at θ = 0. In all cases the peak of dQ occurs on the outside equator θ = 0, as one would expect. For $\xi_0 < 0.1$ the plot cannot be distinguished from the $\xi_0 = 0.1$ plot, though more terms must be added in the sum. Thus one can regard the bottom red curve above as the "fat toroid limit" and the top curve as the "thin toroid limit".

The torus charge density is finite and smooth everywhere, unlike the bowl σ, because a torus has no sharp edges. In general, the torus σ drops monotonically from its maximum value on the outer equator to some finite value on the inner equator. The charge density on the inside surface of the toroid is 0.

Appendix A. Maple code text for plotting the bowl and torus potentials

The following code can be copied from this PDF document and pasted into the Maple V Release 5 (5.00) "classic" white worksheet window (beware PDF page boundaries). It then runs when you hit the enter key and plots should appear (we have verified this). See author's Maple User's Guide for how to break code into separate execution groups.

For more recent versions of Maple, one will likely need to "migrate" the code from our classic .mws file format to the standard .mw format. For example, Maple 2015 contains an "assistant" to do this, as indicated in the Maple 2015 User Manual:

- **Worksheet Migration** - an interface to convert worksheets from Classic Maple (.mws files) to Standard Maple (.mw files).

Code to Plot Bowl Potential

```
restart;

# Construct the charged bowl potential in toroidal coordinates using (8.8b)
A := sqrt(cosh(xi)-cos(u)):
B := sqrt(2)*cos(u/2):
C := sqrt(cosh(xi)-cos(2*u0-u)):
E := sqrt(2)*cos(u0-u/2):
V := (V0/Pi)*(Pi-arccot(B/A)+(A/C)*arccot(E/C));
V0 := 1:
a := 1:
u0 := evalf(Pi/4);

# Routine arctan2Pi
# Given (x,y) somewhere on a circle, return the angle in (0,2Pi) measured CCW from the
# axis. Warning: returned result may include unevaluated multiples of Pi
arctan2Pi := proc(x,y)
local q;
if type(x,numeric) and type(y,numeric) then
    if x = 0 and y = 0 then print("arctan2Pi(0,0) error."); RETURN(0) fi;
    if x = 0 and y > 0 then RETURN(Pi/2) fi;
    if x = 0 and y < 0 then RETURN(3*Pi/2) fi;
    if x > 0 and y = 0 then RETURN(0) fi;
    if x < 0 and y = 0 then RETURN(Pi) fi;
    if x > 0 and y > 0 then q := 0 fi;
    if x < 0 and y > 0 then q := Pi fi;
    if x < 0 and y < 0 then q := Pi fi;
    if x > 0 and y < 0 then q := 2*Pi fi;
    RETURN(arctan(y/x)+q);
else
    'arctan2Pi(x,y)';
fi;
end:

# Routine getu
# Given a,u0,rho,z, compute toroidal bowl-label parameter u in range (u0,u0+2Pi)
getu := proc(rho,z)
global a,u0; local u;
if type(rho,numeric) and type(z,numeric) then
    u := arctan2Pi(rho^2+z^2-a^2,2*a*z);
```

```

    if u < u0 then u := u + evalf(2*Pi) fi; # get in range
    RETURN(u);
else
  'getu(rho,z)';
fi;
end:

# Plot the potential of the charged bowl(an azimuthal slice)
xi := arctanh(2*a*abs(rho)/(a^2+rho^2+z^2)):
u := getu(rho,z):
plot3d(V, rho = -2..2, z = -2..3,numpoints=2000,axes=BOXED, view=0..1);

```

Code to Plot Torus Potential

```

restart;

#For P, we select Bateman (24) which says this
P := (nu,xi) -> evalf(cosh(xi)^nu*hypergeom([-nu/2,1/2-nu/2],[1],tanh(xi)^2));
#Show this agrees with Maple internal P function at some point
evalf(P(3,0.5));
evalf(LegendreP(3,cosh(0.5)));

#For Q, we select Bateman (45) which says this
Q := (nu,xi) -> evalf(sqrt(Pi)*(GAMMA(1+nu)/GAMMA(3/2+nu))*exp(-(1+nu)*xi)*hypergeom([1/2,1+nu],[3/2+nu],exp(-2*xi)));
#Show this agrees with Maple internal Q function at some point
evalf(Q(1,1));
evalf(LegendreQ(1,cosh(1)));

#Routine arctan2Pi
#Given (x,y) somewhere on a circle, return the angle in (0,2Pi) measured CCW from the
x axis. Warning: returned result may include unevaluated multiples of Pi
arctan2Pi := proc(x,y)
local q;
if type(x,numeric) and type(y,numeric) then
  if x = 0 and y = 0 then print("arctan2Pi(0,0) error."); RETURN(0) fi;
  if x = 0 and y > 0 then RETURN(Pi/2) fi;
  if x = 0 and y < 0 then RETURN(3*Pi/2) fi;
  if x > 0 and y = 0 then RETURN(0) fi;
  if x < 0 and y = 0 then RETURN(Pi) fi;
  if x > 0 and y > 0 then q := 0 fi;
  if x < 0 and y > 0 then q := Pi fi;
  if x < 0 and y < 0 then q := Pi fi;
  if x > 0 and y < 0 then q := 2*Pi fi;
  RETURN(arctan(y/x)+q);
else
  'arctan2Pi(x,y)';
fi;
end;

#Routine eps
eps := proc(n) if type(n,numeric) then
  if n=0 then RETURN(1) else RETURN(2) fi;
else 'eps(n)'; fi end;

#Routine getxi
getxi := proc(rho,z)

```

```

global a,xi0; local xi;
if type(rho,numeric) and type(z,numeric) then
  xi := arctanh(2*a*abs(rho)/(a^2+rho^2+z^2));
  if xi > xi0 then xi := xi0 fi; # pin at torus
  if xi < -xi0 then xi := -xi0 fi; # pin at torus
  RETURN(xi);
else
  'getxi(rho,z)';
fi;
end:

#Plot the potential of the torus using (10.1.11)
V := (V0*sqrt(2)/Pi)*sqrt(cosh(xi)-cos(u))*sum(term(n),n=0..N);
term := (n) -> eps(n)*(Q(n-1/2,xi0)/P(n-1/2,xi0))*P(n-1/2,xi)*cos(n*u);
V0 := 10: a := 1: xi0 := 1.0: N := 10:
u:= arctan2Pi(rho^2+z^2-a^2,2*a*z);
xi := getxi(rho,z);
plot3d(Re(V),rho = -2.3..2.3, z = -1.1..1.1, grid = [50,50], axes = boxed, scaling = constrained);

```

Appendix B : Converting expressions from toroidal to cylindrical coordinates

B.1 The conversions

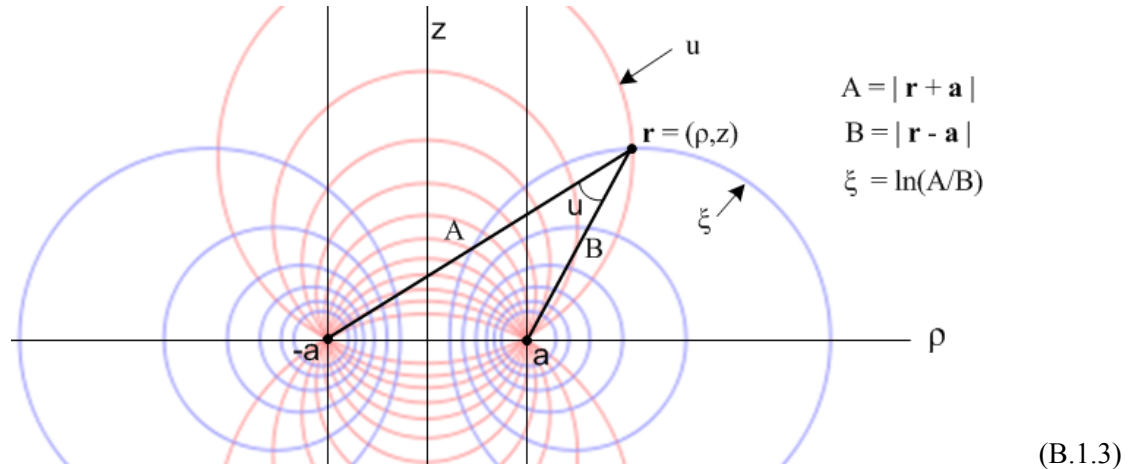
At first this sounds like a task that requires no effort. After all, we know from (1.2.2) that

$$\begin{aligned} x &= a \cos\varphi \operatorname{sh}\xi / (\operatorname{ch}\xi - \cos u) & \rho &= a \operatorname{sh}\xi / (\operatorname{ch}\xi - \cos u) = \sqrt{x^2 + y^2} \\ y &= a \sin\varphi \operatorname{sh}\xi / (\operatorname{ch}\xi - \cos u) & z/\rho &= \sin u / \operatorname{sh}\xi \\ z &= a \sin u / (\operatorname{ch}\xi - \cos u) & 0 \leq \xi \leq \infty, 0 \leq u \leq 4\pi \end{aligned} . \quad (B.1.1)$$

The issue is how to convert expressions like $\operatorname{ch}\xi - \cos u$ to cylindrical coordinates, and there are a few subtleties involved. The following three positive quantities will be useful:

$$A \equiv \sqrt{z^2 + (\rho+a)^2} \quad B \equiv \sqrt{z^2 + (\rho-a)^2} \quad Q \equiv \frac{1}{AB} = \frac{1}{\sqrt{z^2 + (\rho+a)^2} \sqrt{z^2 + (\rho-a)^2}} . \quad (B.1.2)$$

A and B are the distances to the focal points as shown in *Bipolar* Fig (6.1), modified here,



For the ξ coordinate, we invoke Maple, then translate below what it says:

$$\begin{aligned}
 \text{th} &:= 2*a*rho/(a^2+rho^2+z^2); \\
 \text{th} &= 2 \frac{a\rho}{a^2+\rho^2+z^2} \\
 \text{ch2} &:= 1/(1-th^2): \text{simplify}(%): \text{factor}(%); \\
 &\frac{(a^2+\rho^2+z^2)^2}{(\rho^2-2a\rho+a^2+z^2)(\rho^2+2a\rho+a^2+z^2)} \\
 \text{sh2} &:= \text{ch2-1}: \text{simplify}(%): \text{factor}(%); \\
 &4 \frac{a^2\rho^2}{(\rho^2-2a\rho+a^2+z^2)(\rho^2+2a\rho+a^2+z^2)}
 \end{aligned} \tag{B.1.4}$$

The equations above are

$$\begin{aligned}
 \text{th}\xi &= 2ap/(a^2+\rho^2+z^2) && // \text{as appears in (1.2.5)} \\
 \text{ch}^2\xi &= (a^2+\rho^2+z^2)^2/(A^2B^2) = [(a^2+\rho^2+z^2)Q]^2 \\
 \text{sh}^2\xi &= 4a^2\rho^2/(A^2B^2) = [2apQ]^2
 \end{aligned} \tag{B.1.5}$$

Since $\text{ch}\xi$ and $\text{sh}\xi$ are always positive (range of ξ is $(0, \infty)$) one has,

$$\begin{aligned}
 \text{ch}\xi &= (a^2+\rho^2+z^2)Q \\
 \text{sh}\xi &= 2apQ
 \end{aligned} \tag{B.1.6}$$

Notice that

$$e^\xi = \text{ch}\xi + \text{sh}\xi = (a^2+\rho^2+z^2)Q + 2apQ = [(a+\rho)^2 + z^2]Q = [A^2]/(AB) = A/B$$

and therefore

$$\xi = \ln(A/B) = \ln \left[\frac{\sqrt{z^2 + (\rho+a)^2}}{\sqrt{z^2 + (\rho-a)^2}} \right] . \tag{B.1.7}$$

as shown in Fig (B.1.3).

We now repeat the above for coordinate u :

$$\begin{aligned}
 \tanu &:= 2*a*z/(rho^2+z^2-a^2); \\
 tanu &:= 2 \frac{az}{\rho^2+z^2-a^2} \\
 \cosu2 &:= 1/(1+tanu^2):simplify(%):factor(%); \\
 &\quad \frac{(-\rho^2-z^2+a^2)^2}{(\rho^2-2*a*\rho+a^2+z^2)(\rho^2+2*a*\rho+a^2+z^2)} \\
 \sinu2 &:= -cosu2+1:simplify(%):factor(%); \\
 &\quad 4 \frac{a^2 z^2}{(\rho^2-2*a*\rho+a^2+z^2)(\rho^2+2*a*\rho+a^2+z^2)}
 \end{aligned} \tag{B.1.8}$$

The equations above are

$$\begin{aligned}
 \tanu &= 2az/(\rho^2+z^2-a^2) \\
 \cos^2 u &= [(\rho^2+z^2-a^2)/AB]^2 = [(\rho^2+z^2-a^2)Q]^2 \\
 \sin^2 u &= [2az/AB]^2 = [2azQ]^2.
 \end{aligned} \tag{B.1.9}$$

Since u has full range, we don't immediately know the signs to use, so we write for the moment,

$$\begin{aligned}
 \cosu &= \pm (\rho^2+z^2-a^2)Q \\
 \sinu &= \pm 2azQ.
 \end{aligned}$$

It turns out that both signs are determined and are not free. As discussed below (9.1) and as shown in (9.4) the meaning of the $\tan^{-1}u$ operation is really this

$$u = \text{arctan2Pi}(X, Y) = \text{arctan2Pi}(\text{run}, \text{rise}) = \text{arctan2Pi}(\rho^2+z^2-a^2, 2az) \tag{B.1.10}$$

where the arctan2Pi function returns an angle u in the full range $(0, 2\pi)$ with full knowledge of the quadrant of the argument pair. In particular, we can make this table showing the signs of cosu and sinu that arise in the four regions (quadrants) of the arguments $X=\rho^2+z^2-a^2$ and $Y=2az$:

		<u>cosu</u>	<u>sinu</u>
$\rho^2+z^2-a^2 > 0$	$2az > 0$	1Q	+
$\rho^2+z^2-a^2 < 0$	$2az > 0$	2Q	-
$\rho^2+z^2-a^2 < 0$	$2az < 0$	3Q	-
$\rho^2+z^2-a^2 > 0$	$2az < 0$	4Q	+

(B.1.11)

The arctan2Pi function is calibrated so that a point at $z = +\epsilon$ and large ρ will have $u = 0$, consistent with Fig (1.1.2) (a). Notice from the table that

$$\begin{aligned}\text{sign}(\cos u) &= \text{sign}(\rho^2 + z^2 - a^2) \\ \text{sign}(\sin u) &= \text{sign}(z).\end{aligned}\quad (\text{B.1.12})$$

This last result is consistent with $z/\rho = \sin u / \text{sh } \xi$ in (B.1.1). Therefore, the \pm signs shown above are both $+$ and we have

$$\begin{aligned}\cos u &= (\rho^2 + z^2 - a^2)Q \\ \sin u &= 2azQ.\end{aligned}\quad (\text{B.1.13})$$

The ever-popular factor $\text{ch } \xi - \cos u$ is then obtained from (B.1.6) and (B.1.13),

$$\text{ch } \xi - \cos u = (a^2 + \rho^2 + z^2)Q - (\rho^2 + z^2 - a^2)Q = 2a^2Q. \quad (\text{B.1.14})$$

Half-Angle Expressions

Here are some half-"angle" results for ξ ,

$$\begin{aligned}2\text{ch}^2(\xi/2) &= \text{ch } \xi + 1 = (a^2 + \rho^2 + z^2)Q + 1 \\ 2\text{sh}^2(\xi/2) &= \text{ch } \xi - 1 = (a^2 + \rho^2 + z^2)Q - 1\end{aligned}$$

$$\begin{aligned}\sqrt{2} \text{ ch}(\xi/2) &= \sqrt{(a^2 + \rho^2 + z^2)Q + 1} \\ \sqrt{2} \text{ sh}(\xi/2) &= \sqrt{(a^2 + \rho^2 + z^2)Q - 1},\end{aligned}\quad (\text{B.1.15})$$

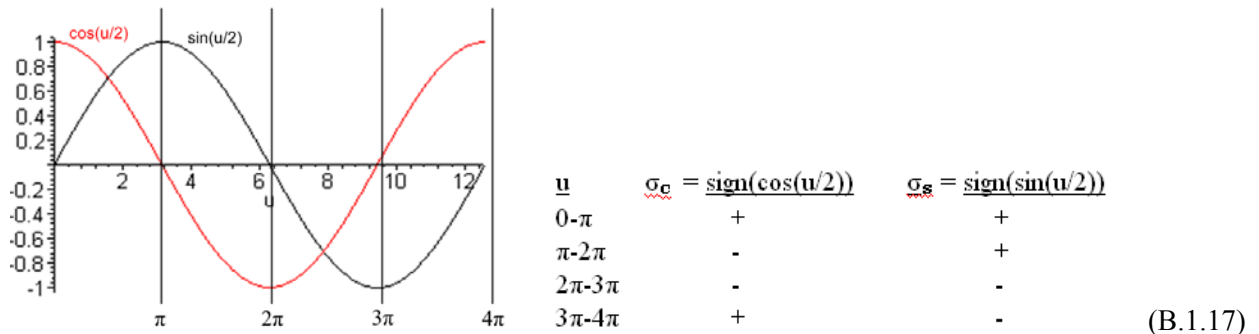
and here are the corresponding results for u ,

$$\begin{aligned}2\cos^2(u/2) &= 1 + \cos u = 1 + (\rho^2 + z^2 - a^2)Q \\ 2\sin^2(u/2) &= 1 - \cos u = 1 - (\rho^2 + z^2 - a^2)Q.\end{aligned}$$

Taking square roots,

$$\begin{aligned}\sqrt{2} \cos(u/2) &= \sigma_c \sqrt{1 + (\rho^2 + z^2 - a^2)Q} \\ \sqrt{2} \sin(u/2) &= \sigma_s \sqrt{1 - (\rho^2 + z^2 - a^2)Q}\end{aligned}\quad (\text{B.1.16})$$

The signs σ_c and σ_s are determined from these plots of the two functions (or the table) :



We may now summarize the above expression conversions:

$$\text{th}\xi = 2ap/(a^2 + p^2 + z^2) \quad A \equiv \sqrt{z^2 + (p+a)^2} \quad B \equiv \sqrt{z^2 + (p-a)^2} \quad (\text{B.1.18})$$

$$\text{ch}\xi = (a^2 + p^2 + z^2)Q \quad Q \equiv \frac{1}{AB} = \frac{1}{\sqrt{z^2 + (p+a)^2} \sqrt{z^2 + (p-a)^2}}$$

$$\text{sh}\xi = 2apQ \quad p = \sqrt{x^2 + y^2} \text{ to convert to Cartesian coordinates}$$

$$\tan u = 2az/(\rho^2 + z^2 - a^2) \quad // \text{ principle branch; } u = \arctan 2 \pi (\rho^2 + z^2 - a^2, 2az) \text{ gives } u \text{ in } (0, 2\pi)$$

$$\cos u = (\rho^2 + z^2 - a^2)Q$$

$$\sin u = 2azQ$$

$$\text{ch}\xi - \cos u = 2a^2Q \quad \xi = \ln(A/B)$$

$$\begin{aligned} \sqrt{2} \text{ ch}(\xi/2) &= \sqrt{(a^2 + p^2 + z^2)Q + 1} \\ \sqrt{2} \text{ sh}(\xi/2) &= \sqrt{(a^2 + p^2 + z^2)Q - 1} \end{aligned}$$

Converting expressions from toroidal to cylindrical coordinates.

$$\begin{aligned} \sqrt{2} \cos(u/2) &= \sigma_c \sqrt{1 + (\rho^2 + z^2 - a^2)Q} \\ \sqrt{2} \sin(u/2) &= \sigma_s \sqrt{1 - (\rho^2 + z^2 - a^2)Q} \end{aligned}$$

B.2 Application: The Disk Potential

The flat disk potential was found in (2.5.4) to be

$$V_{\text{disk}}(\xi, u) = (2V_0/\pi) \cot^{-1} \left[\frac{-\sqrt{2} \cos(u/2)}{\sqrt{\text{ch}\xi - \cos u}} \right] \quad // \xi > 0, \quad u_0 = \pi, \quad \pi \leq u \leq 3\pi. \quad (\text{B.2.1})$$

Based on the angle range, we set $\sigma_c = -1$ using table (B.1.17). Notice that the bipolar parameter a in the disk limit $u = \pi$ is equal to the disk radius.

To convert (B.2.1) to cylindrical coordinates, we look up the pieces in box (B.1.18) above,

$$\begin{aligned} \frac{-\sqrt{2} \cos(u/2)}{\sqrt{\text{ch}\xi - \cos u}} &= \frac{-\sigma_c \sqrt{1 + (\rho^2 + z^2 - a^2)Q}}{\sqrt{2a^2Q}} = \sqrt{\frac{1 + (\rho^2 + z^2 - a^2)Q}{2a^2Q}} \\ &= \sqrt{\frac{2Q^{-1} + 2(\rho^2 + z^2 - a^2)}{4a^2}} = \frac{\sqrt{2AB + 2(\rho^2 + z^2 - a^2)}}{2a}. \end{aligned} \quad (\text{B.2.2})$$

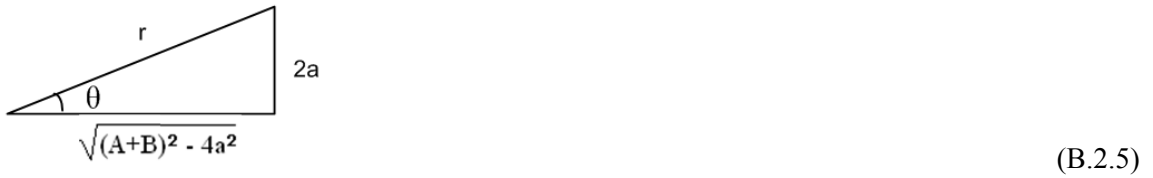
Now compute,

$$\begin{aligned} A^2 + B^2 &= z^2 + (\rho+a)^2 + z^2 + (\rho-a)^2 = 2(\rho^2 + z^2 + a^2) = 2(\rho^2 + z^2 - a^2) + 4a^2 \\ \Rightarrow 2(\rho^2 + z^2 - a^2) &= A^2 + B^2 - 4a^2 . \end{aligned} \quad (B.2.3)$$

Then

$$\theta \equiv \cot^{-1} \left[\frac{-\sqrt{2} \cos(u/2)}{\sqrt{\text{ch}\xi - \cos u}} \right] = \cot^{-1} \left(\frac{\sqrt{2AB + A^2 + B^2 - 4a^2}}{2a} \right) = \cot^{-1} \left(\frac{\sqrt{(A+B)^2 - 4a^2}}{2a} \right) . \quad (B.2.4)$$

Now we conjure up a right triangle whose angle θ has the cotangent shown,



Therefore

$$r^2 = [(A+B)^2 - 4a^2] + [4a^2] = (A+B)^2 \quad \Rightarrow \quad r = A+B \quad (B.2.6)$$

and so

$$\begin{aligned} \sin \theta &= \frac{2a}{r} = \frac{2a}{A+B} \\ \theta &= \cot^{-1} \left[\frac{-\sqrt{2} \cos(u/2)}{\sqrt{\text{ch}\xi - \cos u}} \right] = \sin^{-1} \left(\frac{2a}{A+B} \right) . \end{aligned} \quad (B.2.7)$$

The disk potential has then been converted to cylindrical coordinates :

$$\begin{aligned} V_{\text{disk}}(\xi, u) &= (2V_0/\pi) \cot^{-1} \left[\frac{-\sqrt{2} \cos(u/2)}{\sqrt{\text{ch}\xi - \cos u}} \right] \\ &= (2V_0/\pi) \sin^{-1} \left(\frac{2a}{A+B} \right) \\ &= (2V_0/\pi) \sin^{-1} \left(\frac{2a}{\sqrt{z^2 + (\rho+a)^2} + \sqrt{z^2 + (\rho-a)^2}} \right) . \quad // a = \text{disk radius} \end{aligned} \quad (B.2.8)$$

This result appears in green Jackson p 92 (3.1.78). The Jackson equation should have q/a in place of q , and then $q/a = (2V/\pi)$ by an earlier equation on the same page.

General Case

It would be possible to convert the full bowl potential to cylindrical coordinates. Recall (2.4.14a) ,

$$V(\xi, u) = (V_0/\pi) \left\{ \cot^{-1} \left[-\frac{\sqrt{2} \cos(u/2)}{\sqrt{\text{ch}\xi - \cos u}} \right] + \frac{\sqrt{\text{ch}\xi - \cos u}}{\sqrt{\text{ch}\xi - \cos(2u_0 - u)}} \cot^{-1} \left[\frac{\sqrt{2} \cos(u_0 - u/2)}{\sqrt{\text{ch}\xi - \cos(2u_0 - u)}} \right] \right\} \quad (\text{B.2.9})$$

$$\xi > 0 \quad u_0 \leq u \leq u_0 + 2\pi$$

We have already evaluated the first term above

$$\cot^{-1} \left[-\frac{\sqrt{2} \cos(u/2)}{\sqrt{\text{ch}\xi - \cos u}} \right] = -\sigma_c \sin^{-1} \left(\frac{2a}{A+B} \right). \quad (\text{B.2.10})$$

One would then need various unpleasant computed quantities:

$$\cos(u_0 - u/2) = \cos u_0 \cos(u/2) + \sin u_0 \sin(u/2)$$

$$= [\cos u_0 \sigma_c \sqrt{1 + (\rho^2 + z^2 - a^2)Q} + \sin u_0 \sigma_s \sqrt{1 - (\rho^2 + z^2 - a^2)Q}] / \sqrt{2}$$

$$\cos(2u_0 - u) = \cos(2u_0) \cos u + \sin(2u_0) \sin u$$

$$= \cos(2u_0)(\rho^2 + z^2 - a^2)Q + \sin(2u_0) 2azQ$$

$$= [\cos(2u_0)(\rho^2 + z^2 - a^2) + \sin(2u_0) 2az]Q$$

$$\text{ch}\xi - \cos(2u_0 - u) = 2a^2Q - [\cos(2u_0)(\rho^2 + z^2 - a^2) + \sin(2u_0) 2az]Q$$

$$= [2a^2 - \cos(2u_0)(\rho^2 + z^2 - a^2) - \sin(2u_0) 2az]Q \quad (\text{B.2.11})$$

It does not seem useful to pursue this path, although one could perhaps arrive at a reasonably stated result. In any event, the reader will appreciate that, although the bowl potential looks complicated in toroidal coordinates ξ, u , it is very much more complicated in cylindrical coordinates ρ, z . Results quoted at the end of Appendix D concerning a disk and iris provide a good example of what "more complicated" looks like.

Appendix C: Kelvin's approach to the charged bowl problem

Lord Kelvin (William Thomson, 1824-1907) published his own Collected Works on "electrostatics and mathematically allied subjects" in 1872 and again in 1884, and the latter is available on the web as a Microsoft digitized document. The Contents gives section numbers, not page numbers. There are 42 Articles with 673 sections filling some 600 pages, and the section numbers just increment through all the collected papers.

In the first collected paper (page 1, the ellipsoid paper, "On the Uniform Motion of Heat...", 14p, 1842) Kelvin derives the potential of and charge distribution on a charged conducting ellipsoid and gets the correct result (2.1.2) above. He bases his work on a certain geometric distance p which turns out to be proportional to σ on the ellipsoid: $p = 1/\sqrt{x^2/a^4 + y^2/b^4 + z^2/c^4}$ and $\sigma = Qp/(4\pi abc)$ where a,b,c are the semimajor axes and Q is the total charge on the ellipsoid (see McDonald). His method is very unusual, there is no formal ellipsoidal coordinate system here, but at age 18 he did the whole thing by brute force. He wanders around between the heat, gravitational and electrostatic manifestations of potential theory, but is mostly concerned with heat.

This brings us then to his bowl paper (Article XV, page 178, sections 231-248, "Determination of the distribution...", 14p, 1869). He opens by quoting the above $\sigma = Qp/(4\pi abc)$ formula (he refers to σ by the symbol ρ) and then specializes it first to an elliptical plate then to a circular disk, noting the disk capacitance $C = 2a/\pi$. He finds that $\sigma_{disk}(\rho) = [Q/(4\pi a)](1/\sqrt{a^2-\rho^2})$ on each side, where ρ is our modern-day cylindrical coordinate and a the disk radius (in agreement with half our (4.3.2) with $V = Q/C = Q\pi/2a$). This is the key result upon which his bowl theory is built. Kelvin notes retrospectively that George Green obtained this $\sigma_{disk}(\rho)$ result in 1832.

Kelvin then applies the theory of inversion to relate the disk to the bowl. Since this is crucial to his approach, we pause here for a quick review of this subject.

Inversion Theory in a Nutshell. Consider a set of point charges q_i at positions $\mathbf{r}_i = (r_i, \theta_i, \phi_i)$ in spherical coordinates relative to some origin O. Assume the resulting potential is $\phi(r, \theta, \phi)$. Call this Problem P.

Put an imaginary sphere of radius a around origin O. For each point $\mathbf{r} = (r, \theta, \phi)$ define an "image point" $\mathbf{r}' = (r', \theta', \phi') = (a^2/r, \theta, \phi)$. Points \mathbf{r} and \mathbf{r}' lie on opposite sides of the sphere of radius a along the same ray. It turns out that this 3D mapping $\mathbf{r} \rightarrow \mathbf{r}'$ maps spheres into spheres, somewhat analogous to the fact that linear fractional transformations map circles into circles in the 2D conformal mapping world. The mapping $\mathbf{r} \rightarrow \mathbf{r}'$ could map a sphere into a plane (a sphere of infinite radius).

Now consider Problem P' where all the charges of Problem P are moved to their image points \mathbf{r}'_i relative to this imaginary sphere of radius a , and are scaled as well to be $q'_i = q_i(a/r_i)$. The claim is that the potential ϕ' for Problem P' is related to the potential ϕ for Problem P in this way,

$$\phi'(r, \theta, \phi) = (a/r) \phi(a^2/r, \theta, \phi). \quad \text{relation between potentials in Problems P and P'} \quad (\text{C.1})$$

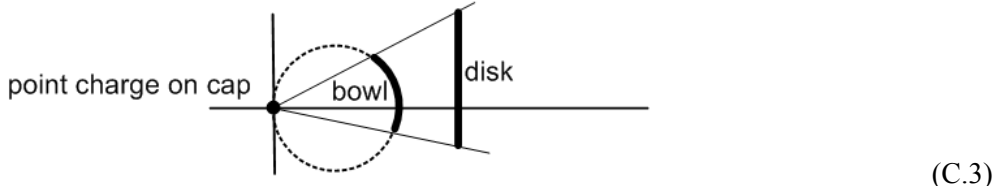
More generally, allowing for continuous charge distributions, one finds that

$q' = (a/r) q$	point charges	
$\sigma'(r, \theta, \phi) = (a/r)^3 \sigma(a^2/r, \theta, \phi)$	surface charges	
$\rho'(r, \theta, \phi) = (a/r)^5 \rho(a^2/r, \theta, \phi)$	volume charges	

(C.2)

For more detail on this subject, see green Jackson 2.6 (this topic was dropped in Jackson's later editions).

Deviating slightly from Kelvin's order of presentation, we tack sideways and ponder the inversion relationship between a charged disk with an added constant potential offset, and a grounded bowl in the presence of a certain point charge. Using the inversion theory, one first finds a inversion mapping using an inversion sphere of radius a which maps the bowl sphere into a plane. This same mapping then maps the bowl into a disk as shown here (the inversion circle is not shown, it lies between the bowl and disk),



The bowl and the disk are shown in the same picture, but each inhabits a separate "problem": the disk problem (Problem P) exists in disk space, while the bowl problem (Problem P') exists in bowl space. In the bowl problem, the bowl is assumed to be grounded ($\phi' = 0$ on the bowl). Suppose the disk is a charged disk with potential V_0 and charge $Q = C_{\text{disk}}V_0$ and potential $\varphi_{\text{disk}}(r, \theta, \phi)$ relative to the origin on the left. We can lower the disk potential to 0 by adding a constant potential $-V_0$ in disk space. From the theory of inversion described above, this causes a point charge $q = -aV_0$ to appear at the origin in bowl space, since $\varphi' = (a/r)\varphi = (a/r)(-V_0)$. The new situation is disk space with a potential $\varphi(r) = \varphi_{\text{disk}}(r) - V_0$ ($\varphi = 0$ on the disk) and a Green's Function situation in bowl space, where we now have a point charge and a grounded bowl ($\varphi' = 0$ on the bowl). One can then apply the (C.1) result that $\varphi'(r) = (a/r)\varphi(r')$ to deduce the potential φ' for the complicated bowl Green's function problem from the relatively simple disk space potential $\varphi(r') = \varphi_{\text{disk}}(r') - V_0$. Notice that the equation $\varphi'(r) = (a/r)\varphi(r')$ is compatible with both the bowl and disk being at zero potential.

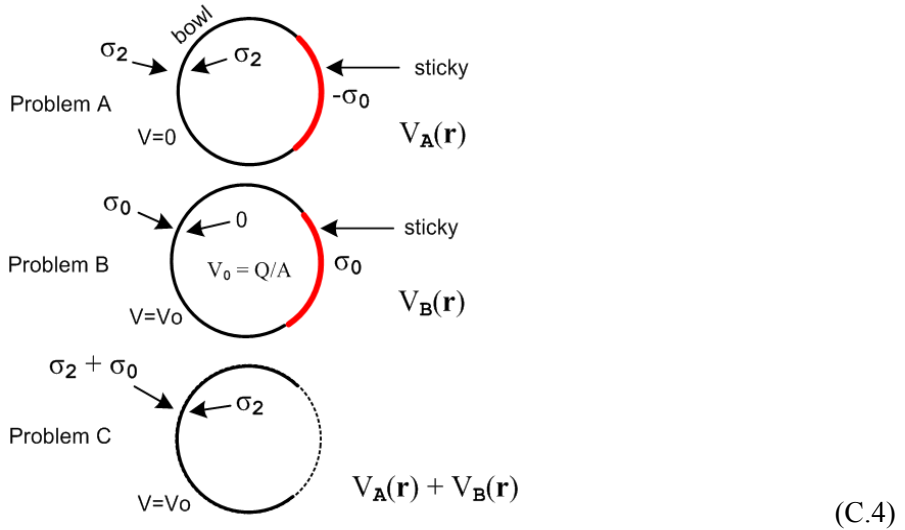
By shifting the charged disk off the symmetry axis as shown in Fig (C.3), Kelvin can cause the point charge to appear at any desired point on the bowl's cap. Since Kelvin knows the disk's charge density $\sigma_{\text{disk}}(\rho)$ stated above, he knows from (C.2) the σ' on the bowl. He does not mention the disk's potential, but that maps into the bowl potential by (C.1). So in the bowl space, we have the grounded bowl with a point charge on the cap, and we know σ' on the bowl. Since σ_{disk} is the same on both sides of the disk, σ' is the same on both sides of the bowl! Basically, the bowl potential is the Green's Function for the bowl with a restricted placement of the Green's point charge.

Kelvin then does two superpositions.

He **first superposes** an infinite number these Green's Function situations to obtain a target uniform charge density $-\sigma_0$ on the bowl's cap. In doing this the point charge has to be properly scaled for each point in the integration as it is made to wander over the cap region. The corresponding bowl σ 's are also being superposed in this process. One then ends up with the final σ on the bowl (let's call it σ_2 , same on both surfaces) as a superposition integral which can be evaluated into trig and inverse trig functions. One can interpret this σ_2 as the charge induced on each surface of a grounded bowl due to the presence of uniform $-\sigma_0$ on the cap. This induced charge on the bowl is brought in from infinity on the traditional "infinitesimally thin wire" grounding the bowl to The Great Metal Sphere At Infinity.

This cap of charge density $-\sigma_0$ is what we call "sticky charge". It is an infinitely thin layer of charge that is magically glued in place so it cannot move, just as the point charge in a Green's function problem is glued to its location and cannot move.

In a **second superposition**, Kelvin superposes Problem A and Problem B to get Problem C:



Problem A is the grounded conducting black bowl of radius R in the presence of a red cap of uniform sticky charge $-\sigma_0$ as just described. The bowl is at $V = 0$ and has σ_2 on each surface.

Problem B is the same conducting bowl carefully prepared to have a uniform free charge density $+\sigma_0$ on its outer surface along with a cap of sticky charge also of $+\sigma_0$. Since we have then a full sphere of uniform σ_0 , the potential *on and inside* the entire bowl sphere is $V_0 = Q/R = (\sigma_0 4\pi R^2)/R = 4\pi R \sigma_0 =$ constant. By the same argument used for a full conducting sphere, this bowl must have $\sigma = 0$ on its inner surface. One might prepare this Problem B by first wrapping a neutral conducting bowl's sphere with a full shell of sticky σ_0 . One then unglues the sticky charge covering just the bowl part of the sphere. The released charges don't move because there is no tangential E field to make them move.

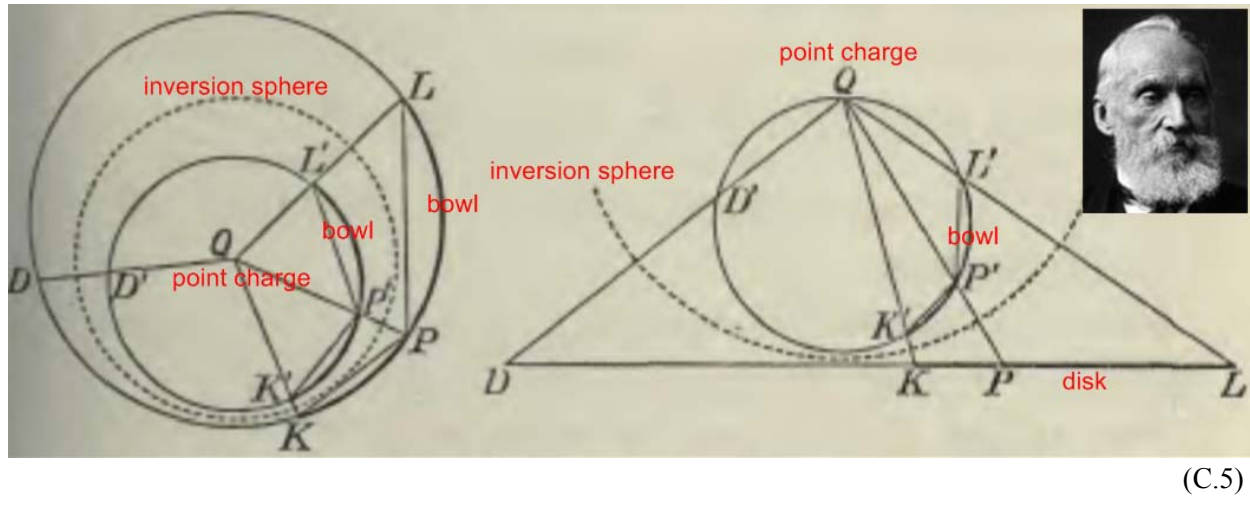
Each of these two problems represents a valid solution to the Laplace equation in the presence of the same conductor. Kelvin forms a third solution by superposing these two problems as Problem C. In this superposed Problem C one has: (1) $V = 0 + V_0 = 4\pi R \sigma_0$ on the bowl ; (2) $\sigma_{in} \equiv \sigma_2 + 0 = \sigma_2$ on the bowl's inner surface; (3) $\sigma_{out} \equiv \sigma_2 + \sigma_0$ on the bowl's outer surface; (4) exact cancellation of the sticky charge on the cap. Notice that $\sigma_{out} - \sigma_{in} = \sigma_0 = V_0/(4\pi R) =$ a constant.

But Problem C is recognized as exactly our "charged bowl problem" for a bowl with potential V_0 , and we have just shown that $\sigma_{out} - \sigma_{in} = \sigma_0 = V/(4\pi R) =$ constant, which is the famous result. And of course we know $\sigma_{in} = \sigma_2$ which came with Problem A. The underlying fact is that a Laplace solution is unique, so if you find something that works, that is the answer. Kelvin's result for $\sigma_{in} = \sigma_2$ is stated in our (4.2.4) and σ_{out} is then found from (4.1.21).

Kelvin, *qua* engineer, uses his hard-won formulas to compute σ_{in} and σ_{out} at several locations on spherical bowls of various shapes. He does this to 5 decimal places and shows the results in a full page graphic, p 186. Had he stopped here, he would have had a great paper, but he had more to say.

Kelvin now knows all about "the charged bowl" problem. Just as he started with a "charged disk" and obtained by inversion the restricted Green's function for a bowl, he now starts with the "charged bowl" and inverts it into either another bowl or a disk, and this time the "inversion-generated point charge at the

"origin" can be made to appear anywhere relative to that bowl or disk. Here are his drawings for these two cases (p 187) with our notations added in red (Kelvin photo wiki),



The inversion sphere is shown dashed, and the point charge is at the inversion origin Q. Thus Kelvin has obtained (in theory) the *fully general Green's Function* for a bowl or a disk. His paper only discusses the charge densities, but the method applies as well to the potential. One can start with the known disk potential (2.5.5),

$$V_{\text{disk}}(\xi, u) = (2V_0/\pi) \sin^{-1} \left[\frac{2a}{\sqrt{(\rho-a)^2 + z^2} + \sqrt{(\rho+a)^2 + z^2}} \right] \quad (2V_0/\pi) = (Q/a) \quad (\text{C.6})$$

and process it through all of Kelvin's steps above.

Appendix D: Smythe's approach to the charged bowl problem

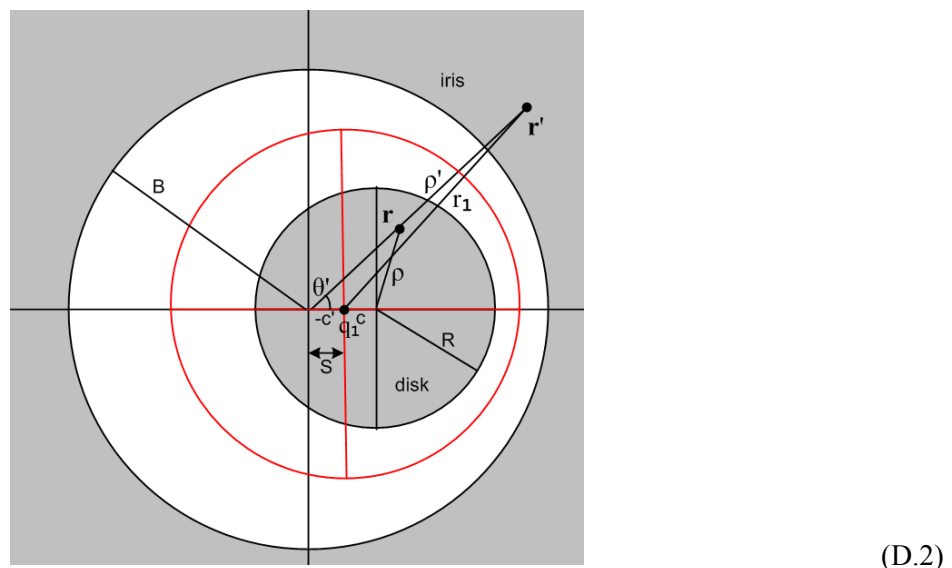
In the Kelvin discussion above we saw an inversion of the on-cap bowl Green's Function problem to an off-axis charged disk problem, Fig (C.3). If the bowl and its on-cap point charge are rotated together so the bowl surface touches the inversion origin, the same bowl Green's Function problem (with the same inversion origin and inversion sphere) can be inverted into an iris Green's Function problem with the point charge in the hole of the iris ("iris" being an infinite grounded conducting plane containing a circular hole). With the bowl in this position, the bowl's cap maps into the hole in the iris and a point charge on the cap maps into a point charge in the hole of the iris:



If one could somehow solve this iris Green's Function problem, one could thereby gain full knowledge of the point-charge-on-cap bowl Green's Function problem, and one could then carry out Kelvin's two superpositions described in Appendix C and thereby obtain the potential and charge densities for the charged bowl problem. This is the approach taken by Smythe in an intriguing sequence of Problems (38 through 42 starting on page 203 of his 2nd Edition book) which we now summarize.

Smythe's Problem Sequence

The starting point is to figure out the Green's Function for a conducting iris with point charge in the hole, and that can be done by inverting the charged disk using the planar inversion arrangement pictured below. The iris hole has radius B while the disk has radius $R < B$. The inversion sphere's cross section is the red circle, and a point charge q_1 is at the center of the red circle marked by the red crosshairs. This location is distance S from the center of the iris hole. The plane of paper is $z' = 0$.



If the iris space has primed cylindrical coordinates $\mathbf{r}' = (\rho', \theta', z')$, the solution to this inversion problem, starting with the charged-disk potential quoted in (C.6) above, is as follows:

$$V'(\mathbf{r}') = 2q_1/(\pi r_1) \cos^{-1} [\sqrt{2} B r_1 / \{ \sqrt{m + (B^2 - S^2)} \sqrt{[(\rho' - B)^2 + z'^2] [(\rho' + B)^2 + z'^2]} \}] \quad (D.3)$$

where

$$m = (\rho'^2 + z'^2)(S^2 - B^2) + B^2(B^2 - S^2 + 2r_1^2)$$

$$r_1^2 = \rho'^2 + S^2 - 2Sp'\cos\theta' + z'^2 \quad \theta' = 0 \text{ in direction of the point charge}$$

$$\sigma'(\mathbf{r}') = -[q_1 / (2\pi^2 r_1^2)] \sqrt{B^2 - S^2} / \sqrt{\rho'^2 - B^2} \quad // \text{either side of the iris, } z'=0 \text{ in } r_1 \quad (D.4)$$

These expressions give the potential at all points in space and the charge density induced on the iris, both caused by the presence of a point charge q_1 located distance S from the center of an iris hole of radius B .

The expression for σ' here is remarkably simple and only appears after considerable brute-force Maple algebra which blindly implements all of Kelvin's many geometry theorems.

In **Problem 38** (p 203) Smythe asks his reader to come up with σ' as shown in (D.4) ($a=B$, $b=S$, $c=\rho'$).

In **Problem 39** he asks the reader to integrate the point charge problem around a circle, to obtain the charge density induced on the iris by a circular ring of charge (radius S) centered within the hole. That result is still amazingly simple:

$$\sigma_2(\rho) = - (q/2\pi^2) (\sqrt{B^2 - S^2} / \sqrt{\rho^2 - B^2}) / (\rho^2 - S^2) \quad // \text{either side} \quad (D.5)$$

where now we remove the primes, and q is the total charge on the ring in the hole.

In **Problem 40** we are instructed to invert this grounded iris + ring charge in hole into a grounded bowl + ring charge on the cap. Fig (D.1) above shows one point on such a ring.

Then in **Problem 42** we do a weighted integral of this bowl-cum-ring situation to obtain a uniform charge density on the cap set to the target amount $-\sigma_0$. This corresponds to Kelvin's first superposition described in Appendix C. We then do Kelvin's second superposition and out pop all the charged bowl results.

Going back now, in **Problem 40** Smythe tells his reader to use "Green's Reciprocal Theorem" to find the potential $V(\theta)$ anywhere on the cap of a charged bowl of potential V_0 . This theorem concerns the charges and potentials on a set of conductors in two "situations", one primed and one unprimed, and states

$$\sum_i V_i Q_i' = \sum_i V_i' Q_i \quad . \quad (D.6)$$

In our application there are only two conductors, one is the bowl, the other is an imagined fine wire in the location of the ring of charge on the bowl's cap. One situation is a charged bowl, the other is the bowl + ring-on-cap Green's function. One quickly finds the potential on the cap to be,

$$V(\theta) = V_0(2/\pi)\sin^{-1}[\cos(\alpha/2)/\cos(\theta/2)], \quad (D.7)$$

where θ, α are θ, u_0 shown in our Fig (4.2.6).

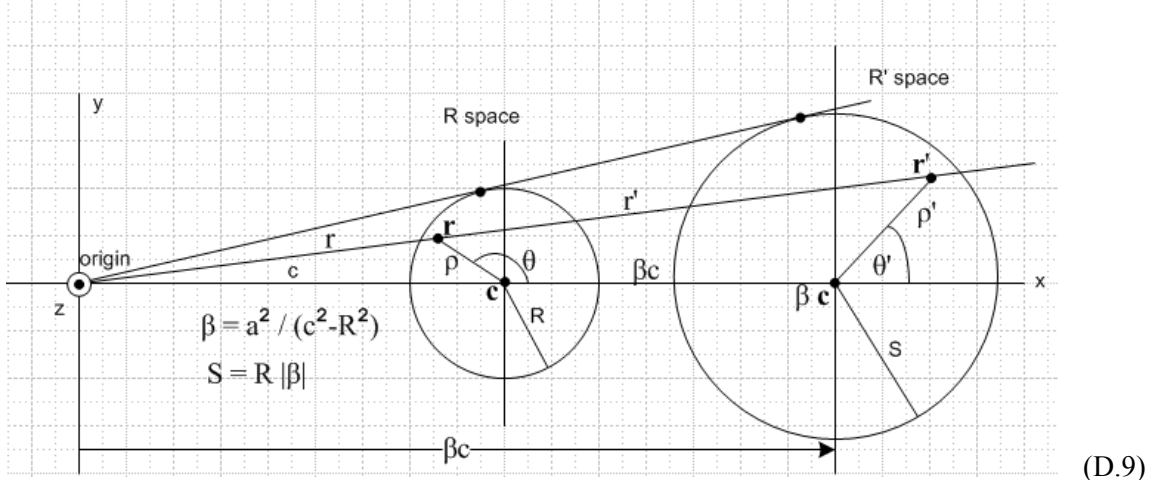
This result has great significance which is brought out in **Problem 41**. One now knows that $V = V_0$ on the bowl, and $V = V(\theta)$ on the cap, so one has a fully prescribed Dirichlet problem and one can then obtain the potential everywhere by assuming an appropriate Smythian form and inverting to find the coefficients. For the exterior problem that atomic superposition is $V(r,\theta) = \sum_{n=0}^{\infty} a_n r^{-n-1} P_n(\cos\theta)$ and the usual Legendre inversion gives

$$\begin{aligned} a_n &= R^{n+1} (2n+1)(1/2) \int_0^\pi P_n(\cos\theta) \sin\theta V(R,\theta,\phi) d\theta \\ &= V_0 R^{n+1} (2n+1)(1/2)^* \\ &\quad \{ (2/\pi) \int_0^\alpha d\theta \sin\theta P_n(\cos\theta) \sin^{-1} [\cos(\alpha/2) / \cos(\theta/2)] + \int_\alpha^\pi d\theta \sin\theta P_n(\cos\theta) \} \end{aligned} \quad (\text{D.8})$$

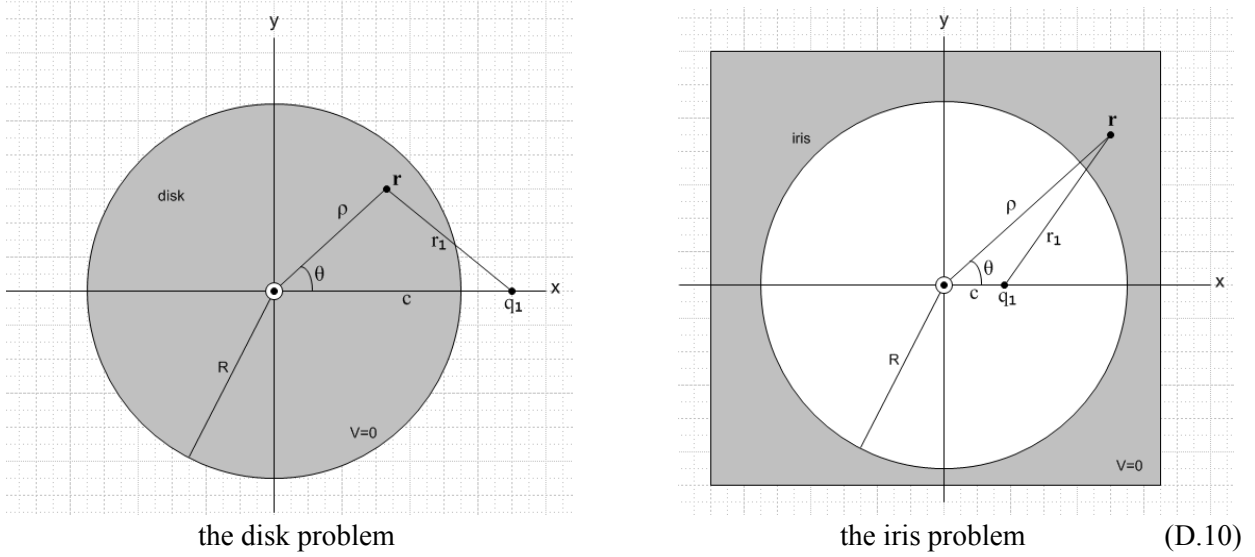
where R is the radius of the bowl's sphere. For $n = 0$ after some work evaluating the first integral one finds that $a_0 = V_0(R/2) \{ [1 - \cos\alpha - (2/\pi)\alpha + (2/\pi)\sin\alpha] + [1 + \cos(\alpha)] \} = V_0(R/\pi) \{ \pi - \alpha + \sin\alpha \}$. For large r , we then have $V \rightarrow a_0/r$ so a_0 is in fact the total charge on the bowl as seen from far away, and we find that the bowl capacitance is $C = R (1/\pi) \{ \pi - \alpha + \sin\alpha \}$, in agreement with (4.4.9) above with $\alpha = u_0$.

Comparing the Disk and Iris Green's Function solutions

We close this appendix with a remark on a related problem which is the Green's Function problem for a disk with the point charge in the plane of (and outside) the disk. One can solve this disk Green's function problem using the following inversion picture,



where R' space contains an isolated charged disk, and R space holds our desired Green's function problem for the disk with point charge at the marked origin. Note that the point charge is distance c from the center of the grounded disk. When this problem is solved, one finds a striking resemblance between its solution and solution (D.3) of the grounded iris with point charge in the hole. We now compare these two Green's function problem solutions :



$$V_{disk}(\rho, \theta, z) = q_1 (2/\pi r_1) \cos^{-1} \left\{ \sqrt{2} R r_1 / \sqrt{m + (c^2 - R^2) \sqrt{[(R-\rho)^2 + z^2] [(R+\rho)^2 + z^2]}} \right\}$$

$$m = (\rho^2 + z^2)(c^2 - R^2) + R^2(R^2 - c^2 + 2r_1^2)$$

$$r_1^2 = (\rho^2 + c^2 + z^2 - 2\rho c \cos\theta) \quad (D.11)$$

$$\sigma_{\text{disk}}(\rho, \theta) = -q_1(1/(2\pi^2 r_1^2)) \sqrt{c^2 - R^2} / \sqrt{R^2 - \rho^2} \quad // \text{each side}$$

$$r_1^2 = (\rho^2 + c^2 - 2cp \cos\theta) \quad (D.12)$$

$$\text{total charge induced on the disk} = -q_1 (2/\pi) \tan^{-1}(R/\sqrt{c^2 - R^2})$$

$$V_{iris}(\rho, \theta, z) = q_1(2/\pi r_1) \cos^{-1} [(\sqrt{2} R r_1 / \sqrt{m + (R^2 - c^2) \sqrt{[(\rho - R)^2 + z^2] [(\rho + R)^2 + z^2]} }]$$

$$m = (\rho^2 + z^2)(c^2 - R^2) + R^2(R^2 - c^2 + 2r_1^2)$$

$$r_1^2 = (\rho^2 + c^2 + z^2 - 2cp \cos \theta) \quad (D.13)$$

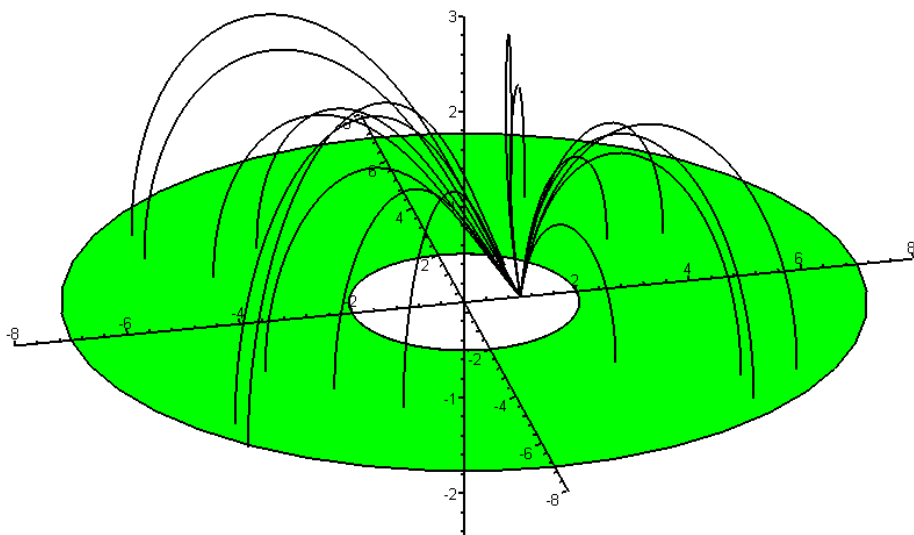
$$\sigma_{\text{iris}}(\rho, \theta) = -q_1 [1/(2\pi^2 r_1^2)] \sqrt{R^2 - c^2} / \sqrt{\rho^2 - R^2} \quad // \text{each side}$$

$$r_1^2 = (\rho^2 + c^2 - 2cp \cos\theta) \quad (D.14)$$

total charge induced on the iris = $-q_1$.

It turns out that the two problems are related by analytic continuation of the variable ρ from $\rho < R$ for the disk problem to $\rho > R$ for the iris problem. The path going directly through $\rho = R$ is blocked by a branch cut of $f(\rho) = \sqrt{(\rho-R)^2 + z^2} = \sqrt{(\rho - a_+)(\rho - a_-)} = \sqrt{\rho - a_+} \sqrt{\rho - a_-}$ joining the points $a_{\pm} = R \pm iz$, so one must continue around either of the branch points with the result that $\sqrt{(\rho-R)^2 + z^2} \rightarrow -\sqrt{(R-\rho)^2 + z^2}$, and this is the only difference in the disk and iris solution sets shown above.

Using the iris Green's Function potential (D.13), one can compute an electric field line by computing $\hat{\mathbf{n}} = \nabla V$ and tracking it in space. In this Maple plot, starting points on the iris were selected by a random number generator, and all field lines dutifully end up at the Green's point charge in the hole:



(D.15)

As expected, each field line launches itself at right angles to the iris surface.

Appendix E: Dual equations and their connection to the charged bowl problem

Sneddon uses the term "dual relations" to cover both dual integral equations and dual series equations, but we shall just call them "dual equations". We can represent a pair of dual equations this way:

$$\begin{array}{lll} A\Psi = f & f = (f_1, f_2) & \text{presented as } [A\Psi]_1 = f_1 \text{ on } I_1 \\ B\Psi = g & g = (g_1, g_2) & \text{presented as } [B\Psi]_2 = g_2 \text{ on } I_2 . \end{array} \quad (E.1)$$

Here A and B are invertible linear operators (perhaps Hankel Transform integral operators) and the other symbols stand for functions of a real variable x . The range I of the variable x is partitioned into two regions I_1 and I_2 so the full interval of interest is $I = I_1 \cup I_2$. The notation $f = (f_1, f_2)$ means that $f(x) = f_1(x)$ on I_1 and $f(x) = f_2(x)$ on I_2 . The dual equation problem is easily stated: given the prescribed functions f_1 and g_2 , find the partner functions f_2 and g_1 (so that you then know f and g on all of I), and also find the solution function $\Psi(x)$ on all of I .

Although A and B are invertible operators, neither dual equation can be inverted because information is missing. For example, we could write $\Psi = A^{-1}f$, but we don't know f , we only know f_1 . The same is true for the second equation: we can write $\Psi = B^{-1}g$, but we only know g_2 . Only by considering both equations of the dual pair can a solution be found. In electrostatics problems, one might have a Dirichlet boundary condition on interval I_1 and a Neumann boundary condition on I_2 , so a dual equation can represent a mixed boundary value problem.

Here is the formal trick used to solve the problem. Although A and B are operators, it is useful to think of them as matrices. It is useful further to think of these matrices as consisting of submatrices so that the row and column spaces are partitioned in the sense of $I = I_1 \cup I_2$. Then for example we could say

$$\begin{array}{lll} A\Psi = f & \leftrightarrow & \begin{pmatrix} A_{11} & A_{12} \\ A_{21} & A_{22} \end{pmatrix} \begin{pmatrix} \Psi_1 \\ \Psi_2 \end{pmatrix} = \begin{pmatrix} f_1 \\ f_2 \end{pmatrix} \\ B\Psi = g & \leftrightarrow & \begin{pmatrix} B_{11} & B_{12} \\ B_{21} & B_{22} \end{pmatrix} \begin{pmatrix} \Psi_1 \\ \Psi_2 \end{pmatrix} = \begin{pmatrix} g_1 \\ g_2 \end{pmatrix} . \end{array} \quad (E.2)$$

The game is to find invertible lower and upper triangular matrices (really operators) L and U such that $LA = UB$. It might seem at first that the existence of such L and U would be unlikely, but an analysis of matrix decomposition theorems shows that in general such L and U do exist. If one applies L to the first equation in (E.1) and U to the second equation, and if one defines

$$S \equiv LA = UB, \quad (E.3)$$

(which S will also be invertible), then equations (E.1) become

$$\begin{array}{ll} S\Psi = Lf \\ S\Psi = Ug . \end{array} \quad (E.4)$$

We now examine the right sides of these two equations in our matrix language,

$$\begin{aligned} Lf &= \begin{pmatrix} L_{11} & 0 \\ L_{21} & L_{22} \end{pmatrix} \begin{pmatrix} f_1 \\ f_2 \end{pmatrix} = \begin{pmatrix} L_{11}f_1 \\ L_{21}f_1 + L_{22}f_2 \end{pmatrix} & L &= \begin{pmatrix} L_{11} & 0 \\ L_{21} & L_{22} \end{pmatrix} \\ Ug &= \begin{pmatrix} U_{11} & U_{12} \\ 0 & U_{22} \end{pmatrix} \begin{pmatrix} g_1 \\ g_2 \end{pmatrix} = \begin{pmatrix} U_{11}g_1 + U_{12}g_2 \\ U_{22}g_2 \end{pmatrix} & U &= \begin{pmatrix} U_{11} & U_{12} \\ 0 & U_{22} \end{pmatrix} . \end{aligned} \quad (E.5)$$

Therefore, since both left hand sides are $S\Psi$, one has

$$Lf = Ug = \begin{pmatrix} L_{11}f_1 \\ U_{22}g_2 \end{pmatrix} . \quad (E.6)$$

Recall that we *know* L and U , and we *know* f_1 and g_2 since they are the prescribed functions (the driving terms on the RHS of the dual equations (E.1), often one of these is 0). The solution to the problem is then obtained as follows. First take either $S\Psi$ equation in (E.4) (say the first one) and invert to get

$$\Psi = S^{-1}(Lf) \leftrightarrow \begin{pmatrix} \Psi_1 \\ \Psi_2 \end{pmatrix} = \begin{pmatrix} S^{-1}_{11} & S^{-1}_{12} \\ S^{-1}_{21} & S^{-1}_{22} \end{pmatrix} \begin{pmatrix} L_{11}f_1 \\ U_{22}g_2 \end{pmatrix} . \quad (E.7)$$

Since we know L, U, S, f_1, g_2 , we have solved the problem for Ψ . To obtain the unknown partner functions use the original equations:

$$\begin{aligned} A\Psi = f &\leftrightarrow \begin{pmatrix} A_{11} & A_{12} \\ A_{21} & A_{22} \end{pmatrix} \begin{pmatrix} \Psi_1 \\ \Psi_2 \end{pmatrix} = \begin{pmatrix} f_1 \\ f_2 \end{pmatrix} \quad \text{so} \quad f_2 = A_{21}\Psi_1 + A_{22}\Psi_2 \\ B\Psi = g &\leftrightarrow \begin{pmatrix} B_{11} & B_{12} \\ B_{21} & B_{22} \end{pmatrix} \begin{pmatrix} \Psi_1 \\ \Psi_2 \end{pmatrix} = \begin{pmatrix} g_1 \\ g_2 \end{pmatrix} \quad \text{so} \quad g_1 = B_{11}\Psi_1 + B_{12}\Psi_2 . \end{aligned} \quad (E.8)$$

Hopefully we have clarified the "basic idea" with this little matrix viewpoint summary. In practice there is of course a *lot* of fine detail. An illustration of the nature of this detail appears in Appendix G below.

It might be noted that Sneddon also considers Triple Equations and the above analysis then involves 3×3 matrices since the variable range is partitioned into $I = I_1 \cup I_2 \cup I_3$. An example of such a problem is the "charged barrel problem" where barrel means a spherical shell with two polar caps removed.

As examples of dual equations, we take a quick look at two famous problems.

The Beltrami disk problem. (Beltrami's 1881 work is reviewed by Sneddon.) An appropriate Smythian form for the charged disk potential can be constructed from cylindrical atoms:

$$V(\rho, z) = \int_0^\infty e^{-k|z|} J_0(k\rho) [k^{-1} a(k)] dk . \quad (E.9)$$

The prescribed potential on the disk is $f_1(\rho)$, and the prescribed charge density is $\sigma \sim \partial_z V = 0$ outside the disk in the $z=0$ plane. Again, this is a "mixed boundary value problem". The dual equations are then

$$\begin{aligned} \int_0^\infty k^{-1} J_0(k\rho) a(k) dk &= f_1(\rho) & \rho < 1 & [A\Psi]_1 = f_1 \\ \int_0^\infty J_0(k\rho) a(k) dk &= 0 & \rho > 1 & [B\Psi]_2 = g_2 = 0 . \end{aligned} \quad (E.10)$$

Here $\Psi(k) = a(k)$, the function to be solved for. A is an integral operator with kernel $K(\rho, k) = k^{-1} J_0(k\rho)$ while B has kernel $J_0(k\rho)$. The matrix sense of A is $A_{\rho, k} = K(\rho, k)$ where both indices of A are continuous real numbers, and similarly for B. Both A and B can be regarded as modified Hankel transforms. The formal matrix method above gives us $a(k)$ which we insert into the Smythian form (E.9) to find solution $V(\rho, z)$. The partner functions are f_2 which is the potential outside the disk in the $z=0$ plane, and g_1 which is the charge density on the disk (sum of both sides).

The appropriate L and U operators for this problem turn out to be gussied-up Abel transform operators (called I and K by Sneddon) known as Erdélyi-Kober operators. These operators can be *interpreted* as fractional integral operators (fractional meaning α is continued off the integers; the disk problem uses $\alpha = 1/2$),

$$R(x) = \mathcal{R}_\alpha \{ f(t); x \} = (1/\Gamma(\alpha)) \int_0^x dt' f(t') (x-t')^{\alpha-1} \quad // \text{matrix: } R = If = Lf \quad (E.11a)$$

Riemann-Liouville 1850

$$W(x) = \mathcal{W}_\alpha \{ f(t); x \} = (1/\Gamma(\alpha)) \int_x^\infty dt' f(t') (t'-x)^{\alpha-1} \quad // \text{matrix: } W = Kf = Uf \quad (E.11b)$$

Weyl 1917

but the fact is that these are really just generalized Abel transforms with fancy names. Like any respectable transform, the Abel transform is invertible (see Appendix F). The disk problem is then solved as outlined above using the Abel transforms L and U and the Hankel transforms A and B.

Setting $f_1(\rho) = V_0 = 1$ of course gives the "charged conducting disk problem".

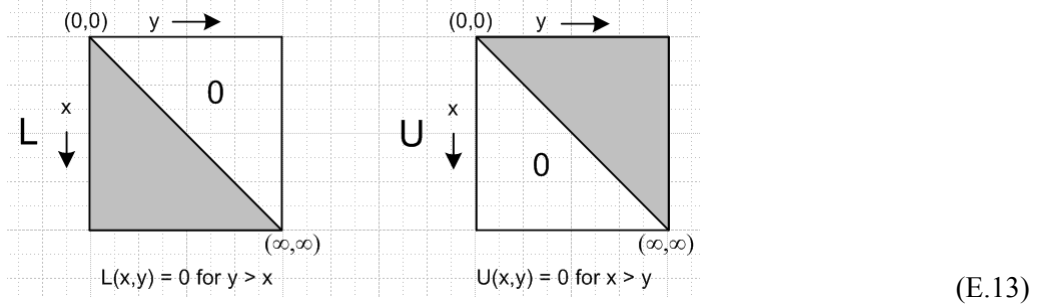
Bateman ET 2 Chapter 13 contains a fairly large collection of specific (E.11) Abel transforms. The Riemann-Liouville ones are in Section 13.1 p 185, and the Weyl ones in Section 13.2 p 201.

How is it that the operators L and U in (E.11) are upper and lower triangular? Consider these two integral equations, where θ is the Heaviside function,

$$\begin{aligned} r(x) &= \int_0^x k(x,y) f(y) dy = \int_0^\infty [k(x,y) \theta(x-y)] f(y) dy \equiv \int_0^\infty [L(x,y)] f(y) dy \quad // r = Lf \\ w(x) &= \int_x^\infty k(x,y) f(y) dy = \int_0^\infty [k(x,y) \theta(y-x)] f(y) dy \equiv \int_0^\infty [U(x,y)] f(y) dy \quad // w = Uf \end{aligned}$$

$$\begin{aligned} L(x,y) &\equiv k(x,y) \theta(x-y) = 0 \text{ when } y > x \\ U(x,y) &\equiv k(x,y) \theta(y-x) = 0 \text{ when } x > y , \end{aligned} \quad (E.12)$$

and consider these graphs showing where the kernels L and U vanish



In the matrix interpretation of the integral equations, x is the row index and y the column index. Fig (E.13) then shows that L is a lower triangular matrix while U is upper triangular, matching (E.5).

Equations like (E.12) where x appears as an integration endpoint are called Volterra equations.

The Corresponding Bowl Problem. An appropriate Smythian form for the unit-radius bowl potential, inside and outside the bowl, can be constructed from spherical atoms,

$$\begin{aligned} V_i(r,\theta) &= \sum_{n=0}^{\infty} a_n r^n P_n(\cos\theta) \\ V_o(r,\theta) &= \sum_{n=0}^{\infty} a_n r^{-n-1} P_n(\cos\theta) \end{aligned} . \quad (\text{E.14})$$

The angle here called θ is called η in our Fig (4.2.6). The (E.14) θ is measured from sphere center and $\theta = 0$ at the base of the bowl. The bowl then corresponds to $0 \leq \theta \leq \theta_0$ and the empty cap to $\theta_0 \leq \theta \leq \pi$. The lip of the bowl is at $\theta = \theta_0$ which in Fig (4.2.6) is called $\pi - u_0$, so the connection is $\theta_0 = \pi - u_0$.

The prescribed potential is $f_1(\theta)$ on the bowl, and the prescribed charge density is $\sigma \sim \partial_r V = 0$ on the cap. The dual equations (dual series equations now) are these:

$$\begin{aligned} \sum_{n=0}^{\infty} P_n(\cos\theta) a_n &= f_1(\theta) & 0 \leq \theta \leq \theta_0 & [A\Psi]_1 = f_1 \\ \sum_{n=0}^{\infty} (2n+1) P_n(\cos\theta) a_n &= 0 & \theta_0 \leq \theta \leq \pi & [B\Psi]_2 = g_2 = 0 \end{aligned} . \quad (\text{E.15})$$

Now we have $\Psi_n = a_n$ and the matrix sense of A is $A_{\theta,n} = P_n(\cos\theta)$ where θ is a continuous angle index and n is a discrete index. As in the previous problem, A is an $\infty \times \infty$ matrix.

Vinogradov et al. show (Section 1.4.3, "Noble's method") that for our bowl problem the appropriate L, U operators are,

$$\begin{aligned} L h(\theta) &= (1/\sqrt{2}) \partial_\theta \int_0^\theta d\phi \sin\phi h(\phi) / \sqrt{\cos\phi - \cos\theta} & // = K_1 h(\theta) \\ U h(\theta) &= (1/\sqrt{2}) \int_\theta^\pi d\phi \sin\phi h(\phi) / \sqrt{\cos\phi - \cos\theta} & // = K_2 h(\theta) \end{aligned} \quad (\text{E.16})$$

where we note that the Volterra θ endpoints cause these operators to have triangular matrices as kernels. If we apply L to the first equation of (E.15) and U to the second, we get (after some work)

$$\begin{aligned} \sum_{n=0}^{\infty} \cos[(n+1/2)\theta] a_n &= L f_1(\theta) & \theta < \theta_0 & \text{or} & S\Psi = Lf & \text{on } I_1 \\ \sum_{n=0}^{\infty} \cos[(n+1/2)\theta] a_n &= 0 & \theta > \theta_0 & \text{or} & S\Psi = Ug = 0 & \text{on } I_2 \end{aligned} \quad (\text{E.17})$$

where both left hand sides are now of the form $S\Psi$ as discussed above in (E.4). In the case of the charged bowl, $f_1(\theta) = V_0 = 1$, we find that $L f_1(\theta) = L 1 = \cos(\theta/2)$ (Maple). Then using (G.4),

$$\int_0^\pi d\theta \cos([n+1/2]\theta) \cos([m+1/2]\theta) = \delta_{n,m} (\pi/2), \quad (E.18)$$

one can trivially invert the equations (E.17) treated as a single equation on $(0,\pi)$ to get $\Psi = S^{-1} L f$, or,

$$a_n = (2/\pi) \int_0^{\theta_0} d\theta \cos([n+1/2]\theta) \cos(\theta/2) = (1/\pi) \left(\frac{\sin(n\theta_0)}{n} + \frac{\sin[(n+1)\theta_0]}{n+1} \right) \quad (E.19)$$

which is the known result Sneddon (8.7.1). Inserting these a_n coefficients into (E.14) gives the potential of the charged unit-radius, unit-potential bowl both inside and outside the bowl. For a bowl of radius R and potential V_0 we then have

$$\begin{aligned} V_{\text{inside}}(r,\theta) &= \frac{V_0}{\pi} \sum_{n=0}^{\infty} \left(\frac{\sin(n\theta_0)}{n} + \frac{\sin[(n+1)\theta_0]}{n+1} \right) (r/R)^n P_n(\cos\theta) \\ V_{\text{outside}}(r,\theta) &= \frac{V_0}{\pi} \sum_{n=0}^{\infty} \left(\frac{\sin(n\theta_0)}{n} + \frac{\sin[(n+1)\theta_0]}{n+1} \right) (r/R)^{-n-1} P_n(\cos\theta) . \end{aligned} \quad (E.20)$$

This may be compared to the result (2.4.14a) for the potential of a charged bowl of label $u_0 = \pi - \theta_0$,

$$V(\xi,u) = \frac{V_0}{\pi} \left\{ \cot^{-1} \left[-\frac{\sqrt{2} \cos(u/2)}{\sqrt{\text{ch}\xi - \cos u}} \right] + \frac{\sqrt{\text{ch}\xi - \cos u}}{\sqrt{\text{ch}\xi - \cos(2u_0 - u)}} \cot^{-1} \left[\frac{\sqrt{2} \cos(u_0 - u/2)}{\sqrt{\text{ch}\xi - \cos(2u_0 - u)}} \right] \right\} \quad (E.21)$$

where the potential both inside and outside the bowl is given by the same unified expression. Moreover, the expression contains no sums or integrals, just elementary functions. (E.21) can be converted from toroidal to cylindrical and then spherical coordinates using the methods of Appendix B.

Appendix F: The Abel Transform in various forms

Here we state the generalized Abel Transform in three different ways. The historical Abel transform problem (tautochrone) involves $\alpha = 1/2$, while "generalized" allows $0 < \alpha < 1$. The Abel transform can be expressed for α outside this range by doing one parts integration for each integer step of shift required (Sneddon). A derivation of the Abel Transform is given in Sneddon Section 2.3 and Vinogradov Section 1.5 in terms of a generic monotonic speed function $h(u)$ where denominators are $[h(x) - h(t)]^\alpha$.

In the S1 forms below, the upper endpoint is the variable x , while in the S2 forms x is the lower endpoint.

For the linear forms (only) we have explicitly done the ∂_t derivatives on the third line of each transform based on the following easily derived facts,

$$\begin{aligned} g(x) &= \int_a^x dt k(x-t)f(t) \quad \Rightarrow \quad \partial_x g(x) = f(a)k(x-a) + \int_a^x dt k(x-t)f'(t) \\ g(x) &= \int_x^b dt k(t-x)f(t) \quad \Rightarrow \quad \partial_x g(x) = -f(b)k(b-x) + \int_x^b dt k(t-x)f'(t), \end{aligned} \quad (\text{F.0})$$

where one does a parts integration with $\partial_x k(t-x) = -\partial_t k(t-x)$, and where one notices that x appears twice in each $g(x)$.

Linear Form of the Generalized Abel Transform:

$$\begin{aligned} \text{S1: } \int_a^x dt f(t) / [x-t]^\alpha &= g(x) \\ \Rightarrow f(t) &= (1/\pi)\sin(\pi\alpha) \partial_t \left\{ \int_a^t du g(u) / [t-u]^{1-\alpha} \right\} \quad (\text{F.1}) \\ &= (1/\pi)\sin(\pi\alpha) \left\{ g(a) / [t-a]^{1-\alpha} + \int_a^t du g'(u) / [t-u]^{1-\alpha} \right\} \end{aligned}$$

$$\begin{aligned} \text{S2: } \int_x^b dt f(t) / [t-x]^\alpha &= g(x) \\ \Rightarrow f(t) &= -(1/\pi) \sin(\pi\alpha) \partial_t \left\{ \int_t^b du g(u) / [u-t]^{1-\alpha} \right\} \quad (\text{F.2}) \\ &= -(1/\pi) \sin(\pi\alpha) \left\{ -g(b) / [b-t]^{1-\alpha} + \int_t^b du g'(u) / [u-t]^{1-\alpha} \right\} \end{aligned}$$

Quadratic Form of the Generalized Abel Transform:

$$\begin{aligned} \text{S1: } \int_a^x dt f(t) / [x^2 - t^2]^\alpha &= g(x) \\ \Rightarrow f(t) &= (2/\pi)\sin(\pi\alpha) \partial_t \left\{ \int_a^t du u g(u) / [t^2 - u^2]^{1-\alpha} \right\} \quad (\text{F.3}) \end{aligned}$$

$$\begin{aligned} \text{S2: } \int_x^b dt f(t) / [t^2 - x^2]^\alpha &= g(x) \\ \Rightarrow f(t) &= -(2/\pi) \sin(\pi\alpha) \partial_t \left\{ \int_t^b du u g(u) / [u^2 - t^2]^{1-\alpha} \right\} \quad (\text{F.4}) \end{aligned}$$

Trig Form of the Generalized Abel Transform:

$$\begin{aligned} S1: \quad & \int_a^x dt f(t) / [\cos(t) - \cos(x)]^\alpha = g(x) \\ \Rightarrow \quad & f(t) = \pi^{-1} \sin(\pi\alpha) \partial_t \left\{ \int_a^t du \sin(u) g(u) / [\cos(u) - \cos(t)]^{1-\alpha} \right\} \end{aligned} \quad (F.5)$$

$$\begin{aligned} S2: \quad & \int_x^b dt f(t) / [\cos(x) - \cos(t)]^\alpha = g(x) \\ \Rightarrow \quad & f(t) = -\pi^{-1} \sin(\pi\alpha) \partial_t \left\{ \int_t^b du \sin(u) g(u) / [\cos(t) - \cos(u)]^{1-\alpha} \right\} \end{aligned} \quad (F.6)$$

and this last case we write again with $\alpha = 1/2$

$$\begin{aligned} S1: \quad & \int_a^x dt f(t) / \sqrt{\cos t - \cos x} = g(x) \\ \Rightarrow \quad & f(t) = \pi^{-1} \partial_t \left\{ \int_a^t du \sin u g(u) / \sqrt{\cos u - \cos t} \right\} \quad // \text{ Sneddon (2.3.5)} \end{aligned} \quad (F.7)$$

$$\begin{aligned} S2: \quad & \int_x^b dt f(t) / \sqrt{\cos x - \cos t} = g(x) \\ \Rightarrow \quad & f(t) = -\pi^{-1} \partial_t \left\{ \int_t^b du \sin u g(u) / \sqrt{\cos t - \cos u} \right\} \quad // \text{ Sneddon (2.3.6)} \end{aligned} \quad (F.8)$$

When $\alpha = 1/2$, the trig form always involves factors of the form $1/\sqrt{\cos a - \cos b}$. There is doubtless a deeper (perhaps group theoretic) explanation, but due to the following integral representations of the P function

$$\begin{aligned} P_n(\cos\theta) &= (\sqrt{2}/\pi) \int_0^\theta d\varphi \cos[(n+1/2)\varphi] / \sqrt{\cos\varphi - \cos\theta} \quad // \text{ GR7 8.823} \\ P_n(\cos\theta) &= (\sqrt{2}/\pi) \int_\theta^\pi d\varphi \sin[(n+1/2)\varphi] / \sqrt{\cos\theta - \cos\varphi} \quad // \theta \rightarrow \pi - \theta, \varphi \rightarrow \pi - \varphi \end{aligned} \quad (F.9)$$

there is a close connection between Legendre functions and Abel transforms in the solution of dual series equations of the type discussed in Appendix E. The integrals (F.9) are called the Mehler-Dirichlet integrals for P_n and they are derived in Section 15.231 of Whittaker and Watson.

Corresponding Bessel J_0 representations also expose this Abel transform connection (though in the Abel quadratic form)

$$\begin{aligned} J_0(k\rho) &= (1/\pi) \int_0^\rho dx \cos(kx) / \sqrt{\rho^2 - x^2} \quad // \text{ Vinogradov 1.156} \\ J_0(k\rho) &= (1/\pi) \int_\rho^\infty dx \cos(kx) / \sqrt{x^2 - \rho^2}. \quad // \text{ Vinogradov 1.157} \end{aligned} \quad (F.10)$$

Here are two interesting expansions which in certain circumstances allow for the solution of dual equation problems by the use of *two sequential* Abel transforms. The first operates in the Legendre world, the second in the Bessel world:

$$\sum_{n=0}^{\infty} P_n(\cos\theta) P_n(\cos\theta') = (1/\pi) \int_0^{\min(\theta, \theta')} d\phi \frac{1}{[\sqrt{\cos\phi - \cos\theta} \sqrt{\cos\phi - \cos\theta'}]} \quad (F.11)$$

$$\int_0^{\infty} J_n(rx) J_n(r'x) dx = (2/\pi) (rr')^{-n} \int_0^{\min(r, r')} ds s^{2n} / [\sqrt{r^2 - s^2} \sqrt{r'^2 - s^2}] \quad (F.12)$$

The main idea is that on the RHS the variables of interest appear in *factorized* Abel-transform-ready form. The first appears as Vinogradov 1.107 and the second as 2.169. Vinogradov et al. have much to say about Abel transforms in the context of dual equations. We shall derive (F.11) in Appendix G, and then use it.

Since ours is mainly a document about the toroidal charged bowl problem, we note this alternate evaluation of the above double Bessel integral (GR7 p696 6.612.3),

$$\int_0^{\infty} J_n(rx) J_n(r'x) dx = (1/\pi) (rr')^{-1/2} Q_{n-1/2}[(r^2 + r'^2)/(2rr')] \quad (F.13)$$

So in the midst of a cylindrical and spherical coordinates discussion, we are somewhat surprised to find ourselves staring at a toroidal Q function as seen in the toroidal atomic forms (2.2.3) (1).

Appendix G: Solving the charged bowl problem using a double Abel transform

The steps given in this lengthy and tedious Appendix are typical of what one encounters in a dual equations problem. In particular, one often encounters painful integrals. Sometimes there are "easy ways" to do integrals, but when the easy ways are not known, one must resort to brute force, as done below. This Appendix closely follows Section 1.4.1 of Vinogradov et al. They in turn are presenting 1964 work of W.E. Williams. Unlike Vinogradov, we try to show all of the waypoints of the calculation.

In Appendix E we outlined a matrix method for solving dual equations in this framework

$$\begin{array}{lll} A\Psi = f & f = (f_1, f_2) & \text{presented as } [A\Psi]_1 = f_1 \text{ on } I_1 \\ B\Psi = g & g = (g_1, g_2) & \text{presented as } [B\Psi]_2 = g_2 \text{ on } I_2 \end{array} \quad (E.1)$$

where the problem is to solve for the "potential" Ψ and the partner functions f_2 and g_1 if one is given A and B and the driving functions f_1 and g_2 . We placed the $V_0=1$ $R=1$ charged bowl problem into this framework according to

$$\begin{array}{lll} \sum_{n=0}^{\infty} P_n(\cos\theta) a_n = 1 & \theta \text{ in } (0, \theta_0) & [A\Psi]_1 = f_1(\theta) = 1 \\ \sum_{n=0}^{\infty} (2n+1) P_n(\cos\theta) a_n = 0 & \theta \text{ in } (\theta_0, \pi) & [B\Psi]_2 = g_2(\theta) = 0 \end{array} \quad (E.15)$$

In the matrix method, one formally finds Ψ first, and then from that gets the partner functions f_2 and g_1 . As one quickly learns from reading Sneddon's reviews, there are *many* variations of this general method. Sometimes the batting order is to first find the partner function g_1 and then from it obtain Ψ and f_2 . That is exactly what we are going to do below.

G.1 Find g_1

The starting point is $B\Psi = g = (g_1, g_2)$ where $g_2 = 0$ since there is no charge density on the cap of a charged bowl. The unknown partner function g_1 is proportional to the total charge density on the bowl. We have

$$g_1(\theta) = \sum_{n=0}^{\infty} (2n+1) P_n(\cos\theta) a_n = \partial_r V_i - \partial_r V_o = 4\pi[\sigma_i(\theta) + \sigma_o(\theta)] \quad \theta \text{ in } (0, \theta_0)$$

from Gauss's Law where σ is expressed in cgs units. For a bowl of radius R ,

$$g_1 = 4\pi R(\sigma_i + \sigma_o). \quad (G.0)$$

The second equation of (E.15) above may be written as ($z = \cos\theta$ in all that follows)

$$\sum_{n=0}^{\infty} (2n+1) P_n(z) a_n = g(\theta) = \begin{cases} g_1(\theta) & \theta \text{ in } (0, \theta_0) \\ 0 & \theta \text{ in } (\theta_0, \pi) \end{cases}. \quad (G.1)$$

Applying $\int_{-1}^1 dz P_n(z)$ to both sides and using $\int_{-1}^1 dz P_n(z) P_m(z) = \delta_{n,m} 2/(2n+1)$ one finds that

$$a_n = (1/2) \int_{-1}^1 dz P_n(z) g(\theta) = (1/2) \int_0^{\theta_0} d\theta \sin\theta P_n(z) g_1(\theta) . \quad (G.2)$$

If we install this a_n into our first dual equation of (E.15), $\sum_{n=0}^{\infty} P_n(z') a_n = V_0 = 1$, we get

$$\sum_{n=0}^{\infty} P_n(z') [(1/2) \int_{-1}^1 dz P_n(z) g(\theta)] = 1$$

or

$$\int_{-1}^1 dz g(\theta) [(1/2) \sum_{n=0}^{\infty} P_n(z) P_n(z')] = 1$$

or

$$\int_{-1}^1 dz g(\theta) K(\theta, \theta') = 1 \quad \text{where } K(\theta, \theta') \equiv (1/2) \sum_{n=0}^{\infty} P_n(z) P_n(z') . \quad (G.3)$$

Thus, $K(\theta, \theta')$ is the kernel of an integral equation we want to solve for g .

Digressing momentarily, if one considers the "string problem with the left end offset "

$$u''(\theta) = -n^2 u(\theta) \quad u(0) = 1 \quad u(\pi) = 0$$

one finds that the eigenfunctions $\cos([n+1/2]\theta)$ form a complete set with completeness

$$\sum_{n=0}^{\infty} \cos([n+1/2]x) \cos([n+1/2]x') = (\pi/2) \delta(x-x') \quad (G.4)$$

and if the right end instead is offset, one gets the same result with $\cos \rightarrow \sin$.

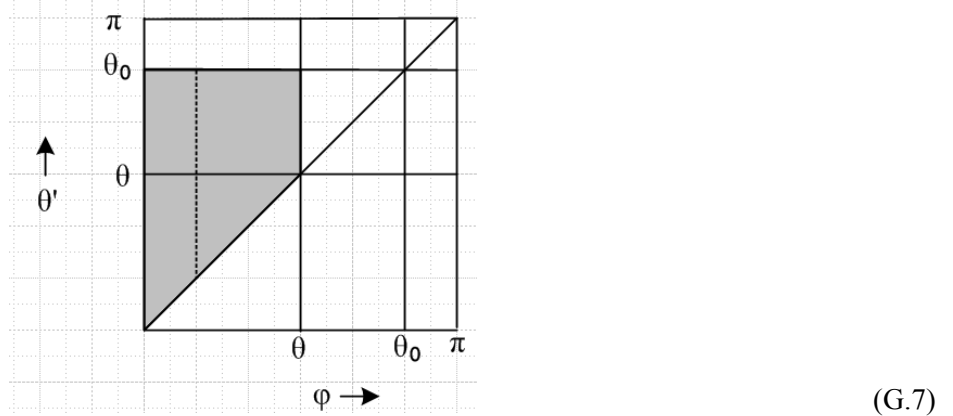
Now, using the integral representation (F.9) for each P function in (G.3) along with (G.4), we get

$$K(\theta, \theta') = (1/2\pi) \int_0^{\min(\theta, \theta')} d\varphi \left\{ 1/\sqrt{\cos\varphi - \cos\theta} \quad 1/\sqrt{\cos\varphi - \cos\theta'} \right\} . \quad (G.5)$$

which was quoted as (F.11) in Appendix F. Equation (G.3) then says

$$1 = \int_0^{\theta_0} d\theta' [\sin\theta' g_1(\theta')] (1/2\pi) \int_0^{\min(\theta, \theta')} d\varphi \left\{ 1/\sqrt{\cos\varphi - \cos\theta} \quad 1/\sqrt{\cos\varphi - \cos\theta'} \right\} \quad (G.6)$$

where we have used the fact that $g(\theta) = 0$ on (θ_0, π) . Pondering the region of the double integration



we can swap the integration order to obtain

$$2\pi = \int_0^\theta d\varphi \frac{1}{\sqrt{\cos\varphi - \cos\theta}} \int_{\varphi}^{\theta_0} d\theta' [\sin\theta' g_1(\theta')] \frac{1}{\sqrt{\cos\varphi - \cos\theta'}} \quad \theta \leq \theta_0 . \quad (\text{G.8})$$

The plan is now to solve this equation for g_1 using a double Abel transform. We can break (G.8) into two pieces, each an Abel transform, in this way

$$2\pi = \int_0^\theta d\varphi h(\varphi) \frac{1}{\sqrt{\cos\varphi - \cos\theta}} \quad \varphi \leq \theta \leq \theta_0 \quad (\text{G.9})$$

$$h(\varphi) \equiv \int_\varphi^{\theta_0} d\theta' [\sin\theta' g_1(\theta')] \frac{1}{\sqrt{\cos\varphi - \cos\theta'}} . \quad (\text{G.10})$$

Using Abel transform (F.7) applied to (G.9) we find that

$$h(\varphi) = 2 \sin\varphi \frac{1}{\sqrt{1-\cos\varphi}} \quad \varphi \text{ in } (0, \theta_0) . \quad (\text{G.11})$$

Using this for the left side of (G.10) we apply Abel transform (F.8) to get

$$[\sin\theta g_1(\theta)] = -(2/\pi) \partial_\theta I \quad (\text{G.12})$$

where

$$I(\theta) = \int_\theta^{\theta_0} du \sin^2 u \left[\frac{1}{\sqrt{1-\cos u}} \right] \left[\frac{1}{\sqrt{\cos\theta - \cos u}} \right] . \quad (\text{G.13})$$

This integral can be transformed into a simpler form which can be evaluated,

$$\begin{aligned} I(\theta) &= \int_\theta^{\theta_0} du \sin^2 u \left[\frac{1}{\sqrt{1-\cos u}} \right] \left[\frac{1}{\sqrt{\cos\theta - \cos u}} \right] \\ &= \int_a^b \left[\frac{dx}{\sqrt{1-x^2}} \right] (1-x^2) / \left[\sqrt{1-x} \sqrt{\cos\theta - x} \right] \quad // x = \cos u, a = \cos\theta_0, b = \cos\theta \\ &= \int_a^b dx \sqrt{1+x} / \sqrt{b-x} \end{aligned}$$

$$\begin{aligned}
&= \int_0^c dy \sqrt{d-y} / \sqrt{y} && // y = b-x, c = b-a, d = b+1, d-c = a+1 \\
&= 2 \int_0^{\sqrt{c}} dx \sqrt{d-x^2} && // y = x^2 \quad c = \cos\theta - \cos\theta_0 \\
&= \sqrt{c} \sqrt{d-c} + d \sin^{-1}(\sqrt{c} / \sqrt{d}) . && // \text{Maple} \quad d = \cos\theta + 1
\end{aligned} \tag{G.14}$$

Then using $\partial_\theta = -\sin\theta (\partial_c + \partial_d)$ we can rewrite (G.12) as

$$[\sin\theta g_1(\theta)] = -(2/\pi) \partial_\theta I = (2/\pi) \sin\theta (\partial_c + \partial_d) I$$

so that

$$\begin{aligned}
g_1(\theta) &= (2/\pi) (\partial_c + \partial_d) I = (2/\pi) \{ \sqrt{d-c} / \sqrt{c} + \sin^{-1}(\sqrt{c} / \sqrt{d}) \} \\
&= (2/\pi) \{ \sqrt{a+1} / \sqrt{b-a} + \sin^{-1}(\sqrt{b-a} / \sqrt{b+1}) \} .
\end{aligned}$$

Using the fact that $\sin^{-1}(\sqrt{b-a} / \sqrt{b+1}) = \pi/2 - \sin^{-1}[\sqrt{1+a} / \sqrt{1+b}]$ we find

$$\begin{aligned}
g_1(\theta) &= (2/\pi) \{ \sqrt{1+a} / \sqrt{b-a} + \pi/2 - \sin^{-1}[\sqrt{1+a} / \sqrt{1+b}] \} \\
&= (2/\pi) \{ \sqrt{2} \cos(\theta_0/2) / \sqrt{\cos\theta - \cos\theta_0} + \pi/2 - \sin^{-1}[\cos(\theta_0/2) / \cos(\theta/2)] \} \\
&= \frac{2}{\pi} \{ \frac{\sqrt{2} \cos(\theta_0/2)}{\sqrt{\cos\theta - \cos\theta_0}} + \frac{\pi}{2} - \sin^{-1}(\frac{\cos(\theta_0/2)}{\cos(\theta/2)}) \} .
\end{aligned}$$

This is our corrected version of Vinogradov equation (1.111),

$$g(\vartheta) = \frac{\sqrt{2}}{\pi} \left\{ \frac{2 \cos \frac{1}{2}\theta_0}{\sqrt{\cos \vartheta - \cos \theta_0}} + \frac{\pi}{2} - \arcsin \left(\frac{\cos \frac{1}{2}\theta_0}{\cos \frac{1}{2}\theta} \right) \right\} . \tag{1. 111}$$

// wrong

where they seem to have $2 \leftrightarrow \sqrt{2}$. So the final result for $g_1(\theta)$ can be stated,

$$\begin{aligned}
g_1(\theta) &= \frac{2}{\pi} \{ \frac{\sqrt{2} \cos(\theta_0/2)}{\sqrt{\cos\theta - \cos\theta_0}} + \frac{\pi}{2} - \sin^{-1}(\frac{\cos(\theta_0/2)}{\cos(\theta/2)}) \} \\
&= \frac{2}{\pi} \{ \frac{\sqrt{2} \cos(\theta_0/2)}{\sqrt{\cos\theta - \cos\theta_0}} + \cos^{-1}(\frac{\cos(\theta_0/2)}{\cos(\theta/2)}) \} . \quad \theta \leq \theta_0
\end{aligned} \tag{G.15}$$

where on the last line we use $\pi/2 - \sin^{-1}(x) = \cos^{-1}(x)$.

To summarize: using a double Abel transform, we have solved our dual equation problem for the partner function g_1 , the total charge density on the bowl (sum of both sides).

G.2 Run a check on g_1

As a check on (G.15), since $g_1 = 4\pi R(\sigma_i + \sigma_o)$ from (G.0) and since $\sigma_o + \sigma_i = 2\sigma_i + (V_0/4\pi R)$ from (4.1.21), we can use the Kelvin result (4.2.3) for σ_i (with $a = u_0$) to claim,

$$\begin{aligned}\sigma_o + \sigma_i &= (V_0/2\pi^2 R) \left\{ \sqrt{1-\cos\alpha} / \sqrt{\cos\alpha - \cos\theta} - \tan^{-1} [\sqrt{1-\cos\alpha} / \sqrt{\cos\alpha - \cos\theta}] \right\} + V_0/(4\pi R) \\ &= V_0/(2\pi^2 R) \left\{ \sqrt{1-\cos\alpha} / \sqrt{\cos\alpha - \cos\theta} - \tan^{-1} [\sqrt{1-\cos\alpha} / \sqrt{\cos\alpha - \cos\theta}] + \pi/2 \right\}.\end{aligned}$$

But for comparison we have to flip the z axis which takes all $\cos \rightarrow -\cos$ (recall that $\theta_0 = \pi - u_0$) to get,

$$\sigma_o + \sigma_i = V_0/(2\pi^2 R) \left\{ \sqrt{1+\cos\theta_0} / \sqrt{\cos\theta - \cos\theta_0} - \tan^{-1} [\sqrt{1+\cos\theta_0} / \sqrt{\cos\theta - \cos\theta_0}] + \pi/2 \right\}.$$

Finally we use the fact that (draw a small triangle)

$$\tan^{-1} [\sqrt{1+\cos\theta_0} / \sqrt{\cos\theta - \cos\theta_0}] = \sin^{-1} [\sqrt{1+\cos\theta_0} / \sqrt{1+\cos\theta}] = \sin^{-1} [\cos(\theta_0/2) / \cos(\theta/2)]$$

to get

$$\sigma_o + \sigma_i = V_0/(2\pi^2 R) \left\{ \sqrt{2} \cos(\theta_0/2) / \sqrt{\cos\theta - \cos\theta_0} + \pi/2 - \sin^{-1} [\cos(\theta_0/2) / \cos(\theta/2)] \right\}.$$

Setting $V_0 = 1$ and $R = 1$ one then has

$$g_1 = 4\pi(\sigma_i + \sigma_o) = (2/\pi) \left\{ \sqrt{2} \cos(\theta_0/2) / \sqrt{\cos\theta - \cos\theta_0} + \pi/2 - \sin^{-1} [\cos(\theta_0/2) / \cos(\theta/2)] \right\}$$

in agreement with (G.15).

G.3 Find a_n

The next step is to determine coefficients a_n by inserting (G.15) for $g_1(\theta)$ into (G.2). This gives

$$a_n = (1/\pi) \int_0^{\theta_0} d\theta \sin\theta P_n(\cos\theta) \left\{ \sqrt{1+\cos\theta_0} / \sqrt{\cos\theta - \cos\theta_0} + \cos^{-1} [\sqrt{1+\cos\theta_0} / \sqrt{1+\cos\theta}] \right\}, \quad (\text{G.16})$$

another unruly integral. The first term can be evaluated using GR7 p 790 7.225.2 (ignore the $P^{-1/2}$ typo)

$$\begin{aligned}\int_{\cos\theta_0}^1 dz P_n(z) / \sqrt{z-\cos\theta_0} &= (n+1/2)^{-1} (1-\cos\theta_0)^{-1/2} [T_n(\cos\theta_0) - T_{n+1}(\cos\theta_0)] \\ &= (n+1/2)^{-1} (1-\cos\theta_0)^{-1/2} [\cos(n\theta_0) - \cos[(n+1)\theta_0]]\end{aligned} \quad (\text{G.17})$$

(Chebyshev T_n) so that

$$\begin{aligned}a_n(\text{1st term}) &= (2/\pi) \cot(\theta_0/2) [\cos(n\theta_0) - \cos[(n+1)\theta_0]] / (2n+1) \\ &= (2/\pi) \cot(\theta_0/2) [2 \sin[(n+1/2)\theta_0] \sin(\theta_0/2)] / (2n+1)\end{aligned}$$

$$\begin{aligned}
&= (4/\pi) \cos(\theta_0/2) \sin[(n+1/2)\theta_0] / (2n+1) \\
&= (2/\pi) \{\sin(n\theta_0) + \sin[(n+1)\theta_0]\} / (2n+1).
\end{aligned} \tag{G.18}$$

The second term integral

$$a_n(2nd \text{ term}) = (1/\pi) \int_0^{\theta_0} d\theta \sin\theta P_n(\cos\theta) \cos^{-1}[\sqrt{1+\cos\theta_0} / \sqrt{1+\cos\theta}] \tag{G.19}$$

is an indefinite integral of P_n times an inverse trig function of an algebraic argument, making this integral a bit difficult to look up in a table. This is where brute force comes in. We put P_n into its integral representation (F.9), and then reverse the integration order using $\int_0^{\theta_0} d\theta \int_0^\theta d\varphi = \int_0^{\theta_0} d\varphi \int_\varphi^{\theta_0} d\theta$ (draw a picture) to get

$$a_n(2nd \text{ term}) = (\sqrt{2}/\pi^2) \int_0^a d\varphi \cos[(n+1/2)\varphi] R$$

where

$$R \equiv \int_\varphi^{\theta_0} d\theta \sin\theta / \sqrt{\cos\varphi - \cos\theta} * \cos^{-1}[\sqrt{1+\cos\theta_0} / \sqrt{1+\cos\theta}] . \tag{G.20}$$

R may be evaluated by setting $x = \sin(\theta/2)$, $a = \cos(\varphi/2)$ and $b = \cos(\theta_0/2)$ to get

$$\begin{aligned}
R &= (2\sqrt{2}) \int_b^a dx x / \sqrt{a^2 - x^2} * \sec^{-1}(x/b) \\
&= -(2\sqrt{2}) \int_b^a dx \partial_x (a^2 - x^2)^{1/2} \sec^{-1}(x/b) \quad // \text{set up for parts} \\
&= (2\sqrt{2}) \int_b^a dx (a^2 - x^2)^{1/2} \partial_x \sec^{-1}(x/b) \quad // \text{"parts" vanish} \\
&= (2\sqrt{2} b) \int_b^a dx x^{-1} (a^2 - x^2)^{1/2} (x^2 - b^2)^{-1/2} \quad // \text{arc trig function is now gone} \\
&= (\sqrt{2} b) \int_\beta^\alpha dy/(y) (\alpha - y)^{1/2} (y - \beta)^{-1/2} \quad // x^2 = y, a^2 = \alpha, b^2 = \beta \\
&= (\sqrt{2} b) (\alpha - 1) \int_0^\infty dz \sqrt{z} / [(z+1)(z+\alpha)] \quad // z = (\alpha - y)/(y - \beta), c = \alpha/\beta = a^2/b^2 \\
&= (\sqrt{2} b) \pi(\sqrt{\alpha} - 1) \quad // \text{regulated partial fractions, } \infty \rightarrow \Lambda \rightarrow \infty \\
&= (\sqrt{2} b) \pi ((a/b) - 1) = (\sqrt{2} \pi) (a - b) \\
&= \sqrt{2} \pi (\cos(\varphi/2) - \cos(\theta_0/2)) .
\end{aligned} \tag{G.21}$$

After this saga, we are left with

$$\begin{aligned}
a_n(\text{2nd term}) &= (2/\pi) \int_0^{\theta_0} d\varphi \cos[(n+1/2)\varphi] [\cos(\varphi/2) - \cos(\theta_0/2)] \\
&= (1/\pi) [(n+1-n \cos\theta_0) \sin(n\theta_0) - n \sin\theta_0 \cos(n\theta_0)] / [n(n+1)(2n+1)] \\
&= (1/\pi) \{ [\sin(n\theta_0)/n - \sin[(n+1)\theta_0]/(n+1)] \} / (2n+1) .
\end{aligned} \tag{G.22}$$

At this point then we have shown that

$$\begin{aligned}
a_n(\text{1st term}) &= (1/\pi) \{ 2\sin(n\theta_0) + 2\sin[(n+1)\theta_0] \} / (2n+1) \\
a_n(\text{2nd term}) &= (1/\pi) \{ \sin(n\theta_0)/n - \sin[(n+1)\theta_0]/(n+1) \} / (2n+1) .
\end{aligned} \tag{G.23}$$

Adding we find

$$\begin{aligned}
a_n &= (1/\pi) \{ [2+1/n] \sin(n\theta_0) + [2-1/(n+1)] \sin[(n+1)\theta_0] \} / (2n+1) \\
&= (1/\pi) \{ (2n+1)/n * \sin(n\theta_0) + (2n+1)/(n+1) * \sin[(n+1)\theta_0] \} / (2n+1) \\
&= (1/\pi) \{ \sin(n\theta_0)/n + \sin[(n+1)\theta_0]/(n+1) \}
\end{aligned} \tag{G.24}$$

which agrees with the result found in (E.19).

G.4 Find Ψ and f_2

For the unit-radius bowl the potential is given by (E.14) with (G.24),

$$\begin{aligned}
V_i(r, \theta) &= (1/\pi) \sum_{n=0}^{\infty} \{ \sin(n\theta_0)/n + \sin[(n+1)\theta_0]/(n+1) \} r^n P_n(\cos\theta) \\
V_o(r, \theta) &= (1/\pi) \sum_{n=0}^{\infty} \{ \sin(n\theta_0)/n + \sin[(n+1)\theta_0]/(n+1) \} r^{-n-1} P_n(\cos\theta) .
\end{aligned} \tag{G.25}$$

Finally, looking at (E.15), the other partner function f_2 is the potential on the cap, $\theta_0 < \theta < \pi$,

$$\begin{aligned}
f_2(\theta) &= (1/\pi) \sum_{n=0}^{\infty} \{ \sin(n\theta_0)/n + \sin[(n+1)\theta_0]/(n+1) \} P_n(\cos\theta) \\
&= (2/\pi) \sin^{-1} \left[\frac{\sin(\theta_0/2)}{\sin(\theta/2)} \right] .
\end{aligned} \tag{G.26}$$

To get this last result, we assume the following obscure Legendre polynomial expansion,

$$\sum_{n=0}^{\infty} \{ \frac{\sin(n\theta_0)}{n} + \frac{\sin[(n+1)\theta_0]}{n+1} \} P_n(\cos\theta) = 2 \sin^{-1} \left[\frac{\sin(\theta_0/2)}{\sin(\theta/2)} \right] \quad \theta_0 \leq \theta \leq \pi . \tag{G.27}$$

We crudely verify (G.27) with a quick Maple test plot using 20 terms of the series so one can see the difference between the two curves,

```

RHS := 2*arcsin(sin(theta0/2)/sin(theta/2));

$$RHS := 2 \arcsin \left( \frac{\sin\left(\frac{1}{2}\theta_0\right)}{\sin\left(\frac{1}{2}\theta\right)} \right)$$

a0 := theta0 + sin(theta0);

$$a0 := \theta_0 + \sin(\theta_0)$$

an := sin(n*theta0)/n + sin((n+1)*theta0)/(n+1);

$$an := \frac{\sin(n\theta_0)}{n} + \frac{\sin((n+1)\theta_0)}{n+1}$$

LHS := a0 + sum(an*LegendreP(n,cos(theta)),n=1..20);

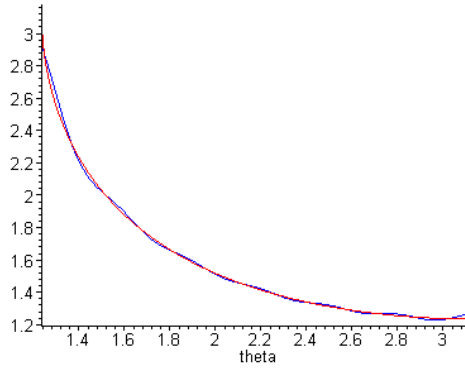
$$LHS := \theta_0 + \sin(\theta_0) + \left( \sum_{n=1}^{20} \left( \frac{\sin(n\theta_0)}{n} + \frac{\sin((n+1)\theta_0)}{n+1} \right) \text{LegendreP}(n, \cos(\theta)) \right)$$

theta0 := 1.2345;

$$\theta_0 = 1.2345$$

plot([RHS,LHS],theta = theta0..Pi,color = [red,blue]);

```



(G.28)

We cannot find series (G.27) in any source, but we know it has to be true for the following reason. Making contact with our previous work, imagine that the angle θ appearing in our Fig (4.2.6) is θ . Then we can say,

$$\begin{aligned} \theta &= \pi - \theta \\ \theta_0 &= \pi - u_0 \quad \text{and set } u_0 = \alpha \end{aligned} \quad . \quad (\text{G.29})$$

Then

$$\frac{\sin(\theta_0/2)}{\sin(\theta/2)} = \frac{\sin([\pi-u_0]/2)}{\sin([\pi-\theta]/2)} = \frac{\cos(u_0/2)}{\cos(\theta/2)} = \frac{\cos(\alpha/2)}{\cos(\theta/2)}$$

so

$$f_2(\theta) = (2/\pi) \sin^{-1} \left[\frac{\cos(\alpha/2)}{\cos(\theta/2)} \right] . \quad (\text{G.30})$$

This agrees with the Smythe potential on the cap result (D.7) with $V_0 = 1$,

$$V(\theta) = V_0 (2/\pi) \sin^{-1} \left[\frac{\cos(\alpha/2)}{\cos(\theta/2)} \right] . \quad (\text{D.7})$$

Appendix H: Support

H.1 Solving for A(τ) and B(τ) in (2.4.10) and double-bowl support

Our first task is to solve equations (2.4.10) for A(τ) and B(τ),

$$\begin{aligned} [A(\tau)\text{ch}(u_0\tau) + B(\tau)\text{sh}(u_0\tau)] &= V_0 \sqrt{2} \frac{\text{ch}[(u_0-\pi)\tau]}{\text{ch}(\pi\tau)} & u'_0 \equiv u_0 + 2\pi \\ [A(\tau)\text{ch}(u'_0\tau) + B(\tau)\text{sh}(u'_0\tau)] &= V_0 \sqrt{2} \frac{\text{ch}[(u_0-\pi)\tau]}{\text{ch}(\pi\tau)} & (2.4.10) . \end{aligned} \quad (\text{H.1.1})$$

Normally we would have Maple solve these equations, but our Maple V is not too smart with the hyperbolic function identities and produces a messy solution of exponentials. Therefore we solve the problem by hand and use Maple to verify the solution.

Since both equations have the same right side, the left sides are also equal,

$$\begin{aligned} [A(\tau)\text{ch}[(u_0 + 2\pi)\tau] + B(\tau)\text{sh}[(u_0 + 2\pi)\tau]] &= [A(\tau)\text{ch}(u_0\tau) + B(\tau)\text{sh}(u_0\tau)] \\ \text{or } A(\tau) [\text{ch}[(u_0+2\pi)\tau] - \text{ch}(u_0\tau)] &= -B(\tau) [\text{sh}[(u_0+2\pi)\tau] - \text{sh}(u_0\tau)] . \end{aligned} \quad (\text{H.1.2})$$

Use the identities

$$\begin{aligned} \text{ch}(a+x) - \text{ch}(x) &= 2 \text{ sh}(a/2+x) \text{ sh}(a/2) \\ \text{sh}(a+x) - \text{sh}(x) &= 2 \text{ ch}(a/2+x) \text{ sh}(a/2) \end{aligned} \quad (\text{H.1.3})$$

with $x = u_0\tau$, $a = 2\pi\tau$, $a/2+x = (\pi+u_0)\tau$ to get

$$\begin{aligned} \text{ch}[(u_0+2\pi)\tau] - \text{ch}(u_0\tau) &= 2 \text{ sh}[(\pi+u_0)\tau] \text{ sh}(\pi\tau) \\ \text{sh}[(u_0+2\pi)\tau] - \text{sh}(u_0\tau) &= 2 \text{ ch}[(\pi+u_0)\tau] \text{ sh}(\pi\tau) . \end{aligned} \quad (\text{H.1.4})$$

Then (H.1.2) becomes,

$$A(\tau) [\text{sh}[(\pi+u_0)\tau] \text{ sh}(\pi\tau)] = -B(\tau) [\text{ch}[(\pi+u_0)\tau] \text{ sh}(\pi\tau)] .$$

so that

$$B(\tau) = -A(\tau) \text{ th}[(\pi+u_0)\tau] \quad (\text{H.1.5})$$

providing a simple relationship between B(τ) and A(τ).

Insert this expression for B(τ) into the first equation of (H.1.1) to get

$$[A(\tau)\text{ch}(u_0\tau) - A(\tau) \text{ th}[(\pi+u_0)\tau] \text{ sh}(u_0\tau)] = V_0 \sqrt{2} \frac{\text{ch}[\tau(u_0-\pi)]}{\text{ch}(\pi\tau)}$$

or

$$\text{ch}(\pi\tau) A(\tau) \{ \text{ch}(u_0\tau) - \text{th}[(\pi+u_0)\tau] \text{ sh}(u_0\tau) \} = V_0 \sqrt{2} \text{ ch}[\tau(u_0-\pi)]$$

or

$$\operatorname{ch}(\pi\tau) A(\tau) \{ \operatorname{ch}[(\pi+u_0)\tau] \operatorname{ch}(u_0\tau) - \operatorname{sh}[(\pi+u_0)\tau] \operatorname{sh}(u_0\tau) \} = V_0 \sqrt{2} \operatorname{ch}[\tau(u_0-\pi)] \operatorname{ch}[(\pi+u_0)\tau]. \quad (\text{H.1.6})$$

Now use identity

$$\operatorname{ch}x \operatorname{ch}y - \operatorname{sh}x \operatorname{sh}y = \operatorname{ch}(x-y) \quad (\text{H.1.7})$$

with $x = [(\pi+u_0)\tau]$ and $y = (u_0\tau)$ to get

$$\operatorname{ch}[(\pi+u_0)\tau] \operatorname{ch}(u_0\tau) - \operatorname{sh}[(\pi+u_0)\tau] \operatorname{sh}(u_0\tau) = \operatorname{ch}(\pi\tau). \quad (\text{H.1.8})$$

Then (H.1.6) may be written

$$\operatorname{ch}^2(\pi\tau) A(\tau) = V_0 \sqrt{2} \operatorname{ch}[\tau(u_0-\pi)] \operatorname{ch}[(\pi+u_0)\tau] \quad (\text{H.1.9})$$

giving

$$A(\tau) = V_0 \sqrt{2} \operatorname{ch}[\tau(u_0-\pi)] \operatorname{ch}[(\pi+u_0)\tau] / \operatorname{ch}^2(\pi\tau). \quad (\text{H.1.10})$$

Then from (H.1.5) that $B(\tau) = -A(\tau) \operatorname{th}[(\pi+u_0)\tau]$,

$$B(\tau) = -V_0 \sqrt{2} \operatorname{ch}[\tau(u_0-\pi)] \operatorname{sh}[(\pi+u_0)\tau] / \operatorname{ch}^2(\pi\tau) \quad (\text{H.1.11})$$

so the solution is then

$$\begin{aligned} A(\tau) &= V_0 \sqrt{2} \operatorname{ch}[(\pi-u_0)\tau] \operatorname{ch}[(\pi+u_0)\tau] / \operatorname{ch}^2(\pi\tau) \\ B(\tau) &= -V_0 \sqrt{2} \operatorname{ch}[(\pi-u_0)\tau] \operatorname{sh}[(\pi+u_0)\tau] / \operatorname{ch}^2(\pi\tau). \end{aligned} \quad (\text{H.1.12})$$

We then use Maple to verify that (H.1.12) really is the solution to (H.1.1). Here f and g are the left sides of (H.1.1), h is the right side, and u0p means u_0' . We want to show that f-h = 0 and g-h = 0.

(% refers to the last calculated object)

```

f := A*cosh(u0*tau) + B*sinh(u0*tau);
f:=A cosh(u0 τ) + B sinh(u0 τ)
g := A*cosh(u0p*tau) + B*sinh(u0p*tau);
g:=A cosh(u0p τ) + B sinh(u0p τ)
h := v0*sqrt(2)*cosh((u0-Pi)*tau)/cosh(Pi*tau);
h:= $\frac{V_0 \sqrt{2} \cosh((u_0 - \pi) \tau)}{\cosh(\pi \tau)}$ 
u0p := u0+2*pi;
u0p=u0+2 π
A := v0*sqrt(2)*cosh((Pi-u0)*tau)*cosh((u0+pi)*tau)/cosh(Pi*tau)^2;
A= $\frac{V_0 \sqrt{2} \cosh((\pi - u_0) \tau) \cosh((u_0 + \pi) \tau)}{\cosh(\pi \tau)^2}$ 
B := -v0*sqrt(2)*cosh((Pi-u0)*tau)*sinh((u0+pi)*tau)/cosh(Pi*tau)^2;
B=- $\frac{V_0 \sqrt{2} \cosh((\pi - u_0) \tau) \sinh((u_0 + \pi) \tau)}{\cosh(\pi \tau)^2}$ 
(f-h)*cosh(Pi*tau)^2:expand(%):simplify(%);
0
(g-h)*cosh(Pi*tau)^2:expand(%):simplify(%);
0

```

(H.1.13)

Double bowl support

The boundary conditions stated in (3.5) are

$$\begin{aligned} [A(\tau)\text{ch}(u_1\tau) + B(\tau)\text{sh}(u_1\tau)] &= V_1 \sqrt{2} \text{ch}[\tau(u_1-\pi)] / \text{ch}(\pi\tau) \\ [A(\tau)\text{ch}(u_0'\tau) + B(\tau)\text{sh}(u_0'\tau)] &= V_0 \sqrt{2} \text{ch}[\tau(u_0-\pi)] / \text{ch}(\pi\tau) . \end{aligned} \quad (3.5)$$
(H.1.14)

Divide the second equation by the first,

$$\frac{A(\tau)\text{ch}(u_0'\tau) + B(\tau)\text{sh}(u_0'\tau)}{A(\tau)\text{ch}(u_1\tau) + B(\tau)\text{sh}(u_1\tau)} = \frac{V_0 \text{ch}[\tau(\pi-u_0)]}{V_1 \text{ch}[\tau(\pi-u_1)]} . \quad (H.1.15)$$

Multiply out and isolate factors A(τ) and B(τ) to find that

$$A(\tau) P = B(\tau) Q \quad (H.1.16)$$

where

$$\begin{aligned} P &\equiv \{ V_1 \text{ch}(u_0'\tau) \text{ch}[\tau(\pi-u_1)] - V_0 \text{ch}(u_1\tau) \text{ch}[\tau(\pi-u_0)] \} \\ Q &\equiv \{ V_0 \text{sh}(u_1\tau) \text{ch}[\tau(\pi-u_0)] - V_1 \text{sh}(u_0'\tau) \text{ch}[\tau(\pi-u_1)] \} . \end{aligned}$$

Multiply the second equation of (H.1.14) by Q

$$[A(\tau)Q\text{ch}(u_0'\tau) + B(\tau)Q\text{sh}(u_0'\tau)] \text{ch}(\pi\tau) = V_0 \sqrt{2} Q \text{ch}[\tau(u_0-\pi)] . \quad (H.1.17)$$

Replace B(τ)Q by A(τ)P in (H.1.17) and solve for A(τ) to get

$$\text{ch}(\pi\tau)A(\tau) = V_0 \sqrt{2} Q\text{ch}[\tau(\pi-u_0)] / [Q\text{ch}(u_0'\tau) + P \text{sh}(u_0'\tau)] . \quad (H.1.18)$$

Replace $A(\tau)P$ by $B(\tau)Q$ by in (H.1.17) and solve for $B(\tau)$ to get

$$\operatorname{ch}(\pi\tau) B(\tau) = V_0 \sqrt{2} P \operatorname{ch}[\tau(\pi-u_0)] / [Q \operatorname{ch}(u_0'\tau) + P \operatorname{sh}(u_0'\tau)] . \quad (\text{H.1.19})$$

The coefficients are then

$$\begin{aligned} A(\tau) &= V_0 \sqrt{2} Q \frac{\operatorname{ch}[\tau(\pi-u_0)]}{[Q \operatorname{ch}(u_0'\tau) + P \operatorname{sh}(u_0'\tau)] \operatorname{ch}(\pi\tau)} \\ B(\tau) &= V_0 \sqrt{2} P \frac{\operatorname{ch}[\tau(\pi-u_0)]}{[Q \operatorname{ch}(u_0'\tau) + P \operatorname{sh}(u_0'\tau)] \operatorname{ch}(\pi\tau)} \end{aligned} \quad (\text{H.1.20})$$

where

$$\begin{aligned} P &= \{ V_1 \operatorname{ch}(u_0'\tau) \operatorname{ch}[\tau(\pi-u_1)] - V_0 \operatorname{ch}(u_1\tau) \operatorname{ch}[\tau(\pi-u_0)] \} \\ Q &= \{ V_0 \operatorname{sh}(u_1\tau) \operatorname{ch}[\tau(\pi-u_0)] - V_1 \operatorname{sh}(u_0'\tau) \operatorname{ch}[\tau(\pi-u_1)] \} . \end{aligned}$$

We then use Maple to verify that (H.1.20) is the solution to (H.1.14),

$$\begin{aligned} A &:= V_0 * \operatorname{sqrt}(2) * Q * \operatorname{cosh}((\operatorname{Pi}-u_0)*\operatorname{tau}) / ((Q * \operatorname{cosh}(u_0 p * \operatorname{tau}) + P * \operatorname{sinh}(u_0 p * \operatorname{tau})) * \operatorname{cosh}(\operatorname{Pi} * \operatorname{tau})) ; \\ A &:= \frac{V_0 \sqrt{2} Q \operatorname{cosh}((\pi - u_0)\tau)}{(Q \operatorname{cosh}(u_0 p \tau) + P \operatorname{sinh}(u_0 p \tau)) \operatorname{cosh}(\pi \tau)} \\ B &:= V_0 * \operatorname{sqrt}(2) * P * \operatorname{cosh}((\operatorname{Pi}-u_0)*\operatorname{tau}) / ((Q * \operatorname{cosh}(u_0 p * \operatorname{tau}) + P * \operatorname{sinh}(u_0 p * \operatorname{tau})) * \operatorname{cosh}(\operatorname{Pi} * \operatorname{tau})) ; \\ B &:= \frac{V_0 \sqrt{2} P \operatorname{cosh}((\pi - u_0)\tau)}{(Q \operatorname{cosh}(u_0 p \tau) + P \operatorname{sinh}(u_0 p \tau)) \operatorname{cosh}(\pi \tau)} \\ P &:= V_1 * \operatorname{cosh}(u_0 p * \operatorname{tau}) * \operatorname{cosh}((\operatorname{Pi}-u_1)*\operatorname{tau}) - V_0 * \operatorname{cosh}(u_1 * \operatorname{tau}) * \operatorname{cosh}((\operatorname{Pi}-u_0)*\operatorname{tau}) ; \\ P &:= V_1 \operatorname{cosh}(u_0 p \tau) \operatorname{cosh}((\pi - u_1)\tau) - V_0 \operatorname{cosh}(u_1 \tau) \operatorname{cosh}((\pi - u_0)\tau) \\ Q &:= V_0 * \operatorname{sinh}(u_1 * \operatorname{tau}) * \operatorname{cosh}((\operatorname{Pi}-u_0)*\operatorname{tau}) - V_1 * \operatorname{sinh}(u_0 p * \operatorname{tau}) * \operatorname{cosh}((\operatorname{Pi}-u_1)*\operatorname{tau}) ; \\ Q &:= V_0 \operatorname{sinh}(u_1 \tau) \operatorname{cosh}((\pi - u_0)\tau) - V_1 \operatorname{sinh}(u_0 p \tau) \operatorname{cosh}((\pi - u_1)\tau) \\ \# \text{ Install } A \text{ and } B \text{ into left sides of (H.1.14) and verify right sides} \\ \operatorname{cosh}(\operatorname{Pi} * \operatorname{tau}) * (A * \operatorname{cosh}(u_1 * \operatorname{tau}) + B * \operatorname{sinh}(u_1 * \operatorname{tau})) : \operatorname{simplify}(\%) ; \\ &\quad \operatorname{cosh}((\pi - u_1)\tau) V_1 \sqrt{2} \\ \operatorname{cosh}(\operatorname{Pi} * \operatorname{tau}) * (A * \operatorname{cosh}(u_0 p * \operatorname{tau}) + B * \operatorname{sinh}(u_0 p * \operatorname{tau})) : \operatorname{simplify}(\%) ; \\ &\quad V_0 \sqrt{2} \operatorname{cosh}((-\pi + u_0)\tau) \end{aligned} \quad (\text{H.1.21})$$

Next, in order so show that (3.2) equals (3.7) for the double bowl, we have to show this:

$$[A(\tau)\operatorname{ch}(u\tau) + B(\tau)\operatorname{sh}(u\tau)] = V_0 \sqrt{2} \frac{\operatorname{ch}[(\pi-u_0)\tau] \operatorname{sh}[(u-u_1)\tau] + \operatorname{ch}[(\pi-u_1)\tau] \operatorname{sh}[(2\pi+u_0-u)\tau]}{\operatorname{ch}(\pi\tau) \operatorname{sh}[(2\pi+u_0-u_1)\tau]} . \quad (\text{H.1.22})$$

This requires a *boatload* of algebra which would be painful to replicate here, so instead of deriving the above equation, we shall verify that it is in fact correct. We first multiple both sides of (H.1.22) by the denominator of the right side to get

$$\begin{aligned} &\operatorname{ch}(\pi\tau) \operatorname{sh}[(2\pi+u_0-u_1)\tau] [A(\tau)\operatorname{ch}(u\tau) + B(\tau)\operatorname{sh}(u\tau)] \quad // \text{LHS} = \text{RHS} \\ &= V_0 \sqrt{2} (\operatorname{ch}[(\pi-u_0)\tau] \operatorname{sh}[(u-u_1)\tau] + \operatorname{ch}[(\pi-u_1)\tau] \operatorname{sh}[(2\pi+u_0-u)\tau]) . \end{aligned} \quad (\text{H.1.23})$$

To assist Maple (which does not like messy fractions), we shall multiply both sides by

$$F = [Q \operatorname{ch}(u_0'\tau) + P \operatorname{sh}(u_0'\tau)] \operatorname{ch}(\pi\tau). \quad (\text{H.1.24})$$

which clears the denominators of A and B visible in (H.1.20). So we then *want to prove* that

$$F^*(\text{LHS}-\text{RHS}) = 0$$

where

$$\begin{aligned} \text{LHS} &= \operatorname{ch}(\pi\tau) \operatorname{sh}[(2\pi+u_0-u_1)\tau] [A(\tau)\operatorname{ch}(u\tau) + B(\tau)\operatorname{sh}(u\tau)] \\ \text{RHS} &= V_0 \sqrt{2} (\operatorname{ch}[(\pi-u_0)\tau] \operatorname{sh}[(u-u_1)\tau] + \operatorname{ch}[(\pi-u_1)\tau] \operatorname{sh}[(2\pi+u_0-u)\tau]) \\ F &= [Q \operatorname{ch}(u_0'\tau) + P \operatorname{sh}(u_0'\tau)] \operatorname{ch}(\pi\tau). \end{aligned} \quad (\text{H.1.25})$$

This is a problem Maple can handle. Continuing the code (H.1.21), we enter the last three expressions,

```
LHS := ( $\cosh(\text{Pi}\tau)\sinh((2\text{Pi}+u_0-u_1)\tau)$ ) * ( $A\cosh(u\tau)+B\sinh(u\tau)$ );
RHS :=  $V_0\sqrt{2}(\cosh((\pi-u_0)\tau)\sinh((u-u_1)\tau)+\cosh((\pi-u_1)\tau)\sinh((2\pi+u_0-u)\tau))$ ;
F := ( $Q\cosh(u_0\tau)+P\sinh(u_0\tau)$ ) *  $\cosh(\text{Pi}\tau)$ ;
F := ( $Q\cosh(u_0\tau)+P\sinh(u_0\tau)$ ) *  $\cosh(\text{Pi}\tau)$ 
```

(H.1.26)

For the double bowl we set $u_0' \equiv u_0 + 2\pi$ and $V_1 = V_0$ as noted below (3.6). Here then is Maple's demonstration that $F^*(\text{LHS}-\text{RHS}) = 0$:

```
u0p :=  $u_0+2\text{Pi}$ ; v1 :=  $V_0$ ;
LHS := ( $\cosh(\text{Pi}\tau)\sinh((2\text{Pi}+u_0-u_1)\tau)$ ) * ( $A\cosh(u\tau)+B\sinh(u\tau)$ );
RHS :=  $V_0\sqrt{2}(\cosh((\pi-u_0)\tau)\sinh((u-u_1)\tau)+\cosh((\pi-u_1)\tau)\sinh((2\pi+u_0-u)\tau))$ ;
F := ( $Q\cosh(u_0\tau)+P\sinh(u_0\tau)$ ) *  $\cosh(\text{Pi}\tau)$ ;
u0p :=  $u_0+2\text{Pi}$ ; v1 :=  $V_0$ ;
F := ( $Q\cosh(u_0\tau)+P\sinh(u_0\tau)$ ) *  $\cosh(\text{Pi}\tau)$ ;
F^*(LHS-RHS) :=  $\text{simplify}(\%)$ ; expand(%);
```

0
(H.1.27)

Next, to verify the claim made below (3.7) we need to show that in the limit $u_1 \rightarrow u_0$, the double bowl potential

$$V(\xi, u) = V_0 \sqrt{2} \sqrt{\operatorname{ch}\xi - \cos u} \int_0^\infty d\tau P_{i\tau-1/2}(\operatorname{ch}\xi) \frac{\operatorname{ch}[(\pi-u_0)\tau] \operatorname{sh}[(u-u_1)\tau] + \operatorname{ch}[(\pi-u_1)\tau] \operatorname{sh}[(2\pi+u_0-u)\tau]}{\operatorname{ch}(\pi\tau) \operatorname{sh}[(2\pi+u_0-u_1)\tau]} \quad (3.7)$$

becomes the single bowl potential

$$V(\xi, u) = V_0 \sqrt{2} \sqrt{\operatorname{ch}\xi - \cos u} \int_0^\infty d\tau P_{i\tau-1/2}(\operatorname{ch}\xi) \frac{\operatorname{ch}[(\pi-u_0)\tau] \operatorname{ch}[(\pi+u_0-u)\tau]}{\operatorname{ch}^2(\pi\tau)} . \quad (2.4.13)$$

This requires showing that, as $u_1 \rightarrow u_0$,

$$\frac{\text{ch}[(\pi-u_0)\tau] \text{sh}[(u-u_1)\tau] + \text{ch}[(\pi-u_1)\tau] \text{sh}[(2\pi+u_0-u)\tau]}{\text{ch}(\pi\tau) \text{sh}[(2\pi+u_0-u_1)\tau]} = \frac{\text{ch}[(\pi-u_0)\tau] \text{ch}[(\pi+u_0-u)\tau]}{\text{ch}^2(\pi\tau)}$$

or

$$\frac{\text{ch}[(\pi-u_0)\tau] \text{sh}[(u-u_0)\tau] + \text{ch}[(\pi-u_0)\tau] \text{sh}[(2\pi+u_0-u)\tau]}{\text{sh}[(2\pi)\tau]} = \frac{\text{ch}[(\pi-u_0)\tau] \text{ch}[(\pi+u_0-u)\tau]}{\text{ch}(\pi\tau)}$$

or

$$\text{ch}(\pi\tau)(\text{sh}[(u-u_0)\tau] + \text{sh}[(2\pi+u_0-u)\tau]) = \text{sh}(2\pi\tau) \text{ch}[(\pi+u_0-u)\tau]. \quad (\text{H.1.28})$$

Maple rises to the occasion:

```
> restart;
> LHS := cosh(Pi*tau)*( sinh((u-u0)*tau)+sinh((2*Pi+u0-u)*tau) );
LHS:=cosh(pi τ)(sinh((u-u0) τ)+sinh((2 π+u0-u) τ))
> RHS := sinh(2*Pi*tau)*cosh((Pi+u0-u)*tau);
RHS:=sinh(2 π τ)cosh((π+u0-u) τ)
> LHS-RHS;
cosh(pi τ)(sinh((u-u0) τ)+sinh((2 π+u0-u) τ))-sinh(2 π τ)cosh((π+u0-u) τ)
> expand(%);
2cosh(pi τ)sinh(tau)cosh(tau0)-2cosh(pi τ)cosh(tau)sinh(tau0)-2cosh(pi τ)^3sinh(tau)cosh(tau0)
+2cosh(pi τ)^3cosh(tau)sinh(tau0)+2sinh(pi τ)^2cosh(pi τ)sinh(tau)cosh(tau0)
-2sinh(pi τ)^2cosh(pi τ)cosh(tau)sinh(tau0)
> simplify(%);
0
(H.1.29)
```

Thus the limit $u_1 \rightarrow u_0$ of the double bowl potential is the single bowl potential.

Finally, we want to verify the claim made in (3.16) that

$$\frac{\text{ch}[\theta\tau] \text{sh}[(u-\pi-\theta)\tau] + \text{ch}[\theta\tau] \text{sh}[(3\pi-\theta-u)\tau]}{\text{ch}(\pi\tau) \text{sh}[(2\pi-2\theta)\tau]} = \frac{\text{ch}(\theta\tau) \text{ch}[(2\pi-u)\tau]}{\text{ch}(\pi\tau) \text{ch}[(\pi-\theta)\tau]}$$

or

$$\frac{\text{sh}[(u-\pi-\theta)\tau] + \text{sh}[(3\pi-\theta-u)\tau]}{\text{sh}[(2\pi-2\theta)\tau]} = \frac{\text{ch}[(2\pi-u)\tau]}{\text{ch}[(\pi-\theta)\tau]}$$

or

$$(\text{sh}[(u-\pi-\theta)\tau] + \text{sh}[(3\pi-\theta-u)\tau]) \text{ch}[(\pi-\theta)\tau] = \text{sh}[(2\pi-2\theta)\tau] \text{ch}[(2\pi-u)\tau]. \quad (\text{H.1.30})$$

Another job for Maple:

```

restart;
LHS := (sinh((u-Pi-theta)*tau) + sinh((3*Pi-theta-u)*tau))*cosh((Pi-theta)*tau);
LHS := (sinh((u - Pi - theta) * tau) + sinh((3 * Pi - theta - u) * tau)) * cosh((Pi - theta) * tau);
RHS := sinh((2*Pi-2*theta)*tau)*cosh((2*Pi-u)*tau);
RHS := sinh((2 * Pi - 2 * theta) * tau) * cosh((2 * Pi - u) * tau)
LHS-RHS:expand(%):simplify(%);
0

```

(H.1.31)

H.2 Computation of the integral in (2.4.7)

Derive the following integral:

$$\int_1^\infty dx P_{i\tau-1/2}(x) / \sqrt{x - \cos u_0} = \sqrt{2} \operatorname{ch}[\tau(u_0 - \pi)] / (\tau \operatorname{sh}(\pi\tau)) \quad 0 \leq u_0 \leq 2\pi. \quad (\text{H.2.1})$$

Start with the left hand side (LHS) and expand part of the integrand using (10.1.8a) with $a=x$ and $b=1$

$$1/\sqrt{x - \cos u_0} = (1/\pi) \sqrt{2} \sum_{n=0}^{\infty} \varepsilon_n Q_{n-1/2}(x) \cos(nu_0) \quad (10.1.8a) \quad (\text{H.2.2})$$

so that

$$\text{LHS} = (\sqrt{2}/\pi) \sum_{n=0}^{\infty} \varepsilon_n \cos(nu_0) \int_1^\infty dx P_{i\tau-1/2}(x) Q_{n-1/2}(x). \quad (\text{H.2.3})$$

Using GR7 page 770 7.114.1 with $\nu = i\tau - 1/2$ and $\sigma = n - 1/2$,

7.114

$$1. \quad \int_1^\infty P_\nu(x) Q_\sigma(x) dx = \frac{1}{(\sigma - \nu)(\sigma + \nu + 1)} \quad [\operatorname{Re}(\sigma - \nu) > 0, \quad \operatorname{Re}(\sigma + \nu) > -1] \\ \text{ET II 324(19)}$$

we find $(\sigma - \nu) = n - i\tau$ and $(\sigma + \nu + 1) = n + i\tau$ so our PQ integral is just $1/(n^2 + \tau^2)$. Then,

$$\text{LHS} = (\sqrt{2}/\pi) \sum_{n=0}^{\infty} \varepsilon_n \cos(nu_0) / (n^2 + \tau^2). \quad (\text{H.2.4})$$

Then use GR7 page 47 1.445.2,

$$2. \quad \sum_{k=1}^{\infty} \frac{\cos kx}{k^2 + \alpha^2} = \frac{\pi}{2\alpha} \frac{\cosh \alpha(\pi - x)}{\sinh \alpha\pi} - \frac{1}{2\alpha^2} \quad [0 \leq x \leq 2\pi] \quad \text{BR* 257, JO (410)}$$

which can be rewritten with $k = n$, $\alpha = \tau$, $x = u_0$, and $\varepsilon_n = 2 - \delta_{n,0}$,

$$\sum_{n=0}^{\infty} \varepsilon_n \frac{\cos(nu_0)}{(n^2 + \tau^2)} = (\pi/\tau) \operatorname{ch}[\tau(\pi - u_0)] / \operatorname{sh}(\pi\tau) \quad 0 \leq u_0 \leq 2\pi \quad (\text{H.2.5})$$

to conclude that

$$\text{LHS} = \sqrt{2} \operatorname{ch}[\tau(\pi - u_0)] / [\tau \operatorname{sh}(\tau\pi)] \quad (\text{H.2.6})$$

and therefore (H.2.1) is validated

H.3 Computation of the integral in (4.4.2)

Derive the following integral:

$$\int_0^\infty dx \operatorname{ch}^2(bx)/\operatorname{ch}^2(x) = [\pi b/\sin(\pi b) + 1]/2 \quad 0 < |b| < 1 . \quad (\text{H.3.1})$$

Start with twice the left hand side,

$$\begin{aligned} & 2 \int_0^\infty dx \operatorname{ch}^2(bx)/\operatorname{ch}^2(x) \\ &= \int_0^\infty dx [\operatorname{ch}(2bx)+1]/\operatorname{ch}^2(x) \\ &= \int_0^\infty dx \operatorname{ch}(2bx)/\operatorname{ch}^2(x) + \int_0^\infty dx/\operatorname{ch}^2(x) \\ &= \int_0^\infty dx \operatorname{ch}(2bx)/\operatorname{ch}^2(x) + 1 . \quad // \text{GR7 3.5.11(8) or Maple for second integral} \end{aligned} \quad (\text{H.3.2})$$

To evaluate the first integral use this integral from GR7 3.512.1,

3.512

$$1. \quad \int_0^\infty \frac{\cosh 2\beta x}{\cosh^{2\nu} ax} dx = \frac{4^{\nu-1}}{a} B\left(\nu + \frac{\beta}{a}, \nu - \frac{\beta}{a}\right) \quad [\operatorname{Re}(\nu \pm \beta) > 0, \quad a > 0, \quad \beta > 0] \\ \text{LI(27)(17)a, EH I 11(26)}$$

with $\beta = b$ and $\nu = 1$ and $a = 1$.

We pause to check the conditions. Requirement $\beta > 0$ indicates that β is real, so $\operatorname{Re}(\beta) = \beta$, as is our ν . So

$$\operatorname{Re}(\nu \pm \beta) > 0 \Rightarrow \nu \pm \beta > 0 \Rightarrow 1 \pm b > 0 \Rightarrow \pm b > -1 \Rightarrow b > -1 \text{ and } b < 1 \text{ so:} \quad -1 < b < 1$$

But condition $\beta > 0$ says $b > 0$. So only condition is this

$$0 < b < 1 . \quad (\text{H.3.3})$$

Applying the above GR7 integral one gets,

$$\int_0^\infty dx \operatorname{ch}(2bx)/\operatorname{ch}^2(x) = B(1+b, 1-b) // B(x,y) \equiv \Gamma(x)\Gamma(y)/\Gamma(x+y)$$

$$= \Gamma(1+b)\Gamma(1-b)/\Gamma(2) = \Gamma(1+b)\Gamma(1-b) \quad (H.3.4)$$

Maple informs us that

```
GAMMA(1+b)*GAMMA(1-b);
  Γ(1+b)Γ(1-b)
simplify(%);
- b π
  ───────────
  sin(π (1+b))
```

so the first term in (H.3.2) is

$$\int_0^\infty dx \operatorname{ch}(2bx)/\operatorname{ch}^2(x) = -\pi b/\sin[\pi(1+b)] = -\pi b/\sin(\pi b + \pi) = +\pi b/\sin(\pi b) . \quad (H.3.5)$$

The integral appearing in (H.3.1) is then

$$\int_0^\infty dx \operatorname{ch}^2(bx)/\operatorname{ch}^2(x) = [\pi b/\sin(\pi b) + 1]/2 . \quad 0 < b < 1 \quad (H.3.6)$$

Replacing b by $|b|$ we get

$$\int_0^\infty dx \operatorname{ch}^2(|b|x)/\operatorname{ch}^2(x) = [\pi |b|/\sin(\pi |b|) + 1]/2 \quad 0 < |b| < 1$$

or

$$\int_0^\infty dx \operatorname{ch}^2(bx)/\operatorname{ch}^2(x) = [\pi b/\sin(\pi b) + 1]/2 \quad 0 < |b| < 1 \quad (H.3.7)$$

H.4 Computation of two integrals used in Appendix J and K

(a) Derive the following integral:

$$\int_0^\pi dx \cos(nx) \frac{1}{b+\cos x} = (\operatorname{sign} b)^{n+1} \frac{\pi}{\sqrt{b^2-1}} (\sqrt{b^2-1} - |b|)^n . \quad b > 1 \text{ or } b < -1 \quad (H.4.1)$$

That is, compute the Fourier Cosine Series Transform of the function $1/(b+\cos x)$.

Start with this integral from GR7 3.613.1,

3.613

$$1.^6 \quad \int_0^\pi \frac{\cos nx dx}{1 + a \cos x} = \frac{\pi}{\sqrt{1 - a^2}} \left(\frac{\sqrt{1 - a^2} - 1}{a} \right)^n \quad [a^2 < 1, \quad n \geq 0] \quad BI (64)(12)$$

$$(H.4.2)$$

Call the above integral $J(a)$ and let $b = 1/a$. Then

$$\begin{aligned}
 J(a) &= \int_0^\pi dx \cos(nx) \frac{1}{1+acox} \frac{b}{b} = b \int_0^\pi dx \cos(nx) \frac{1}{b+\cos x} \\
 \frac{\pi}{\sqrt{1-a^2}} \frac{b}{b} &= b \frac{\pi}{\sqrt{b^2-1}} \\
 \frac{\sqrt{1-a^2}}{a} \frac{b}{b} &= (\sqrt{b^2-1} - b) . \tag{H.4.3}
 \end{aligned}$$

Then

$$b \int_0^\pi dx \cos(nx) \frac{1}{b+\cos x} = b \frac{\pi}{\sqrt{b^2-1}} (\sqrt{b^2-1} - b)^n$$

so we find

$$I(b) \equiv \int_0^\pi dx \cos(nx) \frac{1}{b+\cos x} = b \frac{\pi}{\sqrt{b^2-1}} (\sqrt{b^2-1} - b)^n \quad b > 1, \quad -b = -|b| . \tag{H.4.4}$$

For $b < -1$, the correct analytic continuation is to take $\sqrt{b^2-1} \rightarrow -\sqrt{b^2-1}$ (as verified below) so in this case one finds

$$\begin{aligned}
 I(b) &\equiv \int_0^\pi dx \cos(nx) \frac{1}{b+\cos x} = - \frac{\pi}{\sqrt{b^2-1}} (-\sqrt{b^2-1} - b)^n \quad b < -1, \quad b = -|b| \\
 &= (-1)^{n+1} \frac{\pi}{\sqrt{b^2-1}} (\sqrt{b^2-1} + b)^n \quad b < -1 . \tag{H.4.5}
 \end{aligned}$$

Combining these results,

$$I(b) = \int_0^\pi dx \cos(nx) \frac{1}{b+\cos x} = (\text{sign } b)^{n+1} \frac{\pi}{\sqrt{b^2-1}} (\sqrt{b^2-1} - |b|)^n \tag{H.4.6}$$

and so (H.4.1) has been derived.

Maple numerical integration verification for several cases:

```

f := Int(cos(n*x)*(b+cos(x))^( -1), x=0..Pi);
f := 
$$\int_0^\pi \frac{\cos(nx)}{b + \cos(x)} dx$$

g := signum(b)^(n+1)*(Pi/sqrt(b^2-1))*(sqrt(b^2-1)-abs(b))^n;
g := 
$$\frac{\text{signum}(b)^{(n+1)} \pi (\sqrt{b^2-1} - |b|)^n}{\sqrt{b^2-1}}$$


```

```

b := 1.7 : n := 0 : evalf(f)/evalf(g);
2.285172403
2.285172404
b := 1.7 : n := 3 : evalf(f)/evalf(g);
-.07861038399
-.07861038437
b := -1.7 : n := 0 : evalf(f)/evalf(g);
-2.285172403
-2.285172404
b := -1.7 : n := 3 : evalf(f)/evalf(g);
-.07861038399
-.07861038437

```

(H.4.7)

(b) Derive the following integral:

$$\int_0^\pi dx \cos(nx) \frac{1}{(b+\cos x)^2} = (\text{sign } b)^n \pi (|b| + n\sqrt{b^2-1}) (\sqrt{b^2-1} - |b|)^n \frac{1}{(b^2-1)^{3/2}} \quad b > 1 \text{ or } b < -1$$

(H.4.8)

That is, compute the Fourier Cosine Series Transform of the function $1/(b+\cos x)^2$.

Start with (H.4.4) for $b > 1$

$$I(b) = \int_0^\pi dx \cos(nx) \frac{1}{b+\cos x} = b \frac{\pi}{\sqrt{b^2-1}} (\sqrt{b^2-1} - b)^n. \quad (H.4.4)$$

Apply $\partial_b = d/db$ to get

$$\partial_b I(b) = - \int_0^\pi dx \cos(nx)(b+\cos x)^{-2} = \partial_b \left[\frac{\pi}{\sqrt{b^2-1}} (\sqrt{b^2-1} - b)^n \right]. \quad (H.4.9)$$

Maple does the derivative,

```

f := (Pi/sqrt(b^2-1))*(sqrt(b^2-1) - b)^n;
f :=  $\frac{\pi(\sqrt{b^2-1}-b)^n}{\sqrt{b^2-1}}$ 
-diff(f,b):simplify(%);

$$\frac{(b+n\sqrt{b^2-1})(\sqrt{b^2-1}-b)^n \pi}{(b^2-1)^{\binom{n}{2}}} \quad (H.4.10)$$


```

Thus,

$$\int_0^\pi dx \cos(nx) \frac{1}{(b+\cos x)^2} = \pi (b + n\sqrt{b^2-1}) (\sqrt{b^2-1} - b)^n \frac{1}{(b^2-1)^{3/2}} \quad b > 1, |b| = b \quad . \quad (H.4.11)$$

For $b < -1$, the correct analytic continuation is to take $\sqrt{b^2-1} \rightarrow -\sqrt{b^2-1}$ (as verified below) so in this case one finds,

$$\begin{aligned}
 \int_0^\pi dx \cos(nx) \frac{1}{(b+\cos)^2} &= \pi(b - n\sqrt{b^2-1})(-\sqrt{b^2-1} - b)^n \left[-\frac{1}{(b^2-1)^{3/2}} \right] \\
 &= \pi(-b + n\sqrt{b^2-1})(-\sqrt{b^2-1} - b)^n \frac{1}{(b^2-1)^{3/2}} \\
 &= (-1)^n \pi(-b + n\sqrt{b^2-1})(\sqrt{b^2-1} + b)^n \frac{1}{(b^2-1)^{3/2}} \quad b < -1, -b = |b| .
 \end{aligned} \tag{H.4.12}$$

Combining these results one gets,

$$\int_0^\pi dx \cos(nx) \frac{1}{(b+\cos)^2} = (\text{sign } b)^n \pi(|b| + n\sqrt{b^2-1})(\sqrt{b^2-1} - |b|)^n (b^2-1)^{-3/2} \tag{H.4.13}$$

and so (H.4.8) has been derived.

Maple numerical integration verification for several cases:

```

f := Int(cos(n*x)*(b+cos(x))^(-2), x = 0..Pi);
f := 
$$\int_0^\pi \frac{\cos(nx)}{(b + \cos(x))^2} dx$$

g := (signum(b))^n * Pi * (abs(b) + n*sqrt(b^2-1)) * (sqrt(b^2-1) - abs(b))^n * (b^2-1)^(-3/2),
g := 
$$\frac{\text{signum}(b)^n \pi (|b| + n\sqrt{b^2-1}) (\sqrt{b^2-1} - |b|)^n}{(b^2-1)^{3/2}}$$

b := 1.7 : n := 0 : evalf(f);evalf(g);
2.055446077
2.055446079
b := 1.7 : n := 3 : evalf(f);evalf(g);
-.2422496742
-.2422496756
b := -1.7 : n := 0 : evalf(f);evalf(g);
2.055446077
2.055446079
b := -1.7 : n := 3 : evalf(f);evalf(g);
.2422496742
.2422496756

```

(H.4.14)

H.5 Limits of toroidal functions (and combinations) as $n \rightarrow \infty$

Results below assume $\xi \geq 0$ and $\xi_0 \geq 0$.

From NIST p 366 and p 354 we find that, for large v ,

$$14.15.13 \quad P_v^{-\mu}(\cosh \xi) = \frac{1}{v^\mu} \left(\frac{\xi}{\sinh \xi} \right)^{1/2} I_\mu \left((\nu + \frac{1}{2}) \xi \right) \left(1 + O \left(\frac{1}{v} \right) \right),$$

$$14.15.14 \quad Q_v^\mu(\cosh \xi) = \frac{\nu^\mu}{\Gamma(\nu + \mu + 1)} \left(\frac{\xi}{\sinh \xi} \right)^{1/2} K_\mu \left((\nu + \frac{1}{2}) \xi \right) \left(1 + O \left(\frac{1}{v} \right) \right),$$

uniformly for $\xi \in (0, \infty)$.

and

$$14.3.10 \quad Q_v^\mu(x) = e^{-\mu\pi i} \frac{Q_v^\mu(x)}{\Gamma(\nu + \mu + 1)}. \quad (H.5.1)$$

Our Q function of interest is the unbolded one. Therefore,

$$\begin{aligned} P_v(\text{ch}\xi) &\rightarrow \sqrt{\frac{\xi}{\text{sh}\xi}} I_0[(v+1/2)\xi] \\ Q_v(\text{ch}\xi) &\rightarrow \sqrt{\frac{\xi}{\text{sh}\xi}} K_0[(v+1/2)\xi] \quad v \rightarrow \infty \end{aligned} \quad (H.5.2)$$

so for the toroidal functions

$$\begin{aligned} P_{n-1/2}(\text{ch}\xi) &\rightarrow \sqrt{\frac{\xi}{\text{sh}\xi}} I_0(n\xi) \\ Q_{n-1/2}(\text{ch}\xi) &\rightarrow \sqrt{\frac{\xi}{\text{sh}\xi}} K_0(n\xi) \quad n \rightarrow \infty \end{aligned} \quad (H.5.3)$$

Here I_0 and K_0 are modified Bessel functions. From the same source the large z behaviors of I_0 and K_0 are given by,

10.40.1

$$I_\nu(z) \sim \frac{e^z}{(2\pi z)^{\frac{1}{2}}} \sum_{k=0}^{\infty} (-1)^k \frac{a_k(\nu)}{z^k}, \quad |\text{ph } z| \leq \frac{1}{2}\pi - \delta,$$

10.40.2

$$K_\nu(z) \sim \left(\frac{\pi}{2z} \right)^{\frac{1}{2}} e^{-z} \sum_{k=0}^{\infty} \frac{a_k(\nu)}{z^k}, \quad |\text{ph } z| \leq \frac{3}{2}\pi - \delta,$$

with

Define $a_0(\nu) = 1$,

10.17.1

$$a_k(\nu) = \frac{(4\nu^2 - 1^2)(4\nu^2 - 3^2) \cdots (4\nu^2 - (2k-1)^2)}{k! 8^k}, \quad k \geq 1, \quad (H.5.4)$$

Therefore,

$$\begin{aligned} I_0(z) &\rightarrow \sqrt{\frac{1}{2\pi z}} e^z \\ K_0(z) &\rightarrow \sqrt{\frac{\pi}{2z}} e^{-z} \quad z \rightarrow \infty \end{aligned} \tag{H.5.5}$$

so

$$\begin{aligned} I_0(n\xi) &\rightarrow \sqrt{\frac{1}{2\pi n\xi}} e^{n\xi} \\ K_0(n\xi) &\rightarrow \sqrt{\frac{\pi}{2n\xi}} e^{-n\xi} \quad n \rightarrow \infty \end{aligned} \tag{H.5.6}$$

Putting the pieces together, we find that

$$\begin{aligned} P_{n-1/2}(ch\xi_0) &\rightarrow \sqrt{\frac{\xi_0}{sh\xi_0}} \sqrt{\frac{1}{2\pi n\xi_0}} e^{n\xi_0} = \sqrt{\frac{1}{sh\xi_0}} \sqrt{\frac{1}{2\pi n}} e^{n\xi_0} \\ Q_{n-1/2}(ch\xi_0) &\rightarrow \sqrt{\frac{\xi_0}{sh\xi_0}} \sqrt{\frac{\pi}{2n\xi_0}} e^{-n\xi_0} = \sqrt{\frac{1}{sh\xi_0}} \sqrt{\frac{\pi}{2n}} e^{-n\xi_0} \quad n \rightarrow \infty \end{aligned} \tag{H.5.7}$$

so $P_{n-1/2}(ch\xi_0)$ diverges exponentially as $n \rightarrow \infty$, whereas $Q_{n-1/2}(ch\xi_0)$ converges exponentially. We are interested in several special combinations of functions. First,

$$P_{n-1/2}(ch\xi_0)Q_{n-1/2}(ch\xi_0) \rightarrow \frac{1}{sh\xi_0} \frac{1}{2n} \quad n \rightarrow \infty \tag{H.5.8}$$

which is only mildly convergent as $n \rightarrow \infty$. Next,

$$\frac{Q_{n-1/2}(ch\xi_0)}{P_{n-1/2}(ch\xi_0)} \rightarrow \pi e^{-2n\xi_0} \quad n \rightarrow \infty \tag{H.5.9}$$

which is exponentially convergent. Finally,

$$P_{n-1/2}(ch\xi) \frac{Q_{n-1/2}(ch\xi_0)}{P_{n-1/2}(ch\xi_0)} \rightarrow \sqrt{\frac{1}{sh\xi}} \sqrt{\frac{\pi}{2n}} e^{-n(2\xi_0 - \xi)} \quad n \rightarrow \infty \tag{H.5.10}$$

which is exponentially convergent for $\xi < 2\xi_0$.

H.6 Limits of toroidal functions (and combinations) as $z \rightarrow \infty$

(a) The cases $n = 1, 2, 3, \dots$

We start with this $x \rightarrow \infty$ form from NIST,

$$14.8.12 \quad P_\nu^\mu(x) \sim \frac{\Gamma(\nu + \frac{1}{2})}{\pi^{1/2} \Gamma(\nu - \mu + 1)} (2x)^\nu, \quad \Re \nu > -\frac{1}{2}, \mu - \nu \neq 1, 2, 3, \dots, \quad (H.6.1)$$

Setting $\mu = 0$ we find that

$$P_v(x) \rightarrow (1/\sqrt{\pi}) [\Gamma(v+1/2)/\Gamma(v+1)] (2x)^v \quad v > -1/2 \quad x \rightarrow \infty. \quad (H.6.2)$$

Setting $v = n-1/2$ for $n = 1, 2, \dots$ one finds,

$$P_{n-1/2}(x) \rightarrow (1/\sqrt{\pi}) [\Gamma(n)/\Gamma(n+1/2)] (2x)^{n-1/2} \quad n > 0 \quad x \rightarrow \infty. \quad (H.6.3)$$

For the Q functions one has instead, again from NIST,

14.8.15

$$Q_\nu^\mu(x) \sim \frac{\pi^{1/2}}{\Gamma(\nu + \frac{3}{2})(2x)^{\nu+1}}, \quad \nu \neq -\frac{3}{2}, -\frac{5}{2}, -\frac{7}{2}, \dots,$$

and

$$14.3.10 \quad Q_\nu^\mu(x) = e^{-\mu\pi i} \frac{Q_\nu^\mu(x)}{\Gamma(\nu + \mu + 1)}. \quad (H.6.4)$$

Then

$$Q_v(x) \rightarrow \sqrt{\pi} [\Gamma(v+1)/\Gamma(v+3/2)] (2x)^{-v-1}. \quad (H.6.5)$$

Setting $v = n-1/2$ for $n = 0, 1, 2, \dots$

$$Q_{n-1/2}(x) \rightarrow \sqrt{\pi} [\Gamma(n+1/2)/\Gamma(n+1)] (2x)^{-n-1/2} \quad n = 0, 1, 2, \dots \quad x \rightarrow \infty. \quad (H.6.6)$$

A ratio of interest is this,

$$\begin{aligned} \frac{Q_{n-1/2}(x)}{P_{n-1/2}(x)} &\rightarrow \frac{\sqrt{\pi} [\Gamma(n+1/2)/\Gamma(n+1)] (2x)^{-n-1/2}}{(1/\sqrt{\pi}) [\Gamma(n)/\Gamma(n+1/2)] (2x)^{-n-1/2}} = \pi \frac{\Gamma(n+1/2)/\Gamma(n+1)}{\Gamma(n)/\Gamma(n+1/2)} (2x)^{-2n} \\ &= \pi \frac{\Gamma^2(n+1/2)}{\Gamma(n)\Gamma(n+1)} (2x)^{-2n} \quad n = 1, 2, \dots \quad x \rightarrow \infty. \quad (H.6.7) \end{aligned}$$

(b) The case n = 0

For $Q_{-1/2}(x)$ we use (H.6.6) with n = 0 above to get

$$Q_{-1/2}(x) \rightarrow \sqrt{\pi} [\Gamma(1/2)/\Gamma(1)] (2x)^{-1/2} = (\pi/\sqrt{2}) x^{-1/2} . \quad (H.6.8)$$

The $P_{-1/2}(x)$ function requires much more work, it is a special case. We start with NIST,

$$14.5.25 \quad P_{-\frac{1}{2}}(\cosh \xi) = \frac{2}{\pi \cosh(\frac{1}{2}\xi)} K(\tanh(\frac{1}{2}\xi)) \quad (H.6.9)$$

which relates $P_{-1/2}(x)$ to the complete elliptical integral $K(z)$. As $\xi \rightarrow \infty$, $\tanh(\xi/2) \rightarrow 1$ so we need the behavior of $K(z)$ for z near 1. GR7 8.113.3 gives this expansion of $K(k)$ near $k = 1$ (small k'),

$$3. \quad K = \ln \frac{4}{k'} + \left(\frac{1}{2}\right)^2 \left(\ln \frac{4}{k'} - \frac{2}{1 \cdot 2}\right) k'^2 + \left(\frac{1 \cdot 3}{2 \cdot 4}\right)^2 \left(\ln \frac{4}{k'} - \frac{2}{1 \cdot 2} - \frac{2}{3 \cdot 4}\right) k'^4 \\ + \left(\frac{1 \cdot 3 \cdot 5}{2 \cdot 4 \cdot 6}\right)^2 \left(\ln \frac{4}{k'} - \frac{2}{1 \cdot 2} - \frac{2}{3 \cdot 4} - \frac{2}{5 \cdot 6}\right) k'^6 + \dots$$

where (H.6.10)

$$K (\equiv K(k)) \quad k' = \sqrt{1 - k^2};$$

Keeping only the leading term,

$$K(k) \approx \ln(4/k') = \ln(4/\sqrt{1-k^2}) . \quad (H.6.11)$$

Now if $k = \text{th}(\xi/2)$, then $k' = \sqrt{1-k^2} = \text{sech}(\xi/2)$ so,

$$K(\text{th}(\xi/2)) \approx \ln(4 \text{ ch}(\xi/2)) = (1/2) \ln(16 \text{ ch}^2(\xi/2)) = (1/2) \ln[8(\text{ch}\xi + 1)] . \quad (H.6.12)$$

Therefore,

$$P_{-1/2}(\text{ch}\xi) = \frac{2}{\pi} \frac{1}{\text{ch}(\xi/2)} K(\text{th}(\xi/2)) \approx \frac{2}{\pi} \frac{\sqrt{2}}{\sqrt{\text{ch}\xi + 1}} (1/2) \ln[8(\text{ch}\xi + 1)] \\ \approx \frac{\sqrt{2}}{\pi} \frac{1}{\sqrt{\text{ch}\xi}} \ln(8\text{ch}\xi) \quad \text{large } \xi \quad (H.6.13)$$

which is more simply stated as

$$P_{-1/2}(x) \approx \frac{\sqrt{2}}{\pi} x^{-1/2} \ln(8x) . \quad \text{large } x \quad (H.6.14)$$

We then compute our special n = 0 case Q/P ratio from (H.6.8) and (H.6.14) to be

$$\frac{Q_{-1/2}(x)}{P_{-1/2}(x)} \rightarrow \frac{(\pi/\sqrt{2}) x^{-1/2}}{(\sqrt{2}/\pi) x^{-1/2} \ln(8x)} = (\pi^2/2) 1/\ln(8x) \quad x \rightarrow \infty . \quad (H.6.15)$$

One could argue that $\ln(8x) = \ln(8) + \ln(x) \approx \ln(x)$ for large x , but that would require very large x indeed. For example, if $\ln(x) > 20 \ln(8)$, then $x > 8^{20} \sim 10^{17}$. So we keep the 8.

Taking the first derivative of (H.6.14) we find

$$\begin{aligned} P'_{-1/2}(x) &\approx \frac{\sqrt{2}}{\pi} \partial_x [x^{-1/2} \ln(8x)] = \frac{\sqrt{2}}{\pi} [x^{-1/2} (1/x) - (1/2)x^{-3/2} \ln(8x)] \\ &\approx \frac{\sqrt{2}}{\pi} x^{-3/2} [1 - (1/2)\ln(8x)] . \end{aligned} \quad (H.6.16)$$

H.7 Limits of toroidal functions as $z \rightarrow 1$

From NIST as $x \rightarrow 1$ from above we have

14.8.7

$$P_\nu^\mu(x) \sim \frac{1}{\Gamma(1-\mu)} \left(\frac{2}{x-1} \right)^{\mu/2}, \quad \mu \neq 1, 2, 3, \dots , \quad (H.7.1)$$

Thus we conclude that

$$P_\nu(x) \rightarrow 1 \quad x \rightarrow 1 \quad (H.7.2)$$

which is a well known result. The Q function is more complicated. From NIST,

14.8.9

$$\begin{aligned} Q_\nu(x) &= -\frac{\ln(x-1)}{2\Gamma(\nu+1)} + \frac{\frac{1}{2}\ln 2 - \gamma - \psi(\nu+1)}{\Gamma(\nu+1)} \\ &+ O(x-1), \quad \nu \neq -1, -2, -3, \dots , \end{aligned} \quad (H.7.3)$$

and

$$14.3.10 \quad Q_\nu^\mu(x) = e^{-\mu\pi i} \frac{Q_\nu^\mu(x)}{\Gamma(\nu+\mu+1)}.$$

so the standard $Q_\nu(x)$ function has this behavior

$$Q_\nu(x) = -(1/2) \ln(x-1) + [(1/2)\ln 2 - \gamma - \psi(\nu+1)] \quad x \rightarrow 1+ . \quad (H.7.4)$$

The first term shows logarithmic divergence as $x \rightarrow 1$. The second term is a *constant* where γ is "Euler's constant" (0.557) and $\psi(x) \equiv \partial_x \ln \Gamma(x)$ is the psi function (the digamma function).

Setting $v = n-1/2$ we find that

$$\begin{aligned} P_{n-1/2}(x) &\rightarrow 1 & x \rightarrow 1 \\ Q_{n-1/2}(x) &\rightarrow -\frac{1}{2} \ln(x-1) + [\frac{1}{2} \ln 2 - \gamma - \psi(n+1/2)] & x \rightarrow 1 \end{aligned} \quad (H.7.5)$$

To obtain the behavior of $P_{n-1/2}(x)$ near $x = 1$, we use (7.4.1)

$$P(v, \xi) \equiv P_v(\operatorname{ch}\xi) = (\operatorname{ch}\xi)^v F(-v/2, 1/2-v/2; 1; \operatorname{th}^2\xi) \quad (7.4.1)$$

where $x = \operatorname{ch}\xi$. For small ξ we find, using $F(a, b; c; z) \approx 1 + (ab/c)z + O(z^2)$ and $\operatorname{th}\xi \approx \xi$,

$$\begin{aligned} P(v, \xi) &\approx (1 + \xi^2/2)^v [1 + (-v/2)(1/2-v/2)\xi^2] \\ &= (1 + v\xi^2/2)(1 + (v/2)(v/2-1/2)\xi^2) \\ &= 1 + [(1/2)v + (1/4)v(v-1)]\xi^2 = 1 + (1/4)[2v + v(v-1)]\xi^2 = 1 + (1/4)[v^2 + v]\xi^2 \\ &= 1 + (1/4)v(v+1)\xi^2. \end{aligned} \quad (H.7.6)$$

Then

$$\begin{aligned} P_{n-1/2}(\operatorname{ch}\xi) &\approx 1 + (1/4)(n-1/2)(n+1/2)\xi^2 \\ &\approx 1 + (1/4)[n^2 - 1/4]\xi^2 \quad \xi \rightarrow 0. \end{aligned} \quad (H.7.7)$$

Setting $z = \operatorname{ch}\xi \approx 1 + \xi^2/2$ we have $\xi^2 \approx 2(z-1)$ so then

$$P_{n-1/2}(z) \approx 1 + (1/2)[n^2 - 1/4](z-1) \quad // z \text{ just above 1} \quad (H.7.8)$$

Except for $n = 0$ the correction term is positive, therefore

$$P_{n-1/2}(z) \geq 1 \quad \text{as } z \rightarrow 1+ \text{ for } n = 1, 2, \dots, \infty \quad (H.7.9)$$

Application: Consider

$$\begin{aligned} T(z) &\equiv \sqrt{z^2 - 1} \sum_{n=0}^{\infty} \varepsilon_n [Q_{n-1/2}(z) / P_{n-1/2}(z)] \\ &= \sqrt{z^2 - 1} * 2 * [Q_{-1/2}(z) / P_{-1/2}(z)] + \sqrt{z^2 - 1} \sum_{n=1}^{\infty} \varepsilon_n [Q_{n-1/2}(z) / P_{n-1/2}(z)]. \end{aligned}$$

For z very close to 1 we install $P_{-1/2}(z) = 1$ to get

$$T(z) \approx \sqrt{z^2 - 1} * 2 * Q_{-1/2}(z) + \sqrt{z^2 - 1} \sum_{n=1}^{\infty} \varepsilon_n [Q_{n-1/2}(z) / P_{n-1/2}(z)].$$

But for $n > 0$ we know from (H.7.9) that $P_{n-1/2}(z) \geq 1$, so $[1/P_{n-1/2}(z)] \leq 1$. Therefore,

$$T(z) \leq \sqrt{z^2 - 1} * 2 * Q_{-1/2}(z) + \sqrt{z^2 - 1} \sum_{n=1}^{\infty} \varepsilon_n [Q_{n-1/2}(z)]$$

or

$$T(1) \leq \lim_{z \rightarrow 1+} (\sqrt{z^2 - 1} \sum_{n=0}^{\infty} \varepsilon_n [Q_{n-1/2}(z)])$$

or

$$T(1) \leq \sqrt{2} \lim_{z \rightarrow 1+} (\sqrt{z-1} \sum_{n=0}^{\infty} \varepsilon_n [Q_{n-1/2}(z)]). \quad (H.7.10)$$

In (I.2.17) it is shown that

$$\sum_{n=0}^{\infty} \varepsilon_n \sqrt{z-1} Q_{n-1/2}(z) = (\pi/\sqrt{2}) \quad (I.2.17)$$

and therefore we may conclude that

$$T(1) \leq \pi. \quad (H.7.11)$$

In (I.3.14) we find that $T(1) \approx 2.74$ which meets this inequality.

H.8 Alternate series for T(z) near z = 1

From NIST the Wronskian of the P and Q solutions of the Legendre equation is given by.

14.2.10

$$\mathcal{W}\{P_{\nu}^{\mu}(x), Q_{\nu}^{\mu}(x)\} = -e^{\mu\pi i} \frac{\Gamma(\nu + \mu + 1)}{\Gamma(\nu - \mu + 1)(x^2 - 1)}, \quad (H.8.1)$$

so that

$$W\{P_v(z), Q_v(z)\} = 1/(1-z^2) = P_v(z) Q'_v(z) - P'_v(z) Q_v(z). \quad (H.8.2)$$

Now consider the series

$$\begin{aligned} T(z) &\equiv \sqrt{z^2 - 1} \sum_{n=0}^{\infty} \varepsilon_n [Q_{n-1/2}(z) / P_{n-1/2}(z)] \\ &= \sqrt{z^2 - 1} f(z) \quad f(z) \equiv \sum_{n=0}^{\infty} \varepsilon_n [Q_{n-1/2}(z) / P_{n-1/2}(z)]. \end{aligned} \quad (H.8.3)$$

The derivative of $f(z)$ is given by,

$$\begin{aligned} f'(z) &= \sum_{n=0}^{\infty} \varepsilon_n [P_{n-1/2}(z) Q'_{n-1/2}(z) - Q_{n-1/2}(z) P'_{n-1/2}(z)] / [P_{n-1/2}(z)]^2 \\ &= \sum_{n=0}^{\infty} \varepsilon_n [1/(1-z^2)] / [P_{n-1/2}(z)]^2 \quad // (H.8.2) \\ &= - (z^2 - 1)^{-1} \sum_{n=0}^{\infty} \varepsilon_n 1 / [P_{n-1/2}(z)]^2. \end{aligned} \quad (H.8.4)$$

Then

$$\begin{aligned}
 T'(z) &= (\sqrt{z^2 - 1})' f(z) + \sqrt{z^2 - 1} f'(z) \\
 &= (z/\sqrt{z^2 - 1}) f(z) + \sqrt{z^2 - 1} (- (z^2 - 1)^{-1} \sum_{n=0}^{\infty} \varepsilon_n 1/ [P_{n-1/2}(z)]^2) \\
 &= (1/\sqrt{z^2 - 1}) [z f(z) - \sum_{n=0}^{\infty} \varepsilon_n 1/ [P_{n-1/2}(z)]^2]
 \end{aligned} \tag{H.8.5}$$

so that

$$\sqrt{z^2 - 1} T'(z) = z f(z) - \sum_{n=0}^{\infty} \varepsilon_n 1/ [P_{n-1/2}(z)]^2 . \tag{H.8.6}$$

In the limit $z \rightarrow 1$, assuming $T'(z)$ is not infinite, this says

$$0 = f(z) - \sum_{n=0}^{\infty} \varepsilon_n 1/ [P_{n-1/2}(z)]^2$$

or

$$f(z) = \sum_{n=0}^{\infty} \varepsilon_n 1/ [P_{n-1/2}(z)]^2 . \quad // \text{for } z \text{ very close to 1} \tag{H.8.7}$$

Then from (H.8.3),

$$T(z) = \sqrt{z^2 - 1} f(z) = \sqrt{z^2 - 1} \sum_{n=0}^{\infty} \varepsilon_n \frac{1}{[P_{n-1/2}(z)]^2} \quad \text{for } z \text{ very close to 1} . \tag{H.8.8}$$

Appendix I. Capacitance in the thin-wire and horn torus limits

I.1 The torus thin wire limit $R \rightarrow 0$

Below we shall study the following abstract dimensionless function,

$$T(z) \equiv \sqrt{z^2 - 1} \sum_{n=0}^{\infty} \varepsilon_n [Q_{n-1/2}(z) / P_{n-1/2}(z)] \quad \varepsilon_n = 2 - \delta_{n,0} \quad . \quad (I.1.1)$$

Our interest in $T(z)$ stems from its relation to the toroidal capacitance when $z = \rho_c/R$,

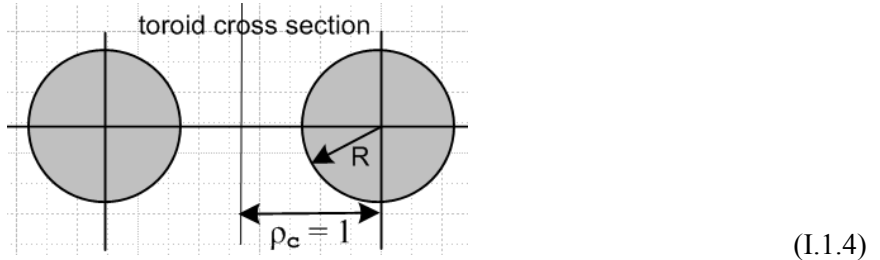
$$\begin{aligned} T(\rho_c/R) &\equiv \sqrt{(\rho_c/R)^2 - 1} \sum_{n=0}^{\infty} \varepsilon_n [Q_{n-1/2}(\rho_c/R) / P_{n-1/2}(\rho_c/R)] \\ &= (1/R)(\pi/2) \{ (2/\pi) \sqrt{\rho_c^2 - R^2} \sum_{n=0}^{\infty} \varepsilon_n [Q_{n-1/2}(\rho_c/R) / P_{n-1/2}(\rho_c/R)] \} \\ &= (\pi/2R) C \quad . \quad // \text{ from (10.4.6)} \end{aligned} \quad (I.1.2)$$

It will be convenient to set $\rho_c = 1$ and write C in the following two ways,

$$C(R) = R (2/\pi) T(1/R)$$

$$C(R) = (2/\pi) \sqrt{1-R^2} \sum_{n=0}^{\infty} \varepsilon_n [Q_{n-1/2}(1/R) / P_{n-1/2}(1/R)] \quad . \quad (I.1.3)$$

Our corresponding picture (10.4.4) with $\rho_c = 1$ is now this,



The "thin-wire limit" is the limit $R \rightarrow 0$. We first separate out the $n = 0$ term in (I.1.3) while also setting $\sqrt{1-R^2} \rightarrow 1$ as $R \rightarrow 0$,

$$C(R) = (2/\pi) Q_{-1/2}(1/R) / P_{-1/2}(1/R) + (4/\pi) \sum_{n=1}^{\infty} [Q_{n-1/2}(1/R) / P_{n-1/2}(1/R)] \quad . \quad (I.1.5)$$

Note that we really set $\sqrt{\rho_c^2 - R^2} \rightarrow \rho_c$ so there is an invisible overall $\rho_c = 1$ factor in the above equation which gives it the dimension of length. If $\rho_c = 10$ cm, one would multiply the above $C(R)$ by 10. As usual for SI units one must add an overall factor of $4\pi\varepsilon$.

Using the small-R Q/P ratios given in (H.6.15) and (H.6.7) one finds that for very small R,

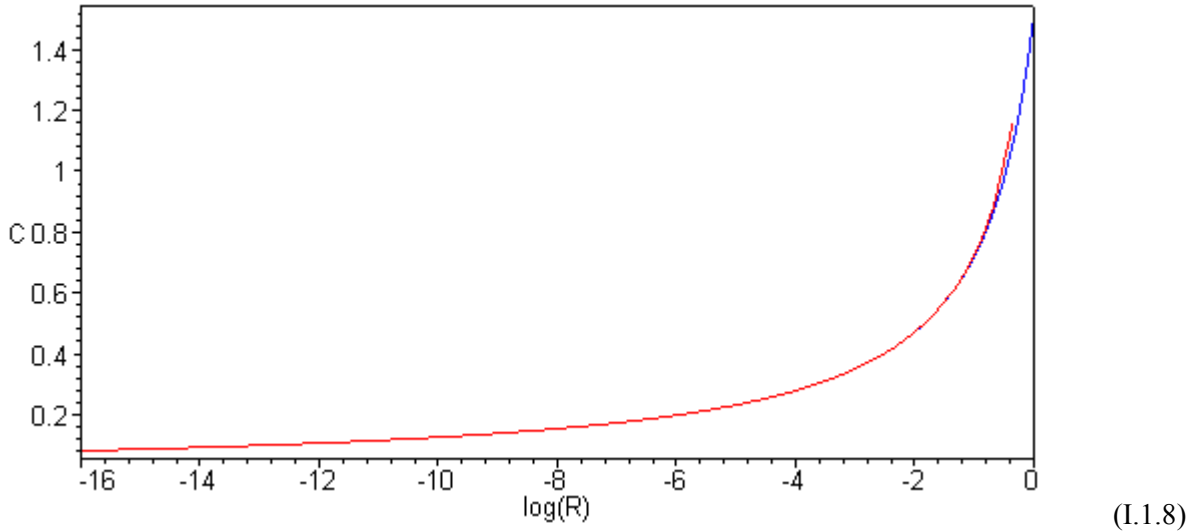
$$\begin{aligned} C(R) &= (2/\pi) \left\{ (\pi^2/2) 1/\ln(8/R) \right\} + (4/\pi) \sum_{n=1}^{\infty} \pi \frac{\Gamma^2(n+1/2)}{\Gamma(n)\Gamma(n+1)} (2/R)^{-2n} . \\ &= \pi / \ln(8/R) + 4 \sum_{n=1}^{\infty} \frac{\Gamma^2(n+1/2)}{\Gamma(n)\Gamma(n+1)} (2/R)^{-2n} . \end{aligned} \quad (I.1.6)$$

As $R \rightarrow 0$, $(2/R)^{-2n} \rightarrow 0$ quickly even for small n, whereas the $n = 0$ log term lingers, so for very small R one can approximate

$$C(R) \approx \pi / \ln(8/R) \equiv C_0(R) . \quad (I.1.7)$$

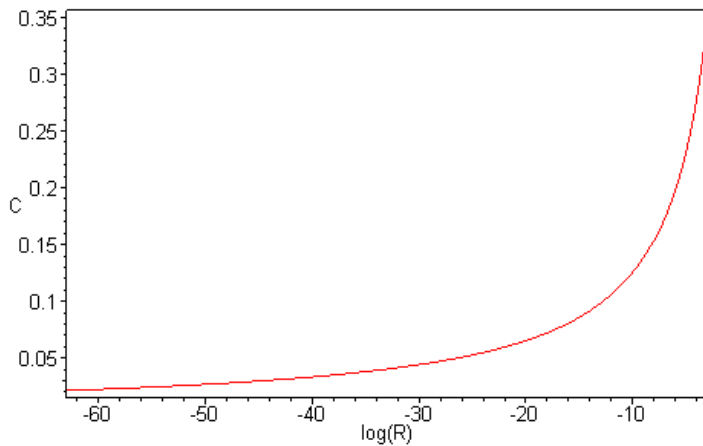
Here is a plot of $C(R)$ in (I.1.3) for R ranging from 10^{-16} to ~ 1 , where we use 20 terms in the sum. The plot also shows $C_0 = \pi / \ln(8/R)$ (blue) for comparison :

```
Digits := 40:
term := (n) -> eps(n)*Q(n-1/2, arccosh(1/R))/P(n-1/2, arccosh(1/R)):
sumterms := sum(term(n), n=0..20):
R := 10^N:
C := (2/Pi)*sqrt(1-R^2)*sumterms:
C0 := Pi/ln(8/R):
plot([C,C0], N=-16..0, axes = boxed, labels = ["log(R)", "C"], color = [red,blue]);
```



The plot shows how gradually capacitance decreases as the wire radius becomes extremely small. It also shows how the $n = 0$ term completely dominates the result for $R < 10^{-3}$. Maple has trouble plotting the full C series for very small R beyond that shown above, but we can plot C_0 to get a result,

```
plot(C0,N=-63..-3,axes = boxed, labels = ["log(R)", "C"]);
```



(I.1.9)

Here as the wire radius drops 60 orders of magnitude, the capacitance drops from 0.3 to .03 .

Thin-wire Capacitance from a simple Arm-waving Analysis

In the thin-wire limit of the torus, where $R \ll \rho_c$, one can make the following simple but somewhat arm-waving model. Very close to the thin wire, the wire looks like an infinitely long straight wire. The solution to that problem is a solution to the 2D Laplace equation for a line charge λ , and one finds outside such a wire that

$$V(r) = 2\lambda \ln(1/r) + k \quad // \text{very close to the wire} \quad (\text{I.1.10})$$

(Purcell p 43, cgs units) where k is a constant. The "2" in this equation is not arbitrary, just as the "1" in the 3D point charge potential $V = 1/r$ is not arbitrary.

Evaluation of (I.1.10) at the wire surface gives

$$V_0 = V(R) = 2\lambda \ln(1/R) + k . \quad (\text{I.1.11})$$

The potential at the torus center is the same as that of a point charge $2\pi\rho_c\lambda$ located distance ρ_c from the center, and that potential is then

$$V_{\text{center}} = (2\pi\rho_c\lambda)/\rho_c = 2\pi\lambda . \quad (\text{I.1.12})$$

Now we imagine that (I.1.10) is also valid at the center of the thin-wire torus, even though that point is not really "close to the wire". One finds, evaluating (I.1.10) at this center point and then using (I.1.12),

$$V(\rho_c) = 2\lambda \ln(1/\rho_c) + k = 2\pi\lambda . \quad (\text{I.1.13})$$

Now setting $\rho_c = 1$ with $R \ll 1$ we find that $k = 2\pi\lambda$. Then from (I.1.11) the potential at the torus surface is

$$\begin{aligned}
V_0 = V(R) &= 2\lambda \ln(1/R) + 2\pi\lambda = 2\lambda [\ln(1/R) + \pi] = 2\lambda [\ln(1/R) + \ln(e^\pi)] \\
&= 2\lambda \ln(e^\pi/R).
\end{aligned} \tag{I.1.14}$$

Now ignoring the potential form (I.1.10) which we applied as far away as the center of the torus, we claim that *very* far from the torus the potential is $V = "q/r" = 2\pi\lambda/r$ and so $V(\infty) = 0$. Somehow we are dealing with multiple scales of largeness in this model. Then the torus is at potential V_0 relative to infinity, and we can then compute the capacitance from $Q = CV_0$ using (I.1.14) to get

$$C = Q/V_0 = (2\pi\lambda)/[2\lambda \ln(e^\pi/R)] = \pi / \ln(e^\pi/R) \approx \pi / \ln(23/R). \tag{I.1.15}$$

We compare this to (I.1.7),

$$C(R) \approx \pi / \ln(8/R). \tag{I.1.7}$$

If $\ln(1/R) \gg \ln(8)$ and $\ln(23)$ then both results say $C(R) = \pi / \ln(1/R)$ and they agree. Again, $\rho_c = 1$.

Thin-wire Capacitance from an Even Simpler Arm-waving Analysis

Here we shall compare a sphere and a torus.

A sphere has area $4\pi R^2$ and surface charge $\sigma = Q/(4\pi R^2)$. The outpointing radial electric field just outside the surface (in cgs units) is $E = 4\pi\sigma = Q/R^2$. Further out $E(r) = Q/r^2$. The potential is then

$$\begin{aligned}
V(r) &= \int_r^\infty E(r')dr' = Q \int_r^\infty dr'/r'^2 = Q/r, \text{ and } V_0 = Q/R \\
\Rightarrow C &= R.
\end{aligned} \tag{I.1.16}$$

A torus has area $4\pi^2\rho_c R$ and surface charge $\sigma = Q/(4\pi^2\rho_c R)$. The outpointing radial electric field just outside the surface is $E = 4\pi\sigma = Q/(\pi\rho_c R)$. Further out, to some distance R_{\max} not too large compared with ρ_c , $E(r) = Q/(\pi\rho_c r)$. The potential is then

$$\begin{aligned}
V(r) &= \int_r^\infty E(r')dr' = (Q/\pi) \int_r^{R_{\max}} dr'/r' = (Q/\pi) \ln(R_{\max}/r), \text{ and } V_0 = (Q/\pi) \ln(R_{\max}/R) \\
\Rightarrow C &= \pi / \ln(R_{\max}/R) \approx \pi / \ln(1/R).
\end{aligned} \tag{I.1.17}$$

We ignore the region beyond $r = R_{\max}$ because E is small there, stored energy is small, and its contribution to capacitance is small. For very small R the result is then $C = \pi / \ln(1/R)$.

In both cases, as $R \rightarrow 0$ the capacitance $C \rightarrow 0$. The approach $C \rightarrow 0$ is much faster for the sphere than for the torus. For the sphere, the charge is all jammed into one point which makes the potential V_0 very large and $C = Q/V_0$ is small. For the torus the charge can spread itself around much better on the thin ring,

resulting in a smaller potential and larger C. In the limit $R = 0$ one can imagine that the charge Q is still present (point charge, line charge), but $V = \infty$ so $C = 0$.

I.2 Warm-up exercises to prepare for the degenerate torus limit

An example with elementary functions

Consider the following relatively simple series on the closed interval $[0,1]$,

$$S(x) = \sum_{k=0}^{\infty} x e^{-2kx}. \quad (\text{I.2.1})$$

The series has the following "partial sum" where k stops at n,

$$S_n(x) = \sum_{k=0}^n x e^{-2kx}. \quad (\text{I.2.2})$$

Notice in passing that

$$S_n(0) = \lim_{x \rightarrow 0} S_n(x) = \sum_{k=0}^n \lim_{x \rightarrow 0} \{ x e^{-2kx} \} = \sum_{k=0}^n \{ 0 \} = 0. \quad (\text{I.2.3})$$

The partial sum (I.2.2) contains a geometric series and can easily be summed. Maple does it :

```

ak := x*exp(-2*k*x);
sn := (n) ->sum(ak,k=0..n):
sn(n):simplify(%);


$$\frac{x(e^{(-2xn)} - e^{(2x)})}{-1 + e^{(2x)}} \quad (\text{I.2.4})$$


```

Rewrite the result multiplying top and bottom by e^{-x} ,

$$S_n(x) = -x \frac{e^{-2xn-x} - e^x}{-e^{-x} + e^x} = -x \frac{e^{-(2n+1)x} - e^x}{2\sinh(x)}. \quad (\text{I.2.5})$$

One can again verify from this form that $S_n(0) = 0$.

With this simple closed form expression for the partial sum, one finds that the full sum $S(x)$ is

$$S(x) = \lim_{n \rightarrow \infty} S_n(x) = x \frac{e^x}{2\sinh(x)}. \quad (\text{I.2.6})$$

Taking the limit $x \rightarrow 0$ gives

$$S(0) = 1/2. \quad (\text{I.2.7})$$

Here then is The Issue: consider these two limits:

$$\begin{aligned} \lim_{n \rightarrow \infty} \{\lim_{x \rightarrow 0} S_n(x)\} &= \lim_{n \rightarrow \infty} \{0\} = 0 \\ \lim_{x \rightarrow 0} \{\lim_{n \rightarrow \infty} S_n(x)\} &= \lim_{x \rightarrow 0} \{S(x)\} = S(0) = 1/2 . \end{aligned} \quad (\text{I.2.8})$$

Interchanging the order of these two limits produces different results. As one learns in calculus courses, the reason for this is that the series $S(x) = \sum_{k=0}^{\infty} x e^{-2kx}$ fails to be *uniformly convergent* on $[0,1]$, having in particular a problem at the $x = 0$ endpoint.

There are several ways to show *a priori* that a series is or is not uniformly convergent on an interval $[0,1]$ where 0 is a potential problem point.

If one knows $S(0)$, as is the case in the above example where $S(0) = 1/2$, then one can check to see if the following is true,

$$\lim_{n \rightarrow \infty} \|S(x) - S_n(x)\| \rightarrow 0 \text{ as } n \rightarrow \infty \quad \text{for all } x \text{ in } [0,1] \quad \Leftrightarrow \quad \text{uniform convergence .} \quad (\text{I.2.9})$$

Here the notation $\|f(x)\|$ means the "max norm" of $f(x)$ which is the maximum value of $|f(x)|$ on the interval in question. In our example, we have from (I.2.6) and (I.2.5),

$$S(x) - S_n(x) = x \frac{e^{-(2n+1)x}}{2\sinh(x)} . \quad (\text{I.2.10})$$

By plotting the function for some value of n , or by studying it a bit, one finds that the max of $|S(x) - S_n(x)|$ occurs at the left endpoint $x = 0$. Thus we have,

$$\|S(x) - S_n(x)\| = S(0) - S_n(0) = 1/2 - 0 = 1/2.$$

and so

$$\lim_{n \rightarrow \infty} \|S(x) - S_n(x)\| = 1/2 . \quad (\text{I.2.11})$$

Since $\lim_{n \rightarrow \infty} \|S(x) - S_n(x)\|$ does not approach 0, we conclude that $S(x)$ is *not* uniformly convergent on the interval $[0,1]$ and therefore we should expect to have the order interchange problem noted in (I.2.8).

Another way to check for uniform continuity is the check this condition (the Cauchy Property),

$$\lim_{n, m \rightarrow \infty} |S_m(x) - S_n(x)| = 0 \quad \text{for all } x \text{ in } [0,1] \quad (\text{I.2.12})$$

This has a formal definition that for any $\epsilon > 0$ one can find N such that, for all x in $[0,1]$, $|S_m(x) - S_n(x)| < \epsilon$ as long as both n and m are $> N$, and N is not allowed to depend on x .

If $S(x)$ is not known, one can use this Cauchy test to check for uniform convergence, but it can take a lot of work since there are three variables at play: x, n, m . In our example one has

$$S_n(x) = -x \frac{e^{-(2n+1)x} - e^x}{2\sinh(x)} \quad (I.2.5)$$

so

$$S_n(x) - S_m(x) = -x \frac{e^{-(2n+1)x}}{2\sinh(x)} + x \frac{e^{-(2m+1)x}}{2\sinh(x)} = \frac{x}{2\sinh(x)} [e^{-(2m+1)x} - e^{-(2n+1)x}]. \quad (I.2.13)$$

In this example, one can take $m = \infty$ and then run the Cauchy test on

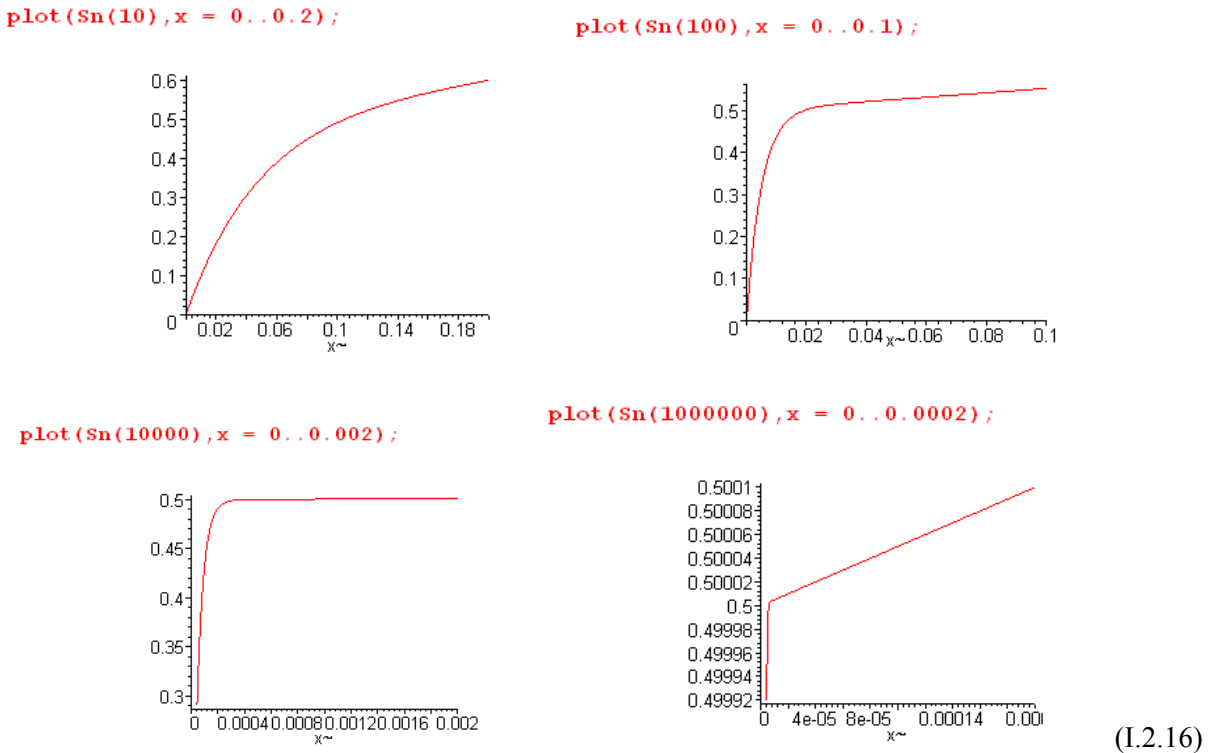
$$S_n(x) - S_\infty(x) = S_n(x) - S(x) = \frac{x}{2\sinh(x)} [e^{-(2n+1)x}]. \quad (I.2.14)$$

As long as $x > 0$ one finds that $|S_m(x) - S_\infty(x)| \rightarrow 0$ as $n \rightarrow \infty$. But if $x = 0$,

$$S_n(x) - S_\infty(x) = \frac{x}{2\sinh(x)} [e^{-(2n+1)x}]|_{x=0} = (1/2) \quad (I.2.15)$$

and thus the Cauchy test fails and the series is not uniformly convergent on $[0,1]$.

Graphically, it is useful to see what happens for this example series near $x = 0$ for some finite number of terms in the sum (I.2.1). Using the code (I.2.4) we plot $S_n(x)$ for various small x ranges for $n = 10, 100, 10000$, and $1,000,000$:



The lower right plot is particularly interesting. If we had no idea that $S(0) = 1/2$ from doing the above analysis, that graph alone would be very convincing evidence that $S(0)$ is extremely close to 0.5. The last three plots are "aiming at 1/2" with increasing targeting precision.

In the degenerate torus limit studied in the next section, the series is more complicated and we don't know how to add up the full series to get the limit, so we are going to use this "aiming method" to determine the limit numerically.

The Q Sum Rule Example

As a second warm-up exercise, recall (10.1.8a),

$$(1/\pi) \sqrt{2/b} \sum_{k=0}^{\infty} \varepsilon_k Q_{k-1/2}(a/b) \cos(kx) = 1/\sqrt{a - b \cos(x)} . \quad // \text{expansion} \quad (10.1.8a)$$

Setting $a = z$, $b = 1$ and $x = 0$ we find that

$$(1/\pi) \sqrt{2} \sum_{k=0}^{\infty} \varepsilon_k Q_{k-1/2}(z) = 1/\sqrt{z-1} \quad \varepsilon_k = 2 - \delta_{k,0}$$

which we rewrite as the following "sum rule" which is valid for all $z \geq 1$:

$$S(z) \equiv \sum_{k=0}^{\infty} \varepsilon_k \sqrt{z-1} Q_{k-1/2}(z) = (\pi/\sqrt{2}) = 2.221441469 . \quad (I.2.17)$$

This series has the following partial sum

$$S_n(z) = \sum_{k=0}^n \varepsilon_k \sqrt{z-1} Q_{k-1/2}(z) . \quad (I.2.18)$$

Near $z = 1$ we know from (H.7.5) that

$$Q_{k-1/2}(z) \approx c_1 \ln(z-1) + c_2$$

where c_1 and c_2 are constants. Letting

$$\delta \equiv z-1$$

then

$$S_n(1+\delta) \approx \sum_{k=0}^n \varepsilon_k \sqrt{\delta} [c_1 \ln(\delta) + c_2] \quad (I.2.19)$$

and then

$$S_n(1) = 0 \quad // \text{since } \sqrt{\delta} \ln(\delta) \rightarrow 0 . \quad (I.2.20)$$

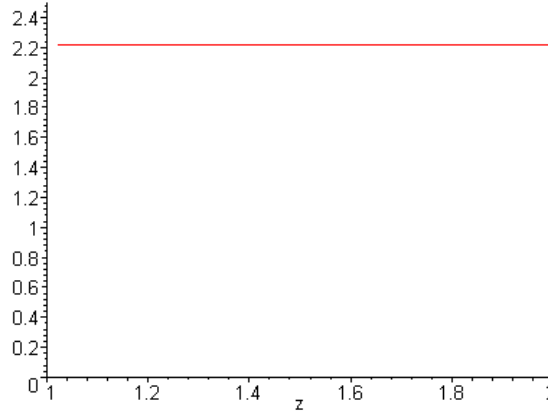
If the series (I.2.17) were uniformly convergent at $z = 1$, one would conclude that

$$S(1) = \lim_{n \rightarrow \infty} S_n(1) = \lim_{n \rightarrow \infty} \{0\} = 0 .$$

But (I.2.17) says $S(1) = 2.22$, so one must conclude that the series is *not* uniformly convergent at $z = 1$.

Suppose one were unaware of the nature of the sum of this series. At first glance, it is certainly not obvious that $S(z)$ is constant in z , but consider a simple plot,

```
Sn := sum(eps(k)*sqrt(z-1)*Q(k-1/2, arccosh(z)), k=0..30):
plot(Sn, z=1..2, view = [1..2, 0..2.5]);
```

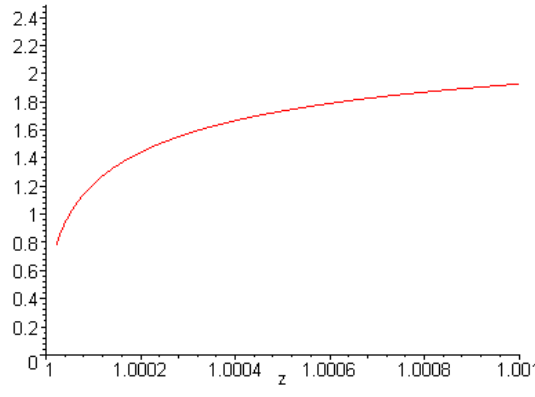


(I.2.21)

So adding only 31 terms, it certainly appears that $S(z)$ is a constant, and that constant is near 2.21.

If we zoom in on the left edge of the above plot, since we are adding a finite number of terms, and since $S_n(1) = 0$, the plot has to dive down to the origin at some point,

```
Sn := sum(eps(k)*sqrt(z-1)*Q(k-1/2, arccosh(z)), k=0..30):
plot(Sn, z=1..1.001, view = [1..1.001, 0..2.5]);
```



(I.2.22)

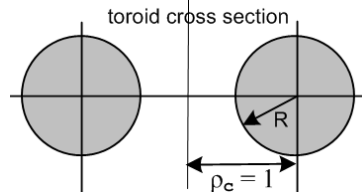
One can prop it back up a bit by increasing the number of terms in the sum, but still being a finite sum it will take the dive at some point just above $z = 1$. If one is looking for the limit $S(1)$ one wants to ignore this diving part of the curve and see where one thinks the curve is "aiming", as in the unzoomed previous plot (I.2.21).

The second example is in fact quite close to the situation below for the degenerate torus limit, but in that case we don't know the limit $S(z=1)$ and we try to find it by the "aiming method".

I.3 Capacitance of a degenerate torus (horn torus)

With $\rho_c = 1$, the capacitance of a torus was given in (I.1.3) as

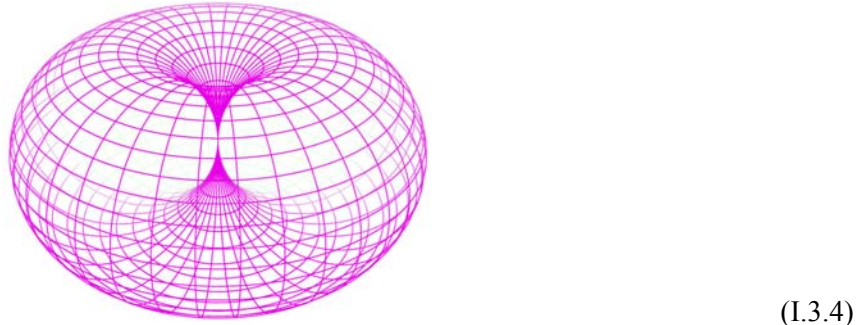
$$C(R) = R (2/\pi) T(1/R) \quad (I.1.3) \quad (I.3.1)$$



where

$$T(z) = \sqrt{z^2 - 1} \sum_{n=0}^{\infty} \varepsilon_n [Q_{n-1/2}(z) / P_{n-1/2}(z)] \quad \varepsilon_n = 2 - \delta_{n,0} \quad . \quad (I.1.1) \quad (I.3.2)$$

When $R = 1$, the hole in the torus just goes away. This situation represents a "degenerate" torus, sometimes called a "horn" torus,



The capacitance of such a torus with $\rho_c = 1$ and $R = 1$ is, from (I.3.1) and (I.3.3),

$$C(1) = (2/\pi) T(1)$$

where

$$T(1) = \lim_{z \rightarrow 1} \left\{ \sqrt{z^2 - 1} \sum_{n=0}^{\infty} \varepsilon_n [Q_{n-1/2}(z) / P_{n-1/2}(z)] \right\} . \quad (I.3.5)$$

The series $T(z)$ shown in (I.3.3) is not uniformly convergent (see Section I.2 above) on the range $z \geq 1$ due to the left endpoint $z = 1$. Thus, to compute $C(R=1) = (2/\pi) T(1)$, we cannot take $\lim_{z \rightarrow 1}$ through the summation symbol. If we *could* do so, we would find that, setting $\delta = z-1$,

$$\begin{aligned} T(1) &= \sum_{n=0}^{\infty} \varepsilon_n \lim_{z \rightarrow 1} \left\{ \sqrt{z^2 - 1} [Q_{n-1/2}(z) / P_{n-1/2}(z)] \right\} \\ &= \sum_{n=0}^{\infty} \varepsilon_n \lim_{\delta \rightarrow 0} \left\{ 2\sqrt{\delta} [(c_1 \ln(\delta) + c_2) / 1] \right\} = 0 . \end{aligned} \quad (I.3.6)$$

Here we use the fact (H.7.2) that $P_{n-1/2}(z) \rightarrow 1$ and (H.7.5) that $Q_{n-1/2}(z) \rightarrow c_1 \ln(\delta) + c_2$. We know the degenerate torus does not have 0 capacitance, and from this fact alone we may conclude that the series is not uniformly convergent on $z \geq 1$.

If we could evaluate the $T(z)$ sum shown in (I.3.3) in terms of known elementary and special functions, we could take the limit of that result to get $T(1)$, as was possible in both our examples (I.2.6) and (I.2.17). But we don't know how to do such an evaluation. For example, we don't know of any integral representations for the function $1/P_{n-1/2}(z)$. If one exists, it could be used with an integral representation of $Q_{n-1/2}(z)$ to possibly allow computation of the infinite sum in (I.3.3), and then maybe the resulting double integration could be reduced to known special functions. We leave this as a problem for the interested reader.

As discussed in the examples of Section I.2, one approach to obtaining a value for $T(1)$ is the "aiming method", and this does give reasonable results.

But first, we can obtain a simple upper bound for $T(1)$. As shown in (H.7.9), $1/P_{n-1/2}(z) \leq 1$ for z just above 1, and therefore, setting $\sqrt{z^2 - 1} \approx \sqrt{2}(z-1)$,

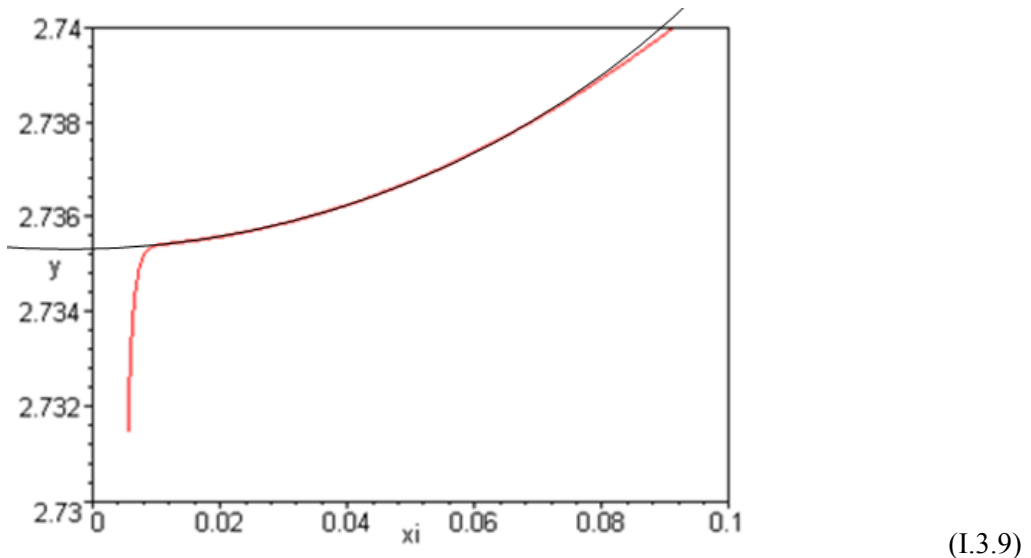
$$T(1) \leq \sqrt{2} \lim_{z \rightarrow 1} \left\{ \sqrt{z-1} \sum_{n=0}^{\infty} \varepsilon_n [Q_{n-1/2}(z)] \right\}. \quad (\text{I.3.7})$$

But (I.2.17) says the sum in $\{\dots\}$ is $\pi/\sqrt{2}$ for any $z \geq 1$ so we conclude that

$$T(1) \leq \pi \approx 3.14. \quad (\text{I.3.8})$$

Now, taking $z = ch\xi$ in (I.3.3), we plot $T(ch\xi)$ as $\xi \rightarrow 0$ with 600 terms in search of a value for $T(1)$:

```
term := (n) -> eps(n)*Q(n-1/2, xi)/P(n-1/2, xi);
T := sinh(xi)*sum(term(n), n=0..600);
plot(T, xi=0..0.1, y=2.73..2.74, numpoints = 20, axes = boxed);
```



With a crude superposed visual fit (black circular segment) the red curve seems to be aiming at this point:

$$2.734 + (3.25/5)(.002) = 2.734 + 0.0013 = 2.7353 \quad . \quad (\text{I.3.10})$$

As shown in the example of (I.2.16), for a finite number of terms in the sum, the plot must dive down to 0 at the very end, and we must ignore that dive in our "aiming method".

It is difficult to get a more accurate value because adding more terms greatly slows down the calculation due to the Q function being near a singularity. In (H.8.8) we derive an alternate series for $T(z)$ which is valid only for z very close to 1,

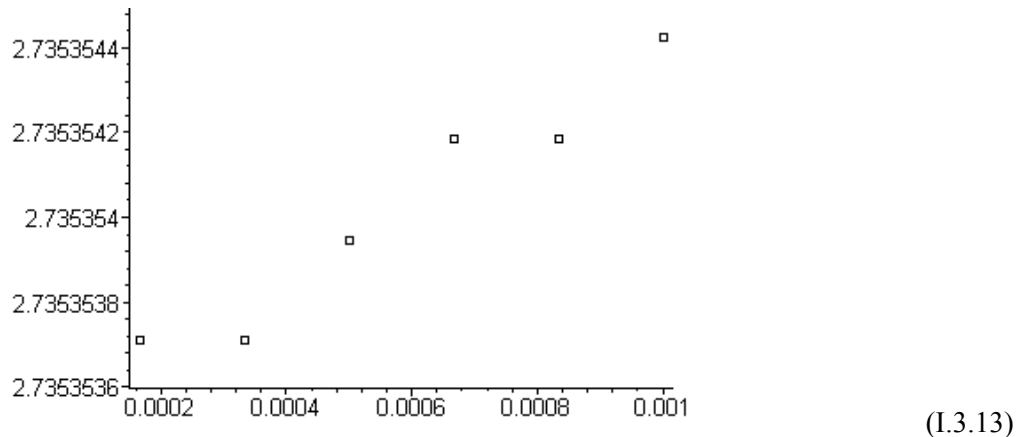
$$T(z) = \sqrt{z^2 - 1} \sum_{n=0}^{\infty} \varepsilon_n \frac{1}{[P_{n-1/2}(z)]^2} \quad z \rightarrow 1 \quad (\text{I.3.11})$$

Using this series, we zoom in on the $T(1)$ limit with the following code,

```
term :=(n) -> eps(n)*1/(P(n-1/2,xi))^2;
T := sinh(xi)*add(term(n),n=0..60000);
M := 6;
for k from 1 to M do
  xi := 0.001*(k/M);
  x[k] := xi;
  t[k] := T;
  print(k,x[k],t[k]);
od:
 1,.000166666666666667, 2.735353613847997
 2,.00033333333333333, 2.735353813969211
 3,.0005000000000000000, 2.735353926506689
 4,.000666666666666667, 2.735354084073598
 5,.00083333333333333, 2.735354286648607
 6,.001, 2.735354534238530
(I.3.12)
```

The code divides the interval $\xi = 0$ to $\xi = .001$ into 6 points and computes $T(\chi\xi)$ for each point using 60,000 terms of the $1/P^2$ series (I.3.11). The following is a plot of the six $(\xi, T(\chi\xi))$ points,

```
P := seq([x[i],t[i]],i=1..M)
pointplot([P],symbol = box);
```



The leftmost point is probably the most correct, giving the following estimated value for $T(1)$,

$$T(1) = 2.7353537 \pm 1 . \quad (\text{I.3.14})$$

where ± 1 refers to the error in the least significant digit.

Therefore, the capacitance of a degenerate torus of radius $R = 1 \text{ cm}$ is

```
evalf(2/Pi)*t[1] :
1.741380194992753
```

$$C(1) = (2/\pi) T(1) = 1.7413802 \pm 1 \text{ cm} . \quad (\text{I.3.15})$$

Appendix J. The Fourier Cosine Series Transform and the Mehler-Fock Transform

Since Morse and Feshbach seem to have an error on this topic (as noted below), and since they have so few errors, we treat this subject very carefully and systematically.

J.1 Regular boundary value problems and associated transforms

In the general theory of the "regular boundary value problem" (also known as the regular Sturm-Liouville problem, see Stakgold Section 4.2), one has second order differential operators L and L_λ of the form

$$\begin{aligned} L &= -\partial_x[p(x)\partial_x] + q(x) \\ L_\lambda &= L - \lambda s(x) \end{aligned} \quad (\text{J.1.1})$$

where p, q, s and $\partial_x p$ are real continuous functions on some finite interval (a, b) and p and s are positive on that interval. The function $s(x)$ is a "weight function" which is 1 in many cases. The boundary conditions at the endpoints a and b must be "unmixed" with real coefficients.

There are three differential equations of interest,

$$\begin{aligned} L_\lambda \phi &= 0 \quad \text{or} \quad L\phi = \lambda s(x)\phi \quad // \text{the eigenvalue problem } (\lambda = \text{eigenvalue}) \\ L_\lambda g(x|\xi;\lambda) &= \delta(x-\xi) \quad // \text{the free-space Green's Function problem for } L_\lambda \\ L_\lambda u &= f . \quad // \text{equation one wants to solve for } u \end{aligned} \quad (\text{J.1.2})$$

The unmixed boundary conditions can be written.

$$\begin{aligned} \alpha_1 h(a) + \alpha_2 h'(a) &= 0 \\ \beta_1 h(b) + \beta_2 h'(b) &= 0 \end{aligned} \quad (\text{J.1.3})$$

where α_i and β_i are real, and where h is any of the functions ϕ , g or u .

The theory shows that the eigenvalues must be real, must have a discrete spectrum, and that the eigenfunctions must be orthogonal with weight $s(x)$. The eigenvalue problem is then written

$$L\phi_n(x) = \lambda_n s(x)\phi_n(x) . \quad (\text{J.1.4})$$

The scale of $\phi_n(x)$ is of course not set by this equation, so one can adjust the scale of each $\phi_n(x)$ so that the $\phi_n(x)$ are orthonormal on (a, b) , where a and b are finite,

$$\int_a^b dx s(x) \bar{\phi}_n(x) \phi_m(x) = \delta_{n,m} \quad (\text{J.1.5})$$

where the overbar indicates complex conjugation.

As Stakgold shows in (4.43), the completeness of the eigenfunctions is given by

$$s(x) \sum_n \varphi_n(x) \bar{\varphi}_n(\xi) = \delta(x-\xi) . \quad // \text{Stakgold (4.43)} \quad (\text{J.1.6})$$

Defining the inner product of two functions as (physics convention)

$$\langle f, g \rangle \equiv \int_a^b dx \bar{f}(x)g(x) \quad (\text{J.1.7})$$

one can write the orthonormality of the eigenfunctions as

$$\langle \sqrt{s} \varphi_n, \sqrt{s} \varphi_m \rangle = \delta_{n,m} . \quad (\text{J.1.8})$$

It turns out that the Green's Function $g(x|\xi; \lambda)$ can be written as an expansion on the eigenfunctions (after all, the eigenfunctions form a complete set),

$$g(x|\xi; \lambda) = \sum_n \varphi_n(x) \bar{\varphi}_n(\xi) / (\lambda_n - \lambda) \quad // \text{Stakgold (4.42)} \quad (\text{J.1.9})$$

and that the solution of $L_\lambda u = f$ is given by,

$$\begin{aligned} u(x) &= \int_a^b dx g(x|\xi; \lambda) f(\xi) d\xi && // \text{Stakgold page 273 top} \\ &= \sum_n \langle f, \varphi_n \rangle / (\lambda_n - \lambda) . && // \text{Stakgold (4.41)} \end{aligned} \quad (\text{J.1.10})$$

An obvious simplification is to define new functions ψ_n

$$\psi_n \equiv \sqrt{s} \varphi_n \quad (\text{J.1.11})$$

and then one has

$$\begin{aligned} \int_a^b dx \bar{\psi}_n(x) \psi_m(x) &= \delta_{n,m} && // \text{orthogonality} \\ \sum_n \psi_n(x) \bar{\psi}_n(\xi) &= \delta(x-\xi) . && // \text{completeness} \end{aligned} \quad (\text{J.1.12})$$

Now expand a function $f(x)$ on this complete set of basis functions,

$$f(x) = \sum_m f_m \psi_m(x) .$$

Apply $\int_a^b dx \bar{\psi}_n(x)$ to "project out" the coefficients f_n .

$$\int_a^b dx \bar{\psi}_n(x) f(x) = \sum_m f_m \int_a^b dx \bar{\psi}_n(x) \psi_m(x) = \sum_m f_m \delta_{n,m} = f_n .$$

Thus our transform may be summarized as

$$\begin{aligned} f(x) &= \sum_n f_n \psi_n(x) && // \text{expansion} \\ f_n &= \int_a^b dx \bar{\psi}_n(x) f(x) . && // \text{projection} \end{aligned} \quad (J.1.13)$$

Stakgold goes on to discuss the *singular* boundary value problem where endpoints a and/or b might be infinite, or where $p(x)$ might vanish in (a,b) , or where some other condition of the regular problem is violated. Our main concern however are is this set of results for the regular problem, as derived above :

$$\begin{aligned} f(x) &= \sum_n f_n \psi_n(x) && // \text{expansion} \\ f_n &= \int_a^b dx \bar{\psi}_n(x) f(x) && // \text{projection} \\ \int_a^b dx \bar{\psi}_n(x) \psi_m(x) &= \delta_{n,m} && // \text{orthogonality} \\ \sum_n \psi_n(x) \bar{\psi}_n(\xi) &= \delta(x-\xi) . && // \text{completeness} \end{aligned} \quad (J.1.14)$$

In the singular case the spectrum of the eigenvalues is usually continuous but can include a discrete part. In the Mehler-Fock transform, studied below in Section J.5, the spectrum is all continuous and the eigenvalues are labeled by the continuous variable τ in the range $(0,\infty)$.

J.2 The Fourier Cosine Series Transform

This should not be confused with the Fourier Cosine Integral Transform which has interval $(0,\infty)$.

For the Fourier Cosine Series Transform we apply the above theory where

variable $x = \theta$

interval $= (a,b) = (0,\pi)$

boundary conditions: $h'(0) = 0$ and $h'(\pi) = 0$

weight function $s(\theta) = 1$

differential operator $L = -\partial_\theta^2$ so $p(\theta) = 1$ and $q(\theta) = 0$

eigenvalue spectrum: $\lambda_n = n^2$ where $n = 0, 1, 2, \dots$

orthonormal eigenfunctions $= \psi_n(\theta) = \sqrt{\varepsilon_n/\pi} \cos(n\theta)$ where $\varepsilon_n = 2 - \delta_{n,0}$. (J.2.1)

Notice the in the last line above the appearance of factor ε_n which equals 1 when $n = 0$, but equals 2 otherwise. This factor appears in the eigenfunctions because it is necessary to make them be orthonormal. The $n = 0$ case is different from all the other cases due to this fact,

```
f := (n,m) ->int(cos(n*theta)*cos(m*theta),theta = 0..Pi);
f = (n,m) → ∫₀^π cos(nθ) cos(mθ) dθ
f(n,n);
1 cos(π n) sin(π n) + π n
2 n
```

For $n = 1, 2, \dots$ the integral is clearly $\pi/2$, but for $n = 0$ the integrand is just 1 so the integral is π . For example,

```
f(0,0);
f(5,5);
1 π
2
```

One then writes

$$\int_0^\pi d\theta \cos(n\theta)\cos(m\theta) = (\pi/\varepsilon_n)\delta_{n,m} \quad (J.2.2)$$

and then the eigenfunctions $\psi_n(\theta) = \sqrt{\varepsilon_n/\pi} \cos(n\theta)$ are orthonormal (and they are real),

$$\int_0^\pi d\theta \psi_n(\theta)\psi_m(\theta) = \delta_{n,m} . \quad (J.2.3)$$

Expanding a real function $f(\theta)$ on the $\psi_n(\theta)$ we get from (J.1.13),

$$\begin{aligned} f(\theta) &= \sum_n f_n \psi_n(\theta) && // \text{expansion} \\ f_n &= \int_a^b dx \psi_n(\theta) f(\theta) && // \text{projection} \end{aligned} \quad (J.2.4)$$

or

$$\begin{aligned} f(\theta) &= \sqrt{\varepsilon_n/\pi} \sum_n f_n \cos(n\theta) \\ f_n &= \sqrt{\varepsilon_n/\pi} \int_0^\pi dx \cos(n\theta) f(\theta) . \end{aligned} \quad (J.2.5)$$

Defining a_n by

$$\sqrt{\varepsilon_n/\pi} f_n = (1/2) \varepsilon_n a_n \quad a_n = 2/\sqrt{\pi \varepsilon_n} f_n \quad f_n = (1/2) \sqrt{\pi \varepsilon_n} a_n \quad (J.2.6)$$

the equations (J.2.5) are written in a more traditional Fourier Series manner,

$$f(\theta) = (1/2) \sum_n \varepsilon_n a_n \cos(n\theta) = a_0/2 + \sum_{n=1}^{\infty} a_n \cos(n\theta)$$

$$a_n = (2/\pi) \int_0^\pi d\theta \cos(n\theta) f(\theta). \quad (J.2.7)$$

The simple factor $\varepsilon_n = 2 - \delta_{n,0}$ is usually called "the Neumann factor" (see etymology below).

After the above very long-winded introduction, we finally arrive at a full statement of the Fourier Cosine Series Transform,

$$f(\theta) = a_0/2 + \sum_{n=1}^{\infty} a_n \cos(n\theta) = (1/2) \sum_{n=0}^{\infty} \varepsilon_n a_n \cos(n\theta) \quad // \text{expansion}$$

$$a_n = (2/\pi) \int_0^\pi d\theta f(\theta) \cos(n\theta) \quad // \text{projection}$$

$$\int_0^\pi d\theta \cos(n\theta) \cos(n'\theta) = (\pi/\varepsilon_n) \delta_{nn}. \quad // \text{orthogonality}$$

$$\sum_{n=0}^{\infty} (\varepsilon_n/\pi) \cos(n\theta) \cos(n\theta') = \delta(\theta-\theta'). \quad // \text{completeness} \quad (J.2.8)$$

As a verification (not a derivation) of these results, consider

$$f(\theta) = (1/2) \sum_{n=0}^{\infty} \varepsilon_n a_n \cos(n\theta)$$

$$= (1/2) \sum_{n=0}^{\infty} \varepsilon_n \left[(2/\pi) \int_0^\pi d\theta' f(\theta') \cos(n\theta') \right] \cos(n\theta)$$

$$= \int_0^\pi d\theta' f(\theta') \left[\sum_{n=0}^{\infty} (\varepsilon_n/\pi) \cos(n\theta') \cos(n\theta) \right] \quad // \text{now use completeness}$$

$$= \int_0^\pi d\theta' f(\theta') \delta(\theta-\theta') = f(\theta). \quad (J.2.9)$$

where we assume uniform convergence, see Section I.2 Going the other direction

$$a_n = (2/\pi) \int_0^\pi d\theta f(\theta) \cos(n\theta)$$

$$= (2/\pi) \int_0^\pi d\theta \left[(1/2) \sum_{m=0}^{\infty} \varepsilon_m a_m \cos(m\theta) \right] \cos(n\theta)$$

$$= \sum_{m=0}^{\infty} (\varepsilon_m/\pi) a_m \left[\int_0^\pi d\theta \cos(m\theta) \cos(n\theta) \right] \quad // \text{now use orthogonality}$$

$$= \sum_{m=0}^{\infty} (\varepsilon_m/\pi) a_m (\pi/\varepsilon_m) \delta_{nm} = a_n. \quad (J.2.10)$$

J.3 Application to $f(\theta) = (a - b \cos \theta)^{1/2}$

Consider the function

$$f(\theta) = 1/\sqrt{a - b \cos \theta} . \quad (\text{J.3.1})$$

The projection coefficients a_n are then given from (J.2.8),

$$\begin{aligned} a_n &= (2/\pi) \int_0^\pi d\theta f(\theta) \cos(n\theta) \\ &= (2/\pi) \int_0^\pi d\theta \cos(n\theta) / \sqrt{a - b \cos \theta} . \end{aligned} \quad (\text{J.3.2})$$

This seemingly simple integral, the Fourier Cosine Series Transform of $1/\sqrt{a - b \cos \theta}$, does not appear in the expected places. Armed with a premonition of the result, we start with the following integral representation of the $Q_v^\mu(z)$ function appearing on GR7 p 961 (also Bateman EH I p 156 (10)),

8.713

$$1. \quad Q_v^\mu(z) = \frac{e^{\mu\pi i} \Gamma\left(\mu + \frac{1}{2}\right)}{\sqrt{2\pi}} (z^2 - 1)^{\frac{\mu}{2}} \left\{ \int_0^\pi \frac{\cos\left(\nu + \frac{1}{2}\right) t dt}{(z - \cos t)^{\mu + \frac{1}{2}}} - \cos\nu\pi \int_0^\infty \frac{e^{-(\nu + \frac{1}{2})t} dt}{(z + \cosh t)^{\mu + \frac{1}{2}}} \right\} \quad [\operatorname{Re} \mu > -\frac{1}{2}, \quad \operatorname{Re}(\nu + \mu) > -1, \quad |\arg(z \pm 1)| < \pi] \quad \text{MO 89}$$

$$(J.3.3)$$

We simultaneously set $\mu = 0$ and $v = n-1/2$. Since $\cos(v\pi) = \cos(n\pi - \pi/2) = \cos(\pi/2 - n\pi) = \sin(n\pi) = 0$, the entire second term conveniently vanishes, leaving us with

$$Q_{n-1/2}(z) = (1/\sqrt{2}) \int_0^\pi dt \cos(nt) / \sqrt{z - \cos t} . \quad (\text{J.3.4})$$

Therefore

$$\begin{aligned} Q_{n-1/2}(a/b) &= (1/\sqrt{2}) \int_0^\pi dt \cos(nt) \frac{1}{\sqrt{(a/b) - \cos t}} * \frac{\sqrt{b}}{\sqrt{b}} \\ &= \sqrt{b/2} \int_0^\pi dt \cos(nt) \frac{1}{\sqrt{a - b \cos t}} \end{aligned}$$

and so

$$\int_0^\pi d\theta \cos(n\theta) / \sqrt{a - b \cos \theta} = \sqrt{2/b} Q_{n-1/2}(a/b) . \quad (\text{J.3.5})$$

The projection coefficients (J.3.2) are therefore

$$a_n = (2/\pi) \sqrt{2/b} Q_{n-1/2}(a/b) . \quad (J.3.6)$$

The corresponding expansion from (J.2.8) is then

$$\begin{aligned} 1/\sqrt{a - b \cos\theta} &= (1/2) \sum_{n=0}^{\infty} \varepsilon_n a_n \cos(n\theta) \\ &= (1/2) (2/\pi) \sqrt{2/b} \sum_{n=0}^{\infty} \varepsilon_n Q_{n-1/2}(a/b) \cos(n\theta) \\ &= (1/\pi) \sqrt{2/b} \sum_{n=0}^{\infty} \varepsilon_n Q_{n-1/2}(a/b) \cos(n\theta) . \end{aligned} \quad (J.3.7)$$

One thus arrives at the transform pair (J.3.7) and (J.3.5),

$$\begin{aligned} 1/\sqrt{a - b \cos(x)} &= (1/\pi) \sqrt{2/b} \sum_{n=0}^{\infty} \varepsilon_n Q_{n-1/2}(a/b) \cos(nx) \quad // \text{expansion} \\ \int_0^\pi dx \cos(nx)/\sqrt{a - b \cos(x)} &= \sqrt{2/b} Q_{n-1/2}(a/b) \quad // \text{projection} \end{aligned} \quad (J.3.8)$$

which we quote as (10.1.8) in Section 10.

If in the expansion one sets $b = 1$, $a = \cosh \mu$ and $x = \eta$ the result is

$$\frac{1}{\sqrt{\cosh \mu - \cos \eta}} = \frac{\sqrt{2}}{\pi} \sum_{n=0}^{\infty} \varepsilon_n Q_{n-1/2}(\cosh \mu) \cos(n\eta) . \quad (J.3.9)$$

It is in this expansion that Morse and Feshbach omit the Neumann factor on page 1304

$$\frac{1}{\sqrt{\cosh \mu - \cos \eta}} = \frac{\sqrt{2}}{\pi} \sum_{n=0}^{\infty} Q_{n-1/2}(\cosh \mu) \cos(n\eta) \quad (10.3.79) \quad // \text{wrong}$$

and this then leads to the omission of the same ε_n factor in the potential for the torus which we quote below (10.1.11).

Morse and Feshbach define their "toroidal harmonics" $Q^{m}_{n-1/2}(ch\mu)$ on page 1329. This seems to be a multiple of their general $Q^{-m}_{n-1/2}(z)$ on page 1327. In any event, when $m = 0$ their functions $Q_{n-1/2}(z)$ seem to be the same as Bateman so there is nothing unusual going on for $n = 0$. So we can rule out something in the definition of $Q_{n-1/2}$ as explaining the above ε_n problem.

A simple application of the expansion (J.3.8) is a representation of the potential $1/R$ of a unit point charge in cylindrical coordinates ρ, z, ϕ . It is easy to show that

$$1/R \equiv 1/|\mathbf{r}-\mathbf{r}'| = 1/\sqrt{\rho^2 + \rho'^2 - 2\rho\rho' \cos(\phi-\phi') + (z-z')^2} . \quad (J.3.10)$$

Now define

$$\begin{aligned}
a &= \rho^2 + \rho'^2 + (z-z')^2 & a/b &= (\rho^2 + \rho'^2 + (z-z')^2)/(2\rho\rho') \\
b &= 2\rho\rho' & \sqrt{2/b} &= 1/\sqrt{\rho\rho'} \\
x &= \varphi-\varphi'
\end{aligned} \tag{J.3.11}$$

and use (J.3.8) so that

$$\begin{aligned}
\frac{1}{R} &= \frac{1}{\sqrt{a - b \cos(x)}} = \frac{1}{\pi} \sqrt{\frac{2}{b}} \sum_{n=0}^{\infty} \epsilon_n Q_{n-1/2}\left(\frac{a}{b}\right) \cos(nx) \\
&= \frac{1}{\pi} \sqrt{\frac{1}{\rho\rho'}} \sum_{n=0}^{\infty} \epsilon_n Q_{n-1/2}\left(\frac{\rho^2 + \rho'^2 + (z-z')^2}{2\rho\rho'}\right) \cos[n(\varphi-\varphi')] .
\end{aligned} \tag{J.3.12}$$

This result appears in Snow (1952) p. 229, where his ϵ_m is half our Neumann factor,

$$(6) \quad \frac{1}{R} = \frac{2}{\pi \sqrt{\rho\rho_1}} \sum_{m=0}^{\infty} \epsilon_m Q_{m-1/2}\left(1 + \frac{D^2}{2\rho\rho_1}\right) \cos[m(\varphi-\varphi_1)], \quad \begin{cases} \epsilon_0 = \frac{1}{2} \\ \epsilon_m = 1, \text{ if } m \neq 0. \end{cases}$$

$$D^2 = (x-x_1)^2 + (\rho-\rho_1)^2 \tag{J.3.13}$$

Comment on the Typewriter:

(J.3.13) is the way one had to write equations into hand-typed papers prior to the advent of "desktop publishing". One could type Latin letters with a typewriter, but Greek letters had to be handwritten in (perhaps the opposite was true for Greek authors). Now with a nice Word normal.dot file (the secret sauce) the author can quickly type the above with a single keystroke for each glyph, more or less, as demonstrated in (J.3.12). This is progress.

Comment on the Neumann Factor.

Morse and Feshbach (1953) refer to ϵ_n by that name on page 1274,

where ϵ_m is the Neumann factor; $\epsilon_0 = 1$, $\epsilon_n = 2$ ($n = 1, 2, 3, \dots$).

In his Treatise "The Theory of Bessel Functions" (1944), Watson uses the term on page 22,

according to the same law as the other terms, it is convenient to introduce *Neumann's factor** ϵ_n , which is defined to be equal to 2 when n is not zero, and to be equal to 1 when n is zero. The employment of this factor, which

* *Journal für Math.* xv. (1836), p. 12. [*Ges. Math. Werke*, vi. (1891), p. 101.]

† *Neueste Schriften der Naturf. Ges. in Danzig*, v. (1855), p. 2.

‡ Neumann, *Theorie der Bessel'schen Functionen* (Leipzig, 1867), p. 7.

and there we see a reference back to Neumann's 1867 *Theory of the Bessel Functions*, page 9,

und kann also, mit Benutzung der früher eingeführten Constanten:

$$\varepsilon_0 = 1, \quad \varepsilon_1 = \varepsilon_2 = \varepsilon_3 = \varepsilon_4 = \dots = 2,$$

auch so ausgedrückt werden:

$$(1.b) \quad \frac{1}{y-x} = \sum_{n=0}^{\infty} \varepsilon_n J^n(x) O^n(y).$$

(<http://gallica.bnf.fr/ark:/12148/bpt6k99615p>) so presumably this is the source of the usage. Incidentally, the latter equation involves "Neumann's polynomials" $O_n(z)$ and appears in NIST as

10.23.12

$$\frac{1}{t-z} = J_0(z) O_0(t) + 2 \sum_{k=1}^{\infty} J_k(z) O_k(t), \quad |z| < |t|.$$

J.4 The Q^2 and QQ' sums

Derive the following sums:

$$\sum_{n=0}^{\infty} \varepsilon_n [Q_{n-1/2}(z)]^2 = (\pi^2/2) \frac{1}{\sqrt{z^2-1}} \quad (J.4.1)$$

$$\sum_{n=0}^{\infty} \varepsilon_n Q_{n-1/2}(z) Q'_{n-1/2}(z) = -(\pi^2/4) z (z^2-1)^{-3/2}. \quad (J.4.2)$$

As far as we know, these series do not appear in any standard references.

Start with the Q function integral representation (J.3.4),

$$Q_{n-1/2}(z) = (1/\sqrt{2}) \int_0^{\pi} dt \cos(nt)/\sqrt{z - \cos t}. \quad (J.3.4)$$

Then

$$\begin{aligned} \sum_{n=0}^{\infty} \varepsilon_n [Q_{n-1/2}(z)]^2 &= (1/2) \sum_{n=0}^{\infty} \varepsilon_n \int_0^{\pi} dt \cos(nt)/\sqrt{z - \cos t} \int_0^{\pi} dt' \cos(nt')/\sqrt{z - \cos t'} \\ &= (1/2) \int_0^{\pi} dt \int_0^{\pi} dt' \frac{1}{\sqrt{z - \cos t} \sqrt{z - \cos t'}} [\sum_{n=0}^{\infty} \varepsilon_n \cos(nt) \cos(nt')]. \end{aligned} \quad (J.4.3)$$

The sum here is recognized as the Fourier Cosine Series Transform completeness relation which is the last line of (J.2.8),

$$\sum_{n=0}^{\infty} (\varepsilon_n/\pi) \cos(n\theta) \cos(n\theta') = \delta(\theta - \theta'). \quad // \text{completeness} \quad (J.2.8)$$

Therefore

$$\begin{aligned} \sum_{n=0}^{\infty} \varepsilon_n [Q_{n-1/2}(z)]^2 &= (1/2) \int_0^\pi dt \int_0^\pi dt' \frac{1}{\sqrt{z - cost} \sqrt{z - cost'}} [\pi \delta(t-t')] \\ &= (\pi/2) \int_0^\pi dt \frac{1}{z - cost} = -(\pi/2) \int_0^\pi dt \frac{1}{-z + cost}. \end{aligned} \quad (J.4.4)$$

Recall now (H.4.1),

$$\int_0^\pi dx \cos(nx) \frac{1}{b + \cos x} = (\text{sign } b)^{n+1} \frac{\pi}{\sqrt{b^2 - 1}} (\sqrt{b^2 - 1} - |b|)^n \quad b > 1 \text{ or } b < -1. \quad (H.4.1)$$

Set $n = 0$ and $b = -z$ to get

$$\int_0^\pi dx \frac{1}{-z + \cos x} = (-1)^{0+1} \frac{\pi}{\sqrt{z^2 - 1}} = -\frac{\pi}{\sqrt{z^2 - 1}}. \quad (J.4.5)$$

Therefore

$$\sum_{n=0}^{\infty} \varepsilon_n [Q_{n-1/2}(z)]^2 = -(\pi/2) [-\frac{\pi}{\sqrt{z^2 - 1}}] = (\pi^2/2) \frac{1}{\sqrt{z^2 - 1}} \quad (J.4.6)$$

which is the result claimed in (J.4.1).

For numerical verification, we enter the two allegedly equal functions

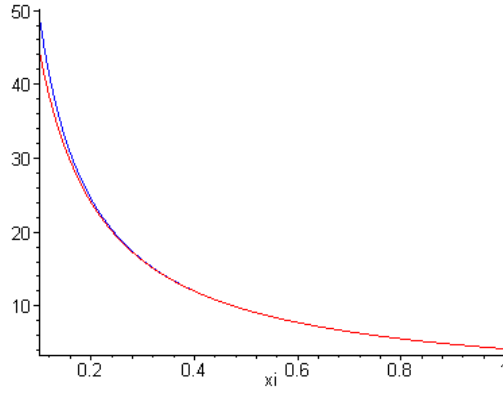
$$\begin{aligned} f &:= (\mathbf{N}) \rightarrow \text{sum}(\text{eps}(n) * (Q(n-1/2, xi))^2, n=0..N); \\ f &:= N \rightarrow \sum_{n=0}^N \text{eps}(n) Q\left(n - \frac{1}{2}, \xi\right)^2 \\ g &:= (\mathbf{Pi}^{2/2}) / \sinh(xi); \\ g &:= \frac{1}{2} \frac{\pi^2}{\sinh(\xi)} \end{aligned}$$

and then code for Q and ε ,

$$\begin{aligned} Q &:= (\nu, xi) \rightarrow \\ &\text{evalf}(\sqrt{\mathbf{Pi}} * (\text{GAMMA}(1+\nu) / \text{GAMMA}(3/2+\nu)) * \exp(-(1+\nu)*xi) * \text{hypergeom}([1/2, 1+\nu], [3/2+\nu], \exp(-2*xi))); \\ Q &:= (\nu, \xi) \rightarrow \text{evalf}\left(\frac{\sqrt{\pi} \Gamma(1+\nu) e^{-(1+\nu)\xi} \text{hypergeom}\left(\left[\frac{1}{2}, 1+\nu\right], \left[\frac{3}{2}+\nu\right], e^{(-2)\xi}\right)}{\Gamma\left(\frac{3}{2}+\nu\right)}\right) \\ \text{eps} &:= \text{proc}(n) \text{ if type}(n, \text{numeric}) \text{ then} \\ &\quad \text{if } n=0 \text{ then RETURN}(1) \text{ else RETURN}(2) \text{ fi;} \\ &\text{else 'eps}(n)'; \text{ fi end:} \end{aligned}$$

Here then is a plot of f in red and g in blue,

```
plot([f(5),g],xi = 0.1..1, color = [red,blue]);
```



(J.4.7)

Here we intentionally use a small number of terms $N = 5$ so the curves can be distinguished.

Now differentiate the sum (J.4.6) as follows,

$$\partial_z \left\{ \sum_{n=0}^{\infty} \varepsilon_n [Q_{n-1/2}(z)]^2 \right\} = \partial_z [(\pi^2/2) (z^2-1)^{-1/2}] = -(\pi^2/2) z (z^2-1)^{-3/2}. \quad (\text{J.4.8})$$

But the left side can be written

$$\partial_z \left\{ \sum_{n=0}^{\infty} \varepsilon_n [Q_{n-1/2}(z)]^2 \right\} = \sum_{n=0}^{\infty} \varepsilon_n \partial_z [Q_{n-1/2}(z)]^2 = 2 \sum_{n=0}^{\infty} \varepsilon_n Q_{n-1/2}(z) Q'_{n-1/2}(z) \quad (\text{J.4.9})$$

Thus one arrives at the following sum :

$$\begin{aligned} \sum_{n=0}^{\infty} \varepsilon_n Q_{n-1/2}(z) Q'_{n-1/2}(z) &= -(\pi^2/4) z (z^2-1)^{-3/2} \\ \text{or} \quad \sum_{n=0}^{\infty} \varepsilon_n Q_{n-1/2}(\operatorname{ch}\xi) Q'_{n-1/2}(\operatorname{ch}\xi) &= -(\pi^2/4) \operatorname{ch}\xi / \operatorname{sh}^3\xi. \end{aligned} \quad (\text{J.4.10})$$

The first line is the claimed sum (J.4.2).

J.5 The Generalized Mehler-Fock Transform

Here the interval for z is $(1, \infty)$ so the associated boundary value problem is singular and the spectrum is continuous. We nevertheless can fit this transform into the context of Section J.1 above. First, we note that $P_v^\mu(z)$ and $Q_v^\mu(z)$ satisfy the Legendre equation

$$\{- (z^2-1)\partial_z^2 - 2z\partial_z + [v(v+1)+\mu^2/(z^2-1)]\} P_v^\mu(z) = 0. \quad (\text{J.5.1})$$

We then define the L operator of (J.1.1) to be

$$L = \{- (z^2-1)\partial_z^2 - 2z\partial_z + \mu^2/(z^2-1)\}. \quad (\text{J.5.2})$$

Then (J.5.1) says,

$$L P_v^\mu(z) = -v(v+1)P_v^\mu(z) \quad (J.5.3)$$

so the $P_v^\mu(z)$ (and $Q_v^\mu(z)$) are eigenfunctions of L with eigenvalues $\lambda_v = -v(v+1)$. The parameter μ is just a bystander parameter in the analysis.

Recall from (J.1.1) that

$$L = -\partial_z[p(z)\partial_z] + q(z) . \quad (J.1.1)$$

For our current Legendre problem we have

$$p(z) = (z^2 - 1) \quad \partial_z p(z) = 2z \quad q = \mu^2/(z^2 - 1) \quad (J.5.4)$$

so that

$$\begin{aligned} [-\partial_z[p(z)\partial_z] + q(z)] f &= [-p(z)\partial_z^2 f - (\partial_z p)\partial_z f + q(z) f] \\ &= [-(z^2 - 1)\partial_z^2 f - 2z\partial_z f + \mu^2/(z^2 - 1)f] \\ &= [-(z^2 - 1)\partial_z^2 f - 2z\partial_z f + \mu^2/(z^2 - 1)f] \\ &= Lf \text{ with } L \text{ as shown in (J.5.2)} . \end{aligned} \quad (J.5.5)$$

So things fit pretty well into the mold of Section J.1, except the problem is singular in that one of the interval endpoints is infinite, and $p(z)$ vanishes at the $z = 1$ endpoint.

For general values of v , neither the functions $P_v^\mu(z)$ nor $Q_v^\mu(z)$ are suitable oscillatory functions on the interval $z = (1, \infty)$. As shown in (H.6.1) the $P_v^\mu(z)$ diverge as z^v , and from (H.7.3) the $Q_v^\mu(z)$ are singular at $z = 1$. However, when one has $v = i\tau - 1/2$, the $P_v^\mu(z)$ become suitable since they are finite at $z = 1$ and since they are reasonable as $z \rightarrow \infty$ since $P_{i\tau-1/2}^\mu(z)$ goes as $z^{-1/2}$. The oscillatory $P_v^\mu(z)$ (at least for $\mu = 0$) are shown in Fig (7.4.5) and Fig (7.4.8) above. Thus, the $P_{i\tau-1/2}^\mu(z)$ are candidates for being the eigenfunctions of a Sturm-Liouville problem as discussed in Section J.1 above, and are thus associated with a transform corresponding to that problem. That transform is the generalized Mehler-Fock Transform.

We continue with our comparison with Section J.1. For $v = i\tau - 1/2$ we find $v(v+1) = -(\tau^2 + 1/4)$, so

$$L P_{i\tau-1/2}^\mu(z) = (\tau^2 + 1/4)P_{i\tau-1/2}^\mu(z) . \quad (J.5.6)$$

The eigenvalues are then

$$\lambda_\tau = \tau^2 + 1/4 \quad (J.5.7)$$

which shows that $\tau = 0$ to ∞ covers the entire spectrum (no need for negative τ). We also see from (J.5.6) and (J.1.2) that the weight function $s(z) = 1$.

Recall the orthonormality condition (J.1.5) ($*$ = complex conjugation) ,

$$\int_a^b dx s(x) \varphi_n(x)^* \varphi_m(x) = \delta_{n,m} . \quad (J.1.5)$$

In the current context, the $P^{\mu}_{i\tau-1/2}(z)$ are not properly normalized to be orthonormal, but they are orthogonal as follows,

$$\int_1^\infty dz [P^{\mu}_{i\tau-1/2}(z)]^* [P^{\mu}_{i\tau'-1/2}(z)] = \delta(\tau-\tau') / h(\tau, \mu) \quad (J.5.8)$$

where

$$h(\tau, \mu) = (\tau/\pi) \operatorname{sh}(\pi\tau) \Gamma(1/2-\mu+i\tau) \Gamma(1/2-\mu-i\tau) \quad (J.5.9)$$

which is a real quantity for real μ and τ . Note that we are just claiming that this is the correct normalization factor, we have not proved that it is correct, and it is not easy to prove.

Since $P_{-v-1}(z) = P_v(z)$ for any v (which follows from (J.5.3)), we know that $P^{\mu}_{i\tau-1/2}(z) = P^{\mu}_{-i\tau-1/2}(z)$. Assuming that μ is real, and since z in $(1, \infty)$ is real, we know that $P^{\mu}_{i\tau-1/2}(z)$ is real, so we can remove the asterisk in (J.5.8) to get

$$\int_1^\infty dz P^{\mu}_{i\tau-1/2}(z) P^{\mu}_{i\tau'-1/2}(z) = \delta(\tau-\tau') / h(\tau, \mu) . \quad // \text{orthogonality} \quad (J.5.10)$$

It is then easy to show that the statement of completeness must be

$$\int_0^\infty d\tau h(\tau, \mu) P^{\mu}_{i\tau-1/2}(z) P^{\mu}_{i\tau-1/2}(z') = \delta(z-z') . \quad // \text{completeness} \quad (J.5.11)$$

We could define some normalized Mehler functions

$$\tilde{P}^{\mu}_{i\tau-1/2}(z) \equiv \sqrt{h(\tau, \mu)} P^{\mu}_{i\tau-1/2}(z) \quad (J.5.12)$$

and then our orthogonality and completeness relations would be

$$\begin{aligned} \int_1^\infty dz \tilde{P}^{\mu}_{i\tau-1/2}(z) \tilde{P}^{\mu}_{i\tau'-1/2}(z) &= \delta(\tau-\tau') \quad // \text{orthogonality} \\ \int_0^\infty d\tau \tilde{P}^{\mu}_{i\tau-1/2}(z) \tilde{P}^{\mu}_{i\tau-1/2}(z') &= \delta(z-z') \quad // \text{completeness} \end{aligned} \quad (J.5.13)$$

in analogy with our two earlier equations for the case $s(x) = 1$ and $\varphi_n(x)$ real,

$$\int_a^b dx \varphi_n(x) \varphi_m(x) = \delta_{n,m} \quad // \text{ orthogonality} \quad (J.1.5)$$

$$\sum_n \varphi_n(x) \varphi_n(\xi) = \delta(x-\xi) . \quad // \text{ completeness} \quad (J.1.6)$$

Making a simple choice of how to allocate the factor $h(\tau, \mu)$, the transform associated with the above Sturm-Liouville problem is the generalized Mehler-Fock transform (2.4.1),

$$g(y) = \int_0^\infty d\tau P_{i\tau-1/2}^\mu(y) f(\tau) \quad // \text{ expansion}$$

$$f(\tau) = h(\tau, \mu) \int_1^\infty dy P_{i\tau-1/2}^\mu(y) g(y) . \quad // \text{ projection} \quad (2.4.1)$$

One can verify the transform in both directions as we did in (J.2.10) and (J.2.11):

$$g(y) = \int_0^\infty d\tau P_{i\tau-1/2}^\mu(y) f(\tau) = \int_0^\infty d\tau P_{i\tau-1/2}^\mu(y) [h(\tau, \mu) \int_1^\infty dy' P_{i\tau'-1/2}^\mu(y') g(y')] \\ = \int_1^\infty dy' g(y') [\int_0^\infty d\tau h(\tau, \mu) P_{i\tau-1/2}^\mu(y) P_{i\tau'-1/2}^\mu(y')] = \int_1^\infty dy' g(y') \delta(y-y') = g(y)$$

$$f(\tau) = h(\tau, \mu) \int_1^\infty dy P_{i\tau-1/2}^\mu(y) g(y) = h(\tau, \mu) \int_1^\infty dy P_{i\tau-1/2}^\mu(y) [\int_0^\infty d\tau' P_{i\tau'-1/2}^\mu(y) f(\tau')] \\ = \int_0^\infty d\tau' f(\tau') h(\tau, \mu) \{ \int_1^\infty dy P_{i\tau-1/2}^\mu(y) P_{i\tau'-1/2}^\mu(y) \} \\ = \int_0^\infty d\tau' f(\tau') h(\tau, \mu) \{ \delta(\tau-\tau') / h(\tau, \mu) \} = \int_0^\infty d\tau' f(\tau') \delta(\tau-\tau') = f(\tau) . \quad (J.5.14)$$

but note that this verification works for any function $h(\tau, \mu)$ and thus does not determine that function.

We then summarize the generalized Mehler Fock transform in this manner:

$$g(y) = \int_0^\infty d\tau P_{i\tau-1/2}^\mu(y) f(\tau) \quad // \text{ expansion}$$

$$f(\tau) = h(\tau, \mu) \int_1^\infty dy P_{i\tau-1/2}^\mu(y) g(y) \quad // \text{ projection}$$

$$\int_1^\infty dz P_{i\tau-1/2}^\mu(z) P_{i\tau'-1/2}^\mu(z) = \delta(\tau-\tau') / h(\tau, \mu) \quad // \text{ orthogonality}$$

$$\int_0^\infty d\tau h(\tau, \mu) P_{i\tau-1/2}^\mu(z) P_{i\tau-1/2}^\mu(z') = \delta(z-z') \quad // \text{ completeness}$$

$$\text{where } h(\tau, \mu) = (\tau/\pi) \operatorname{sh}(\pi\tau) \Gamma(1/2-\mu+i\tau) \Gamma(1/2-\mu-i\tau) . \quad (J.5.15)$$

For $\mu = 0$ one finds $h(\tau, 0) = \tau \tanh(\pi\tau)$ since $\Gamma(1/2+i\tau)\Gamma(1/2-i\tau) = \pi/\cosh(\pi\tau)$. In this case one gets the regular Mehler-Fock transform,

$$\begin{aligned}
 g(y) &= \int_0^\infty d\tau P_{i\tau-1/2}(y) f(\tau) && // \text{expansion} \\
 f(\tau) &= \tau \tanh(\pi\tau) \int_1^\infty dy P_{i\tau-1/2}(y) g(y) && // \text{projection} \\
 \int_1^\infty dz P_{i\tau-1/2}(z) P_{i\tau'-1/2}(z) &= \delta(\tau-\tau') / [\tau \tanh(\pi\tau)] && // \text{orthogonality} \\
 \int_0^\infty d\tau \tau \tanh(\pi\tau) P_{i\tau-1/2}(z) P_{i\tau-1/2}(z') &= \delta(z-z') . && // \text{completeness} \quad (J.5.16)
 \end{aligned}$$

Note that we have not proved the Mehler-Fock transform, we have merely shown how it fits into the framework of the singular boundary value problem with its associated transform. This transform is in fact very difficult to prove as the reader will discover scanning the web. Some methods involve an intermediate use of the Kontorovich-Lebedev transform which involves second-kind modified Bessel functions (aka Macdonald functions) of imaginary index $K_{iy}(x)$. Other derivations such as Gonzalez and Negrin are more direct but still complicated.

One rarely sees our (J.5.15) statements of orthogonality and completeness, but we did find this one orthogonality statement in Szmytkowski and Bielski,

$$\begin{aligned}
 \int_1^\infty dx P_{-1/2+i\kappa}^{\lambda,\mu}(x) P_{-1/2+i\kappa'}^{\lambda,\mu}(x) &= \frac{2^{\mu-\lambda+1}\pi^2[\delta(\kappa-\kappa')+\delta(\kappa+\kappa')]}{\kappa \sinh(2\pi\kappa)} \\
 &\times \Gamma^{-1}((1-\lambda+\mu)/2+i\kappa) \Gamma^{-1}((1-\lambda+\mu)/2-i\kappa) \\
 &\times \Gamma^{-1}((1-\lambda-\mu)/2+i\kappa) \Gamma^{-1}((1-\lambda-\mu)/2-i\kappa) \\
 (\kappa, \kappa' \in \mathbb{R}; \operatorname{Re}\lambda < 1 \text{ or } \lambda \in \mathbb{N}_+; \mu \in \mathbb{C}), \quad (J.5.17)
 \end{aligned}$$

which involves the so-called generalized Legendre functions $P_v^{\lambda,\mu}$ which reduce to associated Legendre functions when $\lambda = \mu$, so that $P_v^{\mu,\mu} = P_v^\mu$. If one sets $\lambda = \mu$ in the above and restricts to κ and κ' both being in the range $(0, \infty)$ so there can be no hit from $\delta(\kappa+\kappa')$, one gets

$$\begin{aligned}
 \int_1^\infty dx P_{-1/2+i\kappa}^\mu(x) P_{-1/2+i\kappa'}^\mu(x) &= 2\pi^2 \delta(\kappa-\kappa') [1/\kappa \operatorname{sh}(2\pi\kappa)] * 1/\text{fourgamma} \\
 \text{fourgamma} &= \Gamma(1/2+i\tau)\Gamma(1/2-i\tau)\Gamma(1/2-\mu+i\kappa)\Gamma(1/2-\mu-i\kappa) = (\pi/\cosh(\pi\tau)) * \Gamma(1/2-\mu+i\kappa)\Gamma(1/2-\mu-i\kappa)
 \end{aligned}$$

so that

$$\int_1^\infty dx P_{-1/2+i\kappa}^\mu(x) P_{-1/2+i\kappa'}^\mu(x) = \delta(\kappa-\kappa')/h(\kappa, \mu) \quad (J.5.18)$$

which is our orthogonality relation of (J.5.15). There is a restriction to $\mu \in N_+$ (positive integers) but we then analytically continue both sides to general (real) μ . For complex μ , we would restore the * of (J.5.8).

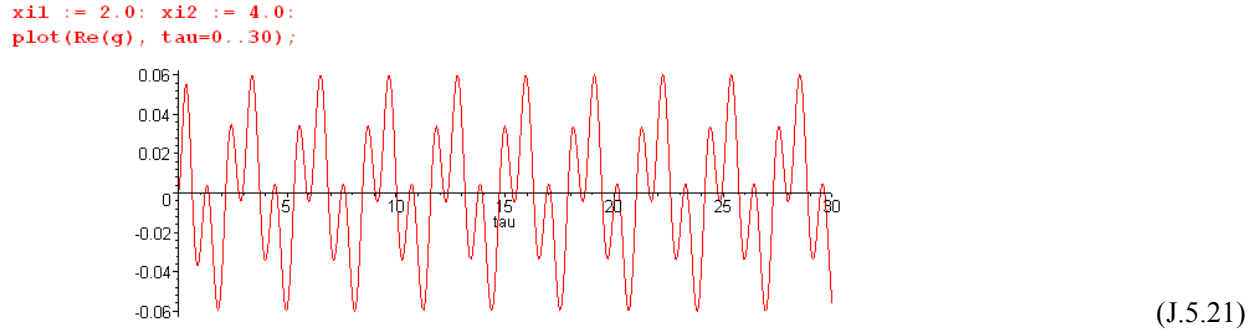
Comment: One might wonder just how these delta function completeness and orthogonality relations work out in the real (engineering) world of Maple. Consider as an example the completeness relation of (J.5.16),

$$\int_0^\infty d\tau \tau \tanh(\pi\tau) P_{i\tau-1/2}(z_1) P_{i\tau-1/2}(z_2) = \delta(z_1 - z_2) . \quad (\text{J.5.19})$$

We enter the P function as in (7.4.4) and then the integrand of the above is

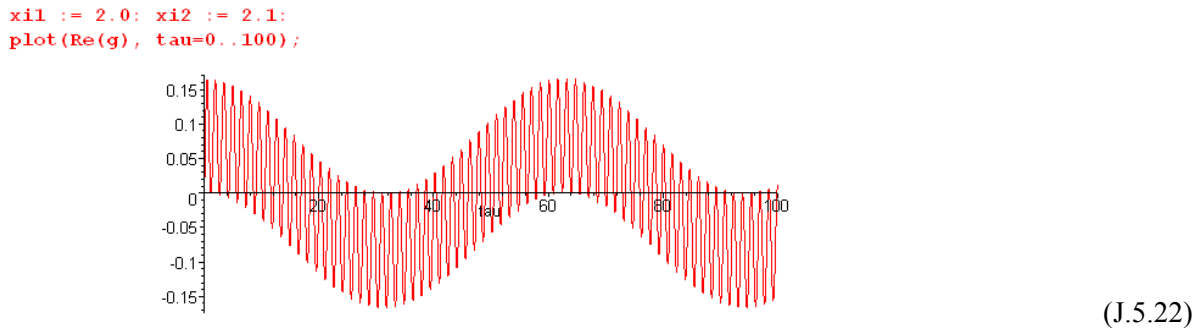
$$\begin{aligned} g &:= \tau \tanh(\pi\tau) P\left(I\tau - \frac{1}{2}, \xi_1\right) P\left(I\tau - \frac{1}{2}, \xi_2\right); \\ g &:= \tau \tanh(\pi\tau) P\left(I\tau - \frac{1}{2}, \xi_1\right) P\left(I\tau - \frac{1}{2}, \xi_2\right) \end{aligned} \quad (\text{J.5.20})$$

The factor τ offsets the $\tau^{-1/2}$ large- τ decay for of the P functions, which results in no decay! Here we plot g for $\xi_1 = 2$ and $\xi_2 = 4$,



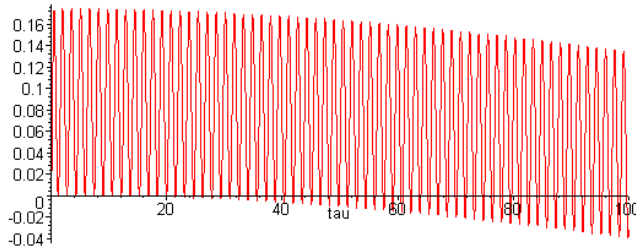
The pattern goes on forever and the area under that infinite curve in the distributional sense is 0, verifying (J.5.19) for these values of $z_1 = \text{ch}\xi_1$ and $z_2 = \text{ch}\xi_2$. One could regulate the integral with a small $e^{-a\tau}$ factor then set $a \rightarrow 0$.

However, if ξ_1 and ξ_2 are close together, the integrand has a different appearance. For example, with $\xi_1 = 2.0$ and $\xi_2 = 2.1$ we get the following, which still has zero area,



As we take $\xi_2 \rightarrow \xi_1$ ($z_2 \rightarrow z_1$) the entire curve becomes the left end of the above curve. For example, here is the above plot with $\xi_1 = 2.00$ and $\xi_2 = 2.01$

```
x1 := 2.0: x2 := 2.01;
plot(Re(g), tau=0..100);
```

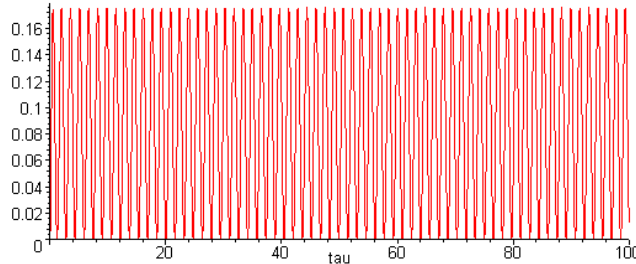


(J.5.23)

For a larger range of τ , the shape of this plot is the same as the previous one and the total area under the curve is still 0. As $z_1 \rightarrow z_2$ the upper endpoint of \int_0^∞ becomes more important in getting zero area.

But, when $z_1 = z_2$ exactly, the entire plot is positive resulting in an infinite integral, and that is the delta function hit,

```
x1 := 2.0: x2 := 2.0;
plot(Re(g), tau=0..100);
```



(J.5.24)

The same idea applies to this simpler completeness relation for the Fourier Cosine Integral Transform,

$$\int_0^\infty dk \cos(kz) \cos(kz') = (\pi/2)\delta(z-z') \quad // \text{completeness}$$

Appendix K: Integration of torus surface charge density

K.1 Warmup Exercises: Circumference and Area of a Torus

Circumference

Consider a torus of label ξ_0 . A cross section of the solid toroidal tube is a round disc. Let ds be a differential *distance* ds along the perimeter of this disc. Then using the scale factor h_u one has from (1.2.3),

$$ds = (h_u du) = a/(ch\xi_0 - cosu) * du . \quad (K.1.1)$$

Integrating around the tube means running u from 0 to 2π as shown in Fig (10.1.2). Thus,

$$\text{circumference} = a \int_0^{2\pi} du (ch\xi_0 - cosu)^{-1} = -a \int_0^{2\pi} du (-ch\xi_0 + cosu)^{-1} . \quad (K.1.2)$$

We invoke integral (H.4.1),

$$\int_0^\pi dx \cos(nx) \frac{1}{b+\cos x} = (\text{sign } b)^{n+1} \frac{\pi}{\sqrt{b^2-1}} (\sqrt{b^2-1} - |b|)^n \quad b > 1 \text{ or } b < -1 \quad (H.4.1)$$

and apply it to the case $n = 0$ and $b = -ch\xi_0$ to find

$$\text{circumference} = -a * 2 * [(-1)^1 \frac{\pi}{sh\xi_0}] = 2\pi a / sh\xi_0 = 2\pi R \quad // (1.2.7)$$

which is the expected result.

Area

Next, let dA be a differential patch of *area* on the torus of label ξ_0 . Then from (1.2.3),

$$\begin{aligned} dA &= (h_u du)(h_\phi d\phi) = a/(ch\xi_0 - cosu) * a sh\xi_0/(ch\xi_0 - cosu) * du d\phi \\ &= a^2 sh\xi_0 (ch\xi_0 - cosu)^{-2} du d\phi . \end{aligned} \quad (K.1.4)$$

The area of the torus is then

$$\begin{aligned} A &= \int_0^{2\pi} d\phi \int_0^{2\pi} du [a^2 sh\xi_0 (ch\xi_0 - cosu)^{-2}] \\ &= 2\pi * a^2 sh\xi_0 * \int_0^{2\pi} du (-ch\xi_0 + cosu)^{-2} . \end{aligned} \quad (K.1.5)$$

We invoke integral (H.4.8),

$$\int_0^\pi dx \cos(nx) \frac{1}{(b+\cos x)^2} = (\text{sign } b)^n \pi (|b| + n\sqrt{b^2-1}) (\sqrt{b^2-1} - |b|)^n \frac{1}{(b^2-1)^{3/2}} \quad b > 1 \text{ or } b < -1 \quad (H.4.8)$$

and apply it to the case $n = 0$ and $b = -ch\xi_0$ to find

$$\int_0^{2\pi} du (-ch\xi_0 + \cos u)^{-2} = 2 * \pi * ch\xi_0 * 1 * 1 / sh^3\xi_0 = 2\pi ch\xi_0 / sh^3\xi_0 \quad (K.1.6)$$

so

$$A = (2\pi a^2 \sin \xi_0) * (2\pi ch\xi_0 / sh^3\xi_0) = 4\pi^2 a^2 (ch\xi_0) / (sh\xi_0)^2 \\ = 4\pi^2 [a/sh\xi_0] [a/th\xi_0] = 4\pi^2 R \rho_c . \quad // (1.2.7)$$

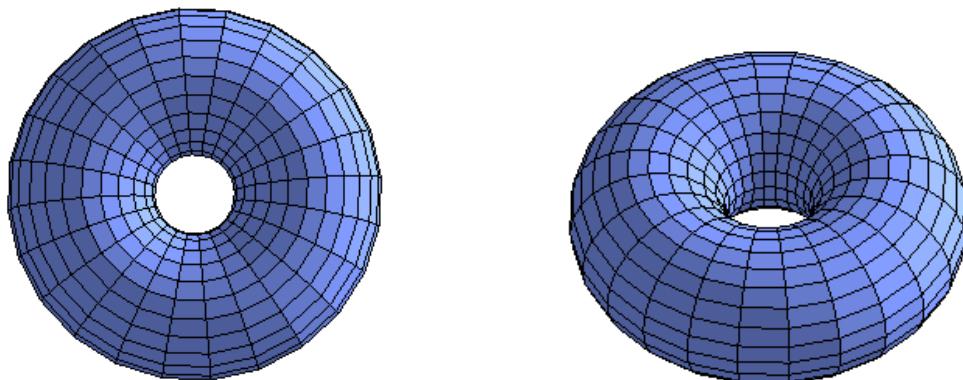
which is the correct area of a torus of tube radius R and centerline radius ρ_c .

Pappus of Alexandria (290-350 A.D. !)

If the torus were a cylinder of length $2\pi\rho_c$ and circumference $2\pi R$, the cylinder area would be $4\pi^2 R \rho_c$. The fact that this is still correct if the cylinder is bent into a torus follows from Pappus's centroid theorem. When the cylinder is bent into a torus, the inside part has less area than half the cylinder, while the outside part has more, but the deficit and excess exactly cancel. Since we happen to have the tools handy, we can compute the inside and outside areas numerically as follows (see Fig 10.1.2),

$$A_{\text{outside}} = 2\pi * a^2 sh\xi_0 * 2 * \int_0^{\pi/2} du (-ch\xi_0 + \cos u)^{-2} = 4\pi a^2 sh\xi_0 \int_0^{\pi/2} du (-ch\xi_0 + \cos u)^{-2} \\ A_{\text{inside}} = 2\pi * a^2 sh\xi_0 * 2 * \int_{\pi/2}^\pi du (-ch\xi_0 + \cos u)^{-2} = 4\pi a^2 sh\xi_0 \int_{\pi/2}^\pi du (-ch\xi_0 + \cos u)^{-2} \quad (K.1.8)$$

Setting $\xi_0 = 1$ and $a = 1$ to have an example (below is the $\xi_0 = 1$ toroid, see also Fig (1.1.3)),



(K.1.9)

```

Aoutside := 4*pi*a^2*sinh(xi0)*Int((-cosh(xi0)+cos(u))^-2,u = 0..pi/2);
Aoutside := 4 pi a2 sinh(xi0) ∫1/2 π0 1 / (-cosh(xi0) + cos(u))2 du

Ainside := 4*pi*a^2*sinh(xi0)*Int((-cosh(xi0)+cos(u))^-2,u = pi/2..pi);
Ainside := 4 pi a2 sinh(xi0) ∫π1/2 π 1 / (-cosh(xi0) + cos(u))2 du

Aformula := 4*pi^2*a^2*cosh(xi0)/sinh(xi0)^2;
Aformula := 4 π2 a2 cosh(xi0) / sinh(xi0)2

a := 1; xi0 := 1;
Aout := evalf(Aoutside);
Aout := 38.88268077

Ain := evalf(Ainside);
Ain := 5.225983892

Aout + Ain;
44.10866466

Atot := evalf(Aformula);
Atot := 44.10866464

Aout/Atot;
.8815202430

Ain/Atot;
.1184797575
(K.1.10)

```

So for this $\xi_0 = 1$ example, the outside area accounts for 88% of the total while the inside is 12%.

K.2 Integration of the toroidal surface charge density

Recall the surface charge density on a torus of label ξ_0 from (10.5.10),

$$\sigma(u; \xi_0) = \frac{V_0}{4\pi R} \left[\frac{1}{2} + \frac{\sqrt{2}}{\pi} (\text{ch}\xi_0 - \cos u)^{3/2} \sum_{n=0}^{\infty} \varepsilon_n P'_{n-1/2}(\text{ch}\xi_0) \frac{Q_{n-1/2}(\text{ch}\xi_0)}{P_{n-1/2}(\text{ch}\xi_0)} \cos(nu) \right]. \quad (\text{K.2.1})$$

Our task is to analytically integrate this quantity over the surface of the torus and then to show that the integral is the expected result. The differential area dA is the same as (K.1.4),

$$dA = (h_u du)(h_\phi d\phi) = a^2 \text{sh}\xi_0 (\text{ch}\xi_0 - \cos u)^{-2} du d\phi. \quad (\text{K.2.2})$$

Then the total charge Q on the torus is given by (there is of course no ϕ dependence in σ)

$$\begin{aligned}
Q &= \int \int \sigma dA = \int_0^{2\pi} d\varphi \int_0^{2\pi} du \sigma(u; \xi_0) [a^2 \operatorname{sh}\xi_0 (\operatorname{ch}\xi_0 - \cos u)^{-2}] \\
&= 2\pi a^2 \operatorname{sh}\xi_0 \int_0^{2\pi} du \sigma(u; \xi_0) (\operatorname{ch}\xi_0 - \cos u)^{-2}. \tag{K.2.3}
\end{aligned}$$

In (K.2.1) we have highlighted in red the two places where $\sigma(u; \xi_0)$ depends on u . We shall therefore need the following two integrals:

$$\begin{aligned}
&\int_0^{2\pi} du (\operatorname{ch}\xi_0 - \cos u)^{-2} \\
&\int_0^{2\pi} du (\operatorname{ch}\xi_0 - \cos u)^{3/2} (\operatorname{ch}\xi_0 - \cos u)^{-2} \cos(nu) = \int_0^{2\pi} du \cos(nu) (\operatorname{ch}\xi_0 - \cos u)^{-1/2}. \tag{K.2.4}
\end{aligned}$$

The first integral has already been evaluated in (K.1.6) to be $2\pi \operatorname{ch}\xi_0 / \operatorname{sh}^3 \xi_0$. The second integral is evaluated in (J.3.4) to be $2 * \sqrt{2} Q_{n-1/2}(\operatorname{ch}\xi_0)$. Thus,

$$\begin{aligned}
&\int_0^{2\pi} du 1 (\operatorname{ch}\xi_0 - \cos u)^{-2} = 2\pi \operatorname{ch}\xi_0 / \operatorname{sh}^3 \xi_0 \quad // (K.1.6) \\
&\int_0^{2\pi} du (\operatorname{ch}\xi_0 - \cos u)^{3/2} (\operatorname{ch}\xi_0 - \cos u)^{-2} \cos(nu) = 2\sqrt{2} Q_{n-1/2}(\operatorname{ch}\xi_0). \quad // (J.3.4) \tag{K.2.5}
\end{aligned}$$

Inserting (K.2.1) for $\sigma(u; \xi_0)$ into (K.2.3) for Q , and then supplying the two integrals (K.2.5), we get

$$\begin{aligned}
Q &= 2\pi a^2 \operatorname{sh}\xi_0 \int_0^{2\pi} du \sigma(u; \xi_0) (\operatorname{ch}\xi_0 - \cos u)^{-2} \\
&= [2\pi a^2 \operatorname{sh}\xi_0 * \frac{V_0}{4\pi R}] * \frac{1}{2} * 2\pi \operatorname{ch}\xi_0 / \operatorname{sh}^3 \xi_0 \\
&\quad + [2\pi a^2 \operatorname{sh}\xi_0 \frac{V_0}{4\pi R}] * \frac{\sqrt{2}}{\pi} \sum_{n=0}^{\infty} \varepsilon_n P'_{n-1/2}(\operatorname{ch}\xi_0) \frac{Q_{n-1/2}(\operatorname{ch}\xi_0)}{P_{n-1/2}(\operatorname{ch}\xi_0)} * 2\sqrt{2} Q_{n-1/2}(\operatorname{ch}\xi_0) \\
&= \frac{V_0}{2R} a^2 \operatorname{sh}\xi_0 \left\{ \pi (\operatorname{ch}\xi_0)(1/\operatorname{sh}^3 \xi_0) + \frac{4}{\pi} \sum_{n=0}^{\infty} \varepsilon_n P'_{n-1/2}(\operatorname{ch}\xi_0) \frac{[Q_{n-1/2}(\operatorname{ch}\xi_0)]^2}{P_{n-1/2}(\operatorname{ch}\xi_0)} \right\}. \tag{K.2.6}
\end{aligned}$$

The reader is hopefully wondering how on earth one can do the sum on n with $P' Q^2 / P$ sitting there.

Consider then this sum,

$$\sum_{n=0}^{\infty} \varepsilon_n P'_{n-1/2}(\operatorname{ch}\xi_0) \frac{[Q_{n-1/2}(\operatorname{ch}\xi_0)]^2}{P_{n-1/2}(\operatorname{ch}\xi_0)}. \tag{K.2.7}$$

Recall the Wronskian of P and Q from (H.8.2),

$$W\{P_v(z), Q_v(z)\} = 1/(1-z^2) = P_v(z) Q'_v(z) - P'_v(z) Q_v(z). \tag{H.8.2}$$

With $z = \text{ch}\xi_0$ and $v = n-1/2$ this says

$$P'_{n-1/2}(\text{ch}\xi_0) Q_{n-1/2}(\text{ch}\xi_0) = (1/\text{sh}^2\xi_0) + P_{n-1/2}(\text{ch}\xi_0) Q'_{n-1/2}(\text{ch}\xi_0) . \quad (\text{K.2.8})$$

Installing this into the sum (K.2.7) gives two sums. The first sum is,

$$(1/\text{sh}\xi_0)^2 \sum_{n=0}^{\infty} \varepsilon_n \frac{Q_{n-1/2}(\text{ch}\xi_0)}{P_{n-1/2}(\text{ch}\xi_0)} \quad // \text{first sum} \quad (\text{K.2.9})$$

while the second sum is

$$\begin{aligned} & \sum_{n=0}^{\infty} \varepsilon_n P_{n-1/2}(\text{ch}\xi_0) \frac{Q_{n-1/2}(\text{ch}\xi_0) Q'_{n-1/2}(\text{ch}\xi_0)}{P_{n-1/2}(\text{ch}\xi_0)} \\ &= \sum_{n=0}^{\infty} \varepsilon_n Q_{n-1/2}(\text{ch}\xi_0) Q'_{n-1/2}(\text{ch}\xi_0) \\ &= -(\pi^2/4) \text{ch}\xi_0 / \text{sh}^3\xi_0 \quad // \text{second sum} \end{aligned} \quad (\text{K.2.10})$$

where we use the result (J.4.8) for the QQ' sum.

We now install these two sums into (K.2.6) to get

$$\begin{aligned} Q &= \frac{V_0}{2R} a^2 \text{sh}\xi_0 \left\{ \pi (\text{ch}\xi_0)(1/\text{sh}^3\xi_0) + \frac{4}{\pi} [\text{second sum} + \text{first sum}] \right\} \\ &= \frac{V_0}{2R} a^2 \text{sh}\xi_0 \left\{ \pi (\text{ch}\xi_0)(1/\text{sh}^3\xi_0) + \frac{4}{\pi} [-(\pi^2/4) \text{ch}\xi_0 / \text{sh}^3\xi_0 + (1/\text{sh}\xi_0)^2 \sum_{n=0}^{\infty} \varepsilon_n \frac{Q_{n-1/2}(\text{ch}\xi_0)}{P_{n-1/2}(\text{ch}\xi_0)}] \right\} \\ &= \frac{V_0}{2R} a^2 \text{sh}\xi_0 \left\{ \frac{4}{\pi} (1/\text{sh}\xi_0)^2 \sum_{n=0}^{\infty} \varepsilon_n \frac{Q_{n-1/2}(\text{ch}\xi_0)}{P_{n-1/2}(\text{ch}\xi_0)} \right\} \quad // \text{two terms cancel} \\ &= \frac{V_0}{2R} \frac{4}{\pi} a (\text{a}/\text{sh}\xi_0) \sum_{n=0}^{\infty} \varepsilon_n \frac{Q_{n-1/2}(\text{ch}\xi_0)}{P_{n-1/2}(\text{ch}\xi_0)} \\ &= V_0 \frac{2a}{\pi} \sum_{n=0}^{\infty} \varepsilon_n \frac{Q_{n-1/2}(\text{ch}\xi_0)}{P_{n-1/2}(\text{ch}\xi_0)} \end{aligned} \quad (\text{K.2.11})$$

The implied capacitance of the torus is then

$$C = \frac{2a}{\pi} \sum_{n=0}^{\infty} \varepsilon_n \frac{Q_{n-1/2}(\text{ch}\xi_0)}{P_{n-1/2}(\text{ch}\xi_0)} \quad (\text{K.2.12})$$

which agrees with the result (10.4.3) which was found completely independently by taking the far-away limit of the potential (10.1.11). We regard this as a reasonable validity check on (K.2.1) for σ .

Appendix L: Some Mehler Integrals

Since the six Mehler integrals stated in (7.1.3) through (7.1.8) do not generally appear in standard references, and since there are sometimes typos where they do appear, we derive all of them here in full detail, hopefully providing the reader with a traceable source for these integrals. For each integral we provide at least one external verification.

- | | | |
|-----|---------|---|
| L.1 | (7.1.1) | $\int_0^\infty d\tau P_{i\tau-1/2}(y)$ |
| L.2 | (7.1.2) | $\int_0^\infty d\tau P_{i\tau-1/2}(y) \cos(a\tau)$ |
| L.3 | (7.1.3) | $\int_0^\infty d\tau P_{i\tau-1/2}(y) \cos(a\tau) / \operatorname{ch}(\pi\tau)$ |
| L.4 | (7.1.4) | $\int_0^\infty d\tau P_{i\tau-1/2}(y) \cos(a\tau) / \operatorname{ch}^2(\pi\tau)$ |
| L.5 | (7.1.5) | $\int_0^\infty d\tau P_{i\tau-1/2}(y) \operatorname{ch}(b\tau) / \operatorname{ch}^2(\pi\tau)$ |
| L.6 | (7.1.6) | $\int_0^\infty d\tau P_{i\tau-1/2}(y) \operatorname{sh}(b\tau) \operatorname{sh}(\pi\tau) / \operatorname{ch}^2(\pi\tau)$ |

L.1 Compute $\int_0^\infty d\tau P_{i\tau-1/2}(y)$

Show that

$$I \equiv \int_0^\infty d\tau P_{i\tau-1/2}(y) = \frac{1}{\sqrt{2}} \frac{1}{\sqrt{y-1}} . \quad y > 1 \quad (\text{L.1.1})$$

Start with this P function integral representation from GR7 8.715 (1) page 962,

$$1. \quad P_\nu^\mu(\cosh \alpha) = \frac{\sqrt{2} \sinh^\mu \alpha}{\sqrt{\pi} \Gamma(\frac{1}{2} - \mu)} \int_0^\alpha \frac{\cosh(\nu + \frac{1}{2}) t dt}{(\cosh \alpha - \cosh t)^{\mu + \frac{1}{2}}} \quad [\alpha > 0, \quad \operatorname{Re} \mu < \frac{1}{2}] \quad \text{MO 87}$$

Set $\mu = 0, \nu = i\tau - 1/2$ to get

$$P_{i\tau-1/2}(\operatorname{ch}\alpha) = (\sqrt{2}/\pi) \int_0^\alpha dx \cos(\tau x) / \sqrt{\operatorname{ch}\alpha - \operatorname{ch}x} \quad y > 1 . \quad (\text{L.1.2})$$

Insert (L.1.2) into (L.1.1) with $y = \operatorname{ch}\alpha$ to get,

$$I = \int_0^\infty d\tau P_{i\tau-1/2}(\operatorname{ch}\alpha) = \int_0^\infty d\tau [(\sqrt{2}/\pi) \int_0^\alpha dx \cos(\tau x) / \sqrt{\operatorname{ch}\alpha - \operatorname{ch}x}]$$

$$= (\sqrt{2}/\pi) \int_0^\alpha dx (1/\sqrt{\cosh \alpha - \cosh x}) \int_0^\infty d\tau \cos(\tau x). \quad (\text{L.1.3})$$

But

$$\begin{aligned} \int_{-\infty}^\infty d\tau e^{i\tau x} &= 2\pi\delta(x) = \int_{-\infty}^\infty d\tau \cos(\tau x) = 2 \int_0^\infty d\tau \cos(\tau x) \\ \Rightarrow \int_0^\infty d\tau \cos(\tau x) &= \pi\delta(x) . \end{aligned} \quad (\text{L.1.4})$$

Using (L.1.4) in (L.1.3),

$$\begin{aligned} I &= (\sqrt{2}/\pi) \int_0^\alpha dx (1/\sqrt{\cosh \alpha - \cosh x}) \pi\delta(x) = (\sqrt{2}/\pi) (\pi) (1/2) 1/\sqrt{\cosh \alpha - \cosh x} \\ &= (1/\sqrt{2}) 1/\sqrt{\cosh \alpha - 1} \quad \alpha > 0 \\ &= (1/\sqrt{2}) 1/\sqrt{y - 1} \quad y > 1 \end{aligned} \quad (\text{L.1.5})$$

which verifies (L.1.1). Note that the integration picks up exactly 1/2 of $\delta(x)$ since the integration starts at $x = 0$. This is a mathematically rigorous fact demonstrable using limits of delta functions sequences.

Verification: The following integral appears in Bateman ET 2 page 330 18.3 (21),

$(21) \quad \int_0^\infty \cos(bx) P_{-\frac{1}{2}+ix}^\mu(\cosh a) dx$ $= 0 \quad 0 < a < b$ $= \frac{(\frac{1}{2}\pi)^{\frac{1}{2}} (\sinh a)^\mu}{\Gamma(\frac{1}{2}-\mu) (\cosh a - \cosh b)^{\mu+\frac{1}{2}}} \quad 0 < b < a$	
--	--

(L.1.6)

Setting $b = 0$, $\mu = 0$ and $\cosh a = y$ the integral states

$$\int_0^\infty d\tau P_{i\tau-1/2}(y) = \sqrt{\pi/2} / [\sqrt{\pi} (y-1)^{1/2}] = (1/\sqrt{2}) (1/\sqrt{y-1}) \quad y > 1 \quad (\text{L.1.7})$$

verifying (L.1.1). Integral (L.1.1) also appears in Oberhettinger and Higgins Table C page 28, the first entry with $a = 1$ and $k = 0$. The above Bateman integral appears as the 2nd integral in that Table.

L.2 Compute $\int_0^\infty d\tau P_{i\tau-1/2}(y) \cos(a\tau)$

Show that [θ is the Heaviside function]

$$I \equiv \int_0^\infty d\tau P_{i\tau-1/2}(y) \cos(a\tau) = \frac{1}{\sqrt{2}} \frac{1}{\sqrt{y-\text{cha}}} \theta(y-\text{cha}) . \quad (\text{L.2.1})$$

This result is the content of Bateman (L.1.6) noted above if we set $\mu = 0$ and $b = a$, and we have (L.1.6) verified in two reference locations. Nevertheless, we compute the integral directly.

Insert the P integral representation (L.1.2) into (L.2.1) to get

$$\begin{aligned} I &= \int_0^\infty d\tau P_{i\tau-1/2}(\text{cha}) \cos(a\tau) = \int_0^\infty d\tau \left[(\sqrt{2}/\pi) \int_0^a dx \cos(\tau x) / \sqrt{\text{cha} - \text{ch}x} \right] \cos(a\tau) \\ &= (\sqrt{2}/\pi) \int_0^a dx (1/\sqrt{\text{cha} - \text{ch}x}) \int_0^\infty d\tau \cos(x\tau) \cos(a\tau) . \end{aligned} \quad (\text{L.2.2})$$

The τ integral is recognized as the completeness relation (or the orthogonality relation) for the Fourier Integral Cosine Transform where $0 \leq z \leq \infty$ and $0 \leq k \leq \infty$:

$$\begin{aligned} f(z) &= \sqrt{2/\pi} \int_0^\infty dk \cos(kz) f^* && // \text{expansion} \\ f^* &= \sqrt{2/\pi} \int_0^\infty dz \cos(kz) f(z) && // \text{projection} \\ \int_0^\infty dz \cos(kz) \cos(k'z) &= (\pi/2)\delta(k-k') && // \text{orthogonality} \\ \int_0^\infty dk \cos(kz) \cos(kz') &= (\pi/2)\delta(z-z') && // \text{completeness} . \end{aligned} \quad (\text{L.2.3})$$

Thus $\int_0^\infty d\tau \cos(x\tau) \cos(a\tau) = (\pi/2)\delta(x-a)$ for $a > 0$ and then from (L.2.2),

$$\begin{aligned} I &= (\sqrt{2}/\pi) \int_0^a dx (1/\sqrt{\text{cha} - \text{ch}x}) (\pi/2) \delta(x-a) = (1/\sqrt{2}) (1/\sqrt{\text{cha} - \text{cha}}) \theta(a - a) \\ &= (1/\sqrt{2}) (1/\sqrt{y - \text{cha}}) \theta(y - \text{cha}) \end{aligned} \quad (\text{L.2.4})$$

which verifies (L.2.1), where θ is the Heaviside function.

Verification:

Oberhettinger and Higgins Table C page 28, second entry.

Bateman (L.1.6) above with $\mu = 0$, $\text{cha} = y$ and $b = a$.

$$\text{L.3 Compute } \int_0^\infty d\tau P_{i\tau-1/2}(y) \cos(i\pi\tau) / \operatorname{ch}(\pi\tau)$$

Show that

$$I \equiv \int_0^\infty d\tau P_{i\tau-1/2}(y) \cos(i\pi\tau) / \operatorname{ch}(\pi\tau) = \frac{1}{\sqrt{2}} \frac{1}{\sqrt{y+\operatorname{cha}}} . \quad (\text{L.3.1})$$

Start with this P function integral representation from GR7 8.713 (3) page 961 (also Bateman HTF 1 3.7 (11), page 156),

$$3. \quad P_\nu^{-\mu}(z) = \sqrt{\frac{2}{\pi}} \frac{\Gamma(\mu + \frac{1}{2})(z^2 - 1)^{\frac{\mu}{2}}}{\Gamma(\nu + \mu + 1)\Gamma(\mu - \nu)} \int_0^\infty \frac{\cosh(\nu + \frac{1}{2})t dt}{(z + \cosh t)^{\mu + \frac{1}{2}}} \\ [\operatorname{Re} z > -1, \quad |\arg(z \pm 1)| < \pi, \quad \operatorname{Re}(\nu + \mu) > -1, \quad \operatorname{Re}(\mu - \nu) > 0] \quad \text{MO 89}$$

$$(11) \quad P_\nu^{-\mu}(z) = (\frac{1}{2}\pi)^{-\frac{\nu}{2}} \frac{\Gamma(\mu + \frac{1}{2})(z^2 - 1)^{\mu/2}}{\Gamma(\nu + \mu + 1)\Gamma(\mu - \nu)} \\ \times \int_0^\infty (z + \cosh t)^{-\mu - \frac{1}{2}} \cosh[(\nu + \frac{1}{2})t] dt \\ \operatorname{Re}(\mu - \nu) > 0, \quad \operatorname{Re}(\mu + \nu + 1) > 0$$

Set $\mu = 0$ to get

$$P_v(y) = \sqrt{2/\pi} \sqrt{\pi} [\Gamma(v+1)\Gamma(-v)]^{-1} \int_0^\infty dt (y + \operatorname{cht})^{-1/2} \operatorname{ch}[(v+1/2)t], \\ \operatorname{Re}(-v) > 0 \text{ and } \operatorname{Re}(v+1) > 0 . \quad (\text{L.3.2})$$

We note from Maple that

$$\begin{aligned} & 1/(\operatorname{GAMMA}(nu+1)*\operatorname{GAMMA}(-nu)) ; \\ & \frac{1}{\Gamma(v+1)\Gamma(-v)} \\ & \operatorname{simplify}(\%) ; \\ & \frac{\sin(\pi(v+1))}{\pi} . \end{aligned} \quad (\text{L.3.3})$$

Setting $v = i\tau - 1/2$ one finds,

$$\begin{aligned} \sin[\pi(v+1)] &= \sin[\pi(i\tau+1/2)] = \sin(\pi/2 + i\pi\tau) = \cos(i\pi\tau) = \operatorname{ch}(\pi\tau) \\ \operatorname{ch}[(v+1/2)t] &= \operatorname{ch}[i\tau t] = \cos(\tau t) . \end{aligned} \quad (\text{L.3.4})$$

Note also that $\operatorname{Re}(-v) = 1/2$ and $\operatorname{Re}(v+1) = 1/2$, so both conditions in (L.3.2) are met. Thus,

$$P_{i\tau-1/2}(y) = \sqrt{2} [\operatorname{ch}(\pi\tau)/\pi] \int_0^\infty dt (y + \operatorname{cht})^{-1/2} \cos(\tau t) . \quad (\text{L.3.5})$$

Now insert (L.3.5) into the integral I of (L.3.1) to get

$$\begin{aligned}
I &\equiv \int_0^\infty d\tau P_{i\tau-1/2}(y) \cos(a\tau) / \operatorname{ch}(\pi\tau) \\
&= \int_0^\infty d\tau [\sqrt{2}/\pi \operatorname{ch}(\pi\tau) \int_0^\infty dt (y + cht)^{-1/2} \cos(\tau t)] \cos(a\tau) / \operatorname{ch}(\pi\tau) \\
&= (\sqrt{2}/\pi) \int_0^\infty d\tau \int_0^\infty dt (y + cht)^{-1/2} \cos(\tau t) \cos(a\tau) \quad // \text{note how } \operatorname{ch}(\pi\tau)'s \text{ canceled} \\
&= (\sqrt{2}/\pi) \int_0^\infty dt (y + cht)^{-1/2} \int_0^\infty d\tau \cos(\tau t) \cos(a\tau) \\
&= (\sqrt{2}/\pi) \int_0^\infty dt (y + cht)^{-1/2} (\pi/2)\delta(t-a) \quad // \text{see (L.2.3)} \\
&= (1/\sqrt{2}) (y + cha)^{-1/2} \tag{L.3.6}
\end{aligned}$$

which then is the claim of (L.3.1).

Verification: Oberhettinger and Higgins Table C page 28, the 4th integral with $k = 0$ and $P_k^k(z) = 1$.

L.4 Compute $\int_0^\infty d\tau P_{i\tau-1/2}(y) \cos(a\tau) / \operatorname{ch}^2(\pi\tau)$

Show that

$$I \equiv \int_0^\infty d\tau P_{i\tau-1/2}(y) \cos(a\tau) / \operatorname{ch}^2(\pi\tau) = \frac{\sqrt{2}}{\pi} \frac{1}{\sqrt{y-cha}} \tan^{-1}\left[\frac{\sqrt{y-cha}}{\sqrt{1+cha}}\right]. \tag{L.4.1}$$

There is surely some simple way to compute this integral, but we don't know what it is so we resort to very ugly brute force with many steps. Start with the integral representation (L.3.5) for P ,

$$P_{i\tau-1/2}(z) = (\sqrt{2}/\pi) \operatorname{ch}(\pi\tau) \int_0^\infty dt (z + cht)^{-1/2} \cos(\tau t). \tag{L.3.5}$$

Install this into (L.4.1) to get,

$$\begin{aligned}
I &= \int_0^\infty d\tau P_{i\tau-1/2}(y) \cos(a\tau) / \operatorname{ch}^2(\pi\tau) \\
&= \int_0^\infty d\tau [(\sqrt{2}/\pi) \operatorname{ch}(\pi\tau) \int_0^\infty dt (y + cht)^{-1/2} \cos(\tau t)] \cos(a\tau) / \operatorname{ch}^2(\pi\tau)
\end{aligned}$$

$$= (\sqrt{2}/\pi) \int_0^\infty dt (y + cht)^{-1/2} \int_0^\infty d\tau \cos(\tau t) \cos(a\tau) / \operatorname{ch}(\pi\tau) \quad (\text{L.4.2})$$

and we now have to evaluate

$$J \equiv \int_0^\infty d\tau \cos(\tau t) \cos(a\tau) / \operatorname{ch}(\pi\tau). \quad (\text{L.4.3})$$

Replace the cosine product as follows,

$$\cos(\tau t) \cos(a\tau) = \operatorname{ch}(ix\tau) \operatorname{ch}(iat) = (1/2) \{ \operatorname{ch}[i(t+a)\tau] + \operatorname{ch}[i(t-a)\tau] \} \quad (\text{L.4.4})$$

so that

$$J = (1/2) \int_0^\infty d\tau \frac{\operatorname{ch}[i(t+a)\tau]}{\operatorname{ch}(\pi\tau)} + (1/2) \int_0^\infty d\tau \frac{\operatorname{ch}[i(t-a)\tau]}{\operatorname{ch}(\pi\tau)}. \quad (\text{L.4.5})$$

We then make use of GR7 3.5.11 (4), page 371,

$$4. \quad \int_0^\infty \frac{\cosh ax}{\cosh bx} dx = \frac{\pi}{2b} \sec \frac{a\pi}{2b} \quad [b > |a|] \quad \text{BI (4)(14)a}$$

Set $b = \pi$ and $a = i(t+a)$ to get

$$\begin{aligned} J &= (1/2) (1/2) \sec [i(t+a)/2] + (1/2) (1/2) \sec [i(t-a)/2] \\ &= (1/4) \{ \operatorname{sech}[(t+a)/2] + \operatorname{sech}[(t-a)/2] \} \\ &= \frac{\operatorname{ch}(t/2)\operatorname{ch}(a/2)}{\operatorname{ch}(t) + \operatorname{ch}(a)}. \end{aligned} \quad (\text{L.4.6})$$

The last line follows from standard identities and we use Maple to verify the result,

$$\begin{aligned} \text{LHS} &:= (1/4) * (\operatorname{sech}((t+a)/2) + \operatorname{sech}((t-a)/2)); \\ &\quad \text{LHS} := \frac{1}{4} \operatorname{sech}\left(\frac{1}{2}t + \frac{1}{2}a\right) + \frac{1}{4} \operatorname{sech}\left(\frac{1}{2}t - \frac{1}{2}a\right) \\ \text{RHS} &:= \cosh(t/2) * \cosh(a/2) / (\cosh(t) + \cosh(a)); \\ &\quad \text{RHS} := \frac{\cosh\left(\frac{1}{2}t\right) \cosh\left(\frac{1}{2}a\right)}{\cosh(t) + \cosh(a)} \\ \text{LHS-RHS} &:= \operatorname{convert}(% , \exp); \operatorname{simplify}(%); \quad 0 \end{aligned} \quad (\text{L.4.7})$$

The integral I is now

$$I = (\sqrt{2}/\pi) \int_0^\infty dt (y + cht)^{-1/2} J$$

$$\begin{aligned}
&= (\sqrt{2}/\pi) \int_0^\infty dt (y + cht)^{-1/2} \frac{ch(t/2)ch(a/2)}{ch(t) + ch(a)} \\
&= (\sqrt{2}/\pi) ch(a/2) \int_0^\infty dt (y + cht)^{-1/2} ch(t/2) (cht + cha)^{-1} \\
&= (1/\pi) ch(a/2) \int_0^\infty dt (y + cht)^{-1/2} (cht + 1)^{1/2} (cht + cha)^{-1}. \tag{L.4.8}
\end{aligned}$$

Now define

$$\alpha \equiv cha \Rightarrow ch(a/2) = \sqrt{1+cha}/\sqrt{2} = \sqrt{1+\alpha}/\sqrt{2} \tag{L.4.9}$$

so that

$$I = \frac{1}{\sqrt{2}\pi} \sqrt{1+\alpha} \int_0^\infty dt (y + cht)^{-1/2} (cht + 1)^{1/2} (cht + \alpha)^{-1}. \tag{L.4.10}$$

Next, change variables to $s = cht$ with $ds = shdt = \sqrt{s^2 - 1} dt$ to get

$$\begin{aligned}
I &= \frac{1}{\sqrt{2}\pi} \sqrt{1+\alpha} \int_1^\infty [ds (s^2 - 1)^{-1/2}] (y+s)^{-1/2} (s+1)^{1/2} (s+\alpha)^{-1} \\
&= \frac{1}{\sqrt{2}\pi} \sqrt{1+\alpha} \int_1^\infty ds (s-1)^{-1/2} (y+s)^{-1/2} (s+\alpha)^{-1}. \tag{L.4.11}
\end{aligned}$$

Now change variables again to $x = s + \alpha$. Then,

$$\int_1^\infty ds = \int_{1+\alpha}^\infty dx \quad s-1 = x - (1+\alpha) \quad y+s = x + (y-\alpha) \quad s+\alpha = x \tag{L.4.12}$$

so now

$$\begin{aligned}
I &= \frac{1}{\sqrt{2}\pi} \sqrt{1+\alpha} \int_{1+\alpha}^\infty dx [x - (1+\alpha)]^{-1/2} [x + (y-\alpha)]^{-1/2} [x]^{-1} \\
&= \frac{1}{\sqrt{2}\pi} \sqrt{1+\alpha} \int_{1+\alpha}^\infty x^{-1} [x + (y-\alpha)]^{-1/2} [x - (1+\alpha)]^{-1/2}. \tag{L.4.13}
\end{aligned}$$

Finally we have a form which can be connected with a hypergeometric function. Consider this integral representation of F from GR8,

$$2.^{12} \quad \int_a^\infty x^{-\lambda} (x+b)^\nu (x-a)^{\mu-1} dx = a^{-\lambda} (b+a)^{\mu+\nu} B(\lambda-\mu-\nu, \mu) {}_2F_1 \left(\lambda, \mu; \lambda-\nu; -\frac{b}{a} \right)$$

$\left[\left| \arg \frac{b}{a} \right| < \pi \text{ or } \left| \frac{b}{a} \right| < 1, \quad 0 < \operatorname{Re} \mu < \operatorname{Re}(\lambda-\nu) \right] \quad \text{ET II 201(8)}$

[The corresponding GR7 equation has a typo reported by your author which got fixed in GR8.] Set

$$a = 1+\alpha \quad \lambda = 1 \quad b = y-\alpha \quad \nu = -1/2 \quad \mu = 1/2 \quad \mu+\nu = 0 . \quad (\text{L.4.14})$$

Then the above GR8 integral says

$$\int_{1+\alpha}^\infty x^{-1} [x + (y-\alpha)]^{-1/2} [x - (1+\alpha)]^{-1/2} = (1+\alpha)^{-1} * 1 * B(1, 1/2) * F(1, 1/2; 3/2; -[y-\alpha]/[1+\alpha]) . \quad (\text{L.4.15})$$

Now

$$B(1, 1/2) = \Gamma(1)\Gamma(1/2)/\Gamma(3/2) = 1 * \sqrt{\pi} / (\sqrt{\pi}/2) = 2 \quad (\text{L.4.16})$$

so then

$$\begin{aligned} I &= \frac{1}{\sqrt{2}\pi} \sqrt{1+\alpha} (1+\alpha)^{-1} 2 F(1, 1/2; 3/2; -[y-\alpha]/[1+\alpha]) \\ &= \frac{\sqrt{2}}{\pi} (1+\alpha)^{-1/2} F(1, 1/2; 3/2; -[y-\alpha]/[1+\alpha]) \\ &= \frac{\sqrt{2}}{\pi} (1+\alpha)^{-1/2} F(1/2, 1; 3/2; -[y-\alpha]/[1+\alpha]) . \quad // \text{recall } \alpha = \text{cha} \end{aligned} \quad (\text{L.4.17})$$

We now make use of GR7 9.121 (27) on page 1007,

$$27. \quad F \left(\frac{1}{2}, 1; \frac{3}{2}; -z^2 \right) = \frac{\arctan z}{z} \quad (\text{L.4.18})$$

where we set $z = \sqrt{\frac{y-\text{cha}}{1+\text{cha}}}$. Then

$$\begin{aligned} I &= \frac{\sqrt{2}}{\pi} (1+\alpha)^{-1/2} \tan^{-1} \sqrt{\frac{y-\text{cha}}{1+\text{cha}}} / \sqrt{\frac{y-\text{cha}}{1+\text{cha}}} \\ &= \frac{\sqrt{2}}{\pi} \frac{1}{\sqrt{y-\text{cha}}} \tan^{-1} \sqrt{\frac{y-\text{cha}}{1+\text{cha}}} \end{aligned} \quad (\text{L.4.19})$$

which is the desired result (L.4.1).

Verification: Oberhettinger and Higgins Table B page 20, the 5th entry. In this entry, the first form agrees with the above. The second form has a typo: the leading $2^{-1/2}$ should be 2^{-1} .

$$\text{L.5 Compute } \int_0^\infty d\tau P_{i\tau-1/2}(y) \operatorname{ch}(b\tau) / \operatorname{ch}^2(\pi\tau)$$

Show that

$$I \equiv \int_0^\infty d\tau P_{i\tau-1/2}(y) \operatorname{ch}(b\tau) / \operatorname{ch}^2(\pi\tau) = \frac{\sqrt{2}}{\pi} \frac{1}{\sqrt{y-\cos b}} \cot^{-1} \left[\frac{\sqrt{1+\cos b}}{\sqrt{y-\cos b}} \right]. \quad (\text{L.5.1})$$

Start with the previous result (L.4.1),

$$\int_0^\infty d\tau P_{i\tau-1/2}(y) \cos(a\tau) / \operatorname{ch}^2(\pi\tau) = \frac{\sqrt{2}}{\pi} \frac{1}{\sqrt{y-\cos a}} \tan^{-1} \left[\frac{\sqrt{y-\cos a}}{\sqrt{1+\cos a}} \right]. \quad (\text{L.4.1})$$

Set $a = ib$ so that

$$\cos(a\tau) = \cos(ib\tau) = \operatorname{ch}(b\tau) \quad \text{and} \quad \operatorname{ch}(a) = \operatorname{ch}(ib) = \cos(b). \quad (\text{L.5.2})$$

Then (L.4.1) becomes

$$\begin{aligned} \int_0^\infty d\tau P_{i\tau-1/2}(y) \operatorname{ch}(b\tau) / \operatorname{ch}^2(\pi\tau) &= \frac{\sqrt{2}}{\pi} \frac{1}{\sqrt{y-\cos b}} \tan^{-1} \left[\frac{\sqrt{y-\cos b}}{\sqrt{1+\cos b}} \right] \\ &= \frac{\sqrt{2}}{\pi} \frac{1}{\sqrt{y-\cos b}} \cot^{-1} \left[\frac{\sqrt{1+\cos b}}{\sqrt{y-\cos b}} \right] \end{aligned} \quad (\text{L.5.3})$$

which is the claimed result (L.5.1). One could replace $\sqrt{1+\cos b} = \sqrt{2} \cos(b/2)$.

Verification: Oberhettinger and Higgins Table B page 20, the 6th entry, but they have a typo. Their result should be this:

$$\begin{aligned} &(1/\sqrt{2}) (1/\sqrt{y-\cos b}) - \frac{\sqrt{2}}{\pi} (1/\sqrt{y-\cos b}) \tan^{-1} \left[\frac{\sqrt{1+\cos b}}{\sqrt{y-\cos b}} \right] \\ &= \frac{\sqrt{2}}{\pi} (1/\sqrt{y-\cos b}) \left(\frac{\pi}{2} - \tan^{-1} \left[\frac{\sqrt{1+\cos b}}{\sqrt{y-\cos b}} \right] \right) = \frac{\sqrt{2}}{\pi} (1/\sqrt{y-\cos b}) \cot^{-1} \left(\frac{\sqrt{1+\cos b}}{\sqrt{y-\cos b}} \right) \end{aligned} \quad (\text{L.5.4})$$

which agrees with our result (L.5.3). But their result is presented instead as

$$2^{-1/2} (y-\cos b)^{-1/2} - 2^{1/2} \pi^{-1} (y-\cos b)^{1/2} \tan^{-1} \left[\frac{\sqrt{1+\cos b}}{\sqrt{y-\cos b}} \right] \quad // \text{ wrong} \quad (\text{L.5.5})$$

where the red 1/2 should be -1/2 (1/2 just prior to \tan^{-1}). This same erroneous exponent also appears in PBM volume 3 on Special Functions (2003), Russian page 181, integral 2.17.24.6,

$$6. \int_0^\infty \frac{\operatorname{ch} bx}{\operatorname{ch}^2 \pi x} P_{ix-1/2}(c) dx = \frac{1}{\sqrt{2(c-\cos b)}} - \frac{\sqrt{2(c-\cos b)}}{\pi} \operatorname{arctg} \sqrt{\frac{1+\cos b}{c-\cos b}} \quad [c > 1].$$

// wrong (L.5.6)

To make sure our form (L.5.1) is the correct form, we do a sample numerical integration. RHS is the right hand side of (L.5.1) while RHS_OH is the right hand side of the "wrong" result (L.5.5) stated above. First, we enter the three items of interest, using our (7.4.1) $P(v,\xi) = P_v(\operatorname{ch}\xi)$ so $P(v,y) = P_v(\operatorname{arccosh}(y))$,

$$\begin{aligned} \text{LHS} &:= \operatorname{int}(P(I\tau-1/2, \operatorname{arccosh}(y)) * \operatorname{cosh}(b\tau)/\operatorname{cosh}(I\tau)^2, \tau = 0..10); \\ LHS &= \int_0^{10} \frac{P\left(I\tau - \frac{1}{2}, \operatorname{arccosh}(y)\right) \operatorname{cosh}(b\tau)}{\operatorname{cosh}(\pi\tau)^2} d\tau \\ \text{RHS} &:= (\sqrt{2}/\pi) * (y-\cos(b))^{-1/2} * \operatorname{arccot}(\operatorname{sqrt}((1+\cos(b))/(y-\cos(b)))); \\ RHS &= \frac{\sqrt{2} \operatorname{arccot}\left(\sqrt{\frac{1+\cos(b)}{y-\cos(b)}}\right)}{\pi \sqrt{y-\cos(b)}} \\ \text{RHS_OH} &:= (1/\sqrt{2}) * (y-\cos(b))^{-1/2} - (\sqrt{2}/\pi) * (y-\cos(b))^{1/2} * \operatorname{arctan}(\operatorname{sqrt}((1+\cos(b))/(y-\cos(b)))); \\ RHS_OH &= \frac{1}{2} \frac{\sqrt{2}}{\sqrt{y-\cos(b)}} - \frac{\sqrt{2} \sqrt{y-\cos(b)} \operatorname{arctan}\left(\sqrt{\frac{1+\cos(b)}{y-\cos(b)}}\right)}{\pi} \end{aligned}$$

Next we enter the P function as in (7.4.1), along with some random values for parameters b and y, then we compare the numeric integral to the two candidate expressions,

$$\begin{aligned} P &:= (\nu, xi) \rightarrow \operatorname{cosh}(xi)^\nu \operatorname{hypergeom}([-nu/2, 1/2-nu/2], [1], \tanh(xi)^2); \\ P &:= (v, \xi) \rightarrow \operatorname{cosh}(\xi)^v \operatorname{hypergeom}\left[\left[-\frac{1}{2}v, \frac{1}{2}-\frac{1}{2}v\right], [1], \tanh(\xi)^2\right] \\ b &:= .7456; y := 2.3456; \\ \operatorname{evalf}(\operatorname{Re}(LHS)); & .2719980019 \\ \operatorname{evalf}(RHS); & .2719980018 \\ \operatorname{evalf}(RHS_OH); & .0978120235 \end{aligned} \quad (L.5.7)$$

Notice that integration to $\tau = 10$ gets the result accurate to 10 decimal places.

Go back now to (L.5.3),

$$\int_0^\infty dt P_{i\tau-1/2}(y) \operatorname{ch}(b\tau) / \operatorname{ch}^2(\pi\tau) = \frac{\sqrt{2}}{\pi} \frac{1}{\sqrt{y-\cos b}} \tan^{-1}\left[\frac{\sqrt{y-\cos b}}{\sqrt{1+\cos b}}\right]$$

$$= \frac{\sqrt{2}}{\pi} \frac{1}{\sqrt{y-\cos b}} \cot^{-1} \left[\frac{\sqrt{1+\cos b}}{\sqrt{y-\cos b}} \right]. \quad (L.5.3)$$

To make the proper analytic continuation in b more obvious, we replace

$$\sqrt{1+\cos b} = \sqrt{2} \cos(b/2)$$

This shows that as b runs along the real axis, the function called " $\sqrt{1+\cos b}$ " in fact changes sign at odd multiples of π , as discussed in Appendix M. Then (L.5.3) can be written as

$$\begin{aligned} \int_0^\infty d\tau P_{i\tau-1/2}(y) \operatorname{ch}(b\tau) / \operatorname{ch}^2(\pi\tau) &= \frac{\sqrt{2}}{\pi} \frac{1}{\sqrt{y-\cos b}} \tan^{-1} \left[\frac{\sqrt{y-\cos b}}{\sqrt{2} \cos(b/2)} \right] \\ &= \frac{\sqrt{2}}{\pi} \frac{1}{\sqrt{y-\cos b}} \cot^{-1} \left[\frac{\sqrt{2} \cos(b/2)}{\sqrt{y-\cos b}} \right]. \end{aligned} \quad (L.5.8)$$

L.6 Compute $\int_0^\infty d\tau P_{i\tau-1/2}(y) \operatorname{sh}(b\tau) \operatorname{sh}(\pi\tau)/\operatorname{ch}^2(\pi\tau)$

Show that

$$I \equiv \int_0^\infty d\tau P_{i\tau-1/2}(y) \operatorname{sh}(b\tau) \operatorname{sh}(\pi\tau)/\operatorname{ch}^2(\pi\tau) = \frac{\sqrt{2}}{\pi} \frac{1}{\sqrt{y+\cos b}} \tan^{-1} \left(\frac{\sqrt{1-\cos b}}{\sqrt{y+\cos b}} \right). \quad (L.6.1)$$

Start by expanding

$$2 \operatorname{sh}(b\tau) \operatorname{sh}(\pi\tau) = \operatorname{ch}[(b+\pi)\tau] - \operatorname{ch}[(b-\pi)\tau] \quad (L.6.2)$$

so then

$$\begin{aligned} I &\equiv \int_0^\infty d\tau P_{i\tau-1/2}(y) \operatorname{sh}(b\tau) \operatorname{sh}(\pi\tau)/\operatorname{ch}^2(\pi\tau) \\ &= (1/2) \int_0^\infty d\tau P_{i\tau-1/2}(y) \operatorname{ch}[(b+\pi)\tau] - (1/2) \int_0^\infty d\tau P_{i\tau-1/2}(y) \operatorname{ch}[(b-\pi)\tau]. \end{aligned} \quad (L.6.3)$$

But (L.5.8) says, replacing b by β ,

$$\int_0^\infty d\tau P_{i\tau-1/2}(y) \operatorname{ch}(\beta\tau) / \operatorname{ch}^2(\pi\tau) = \frac{\sqrt{2}}{\pi} \frac{1}{\sqrt{y-\cos \beta}} \cot^{-1} \left[\frac{\sqrt{2} \cos(\beta/2)}{\sqrt{y-\cos \beta}} \right]. \quad (L.6.4)$$

For the first term in (L.6.3) we set

$$\begin{aligned}\beta &= b+\pi \\ \cos\beta &= \cos(b+\pi) = -\cos(b) \\ \cos(\beta/2) &= \cos(b/2+\pi/2) = -\sin(b/2)\end{aligned}\tag{L.6.5}$$

so

$$\int_0^\infty d\tau P_{i\tau-1/2}(y) \operatorname{ch}[(b+\pi)\tau] / \operatorname{ch}^2(\pi\tau) = \frac{\sqrt{2}}{\pi} \frac{1}{\sqrt{y+\cos b}} \cot^{-1} \left[\frac{-\sqrt{2} \sin(b/2)}{\sqrt{y+\cos b}} \right]. \tag{L.6.6}$$

For the second term in (L.6.3) we set

$$\begin{aligned}\beta &= b-\pi \\ \cos\beta &= \cos(b-\pi) = -\cos(b) \\ \cos(\beta/2) &= \cos(b/2-\pi/2) = \cos(\pi/2-b/2) = \sin(b/2)\end{aligned}\tag{L.6.7}$$

so

$$\int_0^\infty d\tau P_{i\tau-1/2}(y) \operatorname{ch}[(b-\pi)\tau] / \operatorname{ch}^2(\pi\tau) = \frac{\sqrt{2}}{\pi} \frac{1}{\sqrt{y+\cos b}} \cot^{-1} \left[\frac{+\sqrt{2} \sin(b/2)}{\sqrt{y+\cos b}} \right]. \tag{L.6.8}$$

Then,

$$\begin{aligned}I &= (1/2) \int_0^\infty d\tau P_{i\tau-1/2}(y) \operatorname{ch}[(b+\pi)\tau] - (1/2) \int_0^\infty d\tau P_{i\tau-1/2}(y) \operatorname{ch}[(b-\pi)\tau] \\ &= (1/2) \frac{\sqrt{2}}{\pi} \frac{1}{\sqrt{y+\cos b}} \cot^{-1} \left[\frac{-\sqrt{2} \sin(b/2)}{\sqrt{y+\cos b}} \right] - (1/2) \frac{\sqrt{2}}{\pi} \frac{1}{\sqrt{y+\cos b}} \cot^{-1} \left[\frac{+\sqrt{2} \sin(b/2)}{\sqrt{y+\cos b}} \right] \\ &= (1/2) \frac{\sqrt{2}}{\pi} \frac{1}{\sqrt{y+\cos b}} \left\{ \cot^{-1} \left[\frac{-\sqrt{2} \sin(b/2)}{\sqrt{y+\cos b}} \right] - \cot^{-1} \left[\frac{+\sqrt{2} \sin(b/2)}{\sqrt{y+\cos b}} \right] \right\}.\end{aligned}\tag{L.6.9}$$

We now twice use the fact that $\cot^{-1}(x) = \pi/2 - \tan^{-1}(x)$ to rewrite the above as

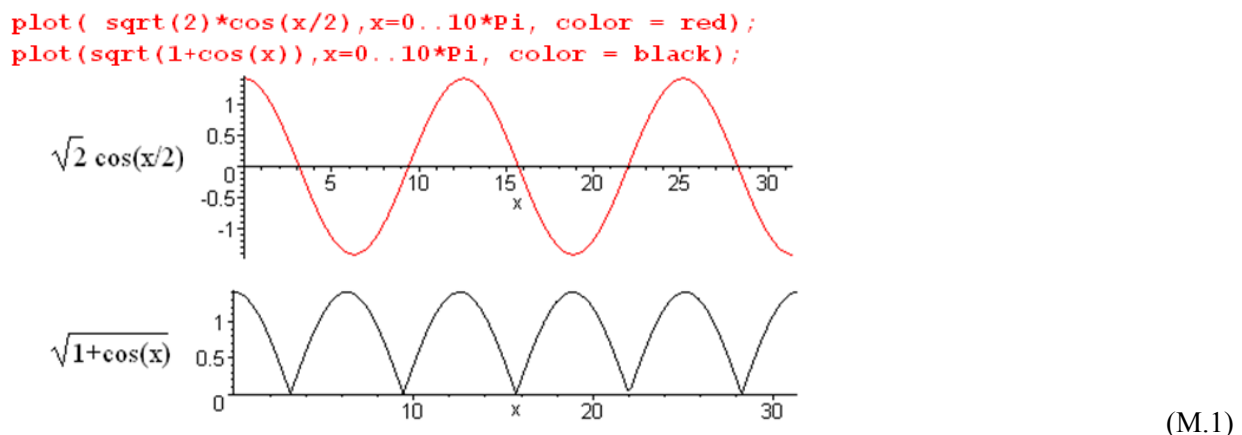
$$\begin{aligned}I &= (1/2) \frac{\sqrt{2}}{\pi} \frac{1}{\sqrt{y+\cos b}} \left\{ \tan^{-1} \left[\frac{+\sqrt{2} \sin(b/2)}{\sqrt{y+\cos b}} \right] - \tan^{-1} \left[\frac{-\sqrt{2} \sin(b/2)}{\sqrt{y+\cos b}} \right] \right\} \\ &= (1/2) \frac{\sqrt{2}}{\pi} \frac{1}{\sqrt{y+\cos b}} \left\{ 2 \tan^{-1} \left[\frac{+\sqrt{2} \sin(b/2)}{\sqrt{y+\cos b}} \right] \right\} \\ &= \frac{\sqrt{2}}{\pi} \frac{1}{\sqrt{y+\cos b}} \tan^{-1} \left(\frac{\sqrt{2} \sin(b/2)}{\sqrt{y+\cos b}} \right) \\ &= \frac{\sqrt{2}}{\pi} \frac{1}{\sqrt{y+\cos b}} \tan^{-1} \left(\frac{\sqrt{1-\cos b}}{\sqrt{y+\cos b}} \right)\end{aligned}\tag{L.6.10}$$

and this is the result claimed in (L.6.1).

Verification: The evaluation shown in (L.6.1) appears in Oberhettinger and Higgins Table B page 20 entry 3.

Appendix M: The behavior of $f(z) = (a+\cos z)^{1/2}$ as an analytic function

The function $f(x) = \sqrt{1+\cos(x)}$ appears in the results of Mehler integrals like (7.1.5) and other places in this document. We comment above (L.5.8) and elsewhere that " $\sqrt{1+\cos(x)}$ changes sign as x passes through odd multiples of π ". This fact is totally obvious when one replaces $\sqrt{1+\cos(x)}$ by $\sqrt{2} \cos(x/2)$. In writing the expression $\sqrt{1+\cos(x)}$ one must be careful about its meaning. Maple (reasonably) interprets this as a positive quantity $|\sqrt{1+\cos(x)}|$ for all real x as seen in the black plot below

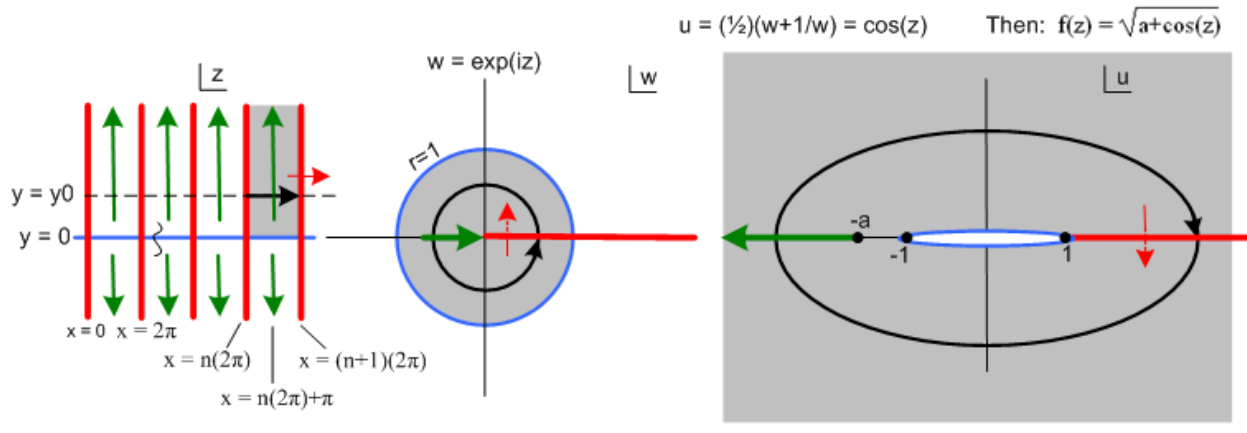


In normal integral evaluations like (7.1.5), if $\sqrt{1+\cos(x)}$ appears on the right side, the usual interpretation is that both sides of the equation are *analytic* in the complex variable x although one might be using the integral for real x . In this case, one gets "the wrong answer" if one uses the black curve above, and plots of potentials come out totally wrong.

This appendix explores the seemingly simple analytic function $f(z) = \sqrt{a+\cos(z)}$ and shows when and in what sense it must change sign at odd multiples of π as z moves "along the real axis". This subject is well addressed in Ahlfors Chapter 3 *Analytic Functions as Mappings*.

Some analytic mappings

Consider the following drawing :



(M.2)

We are considering a three-step mapping of analytic functions:

$$\begin{array}{ll}
 w = e^{iz} & z\text{-plane to } w\text{-plane} \\
 u = (1/2)(w + 1/w) // = \cos(z) & w\text{-plane to } u\text{-plane} \\
 f = \sqrt{a + u} // = \sqrt{a + \cos(z)} & u\text{-plane to } f\text{-plane (not shown)} \quad (M.3)
 \end{array}$$

The drawing shows the z-plane, the w-plane, and the u-plane.

In the z-plane, where $z = x + iy$, the red vertical lines show $x = \text{multiples of } 2\pi$. All the vertical red lines in the z-plane map into the single red half line in the w-plane and then in the u-plane. The red path in the u-plane folds back on itself since $w = 0$ and $w = \infty$ both map to $u = \infty$, while $w = 1$ maps to $u = 1$.

We select a particular region of the z-plane and mark it gray (region is a half-infinite vertical strip). This region maps to the gray disk in the w-plane (radius 1), and that disk in turn maps into all of the u-plane.

Following the Black Ants

We set up a "tracking ant" in the z-plane which wanders along a path indicated by the black arrow. This path is not along the real z axis, but is elevated above it at $y = y_0$ as shown. The ant moves from $n(2\pi)$ to $(n+1)(2\pi)$ in x, while holding $y = y_0$.

As this ant moves in the z-plane along its path, another ant makes a corresponding (mapped) movement in the w- plane, and yet another ant makes a corresponding movement in the u-plane. All ant paths are shown in black.

In the w-plane the ant's path maps into the black circle shown, a simple phasor path.

In the u-plane, the ant's path is an ellipse, and the traversal direction is now clockwise instead of counterclockwise. The reason for the ellipse is this:

$$e^{iz} = e^{ix} e^{-y}$$

$$\begin{aligned} u &= (1/2)(w+1/w) = (1/2)(e^{ix} e^{-y} + e^{-ix} e^y) = (1/2)([\cos x + i \sin x] e^{-y} + [\cos x - i \sin x] e^y) \\ &= \cos x \cosh y - i \sin x \sinh y = u_1 + i u_2 \quad u_1 = \cos x \cosh y \quad u_2 = -\sin x \sinh y \end{aligned} \quad (\text{M.4})$$

Then setting $y = y_0$ for the ant path,

$$\frac{u_1^2}{\cosh^2 y_0} + \frac{u_2^2}{\sinh^2 y_0} = \cos^2 x + \sin^2 x = 1 \quad u = (u_1, u_2). \quad (\text{M.5})$$

This is an ellipse with semi-major axis $\cosh y_0$, semi-minor axis $\sinh y_0$, and focal points at $u = (\pm 1, 0)$.

As x moves along the black arrow in the z -plane starting at $x = n(2\pi)$, $\sin x > 0$ so u gets a negative imaginary part in (M.4) and the ant moves south in the u -plane. That is why the u -plane ant moves clockwise.

The Green Cut

We are interested in the function

$$f(u) = \sqrt{a+u} \quad (\text{M.6})$$

which has a branch point at $u = -a$. We draw the attached green cut off to the left as shown in Fig (M.2). This choice of cut direction makes $\sqrt{a+u}$ unambiguous and real on the positive real axis (the function is "real analytic"). We have then back-mapped this green cut into both the w -plane and the z -plane. There are no green cuts in these two planes, we are just marking the back-image of the u -plane cut location. In the w -plane one sees that the marked green cut location is encountered when the phasor angle x of $e^{iz} = e^{ix} e^{-y}$ passes through odd multiples of π . Then in the z -plane these values of x appear as vertical green lines at odd multiples of π .

This function $f(u)$ has two Riemann sheets which we can regard as

$$\begin{aligned} f(u) &= f_1(u) \equiv +\sqrt{a+u} & \text{Sheet 1} \\ f(u) &= f_2(u) \equiv -\sqrt{a+u} & \text{Sheet 2} \end{aligned} \quad (\text{M.7})$$

just as $\sqrt{4} = \pm 2$. Imagine that Sheet 1 is the one displayed in the u -plane above. Then Sheet 2 lies underneath Sheet 1. An ant moving on Sheet 1 passes through the cut onto Sheet 2. Since the ant is constrained to the surface, it cannot jump across the cut, but has to descend onto Sheet 2. The connection between the sheets is bidirectional which makes it impossible to model physically. Here is the cut seen edge on



Think of Fig (M.8) as two levels of a parking garage that has separate up and down ramps between the levels. Thus for the particular path shown above in the z -plane, the function $f(u) = \sqrt{a+u}$ changes sign each time that z -plane path passes through an odd multiple of π .

The real-axis path as a limit

The ant path shown in the z -plane is elevated at some $y_0 > 0$. We now lower this path to the real axis (shown in blue). As this happens, the black circle in the w -plane moves toward the blue circle perimeter of the gray disk, and the black elliptical path in the u -plane shrinks to the thin blue path shown there. If $a > 1$, this new elliptical path completely avoids the cut, and one finds that $f(u) = \sqrt{a + \cos(z)}$ does not change sign, because we just stay on Sheet 1 for the entire path, so the effect of switching sheets does not occur. Notice that the blue thin ellipse in its limiting sense passes to the left of the focal point $u = -1$.

Now what happens if $a = 1$ and we have the function $f(u) = \sqrt{1+u}$? Go back to the ant path up at $y = y_0$, and draw the green cut starting at $u = -1$ in the u -plane. We then have the sign-switching action as the ant passes odd multiples of π . As we take this ant path down to the blue x axis in the z -plane, the elliptical path in the u -plane always encounters the cut, and we then still have the sign swapping effect. The ant path, no matter how thin its ellipse might be in the u -plane, always passes to the left of the point $a = -1$ and this ant is forced to take the dive.

Our conclusions are:

1. The function $f(x) = \sqrt{a + \cos(x)}$ for $a > 1$ does not change sign as x passes through odd multiples of π .
2. The function $f(x) = \sqrt{1 + \cos(x)}$ *does* change sign as x passes through odd multiples of π . (M.9)

At $x = 0$ we assume that $f(0) = \sqrt{2} > 0$.

Theorem: Given the analytic function $f(z) = \sqrt{1 + \cos(z)}$, if we run z along a real path on the x -axis, taking that path to be the limiting path of a complex path above the real axis, then

$$f(x) = (-1)^\eta |\sqrt{1 + \cos(x)}| \text{ where } \eta = \text{floor}[(x+\pi)/2\pi]. \quad (\text{M.10})$$

Here the factor $(-1)^\eta$ implements the sign changes discussed above. Each time x passes through an odd multiple of π , η increases by 1, causing the desired sign change.

It is of course a lot easier to implement $\sqrt{1 + \cos(x)}$ as $\sqrt{2} \cos(x/2)$.

References

Alphabetical by last name of lead author. Links last verified 28 Dec 2015.

L. A. Ahlfors, *Complex Analysis, 2nd Ed.* (McGraw-Hill, New York, 1966) .

[Bateman] A. Erdelyi et al., *Higher Transcendental Functions*, Volumes 1,2, and 3 (McGraw-Hill, New York, 1953); *Tables of Integral Transforms*, Volumes 1 and 2 (McGraw-Hill, New York, 1954). This is the 5-volume Bateman Manuscript Project. We shall follow the GR7 convention by referring to these five volumes as EH I,II,III and ET I,II (Erdelyi Higher, Erdelyi Transform).

B.J. Gonzalez and E.R. Negrin, "Mehler-Fock Transforms of Generalized Functions via the Method of Adjoints", *Proc. Amer. Math. Soc.*, Vol. 125, No. 11 (Nov, 1997), pp. 3243-3253.

[GR7] I.S. Gradshteyn and I.M. Ryzhik, *Table of Integrals, Series, and Products, 7th Ed.* (Academic Press, New York, 2007). The 8th Edition [GR8] appeared 2 Oct 2014 (no CD). Dan Zwillinger is collecting errata here for the 9th Edition : <http://www.mathtable.com/gr/>

E.W. Hobson, *The Theory of Spherical and Ellipsoidal Harmonics* (Cambridge University Press, Cambridge, 1931). Chapter XI concerns ellipsoidal harmonics, about 50 pages. This presentation seems more readable than Chapter 23 of Whittaker and Watson (see below).

H. Hu and R.G. Larson, " Evaporation of a Sessile Droplet on a Substrate", *J. Phys. Chem. B* (2002), 106, 1334-1344. Points out that 19th century toroidal potential theory has a role in DNA processing.

J.D. Jackson, *Classical Electrodynamics* (Wiley, New York, 1962). This is the first edition with a green cover. Later editions (red cover 1975 and blue cover 1998) omit discussion of the inversion method to make room for more exciting subjects.

Kelvin (W. Thomson), *Reprint of Papers on Electrostatics and Magnetism, 2nd. Ed.* (Macmillan, London, 1884). Like several other items in this Reference list, this out-of-print book is available on the web (this one "Digitized by Microsoft"). Converting PDF to DJVU makes things smaller and faster and maintains searchability.

N.N. Lebedev, *Special Functions and their Applications* (Prentice-Hall, Englewood Cliffs,N.J, 1965). There is a 1972 Dover edition.

N.N. Lebedev, I.P. Skalskaya and Y.S. Uflyand, *Worked Problems in Applied Mathematics* (Dover, New York, 1965). There are not many books like this one. In the first 2/3 of the book, 566 problems requiring many mathematical techniques from various fields of physics and engineering are presented with solutions or hints as to their solution, and in the last 1/3 a subset of these problems is solved (but not those discussed in the current paper). There is a recent 2010 Dover edition.

[Bipolar] P. Lucht, "Bipolar Coordinates and the Two-Cylinder Capacitor" (2015),
<http://user.xmission.com/~rimrock>. If not there, search on "Phil Lucht Documents" or the title.

P. Lucht, "A Maple User's Guide" (2015), see above.

P. Lucht, "Tensor Analysis and Curvilinear Coordinates" (2015), see above.

Maple (Maplesoft), a symbolic computer algebra system, today officially Maple 2015. See wiki for comments about Maple's history versus Mathematica and other systems. See author's Maple User Guide.

K.T. McDonald, "Conducting Spherical Shell with a Circular Orifice" (2002) This paper discusses the bowl problem in several ways, and reviews some of Kelvin's papers noted above. The current paper tries to fill in Section 2.5 of this document. See <http://www.hep.princeton.edu/~mcdonald/examples/>.

P. Moon and D.E. Spencer, *Field Theory Handbook, Including Coordinate Systems, Differential Equations and their Solutions* (Springer-Verlag, Berlin, 1961). This book is not about quantum field theory or anything like that, it is about curvilinear coordinate systems, how the Laplace and Helmholtz equations appear in each system, and what the solutions of these equations look like. This husband and wife team wrote several excellent books. Long ago they were strangely involved in an accident involving a test of general relativity.

P.M. Morse and H. Feshbach, *Methods of Theoretical Physics* (McGraw-Hill, New York, 1953). This 2000 page behemoth is simply amazing.

F. Oberhettinger and T.P. Higgins, *Tables of Lebedev, Mehler and Generalized Mehler Transforms* (Boeing Scientific Research Laboratories, Mathematical No. 246, 1961). A 48 page monograph with about 16 transforms per page. The first author is a member of A. Erdelyi et al. mentioned above. We obtained this book by interlibrary loan from the Coe library at the University of Wyoming.

[NIST] F.W.J. Olver, D.W. Lozier, R.F. Boisvert and C.W. Clark, *NIST Handbook of Mathematical Functions* (Cambridge University Press, 2010). NIST is the U.S. National Institute of Standards and Technology which published the world-famous earlier edition in 1964 with editors Abramowitz and Stegun, known affectionately as "A&S". The greatly expanded 2010 edition (968 p) can be accessed online at dlmf.nist.gov which also has errata. The book ($\geq \$20$) comes with a CD containing a bookmarked PDF file which of course has been bootlegged onto the web. Olver died in 2013.

[PBM] A.P. Prudnikov, Y.A. Brychkov and O.I. Marichev, *Integrals and Series: More Special Functions, Vol 3* (Gordon and Breach, New York, 1996). A huge 5 volume set similar to the Bateman / Erdelyi set plus Gradshteyn & Ryzhik. The Russian editions are perhaps more available and can easily be used by non-Russian readers. Here are a few useful words:

оглавление = table of contents	ряды = series	сумма = sum
глава = chapter	преобразовать = transform	
интеграл = integral	функция = function	

<http://www.babylon.com/define/118/russian-english-dictionary.html>

E.M. Purcell, *Electricity and Magnetism*, Berkeley Physics Course Vol. 2 (McGraw-Hill, New York, 1965), a very excellent book. Now in 3rd Edition 2013 with coauthor D.J. Morin.

W.R. Smythe, *Static and Dynamic Electricity*, 2nd Ed. (McGraw-Hill, New York, 1950). This text contains famously difficult problems.

I. Sneddon, *Mixed Boundary Value Problems in Potential Theory* (Wiley, New York, 1966). This book treats dual and triple integral and series equations with examples from electrostatics and from crack theory. A lot of output is obtained from basic Abel and Hankel type transforms.

C. Snow, *Hypergeometric and Legendre Functions with Applications to Integral Equations of Potential Theory*, National Bureau of Standards Applied Mathematics Series No. 19, 427 pages (May 1, 1952),
<http://babel.hathitrust.org/cgi/pt?id=uiug.30112016737360>;

C. Snow, *Formulas for Computing Capacitance and Inductance*, National Bureau of Standards Circular 544, 71 pages (Sept 10, 1954), www.g3ynh.info/zdocs/refs/NBS/Snow_Circ544.pdf or see hathitrust.org.

I. Stakgold, *Boundary Value Problems of Mathematical Physics*, Volumes 1 and 2 (MacMillan, London, 1967). These are astoundingly good books, but the high level of detail (the subject is intrinsically complex) makes them hard to use in a normal "course", which is why the author later put out a condensed single-volume version *Green's Functions and Boundary Value Problems*, now in a third edition. The original two volumes were reprinted with some corrections in 2000 (SIAM, Philadelphia). P. Lucht has a short list of errata on line.

R. Szmytkowski and S.Bielski, "A Direct delta-type orthogonality relation for the on-the-cut generalized associated Legendre functions of the first kind with imaginary second upper indices", *Integral Transforms and Special Functions* (2014), Vol. 25, No.4, 312-317, <http://dx.doi.org/10.1080/10652469.2013.842235> or <http://www.mif.pg.gda.pl/homepages/radek/#publications>.

S.S Vinogradov, P.D. Smith, and E.D Vinogradova, *Canonical Problems in Scattering and Potential Theory, Part I: Canonical Structures in Potential Theory* (Chapman & Hall/CRC, New York, 2001). The bowl problem is treated in Sections 1.4.1-3 of this excellent but very advanced monograph. Chapter 2 incorporates in compact form nearly the entire huge panorama of Sneddon's book. The book is advanced in that it treats impressive variations of already-difficult problems in electrostatics, surfaces with holes and slots and missing pieces. For example,

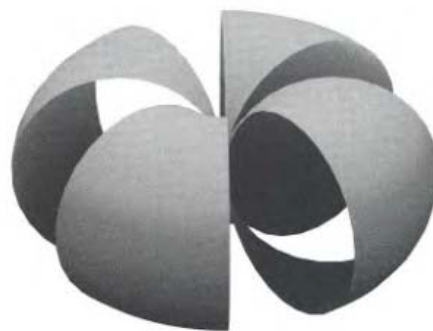


Figure 5.7
A degenerate toroidal shell with four azimuthal cuts.

E.T. Whittaker and G.N. Watson, *A Course in Modern Analysis*, 4th Ed. (Cambridge University Press, Cambridge, 1927). The Mehler-Dirichlet integral is derived in Section 15.231 of this and at least two earlier editions. Beware that the 2nd edition is being sold by Merchant Press and does not include Chapter 23 on Ellipsoidal Harmonics and Lamé Functions. See Kelvin reference above.
